CORRELATION OF THE VAPOR PRESSURE ISOTOPE EFFECT WITH MOLECULAR FORCE FIELDS IN THE LIQUID STATE

by

James S. Pollin

A dissertation submitted to the Graduate Faculty in Chemistry in partial fulfillment of the requirements for the degree of Doctor of Philosophy, The City University of New York.

1976

This manuscript has been read and accepted for the Graduate Faculty in Chemistry in satisfaction of the dissertation requirement for the degree of Doctor of Philosophy.

May 17, 1976
date

Chairman of Examining Committee

5/18/76
date

Leonard H. Schwartz
Executive Officer

Charles E. Heath

B. M.

Supervisory Committee

The City University of New York

Abstract

CORRELATION OF THE VAPOR PRESSURE ISOTOPE EFFECT
WITH MOLECULAR FORCE FIELDS
IN THE LIQUID STATE

by

James S. Pollin

Adviser: Professor Takanobu Ishida

The present work is concerned with the development and application of a new model for condensed phase interactions with which the vapor pressure isotope effect (vpie) may be related to molecular forces and structure. The model considers the condensed phase as being represented by a cluster of regularly arranged molecules consisting of a central molecule and a variable number of molecules in the first coordination shell. The methods of normal coordinate analysis are used to determine the modes of vibration of the condensed phase cluster from which, in turn, the isotopic reduced partition function can be calculated.

Using the medium cluster model, the observed vpie for a series of methane isotopes has been successfully reproduced with better agreement with experiment than has been possible using the simple cell model. We conclude, however, that insofar as the medium cluster model provides a reasonable picture of the liquid state, the vpie is not sufficiently sensitive to molecular orientation to permit an experimental determination of intermolecular configuration in

the condensed phase through measurement of isotopic pressure ratios. The virtual independence of vapor pressure isotope effects on molecular orientation at large cluster sizes is a demonstration of the general acceptability of the cell model assumptions for vpie calculations.

To my wife

ACKNOWLEDGEMENT

The author wishes to express his sincere appreciation to Professor Takanobu Ishida for his guidance, encouragement and assistance during the course of this research. Special thanks are also extended to the thesis committee members, Professors Vojtech Fried, Charles E. Hecht and Avigdor Ronn, for their many helpful comments and suggestions. The invaluable assistance given by Mr. Armand Gazes of the Brooklyn College Data Acquisition Facility and the help given by the staff of the City University Computer Center are gratefully acknowledged.

The United States Energy Research and Development Administration and the City University Faculty Awards Program have contributed to the funding of this research.

TABLE OF CONTENTS

LIST OF TABLES

LIST OF FIGURES

I. INTRODUCTION

This thesis presents the development and application of an original model for condensed phase intermolecular forces for use within the context of the vapor pressure isotope effect. The model considers the condensed phase force field as a set of explicit and well-defined interactions, rather than as a generalized potential. Computational results for a variety of isotopic derivatives of methane will be presented which successfully reproduce experimental observations and provide indications of the important factors involved in determining the isotope effect.

The thesis consists of three major parts: (1) an introduction, in which background information and pertinent theory will be presented; (2) a computational methods section, which shows in detail how model calculations are performed and interpreted; (3) a presentation and discussion of results, with emphasis on the correlation of vapor pressure isotope effects with molecular forces and structure in the condensed phase. Lists of newly developed computer programs are appended. Discussion of material which is original to this research will be integrated with discussions of previous work, rather than presented in a single separate section.

Although this study is largely of a theoretical nature, a brief review of the experimental measurement of vapor pressure isotope effect will first be given.

I-1: Experimental Basis of the Vapor Pressure Isotope Effect

Single component gas-liquid and gas-solid equilibria are characterized by the opposing phenomena of condensation and vaporization. At constant temperature, such an equilibrium state is completely specified by a unique gas-phase pressure. Isotopic substitution in the single component slightly alters the characteristic pressure; this shift is known as the vapor pressure isotope effect (vpie). The correlation of the vpie with molecular structure is significant both theoretically, where it can be of assistance in understanding intermolecular forces, and commercially, where optimum isotope separation is an important industrial process.

The vapor pressure isotope effect is usually expressed as the logarithm of the ratio of equilibrium pressures, $\ell n(P'/P)$, where the primed quantity refers by convention to the pressure of the lighter isotope. The behavior of $\ell n(P'/P)$ for various isotopic pairs as a function of temperature is of primary concern. The vpie is considered normal if, at a given temperature, $\ell n(P'/P) > 0$ and inverse if $\ell n(P'/P) < 0$. The temperature at which the logarithm of the pressure ratio vanishes is called the crossover temperature.

Several techniques have been developed to measure the vapor pressure isotope effect. Because of the strong temperature dependence of vapor pressure, it is not possible to accurately determine the vpie by measuring the pressures of the two species individually; it is necessary to determine the vapor pressures simultaneously at precisely the same temperature. Differential manometry was first used by Keesom and Haantjes (1) for the measurement of the vpie of

neon isotopes. Subsequent studies have employed increasingly sensitive techniques including membrane manometers (2) and differential capacitance gauges (3,4). The compounds under study must be both chemically and isotopically pure when direct vapor pressure measurements are made (5). In addition, the samples must be kept at exactly the same temperature. For example, since a vapor pressure isotope effect is generally on the order of 1%, $P'/P \approx 1.01$; if this ratio is to be determined with one percent precision, the pressure fluctuation, δP, must be limited to $\delta P/P = 0.0001$. From the Clausius-Clapeyron equation,

$$\frac{\delta P}{P} = -\frac{\Delta H_{vap}}{RT^2}\,\delta T \qquad (1)$$

it is seen that a temperature stability, δT, of 0.001 °K is required at 200 °K for a typical latent heat of vaporization of 10 kcal/mole. A cryostat capable of such temperature stability has been described by Bigeleisen, et al. (6) for use below 300 °K.

Distillation techniques provide somewhat indirect and less precise methods for the determination of vapor pressure isotope effects (7,8,9). The principal advantage these techniques have over manometric methods is that only samples of low isotopic composition are needed. The single-stage separation factor, α, is defined as

$$\alpha = \frac{(N'/N)_{vapor}}{(N'/N)_{liquid}} \qquad (2)$$

where N' and N are the equilibrium concentrations of the light and

heavy isotopes in a theoretical stage in the distillation system. The vpie and α are related (10) by

$$\ell n(P'/P) = \left[1 + \frac{P(B_o - V)}{RT}\right]^{-1} \ell n\alpha \qquad (3)$$

where B_o is the second virial coefficient, assumed to be the same for both isotopes (11).

Single-stage distillation experiments are limited by the accuracy of the mass analysis since α is always close to unity. By using an n-stage distillation column, the overall separation factor is increased n-fold (12). In such a multi-stage system, the α factor is given by

$$\frac{X_{top}}{1-X_{top}} = \frac{X_{bottom}}{1-X_{bottom}} \alpha^{n_\infty} \qquad (4)$$

where X_{top} and X_{bottom} are the isotopic atom fractions at the top and bottom of the column and n_∞ is the number of theoretical plates at total reflux. The number of theoretical plates is determined from an analysis of the transient behavior of the distillation column as a function of column parameters and the nature of the distillate. The analysis of multi-stage distillation systems has been described in detail by Cohen (13), Bigeleisen and Ribnikar (8), and Ishida and Wieck (14).

I-2: Historical Overview of Vapor Pressure Isotope Effect Theory

Theoretical interpretation of observed isotope effects began more than fifty years ago with the work of F. A. Lindemann (Lord Cherwell),

who examined the isotopic dependence of vapor pressure in solid-gas equilibria (15). Starting with an equation derived from the theory of monatomic Debye solids, Lindemann obtained an expression for the high temperature isotope effect,

$$\ell n(P'/P) = \frac{1}{RT}\int_0^T (C_p' - C_p)dT + \frac{3}{2}\ell n(\frac{m'}{m}) - \frac{\Delta H_o' - \Delta H_o}{RT} \qquad (5)$$

where C_p', m' and $\Delta H_o'$ are the heat capacity, isotopic mass and latent heat of vaporization at absolute zero for the light isotope and C_p, m and ΔH_o are corresponding quantities for the heavy isotope. An independent derivation of Equation (5) was later given by O. Stern (16). The last term of Equation (5) represents the shift in zero point energy with isotopic substitution, a quantum effect, which was of doubtful validity in 1923. In 1931, Keesom and van Dijk (17) examined the vpie of solid Ne^{20}/Ne^{22}. Their work supported the validity of the Lindemann-Stern equation, thereby demonstrating the existence of the zero point energy and its importance in the vapor pressure isotope effect. In 1934, Scott et al. (18) extended previous calculations of the solid-gas vpie by including consideration of gas imperfections.

The theory of the effect of isotopy on the vapor pressure of liquids has always been somewhat inadequate due in large part to the nature of the liquid-phase distribution function and the quantum corrections that must be applied to the liquid partition function. In 1938, Herzfeld and Teller developed a theory of monatomic liquids (19) by applying the Wigner quantum correction (20) to the Boltzmann dis-

tribution. They obtained an expression for the quantum mechanical partition function, Q, in terms of the classical partition function, Q_{cl}:

$$\frac{Q}{Q_{cl}} = 1 - \frac{\hbar^2}{24(kT)^2}\left\langle \sum \frac{1}{m_i} \frac{\partial^2 U}{\partial x_i^2} \right\rangle + \cdots \qquad (6)$$

where U is the potential energy of the system as a function of all coordinates x. The brackets indicate an average probability distribution in configuration space. Similar expressions for polyatomic molecules are given by Landau and Lifshitz (21) and by Friedmann (22). In general, the Wigner theorem, expressed as a power series of h (23), gives the quantum correction for thermodynamic equilibrium and an expression for the isotope effect. To first order, this expression is

$$\ell n(P'/P) = \frac{\hbar^2}{24(kT)^2}\left(\frac{1}{m'} - \frac{1}{m} \right)\left(\langle \nabla^2 U \rangle_{cond} - \langle \nabla^2 U \rangle_{gas} \right) \qquad (7)$$

where m' and m are isotopic masses and $\langle \nabla^2 U \rangle$ is the mean value of the Laplacian of the intermolecular potential. If many-body forces are neglected in the condensed phase, U is obtained as a pair summation (24),

$$U = \sum_{i>j} u(r_{ij}) \qquad (8)$$

where r_{ij} is the intermolecular distance, and the average Laplacian

is given by (25)

$$\langle \nabla^2 U \rangle = 4\pi n \int_0^\infty g(r) \frac{d}{dr}\left(r^2 \frac{du(r)}{dr} \right) dr \qquad (9)$$

where n is the mean number density and g(r) is the radial distribution function. Bigeleisen, Lee and Mandel (26) have shown that excellent agreement exists between $\langle \nabla^2 U \rangle$ values derived from experimental vpie measurements of Kr, Ar and Xe isotopes and $\langle \nabla^2 U \rangle$ values calculated by Mandel (27) and Verlet (28) using perturbation methods. Rowlinson (29) and Present (30) have examined the effect of many-body forces on the isotope effect.

With Equation (7), Herzfeld and Teller showed that to a first approximation the logarithm of the isotopic pressure ratio is inversely proportional to the square of the absolute temperature with the lighter isotope having the higher vapor pressure at all temperatures. Many examples of the heavy isotope having a higher vapor pressure at some temperatures are known (31). This inverse isotope effect may be explained (32) in terms of a shift in the internal frequencies of vibration upon condensation which is different for the two isotopic species. Such shifts $\delta\nu = \nu_{gas} - \nu_{liquid}$ are observed spectroscopically and correspond to zero point energy changes. The isotopic difference in $\delta\nu$ for non-polar liquids has been explained (33) as a consequence of changes in van der Waals forces.

The observation of inverse isotope effects, and the explanations that have been put forward to explain them, suggest the importance of

molecular structure as well as isotopic mass. Within the framework of a lattice model of the condensed phase, Johns (34) and Devyatykh (35) derived expressions for the vpie of the form

$$\ell n(P'/P) = f(M,M',\theta,\theta') - \frac{\hbar}{2kT}\Sigma(\delta\nu'-\delta\nu) + \ell n\left(\frac{A'B'C'}{ABC}\right) + \frac{\mu_R'-\mu_R}{RT} \qquad (10)$$

where M, θ, and $\delta\nu$ are the molecular mass, the Debye temperature and the frequency shift on condensation. Equation (10) shows that the vpie is not only a function of mass and zero point energy effects, but also a function of μ_R, the chemical potential due to rotation, and A, B, and C, the principal moments of inertia. Rabinovich (36) has suggested an expression for $\ell n(P'/P)$ that separately accounts for the isotope effects on dispersion, orientation, polarization and association energies.

These efforts all suggest an expression for the vpie containing a T^{-1} term as well as a T^{-2} term, and, in general, this is what is observed experimentally. But if the force field in the liquid state is not known, the vapor pressure isotope effect cannot be quantitatively predicted. However, the use of a simplified model of the condensed phase permits the evaluation of the vpie and a correlation of the isotope effect with molecular and intermolecular forces.

In 1961, Bigeleisen (37) introduced a new formulation of the vpie based on a simple cell model of the condensed phase. The simple cell model assumes that each molecule is entrapped in a potential cage formed by the interactions with its nearest neighbors. Stern,

Van Hook and Wolfsberg (38) compared experimental vapor pressure ratios of mono- and dideutero-ethylenes with values calculated using the simple cell model. The calculated dependence of $\ell n(P'/P)$ on temperature was in good agreement with experiment, as were subsequent calculations performed by Ishida and Bigeleisen (39) on other ethylene isotopes and by Bigeleisen, Cragg and Jeevanandam (40) on methane isotopes. However, Van Hook and others (41,42) have shown that there is poor agreement of cell model calculations with experiment for systems that exhibit molecular association or internal rotation in the condesed phase.

In the simple cell model, the condensed phase is considered to exert a generalized influence on the quantum mechanical behavior of the molecule under study, but to be without structure or defined attachment. This study explores a new, somewhat more realistic model for the condensed phase, in which the medium is considered to be a system of specific mass points, each having a weak, but well-defined interaction with the subject molecule. Interactions with the molecules in the first coordination sphere are treated explicitly as part of the condensed phase system, rather than passively or generally as in the simple cell model. The condensed phase molecule is considered to be at the center of a regular convex polyhedron; the molecules of the first coordination shell are at the vertices. If there are m-1 molecules in the coordination shell, the entire aggregate of molecules is called an m-cluster. This new model, the medium cluster model or MCM, is a natural extension of the simple cell theory.

II. THEORY OF VAPOR PRESSURE ISOTOPE EFFECTS

Medium cluster model calculations of vapor pressure isotope effects are based on the same theoretical foundation as simple cell model calculations. In this chapter, the general theoretical framework and specific assumptions of both models are discussed.

II-1: The Born-Oppenheimer Approximation and Partition Function Ratio

An examination of the effect of molecular structure on the vapor pressure isotope effect begins by considering the Schrödinger equation for the polyatomic molecule under study,

$$\hat{H}\,\psi(x,X) = E\,\psi(x,X) \tag{11}$$

where x and X are used to emphasize the dependence of the total wavefunction ψ on both the electronic and nuclear coordinates. The molecular Hamiltonian is

$$\hat{H} = \frac{-\hbar^2}{2}\Sigma\frac{1}{m_\alpha}\nabla_\alpha^2 - \frac{\hbar^2}{2m}\Sigma\nabla_i^2 + \Sigma\Sigma\frac{z_\alpha z_\beta e^2}{r_{\alpha\beta}} - \Sigma\Sigma\frac{z_\alpha e^2}{r_{i\alpha}} + \Sigma\Sigma\frac{e^2}{r_{ij}} \tag{12}$$

where relativistic effects such as spin-orbit coupling are neglected (43). In Equation (12), α and β are nuclear indices and i and j are electronic indices. Nuclear mass is denoted by m_α and electronic mass by m.

The involved nature of Equation (11) may be simplified a great deal by invoking the Born-Oppenheimer approximation by which the total wavefunction is factored into separate electronic and nuclear parts,

$$\psi(x,X) = \psi_{el}(x,X)\, \psi_{nuc}(X) \tag{13}$$

Within this approximation, Equation (11) can be analyzed as two separate problems,

$$\hat{H}_{el}\, \psi_{el}(x,X) = E_{el}\, \psi_{el}(x,X) \tag{14}$$

and

$$\hat{H}_{nuc} \psi_{nuc}(X) = E\, \psi_{nuc}(X) \tag{15}$$

where the electronic Hamiltonian consists of all but the first and third terms of Equation (12). The electronic energy calculated from Equation (14) together with the internuclear repulsion determine the potential field within which the nuclei move. The force constants of these nuclear motions are defined by this potential field and are thus seen to be independent of nuclear mass since only the first term of Equation (12) involves m_α.

The wavefunction in Equation (15) can be further factored into vibrational, rotational and translational wavefunctions,

$$\psi_{nuc}(X) = \psi_{tr}\, \psi_{rot}\, \psi_{vib} \tag{16}$$

where

$$\psi_{vib} = \prod_{i}^{n} \psi_i \tag{17}$$

for n degrees of vibrational freedom. The energy eigenvalues for non-degenerate vibrational motions are given by

$$\epsilon_i = (v_i + \tfrac{1}{2})h\nu_i \qquad [i = 1,2,\ldots,n] \tag{18}$$

where v_i is the vibrational quantum number for the $i^{\underline{th}}$ mode. Since the total vibrational energy, E_{vib}, is the sum of energies of all vibrational modes, the quantum mechanical partition function, q_{vib}, is given by

$$(q_{vib})_{qm} = \sum_{i=1}^{n}\sum_{v_i=1}^{\infty} \exp \frac{-E(v_i)}{kT} \tag{19}$$

or,

$$(q_{vib})_{qm} = \prod_{i=1}^{n} \frac{e^{-u_i/2}}{1 - e^{-u_i}} \tag{20}$$

where

$$u_i = h\nu_i/kT \tag{21}$$

The classical limit of the quantum mechanical partition function is

$$(q_{vib})_{cl} = \lim_{T\to\infty} (q_{vib})_{qm} = \prod_{i=1}^{n} \frac{1}{u_i} \tag{22}$$

Solution of Equation (15) for the energy eigenvalues of rotational motion of a spherical top molecule gives

$$E_{rot,J} = \frac{h^2}{8\pi^2 I} J(J+1) \qquad [J = 0,1,\ldots] \qquad (23)$$

with a degeneracy factor of $(2J+1)^2$. In Equation (23), I is the principal moment of inertia ($I_x = I_y = I_z$). The quantum mechanical rotational partition function is given by

$$(q_{rot})_{qm} = \frac{1}{s}\sqrt{\frac{\pi}{\sigma^3}}\, e^{\sigma/4} \qquad (24)$$

where s is the symmetry number of the molecule accounting for the invariance of the nuclear Hamiltonian under a rotational transformation and σ is the rotational constant given by

$$\sigma = \frac{h^2}{8\pi^2 I k T} \qquad (25)$$

The classical limit of the rotational partition function is

$$(q_{rot})_{cl} = \lim_{T\to\infty} (q_{rot})_{qm} = \frac{1}{s}\sqrt{\frac{\pi}{\sigma^3}} \qquad (26)$$

The quantum mechanical translational partition function for a polyatomic molecule is the same as that calculated from classical mechanics.

The effect of isotopic substitution on chemical equilibria is made manifest only at lower temperatures. Since the classical partition function represents the high temperature limit of the quantum

mechanical partition function, the appropriate quantity with which to examine the isotope effect is a reduced partition function ratio in which the quantum mechanical effects are evaluated in units of the classical limit (44). The isotopic ratio of the reduced partition functions is defined as

$$\frac{s}{s'}f = \frac{(q/q')_{qm}}{(q/q')_{cl}} \tag{27}$$

In this equation, the primed quantity again refers by convention to the lighter isotope under consideration. The factor s/s' is a classical correction, and is included to account for changes in symmetry number in isotopic exchange reactions.

The reduced partition function ratio may be factored into vibrational, rotational and translational parts. Since the quantum mechanical and classical formulation of the translational partition function is the same, one obtains

$$\frac{s}{s'}f = \frac{s}{s'}f_{vib}f_{rot} \tag{28}$$

Comparison of Equations (24) and (26) shows that

$$f_{rot} = \exp(-\frac{\sigma - \sigma'}{4}) \tag{29}$$

For the molecules considered in this research, however, Equation (29) represents a very small correction (45); classical rotation will be assumed so that

$$\frac{s}{s'}f = \frac{s}{s'}f_{vib} \tag{30}$$

Taking isotopic ratios in Equations (20) and (22) and substituting into the definition of the reduced partition function ratio yields

$$\frac{s}{s'}f = \prod_{i=1}^{n} \frac{\left(\frac{u_i\, e^{-u_i/2}}{1 - e^{-u_i}}\right)}{\left(\frac{u_i'\, e^{-u_i'/2}}{1 - e^{-u_i'}}\right)} \tag{31}$$

II-2: Approximations of the Reduced Partition Function Ratio

In order to facilitate machine calculations of reduced partition function ratios and develop a physical interpretation for the factors involved in isotope effects, several approximations to Equation (31) have been introduced.

The G(u) method was proposed by Bigeleisen and Mayer (44) before the computer era to aid hand calculations. The approximation is given to second order (46) by

$$\ell n \frac{s}{s'}f = \sum_i G(u_i)\, \Delta u_i \left[1 + \frac{S(u_i)}{2G(u_i)}\left(\frac{\Delta u_i}{u_i}\right) + \frac{C(u_i) - 2S(u_i)}{6G(u_i)}\left(\frac{\Delta u_i}{u_i}\right)^2\right] \tag{32}$$

where

$$\Delta u_i = u_i' - u_i \tag{33}$$

$$G(u_i) = \frac{1}{2} - \frac{1}{u_i} + \frac{1}{e^{u_i} - 1} \tag{34}$$

$$S(u_i) = \frac{1}{u_i} - \frac{u_i e^{u_i}}{(e^{u_i} - 1)} \tag{35}$$

$$C(u_i) = \frac{2u_i^2 e^{2u_i}}{(e^{u_i} - 1)^3} - \frac{u_i(u_i + 2)e^{u_i}}{(e^{u_i} - 1)^2} \tag{36}$$

Another approximation method with favorable convergence properties was developed by Bigeleisen (47) and Vojta (48). The method is based on a power series expansion of Equation (31). The vibrational reduced partition function ratio is written as

$$\ell n \frac{s}{s'} f = -\sum_i \ell n \left(\frac{\sinh(u_i/2)}{(u_i/2)} \right) + \sum_i \ell n \left(\frac{\sinh(u_i'/2)}{(u_i'/2)} \right) \tag{37}$$

Expanding the hyperbolic sine as an infinite series yields

$$\ell n \frac{s}{s'} f = -\sum_i^n \sum_j^\infty \ell n \left[1 + \left(\frac{u_i}{2\pi j} \right)^2 \right] + \sum_i^n \sum_j^\infty \ell n \left[1 + \left(\frac{u_i'}{2\pi j} \right)^2 \right] \tag{38}$$

which is absolutely convergent for all values of u_i. Since the Taylor series

$$\ell n(1 + y) = \sum_{k=1}^{\infty} (-1)^{k+1} \left(\frac{y^k}{k} \right) \tag{39}$$

is absolutely convergent when $|y| < 1$, it follows that

$$\ell n \frac{s}{s'} f = -\sum_i^n \sum_k^\infty \sum_j^\infty (-1)^{k+1} k^{-1} \left(\frac{u_i}{2\pi j} \right)^{2k} + \sum_i^n \sum_k^\infty \sum_j^\infty (-1)^{k+1} k^{-1} \left(\frac{u_i'}{2\pi j} \right)^{2k} \tag{40}$$

for $u_i, u_i' < 2\pi$. Since

$$\sum_{\ell=1}^{\infty} \frac{1}{\ell^{2k}} = \frac{2^{k-1}\pi^{2k}B_{2k-1}}{(2k)!} \tag{41}$$

where B_i is the $i^{\underline{th}}$ Bernoulli number, Equation (40) can be written as

$$\ell n \frac{s}{s'}f = \sum_{i=1}^{n}\sum_{k=1}^{\infty} \frac{(-1)^{k+1}B_{2k-1}(\Delta u_i)^{2k}}{2k(2k)!} \quad [u_i, u_i' < 2\pi] \tag{42}$$

where u_i is defined by Equation (33). Since the validity of Equation (42) is limited to cases where $u < 2\pi$, the Bernoulli approximation can only be used for frequencies less than about 1300 cm^{-1} at 300°K.

In an effort to extend the utility of the Bernoulli approximation for the reduced partion function ratio, Bigeleisen and Ishida (49,50) expanded Equation (31) as an orthogonal polynomial series,

$$\ell n \frac{s}{s'}f = \sum_{i=1}^{\infty} W_i \frac{(-1)^{i+1}B_{2i-1}}{2i(2i)!}\sum_{j=1}(\Delta u_j)^{2i} \quad [u_j \leq \infty] \tag{43}$$

where W_i is a modulating coefficient explicitly dependent on the number of modes of vibration and the maximum frequency of vibration (50). The modulating coefficients are defined in such a way as to compensate for errors due to truncation of the series. Equation (43) is valid for all positive values of u_i and is thus applicable to the entire molecular frequency spectrum.

II-3: Statistical Thermodynamics of the Vapor Pressure Isotope Effect

In 1961, Bigeleisen (37) developed a quantitative formulation for

the isotope effect on phase equilibria. Since this theory is basic to the purpose of the present research — the development of the medium cluster model — the Bigeleisen formulation will be described in detail.

An expression for the equilibrium vapor pressure isotope effect is obtained by considering the Gibbs free energy in the gas phase and in the condensed phase. For the gas phase, the free energy, G_g, is given in terms of the canonical partition function, Q_g, by

$$G_g = -kT \ell n\, Q_g + PV_g \tag{44}$$

where V_g is the volume of the gas phase. If the gas behaves ideally, the partition function can be written as

$$Q_g = q^N/N! \tag{45}$$

where q is the molecular partition function. If N, the number of molecules is large, then the factorial in Equation (45) may be approximated by the Stirling formula, so that

$$Q_g \approx \left(\frac{eq}{N}\right)^N \tag{46}$$

The total molecular partition function can be factored,

$$q = q_{trans} q_{rot} q_{vib} q_{elec} = q_{trans} q_{int} \tag{47}$$

where q_{int} contains all internal energy states of rotation, vibration and electronic motion. Equation (46) can then be rewritten as

$$Q_g = \left(\frac{eq_{trans}q_{int}}{N}\right)^N = q_{trans}^N \left(\frac{eq_{int}}{N}\right)^N \tag{48}$$

A quantity $\overline{q}_{int}$ is now defined as

$$\overline{q}_{int} = (eq_{int}/N) \tag{49}$$

so that the canonical gas partition function is then

$$Q_g = q_{trans}^N \overline{q}_{int}^N \tag{50}$$

The translational partition function is evaluated in terms of the classical phase integral, $\int \exp\{-\hat{H}(p,x)/kT\}dp\,dx$, where the potential part of $\hat{H}$, the Hamiltonian, vanishes for the ideal gas. The translational partition function is

$$q_{trans} = \frac{(2\pi mkT)^{3/2} V}{h^3} \tag{51}$$

Substitution of Equations (50) and (51) into Equation (44) yields after expansion and rearrangement,

$$\frac{G_g}{RT} = \ell n\, P - \frac{5}{2}\ell n\, T - \frac{3}{2}\ell n\, M - \ell n\, \overline{q}_{int} + \frac{PV_g}{RT} + K \tag{52}$$

where K is a composite of collected fundamental constants and M is the molecular weight. The introduction of factors to account for small

gas-phase imperfections in the penultimate term of Equation (52) gives

$$\frac{G_g}{RT} = \ell n\, P - \frac{5}{2}\ell n\, T - \frac{3}{2}\ell n\, M - \ell n\, \overline{q}_{int} + (1+B_o P^2+\ldots) + K \qquad (53)$$

where B_o is the second virial coefficient given by the state equation,

$$\frac{PV}{RT} = 1 + B_o P^2 + \ldots \qquad (54)$$

For the condensed phase, the Gibbs free energy can be written in a manner analogous to Equation (44):

$$G_c = -kT\ell n\, Q_c + PV_c \qquad (55)$$

where Q_c is the canonical partition function of the condensed phase and V_c is the condensed phase volume. The condensed phase partition function will be further specified below. The assumption of a simple cell model for the liquid state permits a particularly simple formulation for the canonical condensed phase partition function, and it will be shown in Section II-4 that while Q_c is complex for the medium cluster model, the MCM theory yields a simple expression for the reduced partition function ratio.

Dividing Equation (55) by RT gives

$$\frac{G_c}{RT} = -N^{-1}\ell n\, Q_c + \frac{PV_c}{RT} \qquad (56)$$

At equilibrium, $G_c = G_g$, so that the right sides of Equations (53) and

(57) are equal so that

$$\ell n\, P = \frac{5}{2}\ell n\, T + \frac{3}{2}\ell n\, M + \ell n\, \overline{q}_{int} - (1+B_o P^2+\ldots) - N^{-1}\ell n\, Q_c + \frac{PV_c}{RT} + K \qquad (57)$$

Taking a difference between two isotopic species at a given temperature gives

$$\ell n(P'/P) = \ell n\left(\frac{M'}{M}\right)^{3/2}\left(\frac{\overline{q}_{int}'}{\overline{q}_{int}}\right) + (B_o P^2+\ldots) - (B_o P^2+\ldots)' - N^{-1}\ell n\left(\frac{Q_c'}{Q_c}\right) + \frac{1}{RT}(P'V_c' - PV_c) \qquad (58)$$

From Equations (49) and (51), it can be seen that

$$\overline{q}_{int}'/\overline{q}_{int} = q_{int}'/q_{int} \qquad (59)$$

and

$$q_{int}' M'^{3/2} \Big/ q_{int} M^{3/2} = q'V_g'/qV_g \qquad (60)$$

where q' and q are the complete quantum mechanical partition functions for the gas phase. V_g' and V_g are the molal volumes of the light and heavy isotopic gases. In order to compare the two gas partition functions at the same molal volume, a correction factor

of $\int_V^{V'} (\partial \ell n q'/\partial V)\, dV$ is needed. But

$$\int_{V_g}^{V'_g} (\partial \ell n q'/\partial V_g)_T \, dV_g = \frac{1}{RT} \int_{V_g}^{V'_g} P' \, dV_g \tag{61}$$

so that Equation (58) becomes

$$\begin{aligned} \ell n(P'/P) = \ell n \left(\frac{q'}{q}\right)_{qm} + (B_o P^2 + \ldots) - (B_o P^2 + \ldots) \\ - N^{-1} \ell n \left(\frac{Q'_c}{Q_c}\right)_{qm} + \frac{1}{RT} (P'V'_c - PV_c) + \int_{V_g}^{V'_g} P' dV_g \end{aligned} \tag{62}$$

The effect of isotopy on the second virial coefficient has been examined by Van Hook and others (51,52,53) for a variety of compounds. As expected, the effect is small except for high density gases. While the effect of isotopic substitution on molal volume has been studied for only a few compounds (54,55), Wolfsberg (33) has suggested that, in general, the effect is minimal for non-polar compounds. For the purpose of examining the first-order correlation of medium cluster model calculations with the vpie, both of these effects will be neglected. With the ideal gas approximation, $B'_o = B_o = 0$ and all gases have the same molal volume, so that the bracketed terms in Equation (62) vanish,

$$\ell n(P'/P) = \ell n \left(\frac{q'}{q}\right)_{qm} - N^{-1} \ell n \left(\frac{Q'_c}{Q_c}\right)_{qm} \tag{63}$$

In the high temperature limit, all partition functions can be expressed classically by means of the phase integral. By virtue of the isotopic product rule (62) and Equation (51), the ratio of classical partition functions for the condensed and gas phases are both equal to the ratio of masses and symmetry numbers,

$$\left(\frac{q_g'}{q_g}\right)_{cl} = \frac{s}{s'}\prod\left(\frac{m_i'}{m_i}\right)^{3/2} = \left(\frac{q_c'}{q_c}\right)_{cl} \tag{64}$$

Combining Equation (64) with Equation (63) yields the following expression for the vpie:

$$\ell n(P'/P) = \frac{1}{N}\ell n\left(Q_c/Q_c'\right)_{qm} - \ell n\left(q_c/q_c'\right)_{cl} - \ell n\left(\frac{(q/q')_{qm}}{(q/q')_{cl}}\right)_{gas} \tag{65}$$

The nature of the quantum mechanical partition function ratio for the condensed phase must now be considered.

The simple cell theory (56) assumes that each liquid (or solid) molecule moves within its potential cage independently of the motion of the other molecules in the surrounding medium. An equation analogous to Equation (45) can therefore be written for the condensed phase as

$$Q_c = q_c^N/N! \tag{66}$$

if high communal entropy is postulated so that the cells cannot be "labeled" and the molecules are indistinguishable. If communal entropy is considered to be low and the cells are in fixed positions, the factor 1/N! must be omitted and the canonical partition function for the condensed phase is written as

$$Q_c = q_c^N \tag{67}$$

In either case, the first term of Equation (65) becomes

$$\frac{1}{N} \ell n \left(Q_c / Q_c' \right)_{qm} = \ell n \left(q_c / q_c' \right)_{qm} \tag{68}$$

so that the vpie can be written as

$$\ell n(P'/P) = \ell n \frac{s}{s'} f_c - \ell n \frac{s}{s'} f_g \tag{69}$$

where the reduced partition function ratio as defined by Equation (27) has been used.

II-4: The Medium Cluster Model Partition Function

The medium cluster model developed in the course of this research treats the condensed phase molecule together with its first coordination shell. Since a high degree of ordering and symmetry predominate at short range even in the liquid state, there is no great loss of generality if the central molecule and its

surrounding coordination shell are assumed to form a simply connected regular polyhedron. Once past the nearest neighbor shell, some dislocation and disorder is expected, but the assumption of perfect regularity in any small neighborhood is quite realistic (57).

In the medium cluster model, the liquid phase is considered as an assembly of independent clusters with m molecules each. If the clusters are indistinguishable, the condensed phase partition function can be written as

$$Q_c = \frac{q_{cluster}^{N/m}}{(N/m)!} \tag{70}$$

since there are N/m such clusters in a condensed phase system of N total molecules. In Equation (70), $q_{cluster}$ is the complete quantum mechanical "supermolecular" partition function. Each cluster consists of one molecule in a central position in the aggregate and m-1 indistinguishable shell molecules in the first coordination sphere. Using $q_{central}$ and q_{shell} for the molecular partition functions of each type, the cluster partition function may be expressed as

$$q_{cluster} = \frac{q_{shell}^{m-1}}{(m-1)!} \cdot q_{central} \tag{71}$$

Within the context of the medium cluster model, the condensed

phase canonical partition function is therefore given by

$$Q_c = \frac{\left[\frac{q_{shell}^{m-1}}{(m-1)!} \cdot q_{central}\right]^{N/m}}{(N/m)!} \tag{72}$$

If N/m, the number of clusters in the liquid phase, is large, the Stirling approximation can be used so that

$$Q_c = \left[\frac{e\, q_{shell}^{m-1}\, q_{central}}{(m-1)!\ N/m}\right]^{N/m} \tag{73}$$

In general, for an equilibrium system $A \rightleftharpoons B$,

$$\frac{N_A}{N_B} = \frac{q_A}{q_B} \tag{74}$$

where N_A and N_B are the number of each species A and B. Since the shell molecules are considered to be in equilibrium with the central molecules in the medium cluster model,

$$\frac{1}{m-1} = \frac{q_{central}}{q_{shell}} \tag{75}$$

Solving Equation (75) for q_{shell} and substituting in Equation (73),

the condensed phase partition function becomes

$$Q_c = \left(\frac{e(m-1)^{m-1} q_{central}^{m-1} q_{central}}{(m-1)!\ N/m} \right)^{N/m} = \left(\frac{e^{1/m}(m-1)^{\frac{m-1}{m}}\ q_{central}}{[(m-1)!]^{1/m}\ (\frac{N}{m})^{1/m}} \right)^{N} \qquad (76)$$

In the evaluation of the vapor pressure isotope effect using the medium cluster model, the isotopic pairs considered will always be assumed to be in clusters of the same size in the liquid phase. Using Equation (76), the first term in Equation (65) becomes

$$\frac{1}{N} \ell n \left(Q_c / Q_c' \right)_{qm} = \ell n \left(q_{central} / q'_{central} \right)_{qm} \qquad (77)$$

The MCM form of the vpie equation is then

$$\ell n(P'/P) = \ell n \frac{s}{s'} f_{central} - \ell n \frac{s}{s'} f_{gas} \qquad (78)$$

Equation (78) suggests that an evaluation of the vapor pressure isotope effect may be made by considering the central molecule of the cluster as being representative of the entire liquid phase.

II-5: Separation of Internal and External Vibrational Modes

The similarity of Equations (69) and (78) shows that a correspondence exists between the simple cell model and the medium cluster model within the context of the vpie. In order to determine

$\ell n(P'/P)$, both models require an evaluation of the reduced partition function ratio. Using the vibrational reduced partition function ratio as given by Equation (31), the vpie is given for both models as

$$\ell n \frac{P'}{P} = \ell n \prod_{i=1}^{n_c} \left(\frac{u_i e^{-u_i/2}(1-e^{-u_i'})}{u_i' e^{-u_i'/2}(1-e^{-u_i})} \right)_c - \ell n \prod_{i=1}^{n} \left(\frac{u_i e^{-u_i/2}(1-e^{-u_i'})}{u_i' e^{-u_i'/2}(1-e^{-u_i})} \right)_g \quad (79)$$

where the first term extends over all modes of vibration of an independent molecule in the condensed phase (for the simple cell model) or over all modes of vibration for the central molecule of an aggregate (for the medium cluster model). The second term includes all modes of vibration for an independent gas-phase molecule. In general, the number of degrees of vibrational freedom for a condensed phase molecule, n_c, is equal to 3N, where N is the number of atoms in the molecule. In the gas phase, n is 3N-6 (or 3N-5 for linear molecules) since the molecule can rotate and translate freely.

Expanding Equation (79) gives

$$\ell n(P'/P) = \sum^{n_c} \left(\frac{u_i'}{2} - \frac{u_i}{2} \right)_c + \sum^{n_c} \ell n \left(\frac{u_i(1-e^{-u_i'})}{u_i'(1-e^{-u_i})} \right)_c$$

$$- \sum^{n} \left(\frac{u_i'}{2} - \frac{u_i}{2} \right)_g - \sum^{n} \ell n \left(\frac{u_i(1-e^{-u_i'})}{u_i'(1-e^{-u_i})} \right)_g \quad (80)$$

The n_c vibrational modes of a condensed phase molecule consist of six low-frequency external modes and n high-frequency internal modes. Therefore,

$$\ell n(P'/P) = \sum^{n}\left(\frac{u_i'}{2} - \frac{u_i}{2}\right)_c + \sum^{6}\left(\frac{u_i'}{2} - \frac{u_i}{2}\right)_c + \sum^{n} \ell n\left(\frac{u_i(1-e^{-u_i'})}{u_i'(1-e^{-u_i})}\right)_c + \sum^{6} \ell n\left(\frac{u_i(1-e^{-u_i'})}{u_i'(1-e^{-u_i})}\right)_c - \sum^{n}\left(\frac{u_i'}{2} - \frac{u_i}{2}\right)_g - \sum^{n} \ell n\left(\frac{u_i(1-e^{-u_i'})}{u_i'(1-e^{-u_i})}\right)_g \tag{81}$$

$$= \text{I} + \text{II} + \text{III} + \text{IV} + \text{V} + \text{VI}$$

Since all n internal frequencies are large for both the gas and the liquid phase, terms III and VI are respectively negligible compared to II and V. Terms II and IV can be combined as can terms I and V to give

$$\ell n(P'/P) = \sum_{i=1}^{6} \ell n\left(\frac{u_i e^{-u_i/2}(1-e^{-u_i'})}{u_i e^{-u_i'/2}(1-e^{-u_i})}\right)_c - \sum_{i=1}^{n}\left[\left(\frac{u_i'}{2} - \frac{u_i}{2}\right)_g - \left(\frac{u_i'}{2} - \frac{u_i}{2}\right)_c\right] \tag{82}$$

The first term on the right side of Equation (82) is recognized as

the reduced partition function ratio for external modes only, $\ell n \frac{s}{s'} f_{ext}$. Since all external frequencies are small ($u_{ext} \ll 2\pi$), the one-term Bernoulli series approximation of $\ell n \frac{s}{s'} f_{ext}$ can be employed. Using Equation (42), the vpie expression becomes

$$\ell n \frac{P'}{P} = \frac{1}{24} \sum_{i=1}^{6} (u_i'^2 - u_i^2)_c - \sum_{i=1}^{n} \{(\frac{u_i'}{2} - \frac{u_i}{2})_g - (\frac{u_i'}{2} - \frac{u_i}{2})_c\} \quad (83)$$

Recalling the definition of u_i from Equation (21) gives

$$\ell n \frac{P'}{P} = \frac{1}{24} (\frac{h}{kT})^2 \sum_{ext}^{6} (\nu_i'^2 - \nu_i^2)_c - (\frac{h}{2kT}) \sum_{int}^{3N-6} \{(\nu_i'^2 - \nu_i^2)_g - (\nu_i'^2 - \nu_i^2)_c\} \quad (84)$$

where the summation indices int and ext have been added to emphasize the nature of the frequencies considered in each term and n has been explicitly indicated.

Equation (84) has the overall form

$$\ell n(P'/P) = \frac{A}{T^2} - \frac{B}{T} \quad (85)$$

which is observed experimentally for many systems (58,59). With respect to both the simple cell model and the medium cluster model, the B factor relates the isotopic difference in zero-point energy shifts on condensation. B is a function of internal modes of vib-

ration only:

$$B = \left(\frac{h}{2k}\right) \sum_{i=1}^{3N-6} \left\{(\nu_i' - \nu_i)_{gas} - (\nu_i' - \nu_i)_{central}\right\} \qquad (86)$$

The A factor is a function of the low-frequency external modes of vibration in the condensed phase:

$$A = \left(\frac{h^2}{24k^2}\right) \sum_{}^{6} (\nu_i'^2 - \nu_i^2)_{central} \qquad (87)$$

While the simple cell model considers three equal translational and three equal rotational contributions to A for spherical top molecules such as methane, the MCM formalism requires the consideration of more specific, and not necessarily equal, interactions.

This study is an attempt to correlate medium cluster model force fields in the liquid state with the vpie via the A and B factors. The frequencies of vibration used in Equations (86) and (87) have been computed by means of normal coordinate analysis.

III. NORMAL COORDINATE ANALYSIS

While there has been some recent interest in corrections to the Born-Oppenheimer approximation (60,61), the general validity of this approximation, as outlined in Section II-1, has been assumed throughout the course of this study. Within the framework of the Born-Oppenheimer approximation, isotope effects are seen to result from the motion of nuclei of different mass on the same potential energy surface. This implies the necessity of isotope independent force fields in the condensed and gaseous phases from which the frequencies of molecular vibration in Equation (84) can be calculated. Because the shift in frequency due to isotopic replacement is small, and because the vibrational partition function is sensitive to such shifts, large errors would be introduced by the direct substitution of experimental spectroscopic frequencies into Equations (86) and (87).

In this chapter, an outline is given of the method by which vibrational frequencies are calculated from the molecular force field. This methodology of normal coordinate analysis provides the basis for the correlation of the vapor pressure isotope effect with structure and forces in the liquid state. The discussion follows the more detailed treatments given by Wilson, Decius and Cross (62) and Herzberg (63).

III-1. The Potential and Kinetic Energies of a Vibrating System

The internal configuration for an isolated system of N oscillators can be defined by 3N-6 coordinates (3N-5 for a linear system). Thus, for example, the configuration of a bent triatomic molecule ABC is completely determined by the AB distance, the BC distance, and the ABC angle. Such distances and angles are called internal coordinates and define the relative arrangement of atoms within the molecule, but say nothing about the orientation of the entire molecule in space. The three coordinates mentioned above in connection with the ABC molecule are not unique; the AC distance could be substituted for the ABC angle. In general, a set of internal coordinates can be ascribed to any system of oscillating masses which is both complete (that is, sufficient to describe all vibrational degrees of freedom) and linearly independent (64).

For a system with a complete set of n coordinates $s_1, s_2, \ldots, s_n$, where n may be 3N, 3N-5, or 3N-6, the potential energy V can be expressed as an n-dimensional Taylor expansion,

$$V = V_o + \sum_i^n \left(\frac{\partial V}{\partial s_i}\right)_o s_i + \frac{1}{2!} \sum_i^n \sum_j^n \left(\frac{\partial^2 V}{\partial s_i \partial s_j}\right)_o s_i s_j + \ldots \qquad (88)$$

The subscript o indicates a value taken for the equilibrium configuration; V_o is taken to be zero. Further, $\partial V/\partial s = 0$ at the minimum of the interatomic potential surface so that

$$V = \frac{1}{2!}\sum_{i}^{n}\sum_{j}^{n}\left(\frac{\partial^2 V}{\partial s_i \partial s_j}\right)s_i s_j + \frac{1}{3!}\sum_{i}^{n}\sum_{j}^{n}\sum_{k}^{n}\left(\frac{\partial^3 V}{\partial s_i \partial s_j \partial s_k}\right)s_i s_j s_k + \cdots \quad (89)$$

As the molecule is displaced very far from its equilibrium atomic configuration, the anharmonic cubic, quartic, and higher order terms of Equation (89) become significant. If relatively small amplitudes of vibration are assumed, however, Equation (89) becomes a harmonic potential,

$$2V = \sum_{i}^{n}\sum_{j}^{n} f_{ij} s_i s_j \quad (90)$$

where

$$f_{ij} = \left(\frac{\partial^2 V}{\partial s_i \partial s_j}\right)_o \quad (91)$$

These force constants f_{ij} can be arranged in matrix form,

$$\underset{\sim}{F} = \{f_{ij}\} \quad (92)$$

where $f_{ij}=f_{ji}$, so that there can be up to $n(n+1)/2$ independent elements in the array. Equation (90) can be written in matrix notation as

$$2V = \underset{\sim}{S}^{\dagger}\underset{\sim}{F}\underset{\sim}{S} \quad (93)$$

where $\underset{\sim}{S}$ is a column matrix of internal coordinates.

The kinetic energy of a system of N coupled oscillators is given by

$$T = \tfrac{1}{2}\sum_{i}^{3N} m_i \xi_i^2 \tag{94}$$

where ξ_i is the time derivative of the $i^{\underline{th}}$ Cartesian displacement coordinate

$$\xi_i = x_i - x_i^o \tag{95}$$

and m_i is the mass associated with the $i^{\underline{th}}$ coordinate. If the internal coordinates, s_k, are given in terms of the Cartesian coordinates, x_i, by the linear relation

$$s_k = \sum_{i}^{3N} b_{ki} x_i \tag{96}$$

then it can be shown (65) that

$$2T = \sum_{k}^{n}\sum_{\ell}^{n} (g_{k\ell})^{-1} s_k s_\ell \tag{97}$$

or, in matrix notation,

$$2T = \dot{\underset{\sim}{S}}^{\dagger} \underset{\sim}{G}^{-1} \dot{\underset{\sim}{S}} \tag{98}$$

where

$$g_{k\ell} = \sum_{i}^{3N} \frac{1}{m_i} b_{ki} b_{\ell i} \tag{99}$$

The array of $g_{k\ell}$ elements, $\underset{\sim}{G}$, is defined analogously to $\underset{\sim}{F}$ in Equation (92). $\underset{\sim}{G}$ is also symmetric, $g_{k\ell}=g_{\ell k}$. The quantities b_{ij} in Equations (96) and (99) are elements of a matrix $\underset{\sim}{B}$, which is the transformation matrix from Cartesian coordinates to internal coordinates:

$$\underset{\sim}{S} = \underset{\sim}{B}\underset{\sim}{X} \tag{100}$$

where $\underset{\sim}{S}$ and $\underset{\sim}{X}$ are column matrices of internal and Cartesian coordinates respectively. Each of the N atoms in the coupled system contributes one term in each of the three Cartesian directions in Equation (99) so that

$$g_{k\ell} = \sum_{i}^{N} \frac{1}{m_i} (b_{ki_x} b_{\ell i_x} + b_{ki_y} b_{\ell i_y} + b_{ki_z} b_{\ell i_z}) \tag{101}$$

or,

$$g_{k\ell} = \sum_{i}^{N} \mu_i (\vec{\zeta}_{ki} \cdot \vec{\zeta}_{\ell i}) \tag{102}$$

where μ_i is the reciprocal mass of the $i^{\underline{th}}$ atom and the vector $\vec{\zeta}_{ki}$ represents the $i^{\underline{th}}$ atom's contribution to the $k^{\underline{th}}$ internal coordinate, s_k (62). After internal coordinates have been defined, the $\vec{\zeta}$-vectors may be calculated from the relative positions of the N atoms of the system. Together with atomic masses, the $\vec{\zeta}$-vectors thus define the $\underset{\sim}{G}$-matrix.

As an example of the way in which coordinate definitions may be transformed into a matrix of real numbers, consider a linear triatomic molecule ABC with two internal coordinates consisting of an AB stretch and a BC stretch; the remaining two angle coordinates need not be considered. Then,

$$\begin{aligned} \Delta r_{AB} &= s_1 = -x_A + x_B \\ \Delta r_{BC} &= s_2 = - x_B + x_C \end{aligned} \tag{103}$$

where x_A, x_B, and x_C are positive Cartesian displacements of each of the atoms in the same direction. From Equation (100),

$$B = \begin{pmatrix} -1 & 1 & 0 \\ 0 & -1 & 1 \end{pmatrix} \tag{104}$$

so that from Equations (101) and (104) the elements of $\underset{\sim}{G}$ are

$$g_{11} = \mu_A(-1)(-1)+\mu_B(+1)(+1)+\mu_C(0)(0) = \mu_A + \mu_B$$

$$g_{12} = \mu_A(0)(-1)+\mu_B(-1)(+1)+\mu_C(0)(+1) = -\mu_B \qquad (105)$$

$$g_{22} = \mu_A(0)(0)+\mu_B(-1)(-1)+\mu_C(+1)(+1) = \mu_A + \mu_B$$

Since $g_{12}=g_{21}$, the 2x2 $\underset{\sim}{G}$-matrix is thus fully determined. In practice, generalized $\underset{\sim}{G}$-matrix elements are tabulated for the most commonly used coordinates (62).

III-2. The Secular Equation and Normal Coordinates

By considering the equation of motion for the atoms of a molecule, a relation can be derived between the force field and the frequencies of vibration. Legrange's equation of motion,

$$\frac{d}{dt}\left(\frac{\partial T}{\partial \dot{s}_i}\right) + \left(\frac{\partial V}{\partial s_i}\right) = 0 \qquad (106)$$

is applied to Equations (90) and (97):

$$\sum_j g_{ij}^{-1} \ddot{s}_j + \sum_j f_{ij} s_j = 0 \quad [i = 1,2,\ldots,n] \qquad (107)$$

It is assumed that the atoms oscillate in unison with a periodic motion. Thus a reasonable solution of Equation (107) would have the form

$$s_j = A_j \sin(2\pi\nu t) \qquad [i = 1,2,\ldots,n] \tag{108}$$

Substituting this into Equation (107) gives

$$\sum_{j=1}^{n} (f_{ij} - \lambda g_{ij}^{-1}) A_j = 0 \qquad [i = 1,2,\ldots,n] \tag{109}$$

where

$$\lambda = 4\pi^2\nu^2 \tag{110}$$

and A_j is the amplitude of the $j^{\underline{th}}$ mode of vibration. For a non-trivial solution of the set of simultaneous linear equations (109) to exist, the determinant of coefficients of A_j must equal zero; that is

$$|\underset{\sim}{F} - \lambda \underset{\sim}{G}^{-1}| = 0 \tag{111}$$

which is equivalent to

$$|\underset{\sim}{G}\underset{\sim}{F} - \lambda \underset{\sim}{E}| = 0 \tag{112}$$

where $\underset{\sim}{E}$ is the unit matrix. Equation (112) is called the secular equation and provides the sought-after relationship between the molecular force field ($\underset{\sim}{F}$) and the frequencies of vibration from

which the reduced partition function ratio may be calculated. The secular equation is also written as

$$|\underset{\sim}{H} - \lambda \underset{\sim}{E}| = 0 \tag{113}$$

where

$$\underset{\sim}{H} = \underset{\sim}{F}\underset{\sim}{G} \tag{114}$$

In general, $\underset{\sim}{H}$ is not symmetric.

Equation (112) may be solved by direct expansion of the determinant to give a polynomial characteristic equation of the form

$$\lambda^n + c_1\lambda^{n-1} + c_2\lambda^{n-2} + \ldots + c_{n-1}\lambda + c_n = 0 \tag{115}$$

where the coefficients c_i are functions of $\underset{\sim}{F}$ and $\underset{\sim}{G}$ (66). If the secular equation is of low order (say, $n<5$), a direct analytical evaluation of Equation (115) might be the best method for finding the frequency parameters from $\underset{\sim}{F}$ and $\underset{\sim}{G}$. The gas-phase problem for even a small molecule like methane, however, involves a characteristic equation of order 10, and the liquid-phase problem for methane within the framework of the medium cluster model will be seen to involve up to 202 coordinates. An iterative process will be more satisfactory to solve the secular equation for these and similar cases. There are a number of efficient iterative algorithms avail-

able employing matrix diagonalization. The procedure used in this research will be discussed in Section IV-4.

A new set of coordinates $\underset{\sim}{Q} = \{q_i\}$, called normal coordinates, is introduced as a linear combination of internal coordinates,

$$\underset{\sim}{Q} = \underset{\sim}{L}^{-1}\underset{\sim}{S} \tag{116}$$

where $\underset{\sim}{L}^{-1}$ transforms the internal coordinates, s_i, to normal coordinates, q_i. Rearrangement of Equation (116) yields

$$\underset{\sim}{S} = \underset{\sim}{L}\underset{\sim}{Q} \tag{117}$$

The elements of $\underset{\sim}{L}$ are chosen so that in terms of the normal coordinates, the potential and kinetic energies have the form

$$2V = \underset{\sim}{Q}^{\dagger}\underset{\sim}{\Lambda}\underset{\sim}{Q} \tag{118}$$

and

$$2T = \dot{\underset{\sim}{Q}}^{\dagger}\dot{\underset{\sim}{Q}} \tag{119}$$

where $\underset{\sim}{\Lambda}$ is a diagonal matrix. Substitution of Equation (117) into Equations (93) and (98) and comparison with Equations (118) and (119) shows that

$$\underset{\sim}{L}^{\dagger}\underset{\sim}{F}\underset{\sim}{L} = \underset{\sim}{\Lambda} \tag{120}$$

and

$$\underset{\sim}{L}^{\dagger}\underset{\sim}{G}^{-1}\underset{\sim}{L} = \underset{\sim}{E} \tag{121}$$

Combination of Equations (120) and (121) gives

$$\underset{\sim}{L}^{\dagger}\underset{\sim}{G}\underset{\sim}{F}\underset{\sim}{L} = \underset{\sim}{L}^{\dagger}\underset{\sim}{H}\underset{\sim}{L} = \underset{\sim}{\Lambda} \tag{122}$$

The roots, or eigenvalues, of the secular equation are invarient under a similarity transformation (67). The transformed $\underset{\sim}{H}$ of Equation (122) can therefore be substituted into the secular equation, so that in terms of normal coordinates, Equation (112) has the form

$$\underset{\sim}{\Lambda} - \lambda\underset{\sim}{E} = 0 \tag{123}$$

Therefore, the elements of $\underset{\sim}{\Lambda}$ (a diagonal matrix) are the frequency parameters, λ_i, defined by Equation (110).

III-3: Contribution of Internal Coordinates to Normal Coordinates

Solution of the secular equation by simultaneous diagonalization of the $\underset{\sim}{F}$ and $\underset{\sim}{G}$ matrices, as in Equations(120) and (121), defines the $\underset{\sim}{L}$-matrix. The normal coordinates are related to the internal

coordinates through Equation (116). For a molecule with n degrees of vibrational freedom, expansion of Equation (116) gives

$$\begin{aligned} q_1 &= \ell_{11}^{-1}s_1 + \ell_{12}^{-1}s_2 + \ldots + \ell_{1n}^{-1}s_n \\ q_2 &= \ell_{21}^{-1}s_1 + \ell_{22}^{-1}s_2 + \ldots + \ell_{2n}^{-1}s_n \\ &\vdots \\ q_n &= \ell_{n1}^{-1}s_1 + \ell_{n2}^{-1}s_2 \qquad\quad + \ell_{nn}^{-1}s_n \end{aligned} \tag{124}$$

where the ℓ_{ij}^{-1} are elements of the $\underset{\sim}{L}^{-1}$ transformation matrix. For a normal mode of vibration in which the normal coordinate q_k changes with a frequency ν_k, all the internal coordinates involved change with the same frequency. However, the amplitude of each internal coordinate is different; the relative amplitudes of the various internal coordinates are given by

$$\frac{s_1}{\ell_{k1}^{-1}} = \frac{s_2}{\ell_{k2}^{-1}} = \ldots = \frac{s_n}{\ell_{kn}^{-1}} \tag{125}$$

The normal modes may be visualized as a superposition of internal coordinate contributions. The relative amplitudes, ℓ_{ij}^{-1}, can be evaluated (68) from the relations obtained by expanding Equation (122):

$$
\begin{aligned}
&(\Sigma f_{1t}g_{t1} - \lambda_k)\ell_{k1}^{-1} + (\Sigma f_{1t}g_{t2})\ell_{k2}^{-1} + \ldots + (\Sigma f_{1t}g_{tn})\ell_{kn}^{-1} = 0 \\
&(\Sigma f_{2t}g_{t1})\ell_{k1}^{-1} + (\Sigma f_{2t}g_{t2} - \lambda_k)\ell_{k2}^{-1} + \ldots + (\Sigma f_{2t}g_{tn})\ell_{kn}^{-1} = 0 \\
&\quad\vdots \\
&(\Sigma f_{nt}g_{t1})\ell_{k1}^{-1} + (\Sigma f_{nt}g_{t2})\ell_{k2}^{-1} + \ldots + (\Sigma f_{nt}g_{tn} - \lambda_k)\ell_{kn}^{-1} = 0
\end{aligned}
\tag{126}
$$

where the summations are over the index t. If one ℓ_{ki}^{-1} is relatively large compared to all other ℓ_{kj}^{-1} $(i \neq j)$, the $k^{\underline{th}}$ normal vibrational mode can be characterized as being due to displacement of the $i^{\underline{th}}$ internal coordinate alone. If there are two large ℓ_{ki}^{-1} of similar magnitude in the $k^{\underline{th}}$ eigenvector, one can say that the vibration is a mixture of the two internal coordinates involved. In Section IV-5, a detailed discussion will be given of the procedure used in this research to identify vibrational modes that must be included in the reduced partition function ratio.

Another method by which the contribution of each internal coordinate to the $k^{\underline{th}}$ normal mode can be evaluated is to consider the potential energy distribution for a given normal coordinate (69,70). Substitution of the expanded form of Equation (117) into Equation (90) gives

$$
2V = \sum_{t}^{n}\sum_{j>i}^{n}\sum_{i}^{n} f_{ij}\ell_{it}\ell_{jt}q_t^2 \tag{127}
$$

so that for a given mode q_k, the contribution to the total potential energy is

$$(2V)_k = q_k^2 \sum_{j>i}^{n} \sum_{i}^{n} f_{ij} \ell_{ik} \ell_{jk} \tag{128}$$

While Equation (128) is an important and useful relationship for the interpretation of molecular vibrations, it cannot be used for an analysis of condensed phase vibrations because, as is shown by Equation (78), only oscillations of the central molecular part of an m-cluster are considered in the MCM theory as contributing to the liquid-phase reduced partition function ratio.

III-4: The Potential Energy Matrix

In Equations (88) and (89), it was assumed that the potential energy, V, could be expanded as a power series of nuclear displacement coordinates. For small displacements from equilibrium, only the quadratic terms need to be considered. A physical interpretation of the force constants, f_{ij}, appearing in Equation (90) will now be given (62,71).

The diagonal elements of the $\underset{\sim}{F}$-matrix, f_{ii}, are primary force constants; a given f_{ii} is the restoring force in coordinate i caused by unit displacement of that coordinate while keeping all others fixed at their equilibrium positions. If i is a bond length, then f_{ii} is a measure of bond strength (72); if i is a bond angle, then f_{ii} is a measure of the directional forces maintaining the equilibrium configuration of that angle. As a rule, diagonal

force constants are positive quantities.

An interpretation of the off-diagonal elements of the $\underset{\sim}{F}$-matrix is more complex (63,73,74). In order to examine the meaning of an off-diagonal force constant, say $f_{\ell k}$, the right side of Equation (90) may be expanded and like terms collected to give

$$2V = f_{kk}s_k^2 + \sum_{i\neq k}^{n} f_{ii}s_i^2 + 2\sum_{i\neq k}^{n} f_{ik}s_i s_k + 2\sum_{\substack{j\neq k \\ j>i}}^{n}\sum_{i\neq k}^{n} f_{ij}s_i s_j \qquad (129)$$

where the first two terms contain only diagonal force constants with one coordinate k explicitly singled out, and the third term contains only off-diagonal elements of $\underset{\sim}{F}$ on the same row as the singled-out $k^{\underline{th}}$ diagonal term. The last expression in Equation (129) contains all other off-diagonal force constants.

If coordinate k is constrained to a displacement value of $s_k = +1$, the potential energy becomes

$$2V = f_{kk} + \sum_{i\neq k}^{n} f_{ii}s_i^2 + 2\sum_{i\neq k}^{n} f_{ik}s_i + 2\sum_{\substack{j\neq k \\ j>i}}^{n}\sum_{i\neq k}^{n} f_{ij}s_i s_j \qquad (130)$$

As coordinate k is held to its displaced position, the total electronic configuration changes and other coordinates become displaced so as to minimize V. At this new minimum, differentia-

tion with respect to one of the other coordinate displacements, s_ℓ ($\ell \neq k$), gives

$$\left(\frac{\partial V}{\partial s_\ell}\right)_k = 2f_{\ell\ell}s_\ell + 2f_{\ell k} + 2\sum_{i\neq k,\ell}^{n} f_{\ell i}s_i = 0 \qquad (131)$$

In general, primary force constants are larger than off-diagonal constants, so that for small displacements, $f_{\ell\ell}s_\ell \gg f_{\ell i}s_i$, and to a first approximation, the last term of Equation (131) can be neglected. Then,

$$f_{\ell k} \approx -f_{\ell\ell}s_\ell \qquad (132)$$

where s_ℓ is the displacement of coordinate ℓ which would minimize the potential after unit displacement of coordinate k. Equation (132) shows that $f_{\ell k}$ can be interpreted as an interaction constant: if $f_{\ell k}$ is a positive quantity, then positive displacement of coordinate k implies a "stiffening" of coordinate ℓ (62,75).

There is a major difficulty that arises in the determination of a useful F-matrix that will reproduce the observed spectroscopic frequencies of a molecular system. While complete sets of experimental vibrational frequencies may be available, there are often two or more sets of force constants which are equally compatable with observed spectroscopic data; i.e., there is

more than one $\underset{\sim}{F}$ which satisfies Equation (112) for a given set of λ_i (76). Recent attempts have also been made to compute harmonic force constants directly from wavefunctions based on SCF-MO-LCAO approximations to closed-shell ground states (77,78); reliable ab initio quantum mechanical calculations of $\underset{\sim}{F}$ have been performed for a few small polyatomic molecules (79-82). However, in this research, concern is focused, not on a "true" $\underset{\sim}{F}$-matrix, but on a consistent and physically reasonable force field with which the vapor pressure isotope effect can be correlated to the parameters of the liquid-phase medium cluster model.

III-5: The Internal Coordinates and Potential Function for Methane

Although there are always n linearly independent coordinates for a molecule with n degrees of freedom, it is customary to use redundant coordinates so as to retain symmetry in a normal coordinate analysis problem (62). For this reason, methane, with 9 degrees of vibrational freedom, will be described by 10 internal coordinates as shown in Figure 1. The atoms and coordinates are numbered to conform with the labels to be used in MCM calculations. The displacement coordinates consist of four CH bond stretches: Δr_1, Δr_2, Δr_3, Δr_4, and six HCH valence angle bends: $\Delta\alpha_1$, $\Delta\alpha_2$, $\Delta\alpha_3$, $\Delta\alpha_4$, $\Delta\alpha_5$, $\Delta\alpha_6$. A redundancy exists among the angular coordinates. Since the six bond angles together subtend a full 4π steradians, when the angles change from their equilibrium value, the sum of the displacements must equal zero,

$$\sum_{i=1}^{6} \Delta\alpha_i = 0 \qquad (133)$$

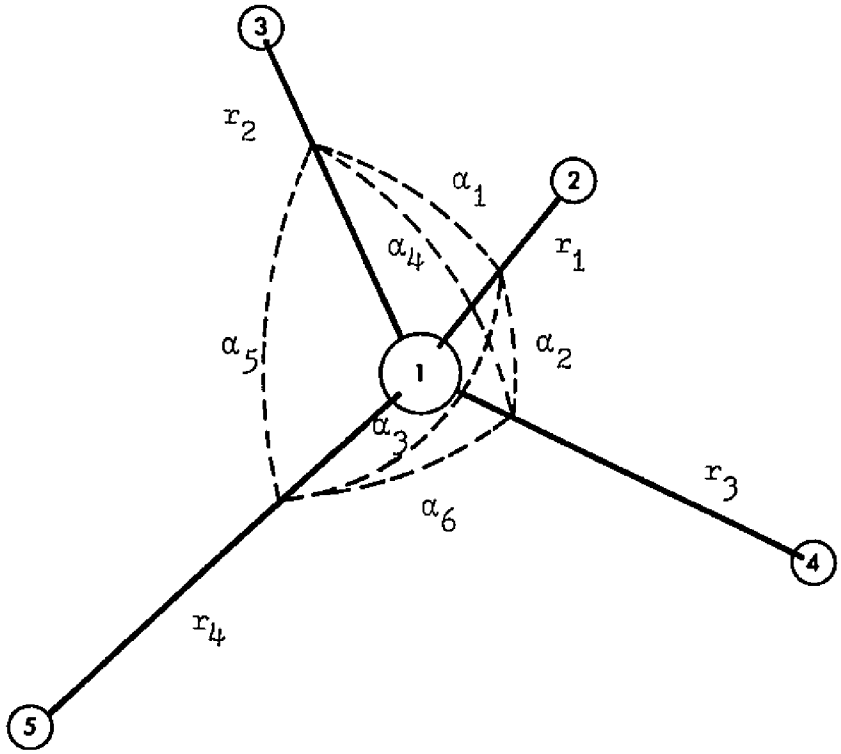

Figure 1. Internal coordinates of methane.

It was stated in Section II-1 that the linear terms $(\partial V/\partial s_i)$ of the expanded potential function vanish at equilibrium. While this description of the potential hypersurface is only valid if the coordinates are independent, it is nevertheless still possible to express the potential energy in quadratic form for systems including redundant coordinates (62,83). The general quadratic potential function for methane, obtained from Equation (90), is

$$
\begin{aligned}
2V = {} & f_r \sum_{i=1}^{4} r_i^2 + 2f_{rr} \sum_{j>i}^{4} \sum_{i=1}^{4} r_i r_j + f_\alpha \sum_{i=1}^{6} \alpha_i^2 \\
& + 2f'_{\alpha\alpha} \sum_{\substack{j>i \\ j+i=7}}^{6} \sum_{i=1}^{6} \alpha_i \alpha_j + 2f''_{\alpha\alpha} \sum_{\substack{j>i \\ j+i\neq 7}}^{6} \sum_{i=1}^{6} \alpha_i \alpha_j \\
& + 2f'_{r\alpha}[r_1(\alpha_1+\alpha_2+\alpha_3) + r_2(\alpha_1+\alpha_4+\alpha_5) \\
& \qquad + r_3(\alpha_2+\alpha_4+\alpha_6) + r_4(\alpha_3+\alpha_5+\alpha_6)] \\
& + 2f''_{r\alpha}[r_1(\alpha_4+\alpha_5+\alpha_6) + r_2(\alpha_2+\alpha_3+\alpha_6) \\
& \qquad + r_3(\alpha_1+\alpha_3+\alpha_5) + r_4(\alpha_1+\alpha_2+\alpha_4)]
\end{aligned}
\tag{134}
$$

where f_r is the primary stretching force constant, f_α is the primary bending force constant, and f_{rr} is the interaction force constant between two carbon-hydrogen stretches. The quantities

$f'_{r\alpha}$ and $f''_{r\alpha}$ are interaction force constants of CH_i stretches respectively with adjacent H_iCH_j and non-adjacent H_jCH_K angle bends; $f'_{\alpha\alpha}$ and $f''_{\alpha\alpha}$ are interaction force constants of H_iCH_j angle bends respectively with adjacent H_iCH_K and non-adjacent H_KCH_ℓ angle bends.

The expression for the potential energy of methane in terms of bond length displacements r_i $(=\Delta r_i)$ and bond angle displacements α_i $(=\Delta\alpha_i)$ can be simplified by considering the redundancy of internal coordinates. The first-order redundancy condition is given by Equation (133). A second-order redundancy formula is obtained by taking the square of both sides of Equation (133) and collecting like terms,

$$\left(\sum_{i=1}^{6}\alpha_i\right)^2 = \sum_{i=1}^{6}\alpha_i^2 + 2\sum_{\substack{j>i\\ i+j=7}}^{6}\sum_{i=1}^{6}\alpha_i\alpha_j + 2\sum_{\substack{j>i\\ i+j\neq 7}}^{6}\sum_{i=1}^{6}\alpha_i\alpha_j = 0 \quad (135)$$

Substituting Equations (133) and (135) into Equation (134) and combining similar terms gives

$$\begin{aligned} 2V = {} & f_r\sum_{i=1}^{4}r_i^2 + 2f_{rr}\sum_{j>i}^{4}\sum_{i=1}^{4}r_ir_j + (f_\alpha - f''_{\alpha\alpha})\sum_{i=1}^{6}\alpha_i^2 \\ & + (f'_{\alpha\alpha} - f''_{\alpha\alpha})\sum_{\substack{j>i\\ i+j=7}}^{6}\sum_{i=1}^{6}\alpha_i\alpha_j + 2(f'_{r\alpha} - f''_{r\alpha})[r_1(\alpha_1+\alpha_2+\alpha_3) \\ & + r_2(\alpha_1+\alpha_4+\alpha_5) + r_3(\alpha_2+\alpha_4+\alpha_6) + r_4(\alpha_3+\alpha_5+\alpha_6)] \end{aligned} \quad (136)$$

Equation (136) shows that the force constants involving angular displacement cannot be determined independently since f_α, $f'_{\alpha\alpha}$, $f''_{\alpha\alpha}$, $f'_{r\alpha}$, and $f''_{r\alpha}$ occur only as difference terms. The spectroscopically accessible angular force constants for gas-phase methane are therefore defined as

$$\varphi_\alpha = f_\alpha - f''_{\alpha\alpha} \tag{137}$$

$$\varphi_{\alpha\alpha} = f'_{\alpha\alpha} - f''_{\alpha\alpha} \tag{138}$$

$$\varphi_{r\alpha} = f'_{r\alpha} - f''_{r\alpha} \tag{139}$$

In order to calculate $\frac{s}{s'}f_g$ for methane isotopes, a reliable mass-independent $\underset{\sim}{F}$-matrix must be used which reproduces the observed gas-phase vibrational frequencies. Bigeleisen, Cragg and Jeevanandam (40) have conducted a study of the vapor pressures of $^{13}CH_4$, $^{14}CH_4$, $^{12}CH_3D$, $^{12}CH_2D_2$, $^{12}CHD_3$, $^{12}CD_4$, $^{12}CH_3T$ relative to $^{12}CH_4$ using a modification of the $\underset{\sim}{F}$-matrix reported by Jones and McDowell (84) to calculate the gas-phase reduced partition function ratio. The Jones-McDowell force constants and the BCJ modified force constants are given in Table I. The BCJ study assumes vanishingly small values for $f''_{\alpha\alpha}$ and $f''_{r\alpha}$ compared to f_α, $f'_{\alpha\alpha}$ and $f'_{r\alpha}$. So that a comparison between medium cluster model and simple cell model results can be made, the Jones-McDowell gas force field as modified by BCJ has been used in the present study, rather than the original Jones-McDowell $\underset{\sim}{F}$ or the more recent $\underset{\sim}{F}$

Table I

Non-zero $\underset{\sim}{F}$-matrix Elements for Gaseous Methane

Jones and McDowell (84)				Bigeleisen, Cragg and Jeevanandam (40)			
f_r	=	5.495	mdyne/Å	f_r	=	5.495	mdyne/Å
f_{rr}	=	0.124	mdyne/Å	f_{rr}	=	0.124	mdyne/Å
φ_α	=	0.549	mdyne·Å	f_α	=	0.568	mdyne·Å
$\varphi_{\alpha\alpha}$	=	0.019	mdyne·Å	$f'_{\alpha\alpha}$	=	0.019	mdyne·Å
$\varphi_{r\alpha}$	=	0.165	mdyne	$f'_{r\alpha}$	=	0.165	mdyne

developed by Hartshorn and Snyder (85).

All non-zero elements of the $\underset{\sim}{G}$-matrix for gas-phase methane are listed in Table II. The carbon-hydrogen distance is denoted by r and the reciprocal mass of the $i^{\underline{th}}$ atom by μ_i. The eigenvalues and eigenvectors of the resulting gas-phase secular equation are shown in Tables III-VI for the four spherical top methanes important to this study. Note that the redundancy in the definition of the internal coordinates has manifested itself as a zero eigenvector for all isotopes. The first four elements of each transformation vector, ℓ^{-1}_{ij} $(j=1,2,3,4)$, represent stretching contributions to the $i^{\underline{th}}$ normal coordinate, q_i, and the last six elements, ℓ^{-1}_{ij} $(j=5,6,7,8,9,10)$, are bending coordinate contributions to q_i. Eigenvalues are given in wavenumbers (cm^{-1}).

III-6: The Simple Cell Model and Condensed Phase Frequencies

The condensed phase part of Equation (69) was evaluated by BCJ (40) using the simple cell model. In this model, the six external modes are due to translation and rotation relative to an external reference frame. These six external coordinates have the form

$$t_1 = M^{-1} \sum_{i=1}^{N} m_i x_i \tag{140}$$

$$t_2 = M^{-1} \sum_{i=1}^{N} m_i y_i \tag{141}$$

$$t_3 = M^{-1} \sum_{i=1}^{N} m_i z_i \tag{142}$$

Table II

General Expressions for the G-matrix Elements of Gaseous Methane

g_r	=	$\mu_C + \mu_H$
g_{rr}	=	$-(\mu_C/3)$
g_α	=	$\frac{1}{r^2}(2\mu_H + \frac{8}{3}\mu_C)$
$g'_{\alpha\alpha}$	=	$-(\mu_H / 2r^2)$
$g''_{\alpha\alpha}$	=	$-\frac{8}{3}(\mu_C / r^2)$
$g'_{r\alpha}$	=	$-\frac{2}{3}\,2^{\frac{1}{2}}(\mu_C / r)$
$g''_{r\alpha}$	=	$-g'_{r\alpha}$

Table III

Eigenvalues and Eigenvectors of the $^{12}CH_4$ Gas Secular Equation

Eigenvalue 1 = 3154.097									
-0.03053	-0.69844	-0.05187	0.78084	0.06640	0.00751	-0.06834	0.06834	-0.00751	-0.06640
Eigenvalue 2 = 3154.097									
0.15557	0.41799	-0.89413	0.32057	-0.05224	0.06727	-0.04337	0.04337	-0.06727	0.05224
Eigenvalue 3 = 3154.097									
-0.89483	0.40413	0.15397	0.33674	0.04469	0.06748	0.05083	-0.05083	-0.06748	-0.04469
Eigenvalue 4 = 3143.741									
-0.49798	-0.49798	-0.49798	-0.49798	0.00000	-0.00000	-0.00000	0.00000	0.00000	-0.00000
Eigenvalue 5 = 1574.215									
-0.00000	-0.00000	-0.00000	-0.00000	0.05554	-0.81472	0.75918	0.75918	-0.81472	0.05554
Eigenvalue 6 = 1574.215									
-0.00000	-0.00000	0.00000	0.00000	-0.90869	0.40625	0.50244	0.50244	0.40625	-0.90869
Eigenvalue 7 = 1357.435									
0.00918	-0.02655	0.03019	-0.01281	0.40343	-0.91400	0.08445	-0.08445	0.91400	-0.40343
Eigenvalue 8 = 1357.435									
-0.02144	0.02428	0.01872	-0.02156	-0.06587	0.06318	0.99847	-0.99847	-0.06318	0.06587
Eigenvalue 9 = 1357.435									
0.02923	0.01020	-0.01169	-0.02774	-0.91553	-0.40730	-0.03463	0.03463	0.40730	0.91553
Eigenvalue 10 = 0.0									
0.0	0.0	0.0	0.0	0.0	0.0	0.0	0.0	0.0	0.0

Table IV

Eigenvalues and Eigenvectors of the $^{13}CH_4$ Gas Secular Equation

Eigenvalue 1 = 3143.741									
0.49798	0.49798	0.49798	0.49798	-0.00000	-0.00000	-0.00000	0.00000	0.00000	0.00000
Eigenvalue 2 = 3143.076									
0.10557	-0.80477	0.04205	0.65715	0.05603	-0.01183	-0.06112	0.06112	0.01183	-0.05603
Eigenvalue 3 = 3143.076									
0.89333	-0.24798	-0.21173	-0.43364	-0.05171	-0.05462	-0.03684	0.03684	0.05462	0.05171
Eigenvalue 4 = 3143.076									
0.10056	0.33191	-0.87904	0.44656	-0.03465	0.06238	-0.04384	0.04384	-0.06238	0.03465
Eigenvalue 5 = 1574.215									
0.00000	0.00000	-0.00000	-0.00000	0.87007	-0.66705	-0.20303	-0.20303	-0.66705	0.87007
Eigenvalue 6 = 1574.215									
0.00000	-0.00000	-0.00000	-0.00000	-0.26790	-0.61956	0.88746	0.88756	-0.61956	-0.26790
Eigenvalue 7 = 1348.914									
0.00806	-0.02811	0.03217	-0.01212	0.44258	-0.88835	0.08966	-0.08966	0.88835	-0.44258
Eigenvalue 8 = 1348.914									
-0.02333	0.02521	0.01973	-0.02161	-0.04151	0.07949	0.99249	-0.99249	-0.07949	0.04151
Eigenvalue 9 = 1348.914									
0.03030	0.01009	-0.01017	-0.03022	-0.89189	-0.44452	-0.00170	0.00170	0.44452	0.89189
Eigenvalue 10 = 0.0									
0.0	0.0	0.0	0.0	0.0	0.0	0.0	0.0	0.0	0.0

Table V

Eigenvalues and Eigenvectors of the $^{14}CH_4$ Gas Secular Equation

Eigenvalue 1 = 3143.741									
-0.49798	-0.49798	-0.49798	-0.49798	-0.00000	0.00000	0.00000	-0.00000	-0.00000	0.00000
Eigenvalue 2 = 3133.685									
-0.87117	0.07356	0.36343	0.43418	0.05637	0.03588	0.03089	-0.03089	-0.03588	-0.05637
Eigenvalue 3 = 3133.685									
-0.02245	-0.07182	0.78022	-0.68595	0.00666	-0.05355	0.05006	-0.05006	0.05355	-0.00666
Eigenvalue 4 = 3133.685									
-0.23295	0.89618	-0.27000	-0.39327	-0.04687	0.03554	0.04426	-0.04426	-0.03554	0.04687
Eigenvalue 5 = 1574.215									
0.00000	-0.00000	-0.00000	-0.00000	0.83124	-0.73714	-0.09410	-0.09410	-0.73714	0.83124
Eigenvalue 6 = 1574.215									
0.00000	0.00000	0.00000	0.00000	0.37126	0.53424	-0.90551	-0.90551	0.53424	0.37126
Eigenvalue 7 = 1341.478									
0.02258	-0.02322	-0.02355	0.02419	0.01348	0.02060	-0.99088	0.99088	-0.02060	-0.01348
Eigenvalue 8 = 1341.478									
0.01494	-0.03005	0.02933	-0.01423	0.31999	-0.93799	-0.01514	0.01514	0.93799	-0.31999
Eigenvalue 9 = 1341.478									
-0.03014	-0.01414	0.01515	0.02913	0.93801	0.31969	0.01940	-0.01940	-0.31969	-0.93801
Eigenvalue 10 = 0.0									
0.0	0.0	0.0	0.0	0.0	0.0	0.0	0.0	0.0	0.0

Table VI

Eigenvalues and Eigenvectors of the $^{12}CD_4$ Gas Secular Equation

Eigenvalue 1 = 2333.201									
-0.26206	0.67351	-0.21859	-0.19286	-0.09090	0.10619	0.10051	-0.10051	-0.10619	0.09090
Eigenvalue 2 = 2333.201									
-0.36048	-0.03614	-0.24743	0.64405	0.08763	0.13431	-0.06265	0.06265	-0.13431	-0.08763
Eigenvalue 3 = 2333.201									
-0.50678	-0.02300	0.58860	-0.05882	0.11705	-0.01808	0.12496	-0.12496	0.01808	-0.11705
Eigenvalue 4 = 2223.804									
0.35226	0.35226	0.35226	0.35226	0.00000	-0.00000	0.00000	-0.00000	0.00000	-0.00000
Eigenvalue 5 = 1113.561									
-0.00000	0.00000	0.00000	-0.00000	-0.03082	-0.54166	0.57248	0.57248	-0.54166	-0.03082
Eigenvalue 6 = 1113.561									
0.00000	0.00000	-0.00000	-0.00000	0.64325	-0.34832	-0.29493	-0.29493	-0.34832	0.64325
Eigenvalue 7 = 1027.032									
-0.00471	0.00971	-0.00615	0.00114	-0.30316	0.65736	0.21601	-0.21601	-0.65736	0.30316
Eigenvalue 8 = 1027.032									
-0.00321	0.00418	0.00749	-0.00846	-0.05867	-0.25940	0.70707	-0.70707	0.25940	0.05867
Eigenvalue 9 = 1027.032									
0.00917	0.00221	-0.00477	-0.00661	-0.06945	-0.26698	-0.15515	0.15515	0.26698	0.68945
Eigenvalue 10 = 0.0									
0.0	0.0	0.0	0.0	0.0	0.0	0.0	0.0	0.0	0.0

$$t_4 = I_{xx}^{-1} \sum_{i=1}^{N} m_i(b_i z_i - c_i y_i) \tag{143}$$

$$t_5 = I_{yy}^{-1} \sum_{i=1}^{N} m_i(c_i x_i - a_i z_i) \tag{144}$$

$$t_6 = I_{zz}^{-1} \sum_{i=1}^{N} m_i(a_i y_i - b_i x_i) \tag{145}$$

where M is the molecular mass. In Equations (140) - (145), x_i, y_i, and z_i are Cartesian displacements of atom i, and a_i, b_i, and c_i are the equilibrium x, y, and z coordinates of atom i. I_{xx}, I_{yy}, and I_{zz} are the principal moments of inertia. Equations (140) - (142) represent infinitismal translations and Equations (143) - (145) are infinitismal rotations. In the gas phase, coordinates t_1 through t_6 have zero frequency, but in the condensed phase, according to the cell model, each of the six external coordinates are subject to harmonic restoring forces. Obviously, these coordinates are not mass independent and, as has been pointed out by Babloyantz (86), an energy hypersurface defined with these coordinates violates the Born-Oppenheimer principal. Stern, Van Hook and Wolfsberg (38), in their study of isotopic ethylenes, therefore abandoned the concept of isotope-dependent external coordinates so that an identical $\underset{\sim}{F}$-matrix could be used for all isotopes. This is done by choosing a basis isotope and subsequently calculating the $\underset{\sim}{G}$-matrices for all other isotopic species by using external coordinates defined in terms of the basis molecule.

If isotopic species α is considered to be the basis molecule, $\underset{\sim}{G}$-matrices for all other isotopes β_1, β_2,... may be constructed as follows. From Equation (140),

$$t_1^{\alpha} = \frac{1}{M^{\alpha}} \sum_{i=1}^{N} m_i x_i = \frac{1}{M^{\alpha}} \sum_{i=1}^{N} (m_i x_i + 0 \cdot y_i + 0 \cdot z_i) \tag{146}$$

Since, from Equation (96),

$$t_1^{\alpha} = \sum_{i=1}^{3N} b_{1i}^{\alpha} x_i \tag{147}$$

the elements of $\underset{\sim}{B}_{\alpha}$ are

$$\begin{array}{lll} b_{11}^{\alpha} = \dfrac{m_1}{M^{\alpha}} & b_{12}^{\alpha} = 0 & b_{13}^{\alpha} = 0 \\ b_{14}^{\alpha} = \dfrac{m_2}{M^{\alpha}} & b_{15}^{\alpha} = 0 & b_{16}^{\alpha} = 0 \\ \cdot & \cdot & \cdot \\ \cdot & \cdot & \cdot \\ \cdot & \cdot & \cdot \\ b_{1,3N-2}^{\alpha} = \dfrac{m_N}{M^{\alpha}} & b_{1,3N-1}^{\alpha} = 0 & b_{1,3N}^{\alpha} = 0 \end{array} \tag{148}$$

where the subscripts are indices of the external portion of $\underset{\sim}{B}_{\alpha}$ only. Then, from Equation (99),

$$g^{\alpha}_{11} = \frac{m_1^2}{m_1 M^{\alpha 2}} + \frac{m_2^2}{m_2 M^2} + \ldots = \frac{1}{M^{\alpha}} \tag{149}$$

Similarly, from Equations (141) and (142),

$$g^{\alpha}_{22} = g^{\alpha}_{33} = \frac{1}{M^{\alpha}} \tag{150}$$

From Equations (143) - (145), one obtains

$$g^{\alpha}_{44} = \frac{1}{I^{\alpha}_{xx}} \qquad g^{\alpha}_{55} = \frac{1}{I^{\alpha}_{yy}} \qquad g^{\alpha}_{66} = \frac{1}{I^{\alpha}_{zz}} \tag{151}$$

The same derivation can be used to show that there are no external-external kinetic interactions, and no external-internal kinetic interaction in species :

$$g^{\alpha}_{t_i t_j} = 0 \qquad [i = j] \tag{152}$$

$$g^{\alpha}_{s_i t_j} = 0 \tag{153}$$

For the basis molecule in the condensed phase, then, the $\underset{\sim}{G}$-matrix only has diagonal external elements. The $\underset{\sim}{G}$-matrices for all other isotopic species β_1, β_2, etc., are found from the basis $\underset{\sim}{B}$-matrix by using the relation

$$\underset{\sim}{G}_{\beta} = \underset{\sim}{B}_{\alpha}\underset{\sim}{M}^{-1}_{\beta}\underset{\sim}{B}^{\dagger}_{\alpha} \qquad (154)$$

where $\underset{\sim}{M}$ is a column matrix of atomic masses. In general, the external part of a condensed phase $\underset{\sim}{G}_{\beta}$ is not diagonal, and non-zero internal-external elements exist.

With this methodology, a single $\underset{\sim}{F}$-matrix may be used for all isotopic species. The force field used by BCJ to evaluate the condensed phase frequencies within the simple cell model is given in Table VII. The resulting liquid phase modes are presented in Table VIII for $^{12}CH_4$, $^{13}CH_4$, $^{14}CH_4$ and $^{12}CD_4$.

The medium cluster model considers a liquid-phase molecule together with its first coordination shell as a total vibrating system. The number of coordinates needed to describe an m-cluster is therefore 3Nm. If the aggregate is considered to rotate and translate freely, then the number of coordinates necessary is 3Nm - 6. For the purpose of evaluating the vpie by means of Equation (84), external modes of vibration have been defined as motions of the central molecule in the cluster relative to the shell molecules, so there is no need to define mass-dependent coordinates such as those in Equations (140) - (145), and unless motion of the cluster as a whole is to be considered as taking place within a "supercell", there is no need to define a basis isotopic species.

Table VII

Non-zero $\underset{\sim}{F}$-Matrix Elements for Simple Cell Theory Liquid Phase Methane Calculations; Ref. (40)

f_r	=	5.452	mdyne/Å
f_{rr}	=	0.124	mdyne/Å
f_α	=	0.565	mdyne·Å
$f'_{r\alpha}$	=	0.175	mdyne
$f'_{\alpha\alpha}$	=	0.019	mdyne·Å
f_{trans}	=	0.057	mdyne/Å
f_{rot}	=	0.0099	mdyne·Å

Table VIII

Liquid Phase Frequencies for Spherical Top Methane Isotopes
Calculated from the Simple Cell Theory; Ref. (40)

$^{12}CH_4$	$^{13}CH_4$	$^{14}CH_4$	$^{12}CD_4$
3140.229 cm^{-1}	3129.403 cm^{-1}	3120.180 cm^{-1}	2321.716 cm^{-1}
3140.229	3129.403	3120.180	2321.716
3140.229	3129.403	3120.180	2321.716
3132.168	3132.168	3132.168	2217.019
1570.305	1570.305	1570.305	1110.803
1570.305	1570.305	1570.305	1110.803
1352.560	1344.009	1336.550	1024.043
1352.560	1344.009	1336.550	1024.043
1352.560	1344.009	1336.550	1024.043
77.693	75.370	73.251	69.451
77.693	75.370	73.251	69.451
77.693	75.370	73.251	69.451
72.285	72.285	72.285	51.133
72.285	72.285	72.285	51.133
72.285	72.285	72.285	51.133

IV. COMPUTATIONAL METHODS

Calculation of the vapor pressure isotope effect within the framework of the medium cluster model of the liquid state may involve an $\underset{\sim}{H}$-matrix with up to 202 x 202 elements for a 13-cluster. This precludes evaluation of the cluster vibrational frequencies on all but the most advanced digital computing systems. The present research has been done with the aid of an IBM System/370 with dual 168 processors.

Computation proceeds in five steps:

(1) Calculation of Cartesian coordinates for all atoms in the cluster. Parameters such as relative molecular orientation and intermolecular distance are specified as input at this stage.

(2) Calculation of the $\underset{\sim}{G}$-matrix for the entire cluster, given the Cartesian coordinates from Step (1), definitions of internal coordinates, and atomic masses.

(3) Construction of an $\underset{\sim}{F}$-matrix for the cluster that is independent of isotopic composition.

(4) Solution of the secular equation by computing the eigenvectors and eigenvalues of $\underset{\sim}{H}$.

(5) Choosing only the eigenvectors and corresponding eigenvalues that represent vibrations of the central molecule of the cluster and subsequent calculation of the vpie parameters A and B from Equations (86) and (87).

In this chapter, each of the above steps will be considered in turn. The computer programs used for the actual calculations are included as an appendix.

IV-1: The Cartesian Coordinate Matrix

The spatial relationships of each part of the cluster to all other parts must be considered in order to construct the kinetic energy matrix. A 2-cluster of methane, for example, can be viewed as a dimolecular aggregate with the carbon-carbon "bond" arranged along the (arbitrary) y-axis and one of the molecules centered on the origin. In order to calculate a set of Cartesian coordinates for all 10 atoms, the coordinates of the methane at the origin is first specified as a 3 x 5 matrix,

$$\underset{\sim}{X}_c = \begin{pmatrix} 0 & x_2 & x_3 & x_4 & x_5 \\ 0 & y_2 & y_3 & y_4 & y_5 \\ 0 & z_2 & z_3 & z_4 & z_5 \end{pmatrix} \tag{155}$$

Two sets of rotational displacements, $\{\theta_1\}$ and $\{\theta_2\}$, are used to transform Equation (155) so that rotated "images", $\underset{\sim}{X}_1'$ and $\underset{\sim}{X}_2'$, of the two methanes are produced. Thus,

$$\underset{\sim}{X}_1' = \begin{pmatrix} 0 & x_2' & x_3' & x_4' & x_5' \\ 0 & y_2' & y_3' & y_4' & y_5' \\ 0 & z_2' & z_3' & z_4' & z_5' \end{pmatrix} \tag{156}$$

$$\underset{\sim}{X}'_2 = \begin{pmatrix} 0 & x'_7 & x'_8 & x'_9 & x'_{10} \\ 0 & y'_7 & y'_8 & y'_9 & y'_{10} \\ 0 & z'_7 & z'_8 & z'_9 & z'_{10} \end{pmatrix} \tag{157}$$

where elements in like columns of $\underset{\sim}{X}'_1$ and $\underset{\sim}{X}'_2$ represent the positions of corresponding atoms in the two molecules. Two position vectors, $\vec{\rho}_1$ and $\vec{\rho}_2$, are introduced to displace each methane to its position in the medium cluster; $\vec{\rho}_1$ is always a null vector so that the "central" molecule maintains its position at the origin. Since the "shell" molecule is displaced along the positive y-axis in a 2-cluster, the Cartesian coordinates for both molecules, $\underset{\sim}{X}_1$ and $\underset{\sim}{X}_2$, are given by $\underset{\sim}{X}_1 = \underset{\sim}{X}'_1$, from Equation (156), and

$$\underset{\sim}{X}_2 = \begin{pmatrix} 0 & x'_7+|\vec{\rho}_2| & x'_8+|\vec{\rho}_2| & x'_9+|\vec{\rho}_2| & x'_{10}+|\vec{\rho}_2| \\ 0 & y'_7+|\vec{\rho}_2| & y'_8+|\vec{\rho}_2| & y'_9+|\vec{\rho}_2| & y'_{10}+|\vec{\rho}_2| \\ 0 & z'_7+|\vec{\rho}_2| & z'_8+|\vec{\rho}_2| & z'_9+|\vec{\rho}_2| & z'_{10}+|\vec{\rho}_2| \end{pmatrix} \tag{158}$$

For the general case of an m-cluster of molecules with N atoms each, the Cartesian coordinates are similarly generated from the coordinates of one central molecule, $\underset{\sim}{X}_c$,

$$\underset{\sim}{X}_c = \begin{pmatrix} x_1 & x_2 & \cdot & \cdot & \cdot & x_N \\ y_1 & y_2 & \cdot & \cdot & \cdot & y_N \\ z_1 & z_2 & \cdot & \cdot & \cdot & z_N \end{pmatrix} \tag{159}$$

and m rotation matrices,

$$\underset{\sim}{\theta}_i^{(xyz)} = \underset{\sim}{\theta}_i^z \, \underset{\sim}{\theta}_i^y \, \underset{\sim}{\theta}_i^x \qquad [i = 1,2,\ldots,m] \qquad (160)$$

where the superscript (xyz) implies a rotation of the $i^{\underline{th}}$ molecule first around the x-axis, followed by rotation around the y-axis, and finally around the z-axis. The order of rotation may be permuted and the rotation process itself takes place according to the right hand convention so that

$$\underset{\sim}{\theta}_i^{(zyx)} = \begin{pmatrix} 1 & 0 & 0 \\ 0 & \cos\theta_x & -\sin\theta_x \\ 0 & \sin\theta_x & \cos\theta_x \end{pmatrix} \begin{pmatrix} \cos\theta_y & 0 & -\sin\theta_y \\ 0 & 1 & 0 \\ \sin\theta_y & 0 & \cos\theta_y \end{pmatrix} \begin{pmatrix} \cos\theta_z & -\sin\theta_z & 0 \\ \sin\theta_z & \cos\theta_z & 0 \\ 0 & 0 & 1 \end{pmatrix} \qquad (161)$$

where θ_x, θ_y, and θ_z are the desired angular displacements. Then,

$$\underset{\sim}{X}_i' = \underset{\sim}{\theta}_i \, \underset{\sim}{X}_c \qquad [i = 1,2,\ldots,m] \qquad (162)$$

Equation (162) produces m superimposed images of the central molecule which may now be displaced to various positions in the cluster by means of m vectors, $\vec{\rho}_i$, where

$$\vec{\rho}_i = \begin{pmatrix} \rho_x \\ \rho_y \\ \rho_z \end{pmatrix} \qquad [i = 1,2,\ldots,m] \qquad (163)$$

These displacement vectors are transformed into a 3 x N translation matrix,

$$\underset{\sim}{P}_i = \vec{\rho}_i \cdot (\text{unit row matrix})$$

$$= \begin{pmatrix} \rho_x \\ \rho_y \\ \rho_z \end{pmatrix} (1\ 1\ \ldots \text{N terms} \ldots 1\ 1) \tag{164}$$

$$= \begin{pmatrix} \rho_x & \rho_x & . & . & . & \rho_x \\ \rho_y & \rho_y & . & . & . & \rho_y \\ \rho_z & \rho_z & . & . & . & \rho_z \end{pmatrix}$$

Then,

$$\underset{\sim}{X}_i = \underset{\sim}{X}'_i + \underset{\sim}{P}_i \qquad [i=1,2,\ldots,m] \tag{165}$$

A final 3 x Nm Cartesian coordinate matrix, $\underset{\sim}{X}$, for the entire cluster is obtained by

$$\underset{\sim}{X} = \underset{\sim}{X}_1 \oplus \underset{\sim}{X}_2 \oplus \ldots \oplus \underset{\sim}{X}_m \tag{166}$$

where $\oplus$ is a process of matrix augmentation in successive columns.

Clusters of 2, 3, 7, 9, and 13 isotopic methanes have been

examined in this study. While arbitrary sets of $\vec{\rho}$-vectors can be used as a basis for non-regular aggregates of molecules, we have examined only symmetric clusters modeled on Platonic solids. The directional components of each $\vec{\rho}$-vector for any such regular m-cluster are fixed, and the lengths of the vectors are equal,

$$\left|\vec{\rho}_2\right| = \left|\vec{\rho}_3\right| = \cdots = \left|\vec{\rho}_m\right| \tag{167}$$

Table IX lists the directional components for $\vec{\rho}$-vectors of interest; simplified cluster diagrams are included in Table X (p. 81). Symmetric 7-, 9-, and 13-clusters correspond to simple cubic, body-centered cubic, and face-centered cubic lattice structures respectively.

The mutual orientation of molecules in the model liquid phase can be changed by means of the m $\underset{\sim}{\theta}$-matrices. Egelstaff, Page and Powels (87) have described a "rocket" geometry for tetrahedral XY_4 molecules in the liquid phase in which nearest neighbor pairs point front-to-end with a Y atom on one molecule located in the crevice formed by three Y atoms on the other. Lowden and Chandler (88) presented evidence in favor of a liquid phase geometry in which two neighboring tetrahedral molecules are interlocked in a staggered antiparallel configuration. Crystallographic studies by Press and coworkers (89,90) have indicated a "gear-like" conformation of CD_4 molecules in the solid state near the triple point. The consequences of each of these intermolecular conforma-

Table IX

Directional Components of the $\vec{\rho}$ - Vectors

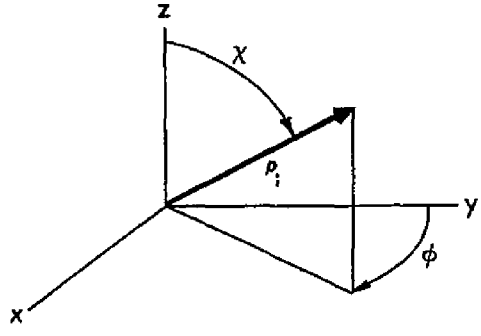

m	i	χ	ϕ
3	2	90°	0°
	3	90°	180°
13	2	90°	0°
	3	90°	60°
	4	90°	120°
	5	90°	180°
	6	90°	240°
	7	90°	300°
	8	45°	30°
	9	45°	150°
	10	45°	270°
	11	135°	90°
	12	135°	210°
	13	135°	330°

m	i	χ	ϕ
7	2	90°	0°
	3	90°	90°
	4	90°	180°
	5	90°	270°
	6	0°	0°
	7	180°	0°
9	2	45°	45°
	3	45°	135°
	4	45°	225°
	5	45°	315°
	6	135°	45°
	7	135°	135°
	8	135°	225°
	9	135°	315°

tions on the vapor pressure isotope effect have been examined in this research using the medium cluster model. The three configurations are pictured for two neighboring methanes in Figure 2.

The $\underset{\sim}{G}$-matrix depends explicitly on molecular geometry and atomic mass. The Jones-McDowell gas-phase $\underset{\sim}{F}$-matrix, given in Table I, was developed when oxygen-16 was the basis for the atomic mass scale; for conformity, all atomic weights used in the present study are those from the 1941 Birge (91) scale. The masses of interest are

$$^{12}C = 12.00386 \text{ daltons}$$

$$^{13}C = 13.00761$$

$$^{14}C = 14.00768$$

$$^{1}H = 1.00813$$

$$^{2}D = 2.01473$$

$$^{3}T = 3.01705$$

The molecular geometry of methane is well known from spectroscopic studies (92). The tetrahedral molecule has a CH valence bond radius of 1.094 Å and an HCH valence bond angle of 109° 28'.

The only remaining cluster parameter which must be specified is the distance between the central and shell molecules in the liquid-phase aggregate, $|\vec{\rho}|$. In order to estimate the intermolecular distance, a potential of the form

$$V(|\vec{\rho}|) = 4\epsilon\left[\left(\frac{\sigma}{|\vec{\rho}|}\right)^{12} - \left(\frac{\sigma}{|\vec{\rho}|}\right)^{6}\right] \qquad (168)$$

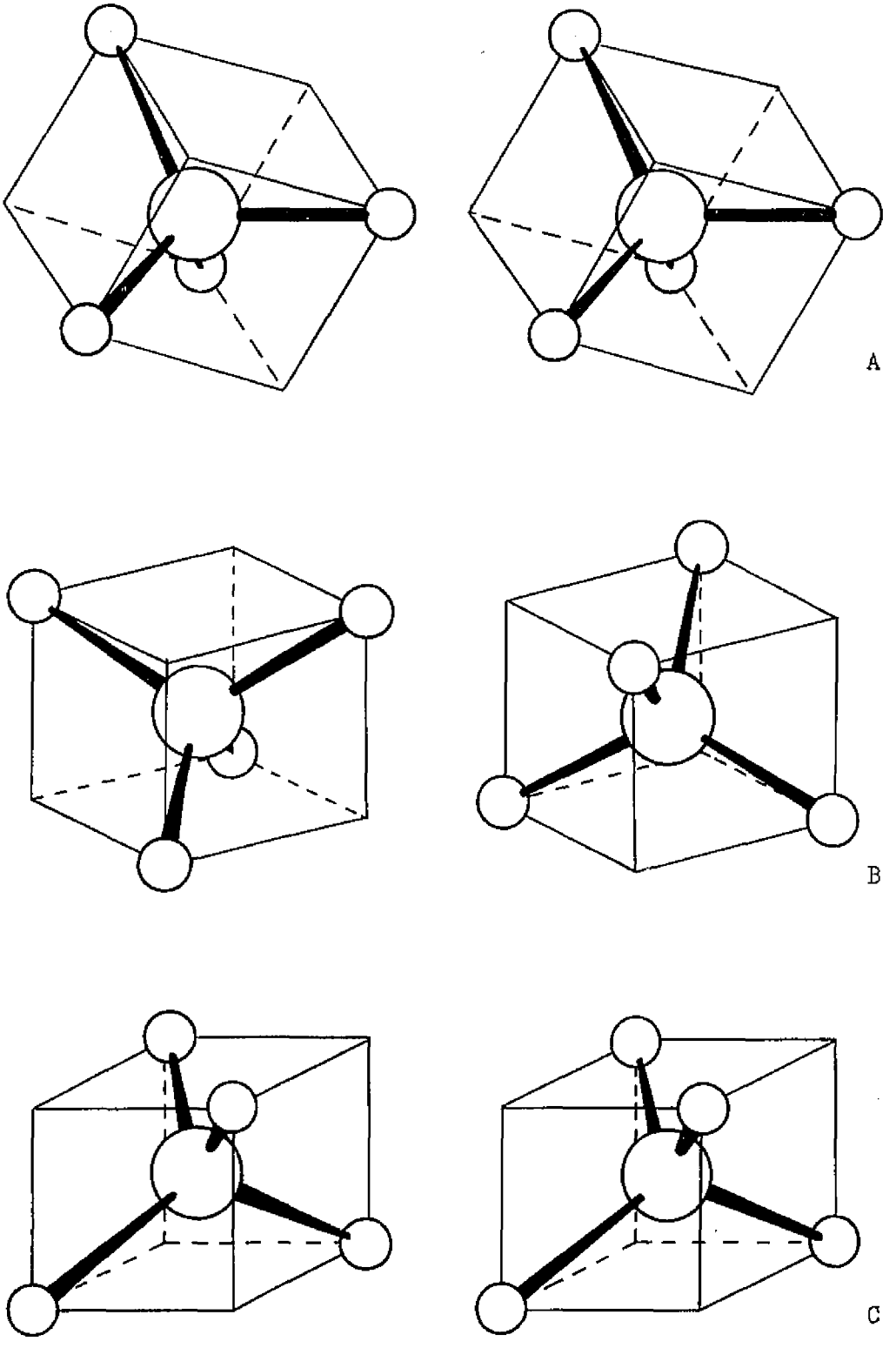

Figure 2. Relative orientations of adjacent methane molecules. A is the rocket geometry, B is the antiparallel geometry, and C is the gear geometry.

was assumed. Equation (168) is the Lennard-Jones (6-12) potential commonly used as a model for non-polar fluid behavior (56,93). The distance of closest approach of two molecules colliding with zero relative kinetic energy is given by σ. The parameter ϵ is the maximum energy of attraction at $|\vec{\rho}| = 2^{1/6}\,\sigma$. The quantities ϵ/k and σ may be determined experimentally from viscosity and thermal conductivity measurements (94,95). From an examination of Lennard-Jones parameters determined from different types of experimental data, Vogel and Ahlert (96,97) and others (98,99) have concluded that 3.817 Å is an optimum σ-value for the successful prediction of the thermodynamic properties of methane. We have therfore examined a range of intermolecular separations in the neighborhood of 3.817 Å with the medium cluster model.

IV-2: Internal Coordinates for Molecular Clusters and the G-matrix

Internal coordinates, s_j, for an m-cluster will now be described. Since the m-cluster contains Nm atoms, the number of vibrational degrees of freedom is 3Nm-6; however, one redundant HCH valence angle bending coordinate has been added for each methane, so that the total number of coordinates is 3Nm-6+m, or 16m-6 for clusters of methane molecules.

Ten coordinates have been used to describe the intramolecular modes of each individual methane. They are the four CH valence bond stretches, r_i, and six HCH valence angle bends, α_i, as shown in Figure 1 (p. 48). There are m such sets of 10 coordinates, together describing the "optical" or "internal" vibrational modes (not to be confused with the general name for all s_j). The defini-

tions of these optical coordinates are given in detail by Wilson, Decius and Cross (62).

The remaining 6m-6 coordinates describe the motion of methane molecules relative to one another in the cluster. These "acoustical" or "external" intermolecular coordinates have been defined in such a way as to simplify the interpretation of $\underset{\sim}{L}^{-1}$ after solution of the secular equation. Since there are m-1 shell molecules and 6m-6 required external coordinates, a procedure has been used by which six external coordinates are defined per shell molecule. The vibrational coordinates are thus described in a systematic fashion for all sized clusters. These intermolecular displacements are pictured in Figures 3 and 4, where a central and a single arbitrary shell molecule of an m-cluster are shown. The lower-case labels "c" and "s" denote central and shell molecules, respectively, in the discussion which follows.

The first of the six (per shell molecule) external coordinates has been defined as an increase in the C_cC_s distance, $R = |\vec{\rho}|$. This carbon-carbon stretch is illustrated in Figure 3a. The $\vec{\zeta}$-vectors for use in Equation (102) are given by

$$\overrightarrow{\zeta_{t(C_c)}} = -\overrightarrow{\zeta_{t(C_s)}} = \overrightarrow{e_{CC}} \qquad (169)$$

where $\overrightarrow{e_{CC}}$ is the unit vector of $\vec{\rho}_i$.

Each of the m-1 peripheral molecules of the cluster can also rotate around the axis formed by $\vec{\rho}_i$. This torsional motion, shown

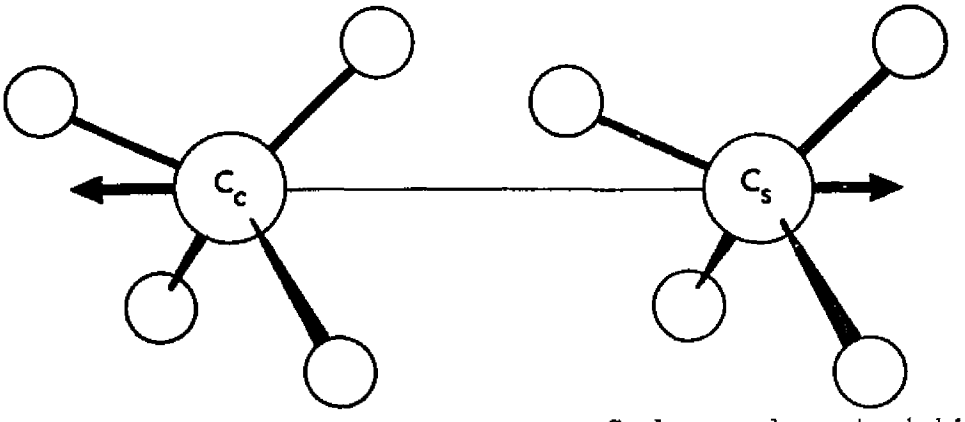

a. Carbon-carbon stretching

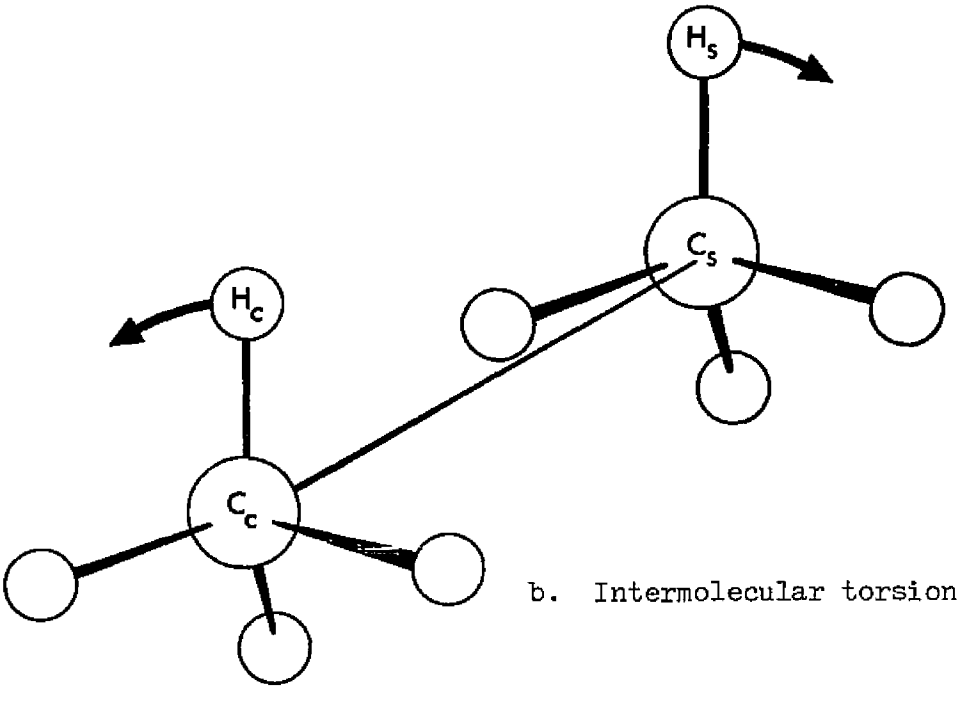

b. Intermolecular torsion

Figure 3. External stretching and torsional coordinates for methane clusters. The molecule on the left is the central methane; the molecule on the right is an arbitrary shell methane.

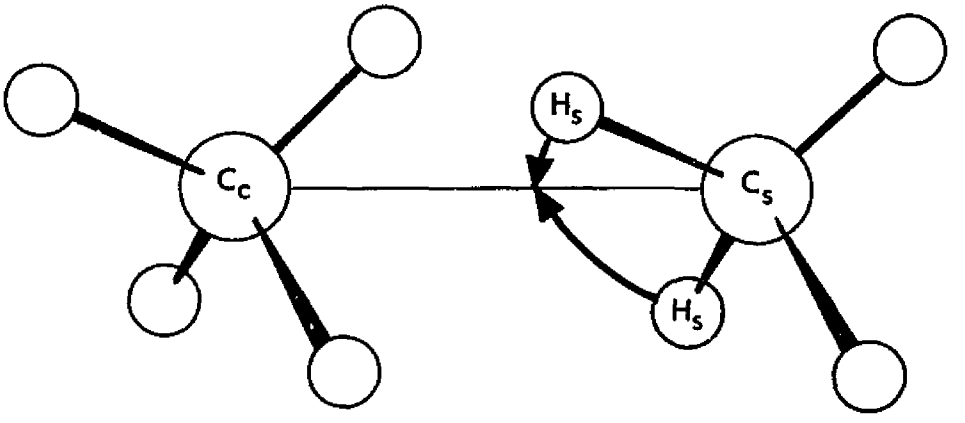

a. Shell nodding

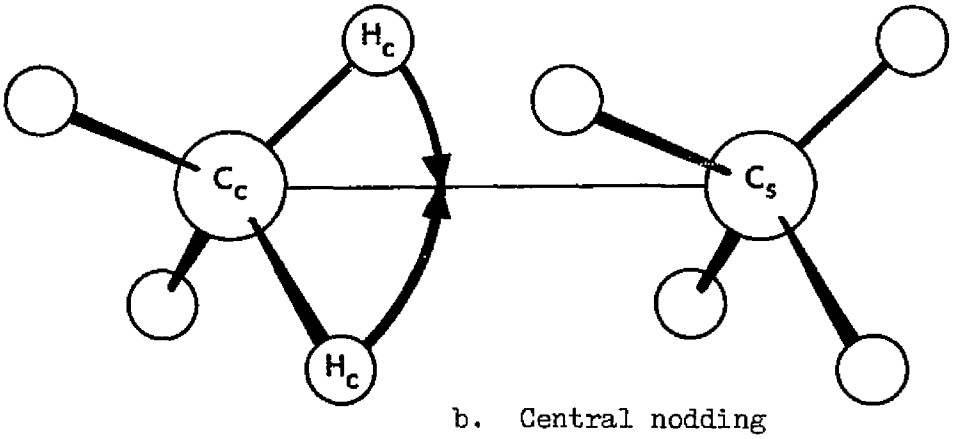

b. Central nodding

Figure 4. External nutational coordinates for methane clusters. The molecule on the left is the central methane; the molecule on the right is an arbitrary shell molecule.

in Figure 3b, has been defined as a change in the angle τ between the plane determined by a hydrogen in the central molecule, H_c, and two carbons C_c and C_s, and the plane determined by the corresponding hydrogen on the shell molecule, H_s, and the same two carbons. The atoms $H_cC_cC_sH_s$ are bonded in sequence. The sign of τ is determined by the following convention: if τ is restricted to the range $-\pi < \tau \leq \pi$, then τ is positive if an observer at the origin looking along $\vec{\rho}_i$ sees the projection of C_sH_s as a clockwise displacement of the projection of C_cH_c. The magnitude of τ is given by

$$\cos\tau = \frac{(\vec{e}^{\,c}_{CH} \times \vec{e}_{CC}) \cdot (\vec{e}_{CC} \times \vec{e}^{\,c}_{CH})}{\sin\beta_c \cdot \sin\beta_s} \tag{170}$$

where $\vec{e}^{\,c}_{CH}$ and $\vec{e}^{\,s}_{CH}$ are unit vectors along the central and shell CH bonds, respectively, and β_c and β_s are the HCC bond angles at the central and shell molecules. The $\vec{\zeta}$-vectors used to calculate G-matrix elements involving the torsional coordinates from Equation (102) are given by

$$\vec{\zeta}_{t(H_c)} = -(\vec{e}^{\,c}_{CH} \times \vec{e}_{CC}) / r \sin^2\beta_c \tag{171}$$

$$\vec{\zeta}_{t(C_c)} = \frac{(R - r\cos\beta_c)(\vec{e}^{\,c}_{CH} \times \vec{e}_{CC})}{rR\sin\beta_c} - \frac{\cos\beta_s(\vec{e}^{\,s}_{CH} \times \vec{e}_{CC})}{R\sin\beta_s} \tag{172}$$

$$\vec{\zeta}_{t(C_s)} = \frac{(R - r\cos\beta_s)(\vec{e}^{\,s}_{CH} \times \vec{e}_{CC})}{rR\sin\beta_s} - \frac{\cos\beta_c(\vec{e}^{\,c}_{CH} \times \vec{e}_{CC})}{R\sin\beta_c} \tag{173}$$

$$\vec{\zeta}_{t(H_s)} = -(\vec{e}^{\,s}_{CH} \times \vec{e}_{CC}) / r \sin^2\beta_s \qquad (174)$$

where R and r are the equilibrium carbon-carbon and carbon-hydrogen distances, respectively.

Four valence angle bends per shell molecule have been defined to complete the description of the acoustical modes. In Figure 4a, two angles are indicated which, when decreased, produce a nutational or "nodding" to the shell molecule with respect to the central molecule. These angles are denoted as β_{s1} and β_{s2}. Figure 4b shows two angles, β_{c1} and β_{c2}, which can be visualized as producing two corresponding nutational motions of the central molecule. While two central nodding coordinates per shell molecule would seem to impart 2(m-1) degrees of rotational freedom to the central molecule, it can be seen that β_{c1} and β_{c2} actually describe "wagging" translational motions of the shell molecules in directions perpendicular to $\vec{\rho}_i$. However, no ambiguity should arise from the continued use of the term "central nutation". An increase in these angles is considered to be a positive displacement of the external coordinate. The $\vec{\zeta}$ - vectors for shell nutation are

$$\vec{\zeta}_{t(H_s)} = (\cos\beta_s \, \vec{e}^{\,s}_{CH} - \vec{e}_{CC}) / r \sin\beta_s \qquad (175)$$

$$\vec{\zeta}_{t(C_s)} = \frac{[(r - R\cos\beta_s)\vec{e}^{\,s}_{CH} + (R - r\cos\beta_s)\vec{e}_{CC}]}{rR\sin\beta_s} \qquad (176)$$

$$\vec{\zeta}_{t(C_c)} = (\cos\beta_s \, \vec{e}_{CC} - \vec{e}^{\,s}_{CH}) / R \sin\beta_s \tag{177}$$

and the $\vec{\zeta}$ - vectors for central nutation (shell molecule "wagging") are

$$\vec{\zeta}_{t(H_c)} = (\cos\beta_c \, \vec{e}^{\,c}_{CH} - \vec{e}_{CC}) / r \sin\beta_c \tag{178}$$

$$\vec{\zeta}_{t(C_c)} = \frac{[(r - R\cos\beta_c)\vec{e}^{\,c}_{CH} + (R - r\cos\beta_c)\vec{e}_{CC}]}{rR\sin\beta_c} \tag{179}$$

$$\vec{\zeta}_{t(C_s)} = (\cos\beta_c \, \vec{e}_{CC} - \vec{e}^{\,c}_{CH}) / R \sin\beta_c \tag{180}$$

Six such external coordinates, R, τ, β_{c1}, β_{c2}, β_{s1}, and β_{s2}, were added to the dimensions of the secular equation for each shell molecule in the cluster. Table X summarizes the number and type of coordinates used for each sized cluster. Using Equations (169), (171) - (180), and $\vec{\zeta}$ - vectors for intramolecular coordinates, a $\underset{\sim}{B}$-matrix may be constructed. The $\underset{\sim}{G}$-matrix is calculated from Equation (101).

In general, the kinetic energy matrix for an m-cluster has the form

Table X

Coordinates for Methane Clusters

Cluster size, m	Number of atoms, mN	Number of coordinates, n	Cluster diagram	CH str.	HCH bend	CC str.	HCCH tors.	β_c nod	β_s nod
1	5	10		4	6	0	0	0	0
3	15	42	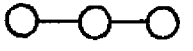	12	18	2	2	2	2
7	35	106	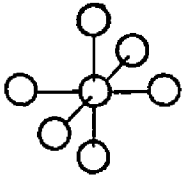	28	42	6	6	12	12
9	45	138	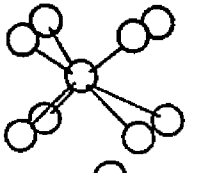	36	54	8	8	16	16
13	65	202	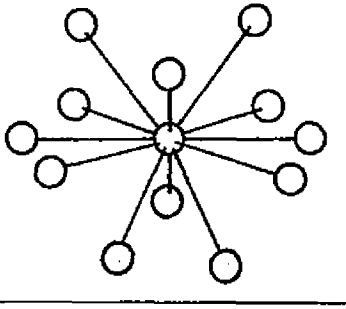	52	78	12	12	24	24

$$\underset{\sim}{G}_m = \begin{pmatrix} \underset{\sim}{G}_c & \underset{\sim}{G}_{cs} & \underset{\sim}{G}_{ce} \\ & \underset{\sim}{G}_s & \\ & \underset{\sim}{G}_{ss} & \underset{\sim}{G}_{se} \\ & & \underset{\sim}{G}_s \\ & & \underset{\sim}{G}_e \end{pmatrix} \qquad (181)$$

where the $\underset{\sim}{G}_c$ area of $\underset{\sim}{G}_m$ consists of elements g_{ij} defined entirely with central molecular internal coordinates; each $\underset{\sim}{G}_s$ area contains elements defined with only internal coordinates of one shell molecule. $\underset{\sim}{G}_e$ consists of kinetic energy terms defined with respect to the (6m-6) external coordinates. The areas labeled $\underset{\sim}{G}_{ss}$, $\underset{\sim}{G}_{se}$, $\underset{\sim}{G}_{cs}$, and $\underset{\sim}{G}_{ce}$ contain elements that express shell-shell kinetic interactions, shell-external interactions, central-shell interactions, and cental-external kinetic interaction, respectively. Because optical coordinates in different molecules never have any atoms in common, elements g_{ij} in areas $\underset{\sim}{G}_{cs}$ and $\underset{\sim}{G}_{ss}$ are always zero. In addition, all m molecules in the cluster are identical with respect to bond lengths, bond angles, and atomic masses, so that

$$(g_{ij})_c = (g_{i+10p,j+10p})_s \quad \begin{bmatrix} i,j=1,2,\ldots,10 \\ p=1,2,\ldots,m-1 \end{bmatrix} \qquad (182)$$

and Equation (181) is then

$$\underset{\sim}{G}_m = \begin{pmatrix} \underset{\sim}{G}_i & & & & \underset{\sim}{G}^c_{ie} \\ & \underset{\sim}{G}_i & & 0 & \\ & & \ddots & & \underset{\sim}{G}^s_{ie} \\ & & & \underset{\sim}{G}_i & \\ & & & & \underset{\sim}{G}_e \end{pmatrix} \qquad (183)$$

where the $\underset{\sim}{G}_i$ are identical sub-matrices of optical coordinates and $\underset{\sim}{G}_e$ contains external-external coordinate kinetic interactions. $\underset{\sim}{G}^c_{ie}$ and $\underset{\sim}{G}^s_{ie}$ contain kinetic interaction terms between internal and external modes.

A 3-cluster of methane molecules will be used to illustrate the way in which coordinates are defined and the structure of the resulting $\underset{\sim}{G}$-matrix. The 3-cluster studied is linear with respect to the carbon atoms (Figure 5); relative molecular orientation is arbitrary for the purpose of defining coordinates.

The coordinates internal to each methane in the cluster require no modification from those of gas-phase methane. They consist of four CH stretches,

$$1 - r(C_1H_2)$$
$$2 - r(C_1H_3)$$
$$3 - r(C_1H_4)$$
$$4 - r(C_1H_5),$$

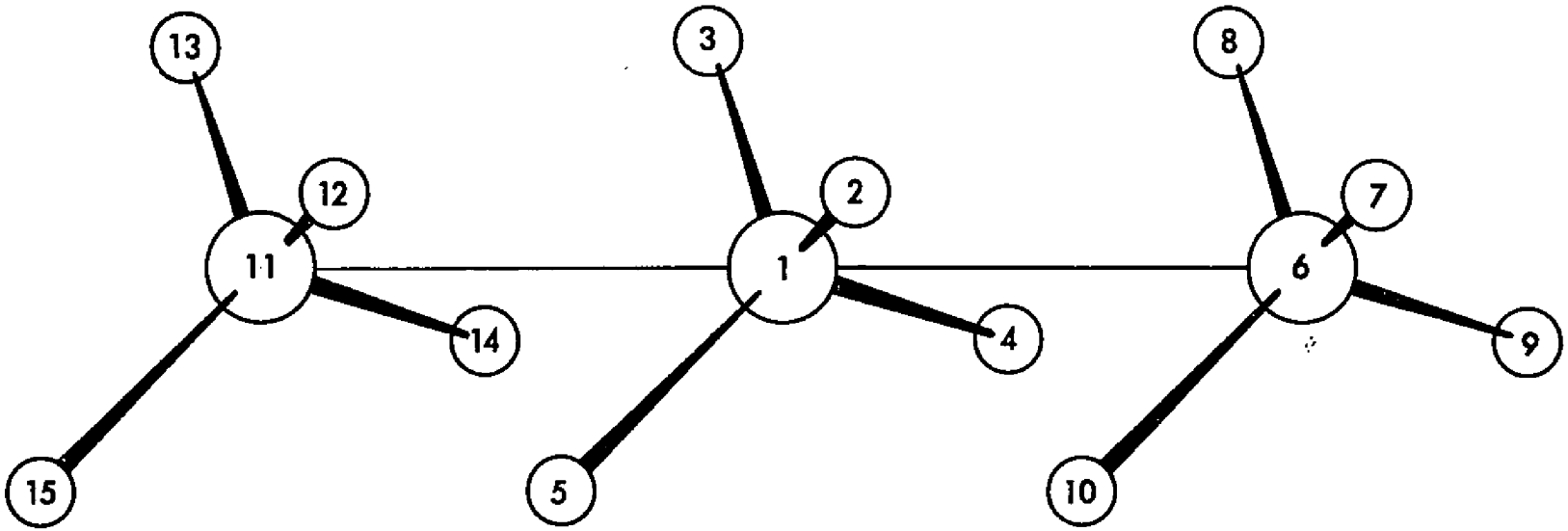

Figure 5. A 3-cluster of methane molecules. The cluster is shown in the gear geometry.

and six bond angle bends,

$$5 - \alpha(H_2C_1H_3)$$
$$6 - \alpha(H_2C_1H_4)$$
$$7 - \alpha(H_2C_1H_5)$$
$$8 - \alpha(H_3C_1H_4)$$
$$9 - \alpha(H_3C_1H_5)$$
$$10 - \alpha(H_4C_1H_5).$$

The internal coordinates of the two shell molecules are defined similarly:

$11 - r(C_6H_7)$	$21 - r(C_{11}H_{12})$
$12 - r(C_6H_8)$	$22 - r(C_{11}H_{13})$
$13 - r(C_6H_9)$	$23 - r(C_{11}H_{14})$
$14 - r(C_6H_{10})$	$24 - r(C_{11}H_{15})$
$15 - \alpha(H_7C_6H_8)$	$25 - \alpha(H_{12}C_{11}H_{13})$
$16 - \alpha(H_7C_6H_9)$	$26 - \alpha(H_{12}C_{11}H_{14})$
$17 - \alpha(H_7C_6H_{10})$	$27 - \alpha(H_{12}C_{11}H_{15})$
$18 - \alpha(H_8C_6H_9)$	$28 - \alpha(H_{13}C_{11}H_{14})$
$19 - \alpha(H_8C_6H_{10})$	$29 - \alpha(H_{13}C_{11}H_{15})$
$20 - \alpha(H_9C_6H_{10})$	$30 - \alpha(H_{14}C_{11}H_{15}).$

External (intermolecular) coordinates are now defined for the 3-cluster; with respect to the peripheral molecule on the right side of Figure 5, these include one "bond" stretch,

$$31 - R(C_1C_{11}),$$

a torsional coordinate around the CC axis,

$$32 - \tau(H_2C_1C_6H_7),$$

two nutational coordinates of the central molecule (shell molecule "wagging"),

$$33 - \beta(H_2C_1C_6)$$
$$34 - \beta(H_3C_1C_6),$$

and two nutational coordinates of the shell molecule defined with correspondingly numbered hydrogens,

$$35 - \beta(H_7C_6C_1)$$
$$36 - \beta(H_8C_6C_1).$$

Six more external coordinates are defined analogously for the peripheral molecule on the left of Figure 5:

$$37 - R(C_1C_{11})$$
$$38 - \tau(H_2C_1C_{11}H_{12})$$
$$39 - \beta(H_2C_1C_{11})$$
$$40 - \beta(H_3C_1C_{11})$$
$$41 - \beta(H_{12}C_{11}C_1)$$
$$42 - \beta(H_{13}C_{11}C_1).$$

These coordinates are sufficient to describe the 42 modes of vibration (including 3 zero modes due to α redundancy) for a 3-cluster of methanes. Larger molecular aggregates studied in this research have been described in an exactly analogous fashion; coordinates for 7-, 9-, and 13-clusters are listed in Tables XI - XIII.

Table XI

Coordinate Definitions for the Methane 7-Cluster

s_1 - s_{30} are the same as those defined for the methane 3-cluster		
31 - $r(C_{16}H_{17})$	57 - $\alpha(H_{27}C_{26}H_{30})$	83 - $R(C_1C_{16})$
32 - $r(C_{16}H_{18})$	58 - $\alpha(H_{28}C_{26}H_{29})$	84 - $\tau(H_2C_1C_{16}H_{17})$
33 - $r(C_{16}H_{19})$	59 - $\alpha(H_{28}C_{26}H_{30})$	85 - $\beta(H_2C_1C_{16})$
34 - $r(C_{16}H_{20})$	60 - $\alpha(H_{29}C_{26}H_{30})$	86 - $\beta(H_3C_1C_{16})$
35 - $\alpha(H_{17}C_{16}H_{18})$	61 - $r(C_{31}H_{32})$	87 - $\beta(H_{17}C_{16}C_1)$
36 - $\alpha(H_{17}C_{16}H_{19})$	62 - $r(C_{31}H_{33})$	88 - $\beta(H_{18}C_{16}C_1)$
37 - $\alpha(H_{17}C_{16}H_{20})$	63 - $r(C_{31}H_{34})$	89 - $R(C_1C_{21})$
38 - $\alpha(H_{18}C_{16}H_{19})$	64 - $r(C_{31}H_{35})$	90 - $\tau(H_2C_1C_{21}H_{22})$
39 - $\alpha(H_{18}C_{16}H_{20})$	65 - $\alpha(H_{32}C_{31}H_{33})$	91 - $\beta(H_2C_1C_{21})$
40 - $\alpha(H_{19}C_{16}H_{20})$	66 - $\alpha(H_{32}C_{31}H_{34})$	92 - $\beta(H_3C_1C_{21})$
41 - $r(C_{21}H_{22})$	67 - $\alpha(H_{32}C_{31}H_{35})$	93 - $\beta(H_{22}C_{21}C_1)$
42 - $r(C_{21}H_{23})$	68 - $\alpha(H_{33}C_{31}H_{34})$	94 - $\beta(H_{23}C_{21}C_1)$
43 - $r(C_{21}H_{24})$	69 - $\alpha(H_{33}C_{31}H_{35})$	95 - $R(C_1C_{26})$
44 - $r(C_{21}H_{25})$	70 - $\alpha(H_{34}C_{31}H_{35})$	96 - $\tau(H_2C_1C_{26}H_{27})$
45 - $\alpha(H_{22}C_{21}H_{23})$	71 - $R(C_1C_6)$	97 - $\beta(H_2C_1C_{26})$
46 - $\alpha(H_{22}C_{21}H_{24})$	72 - $\tau(H_2C_1C_6H_7)$	98 - $\beta(H_3C_1C_{26})$
47 - $\alpha(H_{22}C_{21}H_{25})$	73 - $\beta(H_2C_1C_6)$	99 - $\beta(H_{27}C_{26}C_1)$
48 - $\alpha(H_{23}C_{21}H_{24})$	74 - $\beta(H_3C_1C_6)$	100 - $\beta(H_{28}C_{26}C_1)$
49 - $\alpha(H_{23}C_{21}H_{24})$	75 - $\beta(H_7C_6C_1)$	101 - $R(C_1C_{31})$
50 - $\alpha(H_{24}C_{21}H_{25})$	76 - $\beta(H_8C_6C_1)$	102 - $\tau(H_2C_1C_{31}H_{32})$
51 - $r(C_{26}H_{27})$	77 - $R(C_1C_{11})$	103 - $\beta(H_2C_1C_{31})$
52 - $r(C_{26}H_{28})$	78 - $\tau(H_2C_1C_{11}H_{12})$	104 - $\beta(H_3C_1C_{31})$
53 - $r(C_{26}H_{29})$	79 - $\beta(H_2C_1C_{11})$	105 - $\beta(H_{32}C_{31}C_1)$
54 - $r(C_{26}H_{30})$	80 - $\beta(H_3C_1C_{11})$	106 - $\beta(H_{33}C_{31}C_1)$
55 - $\alpha(H_{27}C_{26}H_{28})$	81 - $\beta(H_{12}C_{11}C_1)$	
56 - $\alpha(H_{27}C_{26}H_{29})$	82 - $\beta(H_{13}C_{11}C_1)$	

Table XII

Coordinate Definitions for the Methane 9-Cluster

s_1 - s_{70} are the same as those defined for the methane 7-cluster

71 - $r(C_{36}H_{37})$
72 - $r(C_{36}H_{38})$
73 - $r(C_{36}H_{39})$
74 - $r(C_{36}H_{40})$
75 - $\alpha(H_{37}C_{36}H_{38})$
76 - $\alpha(H_{37}C_{36}H_{39})$
77 - $\alpha(H_{37}C_{36}H_{40})$
78 - $\alpha(H_{38}C_{36}H_{39})$
79 - $\alpha(H_{38}C_{36}H_{40})$
80 - $\alpha(H_{39}C_{36}H_{40})$
81 - $r(C_{41}H_{42})$
82 - $r(C_{41}H_{43})$
83 - $r(C_{41}H_{44})$
84 - $r(C_{41}H_{45})$
85 - $\alpha(H_{42}C_{41}H_{43})$
86 - $\alpha(H_{42}C_{41}H_{44})$
87 - $\alpha(H_{42}C_{41}H_{45})$
88 - $\alpha(H_{43}C_{41}H_{44})$
89 - $\alpha(H_{43}C_{41}H_{45})$
90 - $\alpha(H_{44}C_{41}H_{45})$
91 - $R(C_1C_6)$
92 - $\tau(H_2C_1C_6H_7)$
93 - $\beta(H_2C_1C_6)$
94 - $\beta(H_3C_1C_6)$
95 - $\beta(H_7C_6C_1)$
96 - $\beta(H_8C_6C_1)$
97 - $R(C_1C_{11})$
98 - $\tau(H_2C_1C_{11}H_{12})$
99 - $\beta(H_2C_1C_{11})$
100 - $\beta(H_3C_1C_{11})$
101 - $\beta(H_{12}C_{11}C_1)$
102 - $\beta(H_{13}C_{11}C_1)$
103 - $R(C_1C_{16})$
104 - $\tau(H_2C_1C_{16}H_{17})$
105 - $\beta(H_2C_1C_{16})$
106 - $\beta(H_3C_1C_{16})$
107 - $\beta(H_{17}C_{16}C_1)$
108 - $\beta(H_{18}C_{16}C_1)$
109 - $R(C_1C_{21})$
110 - $\tau(H_2C_1C_{21}H_{22})$
111 - $\beta(H_2C_1C_{21})$
112 - $\beta(H_3C_1C_{21})$
113 - $\beta(H_{22}C_{21}C_1)$
114 - $\beta(H_{23}C_{21}C_1)$
115 - $R(C_1C_{26})$
116 - $\tau(H_2C_1C_{26}H_{27})$
117 - $\beta(H_2C_1C_{26})$
118 - $\beta(H_3C_1C_{26})$
119 - $\beta(H_{27}C_{26}C_1)$
120 - $\beta(H_{28}C_{26}C_1)$
121 - $R(C_1C_{31})$
122 - $\tau(H_2C_1C_{31}H_{32})$
123 - $\beta(H_2C_1C_{31})$
124 - $\beta(H_3C_1C_{31})$
125 - $\beta(H_{32}C_{31}C_1)$
126 - $\beta(H_{33}C_{31}C_1)$
127 - $R(C_1C_{36})$
128 - $\tau(H_2C_1C_{36}H_{37})$
129 - $\beta(H_2C_1C_{36})$
130 - $\beta(H_3C_1C_{36})$
131 - $\beta(H_{37}C_{36}C_1)$
132 - $\beta(H_{38}C_{36}C_1)$
133 - $R(C_1C_{41})$
134 - $\tau(H_2C_1C_{41}H_{42})$
135 - $\beta(H_2C_1C_{41})$
136 - $\beta(H_3C_1C_{41})$
137 - $\beta(H_{42}C_{41}C_1)$
138 - $\beta(H_{43}C_{41}C_1)$

Table XIII

Coordinate Definitions for the Methane 13-Cluster

s_1 - s_{90} are the same as those defined for the methane 9-cluster		
91 - $r(C_{46}H_{47})$	116 - $\alpha(H_{57}C_{56}H_{59})$	141 - $\beta(H_{12}C_{11}C_1)$
92 - $r(C_{46}H_{48})$	117 - $\alpha(H_{57}C_{56}H_{60})$	142 - $\beta(H_{13}C_{11}C_1)$
93 - $r(C_{46}H_{49})$	118 - $\alpha(H_{58}C_{56}H_{59})$	143 - $R(C_1C_{16})$
94 - $r(C_{46}H_{50})$	119 - $\alpha(H_{58}C_{56}H_{60})$	144 - $\tau(H_2C_1C_{16}H_{17})$
95 - $\alpha(H_{47}C_{46}H_{48})$	120 - $\alpha(H_{59}C_{56}H_{60})$	145 - $\beta(H_2C_1C_{16})$
96 - $\alpha(H_{47}C_{46}H_{49})$	121 - $r(C_{61}H_{62})$	146 - $\beta(H_3C_1C_{16})$
97 - $\alpha(H_{47}C_{46}H_{50})$	122 - $r(C_{61}H_{63})$	147 - $\beta(H_{17}C_{16}C_1)$
98 - $\alpha(H_{48}C_{46}H_{49})$	123 - $r(C_{61}H_{64})$	148 - $\beta(H_{18}C_{16}C_1)$
99 - $\alpha(H_{48}C_{46}H_{50})$	124 - $r(C_{61}H_{65})$	149 - $R(C_1C_{21})$
100 - $\alpha(H_{49}C_{46}H_{50})$	125 - $\alpha(H_{62}C_{61}H_{63})$	150 - $\tau(H_2C_1C_{21}H_{22})$
101 - $r(C_{51}H_{52})$	126 - $\alpha(H_{62}C_{61}H_{64})$	151 - $\beta(H_2C_1C_{21})$
102 - $r(C_{51}H_{53})$	127 - $\alpha(H_{62}C_{61}H_{65})$	152 - $\beta(H_3C_1C_{21})$
103 - $r(C_{51}H_{54})$	128 - $\alpha(H_{63}C_{61}H_{64})$	153 - $\beta(H_{22}C_{21}C_1)$
104 - $r(C_{51}H_{55})$	129 - $\alpha(H_{63}C_{61}H_{65})$	154 - $\beta(H_{23}C_{21}C_1)$
105 - $\alpha(H_{52}C_{51}H_{53})$	130 - $\alpha(H_{64}C_{61}H_{65})$	155 - $R(C_1C_{26})$
106 - $\alpha(H_{52}C_{51}H_{54})$	131 - $R(C_1H_6)$	156 - $\tau(H_2C_1C_{26}H_{27})$
107 - $\alpha(H_{52}C_{51}H_{55})$	132 - $\tau(H_2C_1C_6H_7)$	157 - $\beta(H_2C_1C_{26})$
108 - $\alpha(H_{53}C_{51}H_{54})$	133 - $\beta(H_2C_1C_6)$	158 - $\beta(H_3C_1C_{26})$
109 - $\alpha(H_{53}C_{51}H_{55})$	134 - $\beta(H_3C_1C_6)$	159 - $\beta(H_{27}C_{26}C_1)$
110 - $\alpha(H_{54}C_{51}H_{55})$	135 - $\beta(H_7C_6C_1)$	160 - $\beta(H_{28}C_{26}C_1)$
111 - $r(C_{56}H_{57})$	136 - $\beta(H_8C_6C_1)$	161 - $R(C_1C_{31})$
112 - $r(C_{56}H_{58})$	137 - $R(C_1C_{11})$	162 - $\tau(H_2C_1C_{31}H_{32})$
113 - $r(C_{56}H_{59})$	138 - $\tau(H_2C_1C_{11}H_{12})$	163 - $\beta(H_2C_1C_{31})$
114 - $r(C_{56}H_{60})$	139 - $\beta(H_2C_1C_{11})$	164 - $\beta(H_3C_1C_{31})$
115 - $\alpha(H_{57}C_{56}H_{58})$	140 - $\beta(H_3C_1C_{11})$	165 - $\beta(H_{32}C_{31}C_1)$

(continued)

Table XIII (continued)

166 - $\beta(H_{33}C_{31}C_1)$
167 - $R(C_1C_{36})$
168 - $\tau(H_2C_1C_{36}H_{37})$
169 - $\beta(H_2C_1C_{36})$
170 - $\beta(H_3C_1C_{36})$
171 - $\beta(H_{37}C_{36}C_1)$
172 - $\beta(H_{38}C_{36}C_1)$
173 - $R(C_1C_{41})$
174 - $\tau(H_2C_1C_{41}H_{42})$
175 - $\beta(H_2C_1C_{41})$
176 - $\beta(H_3C_1C_{41})$
177 - $\beta(H_{42}C_{41}C_1)$
178 - $\beta(H_{43}C_{41}C_1)$
179 - $R(C_1C_{46})$
180 - $\tau(H_2C_1C_{46}H_{47})$
181 - $\beta(H_2C_1C_{46})$
182 - $\beta(H_3C_1C_{46})$
183 - $\beta(H_{47}C_{46}C_1)$
184 - $\beta(H_{48}C_{46}C_1)$
185 - $R(C_1C_{51})$
186 - $\tau(H_2C_1C_{51}H_{52})$
187 - $\beta(H_2C_1C_{51})$
188 - $\beta(H_3C_1C_{51})$
189 - $\beta(H_{52}C_{51}C_1)$
190 - $\beta(H_{53}C_{51}C_1)$
191 - $R(C_1C_{56})$
192 - $\tau(H_2C_1C_{56}H_{57})$
193 - $\beta(H_2C_1C_{56})$
194 - $\beta(H_3C_1C_{56})$
195 - $\beta(H_{57}C_{56}C_1)$
196 - $\beta(H_{58}C_{56}C_1)$
197 - $R(C_1C_{61})$
198 - $\tau(H_2C_1C_{61}H_{62})$
199 - $\beta(H_2C_1C_{61})$
200 - $\beta(H_3C_1C_{61})$
201 - $\beta(H_{62}C_{61}C_1)$
202 - $\beta(H_{63}C_{61}C_1)$

IV-3: Construction of the Medium Cluster Force Field

A generalized force field ($\underset{\sim}{F}$-matrix) was constructed for m-cluster models (m = 3,7,9,13) of the liquid state for use in the secular equation. As a first requirement, the liquid-phase $\underset{\sim}{F}$-matrix must reproduce the observed spectroscopic frequency shifts on condensation, $\delta\nu$, for CH_4 within experimental error, where

$$\delta\nu = \nu_{gas} - \nu_{condensed} \tag{184}$$

Since the gas frequencies are already determined by the Jones - McDowell $\underset{\sim}{F}$ (Table I) and a well-defined $\underset{\sim}{G}$ for gaseous methane, and the condensed phase $\underset{\sim}{G}$ is determined from the nature of the model, the frequency shifts on condensation are dependent only on the choice of the F-matrix for the m-cluster.

With the coordinates defined in the previous section, a homologous series of $\underset{\sim}{F}$-matrices for m-clusters (denoted $\underset{\sim}{F}_m$) has the form

$$\underset{\sim}{F}_m = \begin{pmatrix} \underset{\sim}{F}_c & \underset{\sim}{F}_{cs} & \underset{\sim}{F}_{ce} \\ & \underset{\sim}{F}_s & \\ & & \underset{\sim}{F}_{ss} \quad \underset{\sim}{F}_{se} \\ & & \ddots \\ & & \underset{\sim}{F}_s \\ & & \underset{\sim}{F}_e \end{pmatrix} \tag{185}$$

where the areas labeled $\underset{\sim}{F}_c$, $\underset{\sim}{F}_s$, $\underset{\sim}{F}_e$, $\underset{\sim}{F}_{cs}$, $\underset{\sim}{F}_{ss}$, $\underset{\sim}{F}_{ce}$, and $\underset{\sim}{F}_{se}$ have analogous meanings to those labels used with the $\underset{\sim}{G}$-matrix in Equation (181). The ellipsis in Equation (185) indicates the variability in the size of $\underset{\sim}{F}$ for different clusters.

In this study, explicit force interactions between internal coordinates in two different shell molecules have been neglected. This approximation parallels the assumption of independent ligand vibration first proposed by Cotton and Kraihänzel (100) in connection with spectroscopic studies of inorganic coordination compounds. If the approximation is valid for such complexes, it is reasonable to assume its applicability to the much weaker forces postulated in the medium cluster model. We have further assumed that all off-diagonal terms of $\underset{\sim}{F}$ that explicitly involve an interaction of an intramolecular shell force with either an intramolecular central force or an intermolecular external force vanish. Thus,

$$(f_{ij})_{ss} = (f_{ij})_{cs} = (f_{ij})_{se} = 0 \qquad (186)$$

where the outer subscript indicates membership in the appropriate region of the $\underset{\sim}{F}_m$-matrix. These assumptions are altogether valid when one reflects on the nature of the medium cluster model, i.e., only the central molecule represents the bulk liquid phase and the explicit interactions of the shell molecules are of secondary importance.

The area of $\underset{\sim}{F}_m$ in Equation (185) labeled "ce" contains elements representing interactions of intramolecular central forces with

intermolecular external forces. Non-zero force constants in this region will be shown in Section V-4 to have important consequences, but for a preliminary examination of the MCM theory, we have assumed

$$(f_{ij})_{ce} = 0 \tag{187}$$

$\underset{\sim}{F}_m$ in Equation (185) is thus a sparse matrix with non-zero blocks of elements arranged along the major diagonal. Since the internal forces of all m-1 shell molecules are identical, the construction of the $\underset{\sim}{F}$-matrix consisted of finding a central molecular force field, a shell molecular force field, and an external intermolecular force field,

$$\underset{\sim}{F}_m = \underset{\sim}{F}_c \oplus \underset{\sim}{F}_s \oplus \cdots \oplus \underset{\sim}{F}_s \oplus \underset{\sim}{F}_c \tag{188}$$

where $\oplus$ indicates a direct sum.

a. Cental Molecular Forces

The central molecule of the cluster is representative of the condensed phase, so that central molecular force constants are not expected to be very different from those used successfully with the simple cell model. As a first approximation, therefore, the liquid $\underset{\sim}{F}$-matrix used by BCJ (Table VII) was substituted for F_c in Equation (185). F_s and F_e were calculated concurrently by methods to be described later in this section. By slowly varying each $(f_{ij})_c$ element of $\underset{\sim}{F}_c$ and solving the resulting secular equation for each different

$\underset{\sim}{F}_m$, we obtained sets of liquid-phase frequencies for each slightly different central molecular force field. The vapor pressure isotope factors A and B were calculated from Equations (86) and (87) for each small change in $\underset{\sim}{F}_c$ and, finally, we evaluated $(\partial B/\partial f^c_{ij})$ for each element in the central internal region of $\underset{\sim}{F}_m$. The results are shown in Table XIV for 3-, 7-, 9-, and 13-clusters. It was found that $(\partial B/\partial f^c_{ij})$ was nearly linear within a small neighborhood of the BCJ simple cell model $\underset{\sim}{F}$-matrix. Furthermore, as can be seen from Table XIV, the change in B per unit change in any $(f_{ij})_c = f^c_{ij}$ is almost independent of cluster size, m.

The A factor did not change appreciably as the central molecular force constants were varied.

In the BCJ simple cell model, of the five non-zero elements of the gas-phase $\underset{\sim}{F}$-matrix, only f_r, f_α, and $f'_{r\alpha}$ need undergo change upon condensation in order to produce acceptable liquid-phase frequencies. In theory, then, one could obtain an acceptable $\underset{\sim}{F}_c$ in the MCM from the experimental values of B for three isotopes by iteratively solving the equations

$$\Delta B^{13} = \frac{\partial B^{13}}{\partial f^c_r}\Delta f_r + \frac{\partial B^{13}}{\partial f^c_\alpha}\Delta f_\alpha + \frac{\partial B^{13}}{\partial f'^c_{r\alpha}}\Delta f'_{r\alpha} \qquad (189)$$

$$\Delta B^{14} = \frac{\partial B^{14}}{\partial f^c_r}\Delta f_r + \frac{\partial B^{14}}{\partial f^c_\alpha}\Delta f_\alpha + \frac{\partial B^{14}}{\partial f'^c_{r\alpha}}\Delta f'_{r\alpha} \qquad (190)$$

$$\Delta B^{D} = \frac{\partial B^{D}}{\partial f^c_r}\Delta f_r + \frac{\partial B^{D}}{\partial f^c_\alpha}\Delta f_\alpha + \frac{\partial B^{D}}{\partial f'^c_{r\alpha}}\Delta f'_{r\alpha} \qquad (191)$$

Table XIV

Dependence of the Isotopic B Factor on
Central Molecular Force Constants and Cluster Size;
Gear Geometry; $|\vec{\rho}| = 3.817$ Å

Isotope	Cluster size	$(\partial B/\partial f_r^c)$ (°K/mdyne Å^{-1})	$(\partial B/\partial f_\alpha^c)$ (°K/mdyne Å)	$(\partial B/\partial f'^c_{r\alpha})$ (°K/mdyne)
$^{13}CH_4$	m=3	-2.184	3.450	20.781
	m=7	-2.186	3.460	20.781
	m=9	-2.186	3.482	20.778
	m=13	-2.188	3.500	20.791
$^{14}CH_4$	m=3	-4.430	-27.320	38.087
	m=7	-4.450	-27.308	38.075
	m=9	-4.452	-27.296	38.090
	m=13	-4.400	-27.400	38.064
$^{12}CD_4$	m=3	-221.710	-1605.860	-15.491
	m=7	-220.963	-1618.110	-15.501
	m=9	-220.903	-1614.350	-15.504
	m=13	-220.900	-1608.010	-15.494

where

$$\Delta f_{ij} = f_{ij}(\text{trial}) - f^{c}_{ij} \tag{192}$$

$$\Delta B = B(\text{calc}) - B(\text{exp}) \tag{193}$$

and the notation B^{13}, B^{14}, and B^{D} represents the B-values for $^{13}CH_4$, $^{14}CH_4$, and $^{12}CD_4$. Equations (189) - (191) are solved simultaneously for f_r, f_α, and $f'_{r\alpha}$. However, because of inaccuracies in the experimental B's and the slight non-linearity of $(\partial B/\partial f_{ij})$, the required changes in f_r, f_α, and $f'_{r\alpha}$ thus obtained were found to be unrealistic even after some allowance was made for the effect of experimental uncertainties in B. A more reliable procedure would be to assign some elements of $\underset{\sim}{F}_c$ directly on the basis of observed $\delta\nu$, and then optimizing $\underset{\sim}{F}_c$ by means of Equations (189) - (191). Since the totally symmetric stretching mode of $\mathcal{T}_d$ molecules, $\nu(A_1)$, is dependent only on the stretching force constant f_r, an optimum stretching force constant was determined by varying f^{c}_{r} until an acceptable A_1 frequency shift was found (101). With the stretching force constant so fixed, we simultaneously solved

$$\Delta B^{13} = \frac{\partial B^{13}}{\partial f^{c}_{\alpha}} \Delta f_\alpha + \frac{\partial B^{13}}{\partial f'^{c}_{r\alpha}} \Delta f'_{r\alpha} \tag{194}$$

$$\Delta B^{14} = \frac{\partial B^{14}}{\partial f^{c}_{\alpha}} \Delta f_\alpha + \frac{\partial B^{14}}{\partial f'^{c}_{r\alpha}} \Delta f'_{r\alpha} \tag{195}$$

$$\Delta B^{D} = \frac{\partial B^{D}}{\partial f^{c}_{\alpha}} \Delta f_\alpha + \frac{\partial B^{D}}{\partial f'^{c}_{r\alpha}} \Delta f'_{r\alpha} \tag{196}$$

where the ΔB-values are the residual discrepancies between the calculated and experimental B's after the effect of the stretching force constant, f_r^c, has been taken into account. Since this set of equations overdetermines Δf, one equation may be eliminated. The vapor pressure isotope effect of $^{14}CH_4$ is determined by a radioactive tracer technique, which is considerably less accurate than cryostatic manometry or column distillation methods. The experimental B-value in Equation (193) for this isotope is somewhat less dependable than that for $^{13}CH_4$ or $^{12}CD_4$. Therefore, Equation (195) was eliminated from consideration and $\underset{\sim}{F}_c$ was found by solving the two remaining equations simultaneously. The $\underset{\sim}{F}_c$-matrices thus determined for various sized clusters is given in Table XV.

b. Shell Molecular Forces

The one-component condensed phase in the medium cluster model is considered to be a mixture of central- and shell-quasicomponents. Ben-Naim (102) has shown that the mole fractions of quasicomponents in such a mixture-model can be used to gain insight into the way extensive properties are distributed over the various species. Since the shell molecules in a cluster are being used to simulate the entire bulk phase, it would be unrealistic to assign equal force constants to the central and shell components. The shell molecule force constants must reflect the existence of additional hierarchical coordination spheres and the distribution of energy among central and shell molecules. This has been done by considering how the electronic kinetic energy for the entire system changes upon con-

Table XV

Central Molecular Force Field for Liquid Methane
Gear Geometry; $|\vec{\rho}| = 3.817$ Å

	3-Cluster	7-Cluster	9-Cluster	13-Cluster
f_r^c (mdyne/Å)	5.4573	5.4573	5.4573	5.4573
f_α^c (mdyne·Å)	0.5654	0.5612	0.5590	0.5610
f_{rr}^c (mdyne/Å)	0.1240	0.1240	0.1240	0.1240
$f_{r\alpha}'^c$ (mdyne)	0.1901	0.1993	0.1989	0.1996
$f_{\alpha\alpha}'^c$ (mdyne·Å)	0.0190	0.0190	0.0190	0.0190

densation and then apportioning the energy into "shell" and "central" regions. The arguments which follow are due to Bader and coworkers (103,104,105) and Srebrenik (106).

The electronic energy density, $E(\vec{x})$, for the supermolecular aggregate can be expressed as (104)

$$E(\vec{x}) = K(\vec{x}) + V^1(\vec{x}) + V^2(\vec{x}) \tag{197}$$

where $K(\vec{x})$ is the electronic kinetic energy density expressed in the Schrödinger form. The terms $V^1(\vec{x})$ and $V^2(\vec{x})$ represent contributions of the one- and two-electron potential energy densities. Each density term in Equation (197) is indicated as depending on electronic coordinates, $\vec{x}$.

The observable electronic kinetic energy, $<T>$, is defined as

$$<T> = \iiint_V J(\vec{x})\, d\vec{x} \tag{198}$$

where

$$J(\vec{x}) = \tfrac{1}{2} \sum_i \lambda_i \nabla\psi_i(\vec{x}) \cdot \nabla\psi_i(\vec{x}) \tag{199}$$

The λ_i are occupation numbers for the $i^{\underline{th}}$ orbital. From Equation (198), it is seen that $J(\vec{x})$ is dimensionally equivalent to an energy density and it can be shown (107) that the two formulations for kinetic energy density, $K(\vec{x})$ and $J(\vec{x})$, are related by

$$J(\vec{x}) - K(\vec{x}) = \tfrac{1}{4} \nabla^2\gamma(\vec{x}) \tag{200}$$

where $\gamma(\vec{x})$ is the electron charge density. Taking a volume integral of both sides of Equation (200) gives

$$\iiint_V \{J(\vec{x}) - K(\vec{x})\}\,dV = \tfrac{1}{4}\iiint_V \nabla^2\gamma(\vec{x})dV \tag{201}$$

Using the divergence theorem (Green's theorem in three dimensions),

$$\iiint_V \nabla^2 f = \iint_S \frac{\partial f}{\partial \vec{n}} \tag{202}$$

where f is a scalar field and S is an orientable boundary surface of V with normal $\vec{n}$, the right side of Equation (201) becomes

$$\tfrac{1}{4}\iiint_V \nabla^2\gamma(\vec{x})dV = \tfrac{1}{4}\iint_S \frac{d\gamma(\vec{x})}{d\vec{\rho}_i}\,dS \tag{203}$$

where $\vec{\rho}_i$ is the position vector from the central molecule to the $i^{\underline{th}}$ shell molecule. Then,

$$\iiint_V \{J(\vec{x}) - K(\vec{x})\}dV = \tfrac{1}{4}\iint_S \frac{d\gamma(\vec{x})}{d\vec{\rho}_i}dS \tag{204}$$

and in order for the two formulations of the kinetic energy density to be equivalent, i.e., $J(\vec{x}) = K(\vec{x})$, the relation

$$d\gamma(\vec{x}) / d\vec{\rho}_i = 0 \tag{205}$$

must hold at the boundary surface, S. Bader and Beddall (104) have

shown that, within such a boundary surface, it is reasonable to postulate the existence of a virial relationship,

$$-\langle T_i \rangle = \langle V_i \rangle \tag{206}$$

for any part i of a molecular system. The need for such a relationship is evident from Equation (197); the electronic potential energy density change upon condensation cannot be followed because the two-electron potential, $V^2(\vec{x})$, may contain large interaction terms between electrons in different molecules, nor can the total energy density change be followed since it depends on $V^2(\vec{x})$. We may, however, examine the behavior of the electronic kinetic energy, T, which depends on $K(\vec{x})$ or $J(\vec{x})$, and then by using Equation (206), relate the potential energy to the kinetic energy within the boundary defined by Equation (205). The potential energy cannot be examined directly since there is no expression for $V^1(\vec{x}) + V^2(\vec{x})$ analogous to Equation (200).

In a condensed phase, all molecules are equivalent and indistinguishable. The two-quasicomponent medium cluster model, however, imposes the labels "shell" and "central" on the molecules. Nevertheless, for a system of N molecules, the electronic kinetic energy gained on condensation must be the same for each of these two species. Therefore,

$$\sum^{N/m} \langle T_c^* \rangle = \sum^{N-N/m} \langle T_s^* \rangle \tag{207}$$

where

$$\langle T^* \rangle = \langle T \rangle_{condensed} - \langle T \rangle_{gas} \tag{208}$$

In Equation (207), the summation on the left side spans all molecules labeled "central" and that on the right side all molecules labeled "shell". Since all shell molecules are identical in a regular m-cluster,

$$\sum^{N-N/m} \langle T_s^* \rangle = (m-1) \sum^{N/m} \langle T_s^* \rangle \tag{209}$$

so that

$$\sum^{N/m} \langle T_c^* \rangle = (m-1) \sum^{N/m} \langle T_s^* \rangle \tag{210}$$

The summations on the right of Equations (209) and (210) refer to one shell molecule per cluster, not all shell molecules in the condensed phase. Considering only a single cluster as representative of the entire liquid phase gives

$$\langle T_c^* \rangle = (m-1) \langle T_s^* \rangle \tag{211}$$

If the shell and central regions of the cluster are defined in

accordance with the restriction of Equation (205), the two-electron potential between regions is minimized so that the Bader and Beddall relation of Equation (206) can be used to give

$$\langle V_c^* \rangle = (m-1)\langle V_s^* \rangle \tag{212}$$

Since the electronic potentials of all gas molecules are the same, Equation (212) becomes

$$\langle V_c \rangle - \langle V_g \rangle = (m-1)\{\langle V_s \rangle - \langle V_g \rangle\} \tag{213}$$

The Born-Oppenheimer approximation states that the nuclear motions of a molecule can be viewed as occurring in a potential field provided by the electrons. This implies that the forces acting on the nuclei are expressible as gradients of this electronic potential field, and that the force constants are functions of electronic potential energy. If exact wavefunctions are known, the generalized Hellmann-Feynman theorem (43) can be used to calculate force constants. However, an ab initio quantum mechanical evaluation of force constants is not feasible for the present system, so we have assumed that any small change in f_{ij} on condensation is proportional to the change in electronic potential energy. Equation (213) therefore implies

$$(f_{ij})_c - (f_{ij})_g = (m-1)[(f_{ij})_s - (f_{ij})_g] \tag{214}$$

to a first approximation. Considering the entire $\underset{\sim}{F}_m$-matrix,

$$\underset{\sim}{F}_s = \underset{\sim}{F}_g + \frac{1}{m-1}\left(\underset{\sim}{F}_c - \underset{\sim}{F}_g\right) \tag{215}$$

where $\underset{\sim}{F}_c$ and $\underset{\sim}{F}_s$ are the central and shell submatrices appearing in Equation (185), and $\underset{\sim}{F}_g$ is the Jones-McDowell force field for the gas phase. The $(f_{ij})_s$ values used for various sized clusters are given in Table XVI.

c. External Forces

The external intermolecular portion of the potential energy matrix, $\underset{\sim}{F}_e$, consists of m-1 submatrices; since external coordinates are defined in the same way relative to each shell molecule in the cluster, corresponding elements in these external submatrices are equal,

$$(f_{ij})_e = (f_{i+6p,j+6p})_e \quad \begin{bmatrix} i,j = 10m+1,\ldots,16m-6 \\ p = 1,2,\ldots,m-2 \end{bmatrix} \tag{216}$$

Interaction constants are assumed to be zero in the $\underset{\sim}{F}_e$ region. Nutational motion of shell and cental molecules are defined equivalently, and so we chose to use the same value for all diagonal nodding constants, f_β. There are thus three constants to be determined: f_R, the C_cC_s stretching force constant, f_τ, the $H_cC_cC_sH_s$ torsional force constant, and f_β, the $H_cC_cC_s$ and $H_sC_sC_c$ angle bending force constant.

Values for the external force constants were determined by

Table XVI

Shell Molecular Force Field for Liquid Methane
Calculated from Equation (215)

	3-Cluster	7-Cluster	9-Cluster	13-Cluster
f_r^s (mdyne/Å)	5.4762	5.4887	5.4903	5.4919
f_α^s (mdyne·Å)	0.5667	0.5668	0.5668	0.5673
f_{rr}^s (mdyne/Å)	0.1240	0.1240	0.1240	0.1240
$f_{r\alpha}'^c$ (mdyne)	0.1776	0.1707	0.1692	0.1676
$f_{\alpha\alpha}'^c$ (mdyne·Å)	0.0190	0.0190	0.0190	0.0190

a method similar to that used for the elements of $\underset{\sim}{F}_c$. The rate of change of the vpie A factor with small changes in $\underset{\sim}{F}_e$ is nearly linear, so that an appropriate set of external force constants may be obtained by finding $(\partial A/\partial f^e_{ij})$ for each of the three independent external force constants and then calculating an $\underset{\sim}{F}_e$-matrix that reproduces the experimental A values for $^{13}CH_4$, $^{14}CH_4$ and $^{12}CD_4$. The equations used are

$$\Delta A^{13} = \frac{\partial A^{13}}{\partial f_R}\Delta f_R + \frac{\partial A^{13}}{\partial f}\Delta f + \frac{\partial A^{13}}{\partial f_\beta}\Delta f_\beta \qquad (217)$$

$$\Delta A^{14} = \frac{\partial A^{14}}{\partial f}\Delta f_R + \frac{\partial A^{14}}{\partial f}\Delta f + \frac{\partial A^{14}}{\partial f_\beta}\Delta f_\beta \qquad (218)$$

$$\Delta A^{D} = \frac{\partial A^{D}}{\partial f_R}\Delta f_R + \frac{\partial A^{D}}{\partial f}\Delta f + \frac{\partial A^{D}}{\partial f_\beta}\Delta f_\beta \qquad (219)$$

where Δf and ΔA are defined in a manner similar to Equations (192) and (193). As can be seen from Table XVII, values of $(\partial A/\partial f^e_{ij})$ are almost independent of cluster size. This was expected since we assumed no direct potential interaction between shell molecules. Satisfactory agreement of MCM calculated vpie factors with experiment is obtained when the following force constant values are used: $f_R = 0.0555$ mdyne/Å, $f = 0.00375$ mdyne·Å, $f = 0.00520$ mdyne·Å.

In the process of constructing a complete $\underset{\sim}{F}$-matrix for the cluster model of the liquid phase, many off-diagonal elements

Table XVII

Dependence of the Isotopic A Factor on Intramolecular Force Constants and Cluster Size; Gear Geometry; $|\vec{\rho}| = 3.817$ Å

Isotope	Cluster size	$(\partial A/\partial f_R^e)$ ($^\circ K^2/\mu dyne\,Å^{-1}$)	$(\partial A/\partial f^e)$ ($^\circ K^2/\mu dyne\,Å$)	$(\partial A/\partial f_\beta^e)$ ($^\circ K^2/\mu dyne\,Å$)
$^{13}CH_4$	m=3	40.661	8.851	35.662
	m=7	40.664	8.860	35.663
	m=9	40.663	8.865	35.661
	m=13	40.660	8.900	35.658
$^{14}CH_4$	m=3	43.052	8.851	35.905
	m=7	43.055	8.863	35.900
	m=9	43.045	8.866	35.887
	m=13	43.044	8.898	35.875
$^{12}CD_4$	m=3	47.836	31.940	526.02
	m=7	47.841	31.944	557.02
	m=9	47.839	31.963	558.02
	m=13	47.837	31.954	540.002

have been assumed to be negligible. It must be emphasized that the goal of these calculations has not been the determination of a "true" force field, rather, we have been concerned with a correlation of the vapor pressure isotope effect of methane with a reasonable and consistant $\underset{\sim}{F}$-matrix.

IV-4: Solution of the Secular Equation by the Jacobi Method

With the potential and kinetic energy matrices thus defined for the MCM secular equation, the computational method by which Equation (112) was solved will now be discussed.

The solution of the secular equation consists of finding the eigenvectors and eigenvalues of the $\underset{\sim}{H} = \underset{\sim}{G}\underset{\sim}{F}$ matrix. One of the most efficient machine methods of accomplishing this is the simultaneous diagonalization of $\underset{\sim}{F}$ and $\underset{\sim}{G}$ [Equation (116) ff.].

Since $\underset{\sim}{G}$ is a real symmetric matrix, a unitary transformation, $\underset{\sim}{A}$, exists that will diagonalize $\underset{\sim}{G}$ (108). Thus,

$$\underset{\sim}{A}^{\dagger}\underset{\sim}{G}\underset{\sim}{A} = \underset{\sim}{\Gamma} \tag{220}$$

where $\underset{\sim}{\Gamma}$ is the kinetic energy matrix in diagonal form. The actual algorithm for finding $\underset{\sim}{A}$, called the Jacobi method, will be discussed shortly. Rearranging Equation (220), and taking the inverse of both sides gives

$$\underset{\sim}{G}^{-1} = \underset{\sim}{A}\,\underset{\sim}{\Gamma}^{-1}\underset{\sim}{A}^{-1} \tag{221}$$

from which it is seen that $\underset{\sim}{A}$ also diagonalizes $\underset{\sim}{G}^{-1}$,

$$\underset{\sim}{A}^{\dagger}\underset{\sim}{G}^{-1}\underset{\sim}{A} = \underset{\sim}{A}^{\dagger}\underset{\sim}{A}\,\underset{\sim}{\Gamma}^{-1}\underset{\sim}{A}^{-1}\underset{\sim}{A} = \underset{\sim}{\Gamma}^{-1} \tag{222}$$

Since $\underset{\sim}{\Gamma}$ is diagonal with elements γ_i, $\underset{\sim}{\Gamma}^{-1}$ is also diagonal with elements $1/\gamma_i$. A coordinate system $\underset{\sim}{Y}$ is now defined such that

$$\underset{\sim}{S} = \underset{\sim}{A}\underset{\sim}{Y} \tag{223}$$

and

$$\dot{\underset{\sim}{S}} = \underset{\sim}{A}\dot{\underset{\sim}{Y}} \tag{224}$$

where $\underset{\sim}{S}$ is the matrix of internal coordinates. Substituting Equation (224) into Equation (98), where the definition of the kinetic energy is given, yields

$$2T = \underset{\sim}{Y}^{\dagger}\underset{\sim}{\Gamma}^{-1}\underset{\sim}{Y} \tag{225}$$

which can be expressed as

$$2T = \sum_{i=1}^{n} \dot{y}_i^2/\gamma_i \tag{226}$$

A column matrix $\dot{\underset{\sim}{Z}}$ is introduced having elements $\dot{z}_i$ defined by

$$\dot{z}_i = \dot{y}_i/\gamma_i^{\frac{1}{2}} \tag{227}$$

The kinetic energy then becomes

$$2T = \dot{\underset{\sim}{Z}}^{\dagger}\dot{\underset{\sim}{Z}} \tag{228}$$

The $\underset{\sim}{F}$-matrix will now be diagonalized using the same $\underset{\sim}{A}$-matrix used to diagonalize $\underset{\sim}{G}$ as a basis. A matrix $\underset{\sim}{W}$ is constructed consisting of elements w_{ij} defined as

$$w_{ij} = \gamma_i^{\frac{1}{2}} a_{ij} \tag{229}$$

where a_{ij} are the elements of $\underset{\sim}{A}$. Then,

$$\underset{\sim}{A}\underset{\sim}{Y} = \underset{\sim}{W}\underset{\sim}{Z} = \underset{\sim}{S} \tag{230}$$

from Equations (223), (227) and (229). Equation (230) can be used with the definition of the potential energy of the system, Equation (93), to give

$$2V = (\underset{\sim}{W}\underset{\sim}{Z})^{\dagger}\underset{\sim}{F}(\underset{\sim}{W}\underset{\sim}{Z}) = \underset{\sim}{Z}^{\dagger}\underset{\sim}{D}\underset{\sim}{Z} \tag{231}$$

where $\underset{\sim}{D}$ is given by

$$\underset{\sim}{D} = \underset{\sim}{W}^{\dagger}\underset{\sim}{F}\underset{\sim}{W} \tag{232}$$

The $\underset{\sim}{D}$ matrix is symmetric, so that the Jacobi method can be used for its diagonalization,

$$\underset{\sim}{C}^{\dagger}\underset{\sim}{D}\underset{\sim}{C} = \underset{\sim}{\Lambda} \tag{233}$$

where $\underset{\sim}{C}$ is a unitary matrix and $\underset{\sim}{\Lambda}$ is a diagonal matrix. With this transformation, a matrix $\underset{\sim}{Q}$ is defined,

$$\underset{\sim}{Q} = \underset{\sim}{C}^{-1}\underset{\sim}{Z} \tag{234}$$

so that

$$2V = \underset{\sim}{Z}^{\dagger}\underset{\sim}{D}\underset{\sim}{Z} = \underset{\sim}{Q}^{\dagger}\underset{\sim}{C}^{\dagger}\underset{\sim}{D}\underset{\sim}{C}\underset{\sim}{Q} = \underset{\sim}{Q}^{\dagger}\underset{\sim}{\Lambda}\underset{\sim}{Q} \tag{235}$$

and

$$2T = \dot{\underset{\sim}{Z}}^{\dagger}\dot{\underset{\sim}{Z}} = \dot{\underset{\sim}{Q}}^{\dagger}\underset{\sim}{C}^{\dagger}\underset{\sim}{C}\dot{\underset{\sim}{Q}} = \dot{\underset{\sim}{Q}}^{\dagger}\dot{\underset{\sim}{Q}} \tag{236}$$

Comparison of these last two equations with Equations (118) and (119) shows that $\underset{\sim}{Q}$ is indeed the normal coordinate matrix. The

$\underset{\sim}{G}$- and $\underset{\sim}{F}$-matrices have been simultaneously diagonalized to $\underset{\sim}{\Gamma}$ and $\underset{\sim}{\Lambda}$ by using the relations

$$\underset{\sim}{S} = \underset{\sim}{A}\underset{\sim}{Y} = \underset{\sim}{W}\underset{\sim}{Z} = \underset{\sim}{W}\underset{\sim}{C}\underset{\sim}{Q} \tag{237}$$

with the definitions of potential and kinetic energies. The transformation from internal coordinates to normal coordinates, $\underset{\sim}{L}^{-1}$, defined in Equation (116), which diagonalizes $\underset{\sim}{G}$ and $\underset{\sim}{F}$, is thus given by

$$\underset{\sim}{L}^{-1} = (\underset{\sim}{W}\underset{\sim}{C})^{-1} = (\underset{\sim}{W}\underset{\sim}{C})^{\dagger} \tag{238}$$

since $\underset{\sim}{W}$ and $\underset{\sim}{C}$ are both unitary.

The Jacobi method, used in the present work to diagonalize $\underset{\sim}{G}$ and $\underset{\sim}{D}$ in Equations (221) and (233), thereby defining $\underset{\sim}{A}$ and $\underset{\sim}{C}$, is an iterative process well suited for high-speed machine calculations (109,110,111). The method subjects a real n x n symmetric matrix, $\underset{\sim}{R}$, to a sequence of simple unitary transformations which do not alter the eigenvalues of $\underset{\sim}{R}$. Each transformation is an n x n rotation matrix, $\underset{\sim}{O}_k$, of the form

$$\underset{\sim}{O}_k = \begin{pmatrix} \ddots & & \\ & \cos\phi_k & -\sin\phi_k \\ & \sin\phi_k & \cos\phi_k \\ & & \ddots \end{pmatrix} \tag{239}$$

where the ellipses indicate unity along the remainder of the principal diagonal and zero elsewhere. Consider one step in the iterative sequence where $\underset{\sim}{R}$ is transformed to $\underset{\sim}{P}$. If the four elements of Equation (239) are chosen to be in the (i,i), (i,j), (j,i) and (j,j) positions, then

$$\underset{\sim}{P} = \underset{\sim}{O}_k^{-1} \underset{\sim}{R} \underset{\sim}{O}_k \tag{240}$$

with

$$p_{ii} = r_{ii}\cos^2\phi_k + 2r_{ij}\sin\phi_k\cos\phi_k + r_{jj}\sin^2\phi_k \tag{241}$$

$$p_{ji} = p_{ij} = (r_{jj} - r_{ii})\sin\phi_k\cos\phi_k + r_{ij}(\cos^2\phi_k - \sin^2\phi_k) \tag{242}$$

$$p_{jj} = r_{ii}\sin^2\phi_k - 2r_{ij}\sin\phi_k\cos\phi_k + r_{jj}\cos^2\phi_k \tag{243}$$

The trigonometric argument for the $k^{\underline{th}}$ step, ϕ_k, is chosen such that

$$\tan 2\phi_k = 2r_{ij}/(r_{ii} - r_{jj}) \tag{244}$$

yielding

$$p_{ij} = p_{ji} = 0 \tag{245}$$

Each step of the Jacobi method therefore makes a pair of off-diagonal elements zero. Unfortunately, subsequent steps, while creating new pairs of off-diagonal zeros, introduce non-zero elements into formerly zero positions. However, repeated application of Jacobi rotations to that (i,j) position containing the largest off-diagonal element will eventually transform the original matrix to a diagonal matrix (110,111).

An estimate of the number of iterations needed to diagonalize $\underset{\sim}{R}$ can be made as follows. A function $\hat{J}$ is defined as the sum of squares of the off-diagonal elements. It can be shown (112) that if r_{ij} is the largest off-diagonal element of $\underset{\sim}{R}$ in any one step of the Jacobi algorithm, then

$$\hat{J}(\underset{\sim}{P}) = \hat{J}(\underset{\sim}{O}_k \underset{\sim}{R} \underset{\sim}{O}_k) = \hat{J}(\underset{\sim}{R}) - 2r_{ij}^2 \tag{246}$$

Since r_{ij} is the largest off-diagonal element,

$$\hat{J}(R) \leq \frac{2n(n-1)}{2} r_{ij}^2 \tag{247}$$

Combining Equations (246) and (247) gives

$$\hat{J}(\underset{\sim}{P}) \leq \left[1 - \frac{2}{n^2-n}\right] \hat{J}(\underset{\sim}{R}) \tag{248}$$

for each step in the iterative process. After t such steps, we have

$$\hat{J}(\underset{\sim}{P}_t) \leq \left(1 - \frac{2}{n^2-n}\right)^t \hat{J}(\underset{\sim}{R}) \tag{249}$$

The sum of squares of the off-diagonal elements can be made as small as desired, so that if

$$\epsilon = \frac{\hat{J}(\underset{\sim}{P}_t)}{\hat{J}(\underset{\sim}{R})} - \hat{J}(\underset{\sim}{E}) \tag{250}$$

where $\underset{\sim}{E}$ is the n x n unit matrix, then

$$t \approx \frac{\log \epsilon}{\log\left(1 - \frac{2}{n^2-n}\right)} \tag{251}$$

For example, diagonalization of $\underset{\sim}{G}$ and $\underset{\sim}{F}$ for the 13-cluster required use of the Jacobi algorithm for 202 x 202 square matrices. We wanted the sum of off-diagonals to be less than $2^{-27} = 7.4 \times 10^{-9}$, so that the number of iterations carried out exceeded 379,000. The computing system required approximately 2100 μsec for each Jacobi rotation, so that the full diagonalization process took about 13.3 minutes. Access and buffer allocation time typically inflated this figure by about 290%.

The diagonalization steps are by far the most costly portion of the theoretical calculation of the vapor pressure isotope effect. We have made several attempts to increase the efficiency of this

procedure by using the methods of Givens (111) or Householder (112), but improvement in cost effectiveness was not significant.

Final expressions for the transformation matrices $\underset{\sim}{A}$ and $\underset{\sim}{C}$ are given as products of the individual rotations,

$$\underset{\sim}{A} = \underset{\sim}{A}_1 \underset{\sim}{A}_2 \underset{\sim}{A}_3 \cdots \underset{\sim}{A}_t \tag{252}$$

and

$$\underset{\sim}{C} = \underset{\sim}{C}_1 \underset{\sim}{C}_2 \underset{\sim}{C}_3 \cdots \underset{\sim}{C}_t \tag{253}$$

where each term on the right side is analogous to $\underset{\sim}{O}_k$ in Equation (239).

The secular equations were thus solved for each isotopic compound and cluster size under consideration. The eigenvector matrix, $\underset{\sim}{L}^{-1}$, was computed from Equation (238) and given as output; the associated eigenvalue matrix, $\underset{\sim}{\Lambda} = \{\lambda_i\}$, computed from Equation (233), was also printed.

IV-5: Identification of Central Modes

The eigenvectors and corresponding eigenvalues representing vibration of the central molecule had to be identified so that the appropriate frequencies could be used in Equations (86) and (87). We first considered the intramolecular normal modes of the central molecule used to calculate the zero point energy shift on condensation.

The elements of the $i^{\underline{th}}$ row of the transformation matrix, $\underset{\sim}{L}^{-1}$, give the relative contributions of the internal coordinates, s_k, to the $i^{\underline{th}}$ normal mode:

$$q_i = \ell_{i1}^{-1}s_1 + \ell_{i2}^{-1}s_2 + \ldots + \ell_{in}^{-1}s_n \qquad (254)$$

We sought only normal coordinates q_i for which a substantial contribution was made by internal coordinates s_k associated with the central molecule; for methane, $k \leq 10$. A "substantial" contribution can not always be defined precisely. However, when studying the vibrational spectrum of methane isotopes, nine non-zero central modes are expected from among 16m-6 total cluster modes, so that in general, the nine largest row vectors $\vec{\ell}_{ik}^{-1}$ $(k \leq 10)$ of the $\underset{\sim}{L}^{-1}$-matrix were sought. More specifically, if

$$(m-1)\sum_{j=t}^{t'}|\ell_{ij}^{-1}| \gg \sum_{j=t+10}^{t'+10}|\ell_{ij}^{-1}| + \sum_{t+20}^{t'+20}|\ell_{ij}^{-1}| + \ldots + \sum_{t+10(m-1)}^{t'+10(m-1)}|\ell_{ij}^{-1}| \qquad (255)$$

then the $i^{\underline{th}}$ mode was considered to be a major central contributor. In Equation (255), t and t' span the first four internal coordinates when CH stretches are intercompared, or the fifth through tenth internal coordinates when HCH bends are considered. Very often, the inequality in (255) was not completely satisfied for nine of

the 16m-6 cluster vibrations. In these cases use was made of the fact that the central molecule of the cluster is the hypothetical analogue of the true condensed phase. Thus, any vibrational symmetry of the condensed phase modes should be reflected in the MCM eigenvectors. In addition, the nine frequencies chosen as central vibrations should display only a small perturbation from the pattern of degeneracy observed for the gas phase (113).

Because of the qualifying conditions placed on Equation (255) and the limited nature of acceptable central internal modes, the choice of liquid phase eigenvectors could not be made by means of any simple algorithm. For this reason, the full $\underset{\sim}{L}^{-1}$-matrix had to be printed and examined; the selection of cental modes was made manually.

Some examples will clarify the techniques used to choose central eigenvectors. Two typical eigenvectors of a 3-cluster representation of liquid $^{12}CH_4$ is given in Table XVIII. Each eigenvector, $\vec{\ell}^{-1}_{15,k}$ and $\vec{\ell}^{-1}_{18,k}$, is displayed with ten elements per line; the first line contains the amplitude coefficients associated with the internal coordinates of the central molecule; the second and third lines have the coefficients of the left and right shell molecules respectively (see Figure 5, p. 84). The first four elements of each of the first three lines are the relative amplitudes of the CH stretches; the fifth through tenth elements in each of the first three lines are associated amplitudes of HCH bends. The last twelve elements of each of the two eigenvectors represent amplitude coefficients of the intermolecular vibrations and are

Table XVIII

Identification of Central Internal Eigenvectors - 3-Cluster

Eigenvalue 15 = 1573.758

0.00000	0.00031	-0.00000	-0.00031	-0.39214	0.01060	0.38141	0.36849	0.01067	-0.37903
0.00001	-0.00013	-0.00001	0.00014	0.44373	0.07458	-0.51859	-0.51198	0.07457	0.43769
0.00001	-0.00013	-0.00001	0.00014	0.40767	0.14574	-0.55385	-0.54739	0.14571	0.40212
0.00001	-0.06194	0.00534	-0.00832	-0.03741	0.00365	-0.00001	0.06190	-0.00533	0.00752
0.07300	-0.07138								

Eigenvalue 18 = 1571.633

-0.00000	-0.00015	-0.00000	0.00015	0.68927	0.00187	-0.69113	-0.68481	0.00183	0.68298
0.00000	0.00007	0.00000	-0.00007	0.27197	-0.00024	-0.27173	-0.27493	-0.00023	0.27516
0.00000	0.00008	0.00000	-0.00007	0.27208	-0.00046	-0.27162	-0.27482	-0.00045	0.27527
-0.00000	0.02981	0.00094	0.00053	0.00012	0.00034	0.00000	-0.02987	-0.00099	-0.00012
-0.00023	-0.00061								

not considered here.

In q_{15}, the internal coordinate contributions from central HCH bends are greatly outweighed in absolute value by positionally corresponding contributions from the shell molecules. Equation (255) is therefore not satisfied for t,t' = 5,10 and so ν_{15} = 1573.758 cm^{-1} is not included in Equation (86) when calculating the vpie B factor. In q_{18}, the contributions from internal bending coordinates satisfy Equation (255), so that ν_{18} = 1571.633 cm^{-1} is included in Equation (86) as a central vibration.

Another example is given in Table XIX, where two eigenvectors of a 9-cluster liquid $^{12}CD_4$ model are shown. The first line of 10 elements in each vector is the central molecular contribution to the mode; the next eight lines are shell contributions and the final 48 elements are amplitude coefficients for the acoustic modes. Both modes are primarily CH stretching vibrations, but q_{10} is seen to consist of large amplitude shell CH stretches and only small amplitude central CH stretches, while in q_9, the amplitude coefficients for central CH stretching are larger than those for shell stretching. Accordingly, ν_9 = 2321.702 cm^{-1} is included when B is calculated.

As a final example of the selection process for optical frequencies, two eigenvectors, $\vec{\ell}^{-1}_{6,k}$ and $\vec{\ell}^{-1}_{7,k}$, are shown in Table XX for a $^{12}CD_4$ 7-cluster. The first line of ten elements represents the amplitude coefficients of the central molecular vibration and the next six lines contain coefficients associated with each of

Table XIX

Identification of Central Internal Eigenvectors - 9-Cluster

Eigenvalue 9 = 2321.702

0.56605	-0.02491	-0.53485	-0.00628	-0.11697	-0.00662	-0.12100	0.12094	0.00678	0.11692
0.00067	-0.00028	-0.00110	-0.00031	-0.02304	-0.01227	0.04612	-0.04612	0.01227	0.02304
-0.00056	0.00003	0.00077	-0.00231	0.00026	-0.00853	0.00008	-0.00011	0.00853	-0.00026
0.00152	-0.00119	0.00070	-0.00103	0.01740	0.00044	-0.01854	-0.01680	0.00045	0.01706
0.00002	-0.00008	-0.00008	0.00003	0.00864	0.00021	-0.00815	-0.00937	0.00020	0.00847
-0.00451	-0.00388	0.00049	-0.00252	-0.00221	0.01291	0.01728	-0.01683	-0.01331	0.00215
-0.00000	0.00345	0.00088	0.00071	-0.00297	-0.00011	0.00357	0.00256	-0.00012	-0.00294
0.00012	0.00001	-0.00021	-0.00101	0.00016	-0.00017	-0.00028	-0.00030	0.00032	0.00028
0.00056	0.00027	-0.00087	0.00009	0.00007	0.00019	0.00000	-0.00000	-0.00020	-0.00006
0.00002	0.00000	0.00000	-0.00003	-0.00003	-0.00077	-0.00001	-0.00008	-0.00000	-0.00008
0.00000	0.00003	-0.00045	-0.00022	-0.00101	-0.00000	0.00003	-0.00100	-0.00000	-0.00000
-0.00000	-0.00012	-0.00009	0.00000	0.00076	-0.00011	0.00000	-0.00003	0.00000	0.00051
-0.00000	-0.00002	-0.00002	-0.00006	0.00006	-0.00000	-0.00010	-0.00003	-0.00009	0.00000
0.00025	0.00000	0.00044	-0.00021	0.00004	-0.00007	0.00030	0.00044		

(continued)

Table XIX (continued)

Eigenvalue 10 = 2320.906

0.00267	-0.00259	-0.00263	-0.00000	0.00856	0.00040	-0.00077	0.00078	-0.00041	-0.00857
0.00890	-0.12780	-0.12882	0.00787	-0.01000	0.00480	0.00011	-0.00012	-0.00482	-0.00998
0.12099	-0.08799	0.08804	0.13471	0.00009	0.00374	0.00004	-0.00001	-0.00374	-0.00012
0.06778	0.23282	0.07001	-0.22278	0.00000	0.00055	0.00071	-0.00022	-0.00033	-0.00072
-0.24098	-0.01272	-0.24566	0.00043	0.00129	-0.00222	-0.00006	0.00008	0.00219	-0.00130
-0.22074	-0.01337	-0.24771	0.00056	0.00127	-0.00220	-0.00004	0.00007	0.00216	-0.00128
0.06779	0.23290	0.07005	-0.22301	0.00002	0.00058	0.00073	-0.00024	-0.00035	-0.00073
0.12098	-0.08803	0.08810	0.13482	0.00009	0.00375	0.00002	-0.00001	-0.00373	-0.00012
0.00888	-0.12782	-0.12880	0.00789	-0.00998	0.00480	0.00011	-0.00012	-0.00481	-0.01000
-0.00389	-0.02266	0.00000	-0.00000	-0.00788	-0.01000	-0.00389	0.00067	-0.00202	-0.00000
0.00000	-0.00002	-0.00009	0.00067	-0.00452	-0.06260	-0.00000	0.00566	-0.00010	0.00000
0.00373	-0.00009	-0.00022	0.00033	-0.00010	0.00000	0.00034	0.00044	-0.00092	0.00201
0.00000	0.00478	-0.00033	0.00022	-0.00029	0.00018	0.00079	0.00095	-0.00177	-0.01002
-0.00056	0.00363	-0.00290	-0.00100	-0.00000	-0.00000	-0.00190	0.00108		

Table XX

Identification of Central Internal Eigenvectors - 7-Cluster

Eigenvalue 6 = 2321.990

-0.61457	0.62385	-0.61501	0.61909	-0.00000	0.00020	0.00003	-0.00004	-0.00018	0.00000
0.00927	-0.00251	0.00171	-0.00017	-0.00002	-0.00045	-0.00024	0.00025	0.00043	0.00002
0.00645	-0.00456	-0.00029	-0.00099	0.00098	0.00095	-0.00110	-0.00118	-0.00075	0.00110
0.00097	-0.00782	-0.00648	0.00107	0.00006	-0.00006	0.00000	-0.00000	0.00005	-0.00005
-0.00104	0.00397	0.00092	0.01007	0.00001	0.00001	-0.00006	0.00006	-0.00000	-0.00001
0.29789	-0.28309	-0.21008	0.21722	-0.00034	-0.00210	-0.00066	0.00165	0.00101	0.00044
0.30004	-0.29610	0.27957	-0.29113	0.00001	0.00000	-0.00000	-0.00000	0.00001	-0.00002
0.00278	-0.00039	0.00028	-0.00022	0.00000	0.00000	-0.00000	-0.00000	0.00046	0.00085
-0.00006	-0.00100	-0.00099	-0.00038	0.00028	0.00048	-0.00109	0.00055	0.00133	-0.00101
0.00000	0.00000	-0.00044	-0.00029	-0.00167	-0.00005	-0.00111	-0.00020	-0.00000	0.00333
0.00167	0.00122	0.00155	-0.00000	-0.00177	0.00088				

(continued)

Table XX (continued)

Eigenvalue 7 = 2320.069

-0.59121	-0.10728	0.62108	-0.18901	0.11804	-0.01926	0.12711	-0.12720	0.01900	-0.11770
-0.06287	-0.00045	0.04567	-0.00897	0.00456	-0.00076	-0.00020	-0.00000	-0.00360	0.00001
0.00499	0.00250	-0.03078	0.00111	0.00005	-0.00000	-0.00280	0.00235	0.00051	-0.00001
-0.07299	-0.00077	0.05009	-0.00726	-0.00000	0.00390	0.00121	-0.00120	-0.00380	0.00010
0.08724	0.00345	-0.01211	0.00567	0.00045	-0.00035	-0.00011	-0.00007	0.00025	-0.00017
-0.10045	-0.09784	0.00673	-0.10007	0.00014	-0.00000	-0.00016	-0.00015	0.00017	0.00000
-0.08974	0.00579	-0.07921	-0.11253	0.00124	0.00378	-0.09002	0.09055	-0.00180	-0.00375
0.00313	-0.00278	-0.00856	-0.08479	-0.03312	0.06544	0.00313	0.00278	-0.08771	0.00567
0.00552	-0.00066	-0.00313	-0.00077	-0.00034	0.00433	-0.00001	-0.00003	-0.00313	-0.00076
-0.00000	-0.00000	0.00232	-0.01910	-0.00313	-0.00077	-0.00600	-0.00281	-0.00000	0.00000
0.00313	0.00076	-0.00064	0.00442	0.00004	0.00000	0.00004			

the shell molecules. The last 36 elements of each eigenvector are the amplitude coefficients of the intermolecular coordinates. Both q_6 and q_7 satisfy Equation (255). However, an examination of the first 10 components of $\vec{\ell}^{-1}_{6,k}$, and comparison with the gas-phase eigenvectors of $^{12}CD_4$ in Table VI, shows that the vibrations of the central molecule of the cluster do not represent anything close to a vibrational mode of gaseous $^{12}CD_4$ with respect to the symmetry and magnitude of eigenvector elements. Normal mode q_7 roughly coincides with a gas-phase vibration, in addition to meeting the requirement of Equation (255). Thus, ν_7 is considered to be a central mode, and is counted in Equation (86), while ν_6 is not.

The intermolecular vibrations of the entire cluster are used as surrogate external frequencies in the calculation of the vpie A factor given by Equation (87). In general, only those motions that displace the central molecule relative to the shell molecules are considered in the MCM theory as proper acoustic modes. For example, a normal mode representing a symmetric CCC stretch in a (linear) 3-cluster merely indicates a simultaneous outward motion of the two shell molecules; no net movement of the central methane relative to a shell-molecular reference frame is apparent and the mode is not counted as an external vibration of the central molecule or included in Equation (87). This is illustrated in Table XXI, where two eigenvectors of a 3-cluster of $^{14}CH_4$ are presented. As in the previous examples, intermolecular orientation is arbitrary for the purpose of demonstrating eigenvector interpretation. In each eigenvector, the first three lines contain internal co-

Table XXI

Identification of Central External Eigenvectors - 3-Cluster Stretching Modes

Eigenvalue 29 = 106.403

0.00000	0.00000	-0.00000	-0.00000	-0.00000	0.00000	0.00000	-0.00000	-0.00000	0.00000
-0.00009	0.00009	-0.00009	0.00009	0.00000	0.00089	-0.00000	-0.00000	-0.00089	-0.00000
0.00009	-0.00009	0.00009	-0.00009	-0.00000	-0.00089	0.00000	0.00000	0.00090	0.00000
-0.16638	0.00171	0.00002	0.00004	-0.00098	-0.00199	-0.16638	0.00171	0.00002	0.00005
-0.00098	-0.00199								

Eigenvalue 30 = 98.005

-0.00031	0.00031	-0.00031	0.00034	0.00001	0.00313	0.00000	-0.00001	-0.00313	-0.00000
0.00015	-0.00015	0.00015	-0.00015	-0.00001	-0.00156	0.00000	0.00000	0.00156	0.00000
0.00015	-0.00015	0.00015	-0.00015	-0.00001	-0.00156	0.00000	0.00000	0.00156	0.00000
0.28782	-0.00203	0.00241	0.00298	0.00094	0.00116	-0.28782	-0.00203	-0.00241	-0.00299
-0.00095	-0.00116								

ordinate amplitude coefficients of the central, left and right molecules, respectively. The last twelve elements are ℓ_{ij}^{-1}-values for the intermolecular coordinates as described previously. Of the last twelve, the first and seventh elements — $\ell_{29,31}^{-1}$ and $\ell_{29,37}^{-1}$ in the first eigenvector in Table XXI and $\ell_{30,31}^{-1}$ and $\ell_{30,37}^{-1}$ in the second — are amplitude coefficients for the C_1-C_6 and C_1-C_{11} "bond" stretches. In q_{29},

$$\ell_{29,31}^{-1} \approx \ell_{29,37}^{-1} \tag{256}$$

in both sign and magnitude, so that $R(C_1C_6)$ and $R(C_1C_{11})$ are vibrating in phase symmetrically; thus, the displacement of the central molecule is zero, and the frequency of the mode, $\nu_{29} = 106.403\ cm^{-1}$, is not included in the calculation of the A factor. In q_{30},

$$-\ell_{30,31}^{-1} \approx \ell_{30,37}^{-1} \tag{257}$$

and the two C_cC_s "bonds" are vibrating asymmetrically. The central molecule must be moving in such a way as to maintain the center of mass for the cluster. This central motion qualifies q_{30} as a surrogate liquid external mode — in particular, a translational mode — and so $\nu_{30} = 98.005\ cm^{-1}$ is included in Equation (87).

Table XXII and Figures 6 and 7 show this principle for a 7-cluster of $^{12}CH_4$. The first seven lines of each eigenvector represent intra-

Table XXII

Identification of Central External Eigenvectors - 7-Cluster Stretching Modes

Eigenvalue 74 = 101.339

0.00522	-0.00356	-0.00181	0.00820	-0.00019	-0.00000	-0.00678	0.00680	0.00055	-0.00038
-0.00698	-0.00321	-0.00200	0.00699	0.00000	0.00000	0.00000	-0.00000	-0.00000	-0.00000
-0.00000	-0.00459	0.00231	0.00750	0.00000	-0.00001	-0.00003	0.00004	-0.00000	0.00000
0.00089	-0.00045	-0.00000	-0.00384	0.00000	-0.00000	-0.00000	0.00000	0.00000	-0.00000
-0.00137	-0.07231	0.00856	-0.00421	-0.00581	-0.00414	0.00594	-0.00067	-0.00333	0.00801
0.00222	0.00276	-0.00002	-0.00006	-0.00639	0.00282	0.00693	-0.00110	-0.00820	0.00594
0.00493	-0.00287	0.00496	0.00202	-0.00000	-0.00000	0.00000	0.00000	-0.00000	0.00000
-0.97201	-0.00067	-0.00674	0.00684	0.00333	0.00229	-0.83002	-0.00004	-0.00330	0.00663
0.00202	0.00055	0.96000	-0.00045	-0.00000	-0.00000	-0.00033	0.00228	0.84126	0.00078
-0.00087	0.00561	-0.00616	0.00045	0.00000	0.00000	0.00000	0.00000	-0.00000	-0.00000
0.00000	0.00000	-0.00000	0.00000	-0.00000	0.00000				

(continued)

Table XXII (continued)

Eigenvalue 76 = 97.602

0.00000	-0.00450	-0.00279	0.00277	-0.01204	-0.00388	0.00722	0.00109	-0.00008	0.00769
0.00000	0.00000	-0.00000	0.00000	0.00000	0.00000	-0.00000	-0.00000	0.00000	0.00000
0.00344	0.00060	-0.00056	-0.00210	-0.00006	-0.00465	-0.00297	0.00068	0.00045	0.00655
-0.00000	-0.00000	0.00000	0.00000	-0.00000	-0.00000	0.00000	0.00000	-0.00000	-0.00000
0.00077	-0.00320	-0.00111	0.00912	0.00005	-0.00632	0.00929	-0.00027	-0.00000	-0.00275
-0.00555	0.00220	-0.00204	-0.00115	-0.00684	-0.00229	-0.00038	0.00620	0.00200	0.00131
0.00409	-0.00000	-0.00000	0.00398	-0.00993	-0.00022	-0.00285	0.00285	0.00030	0.00985
0.71111	-0.00005	-0.00062	0.00051	0.00000	0.00040	0.71097	-0.00000	0.00000	0.00000
0.00000	0.00000	0.71111	0.00008	-0.00067	-0.00002	-0.00082	0.00001	0.71097	0.00000
0.00000	0.00000	-0.00000	0.00000	0.80420	0.00109	0.00682	-0.00057	-0.00225	0.00022
-0.80422	0.00109	0.00393	-0.00202	0.00000	0.00058				

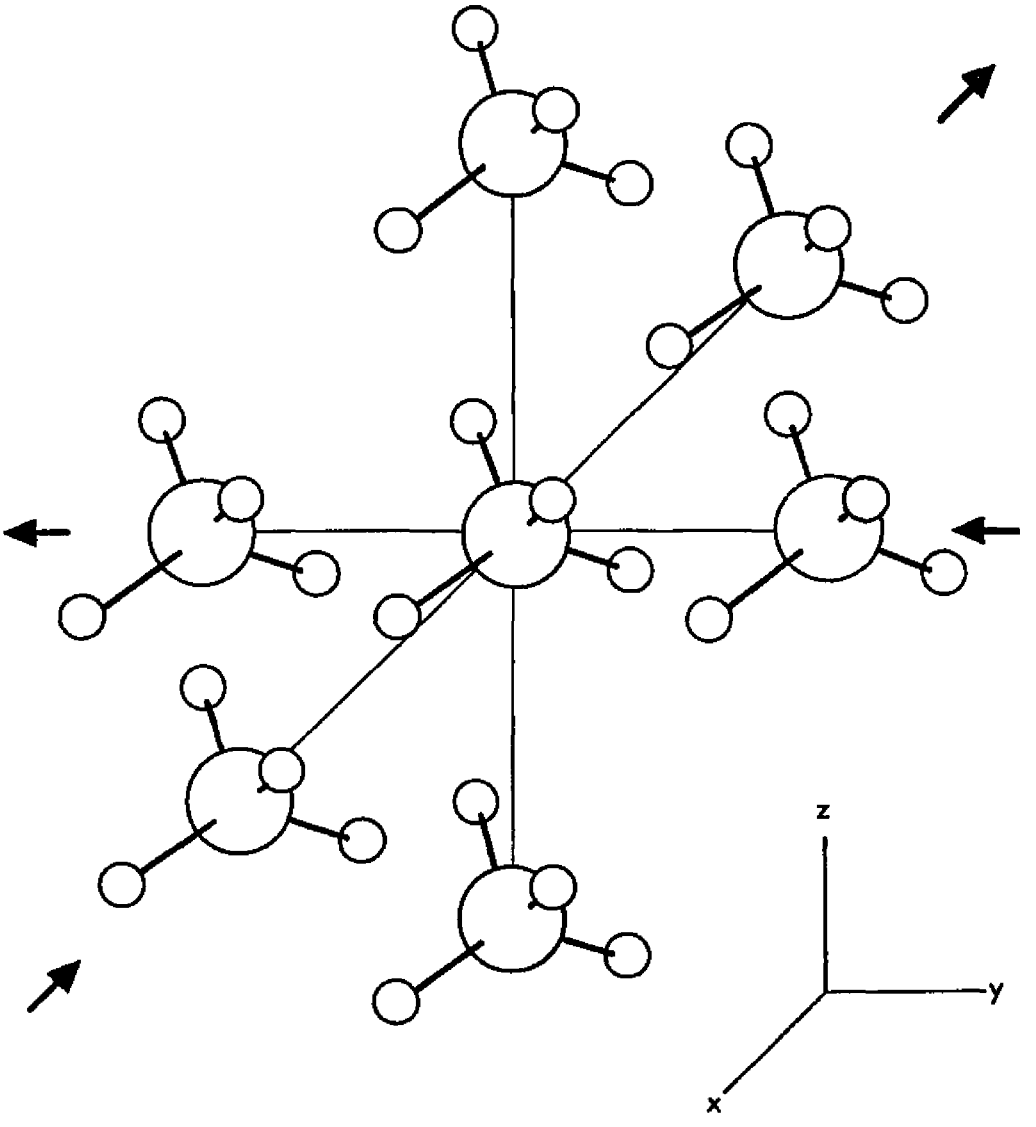

Figure 6. Asymmetric stretching of the 7-cluster in the x- and y-directions. The cluster is shown in the gear geometry.

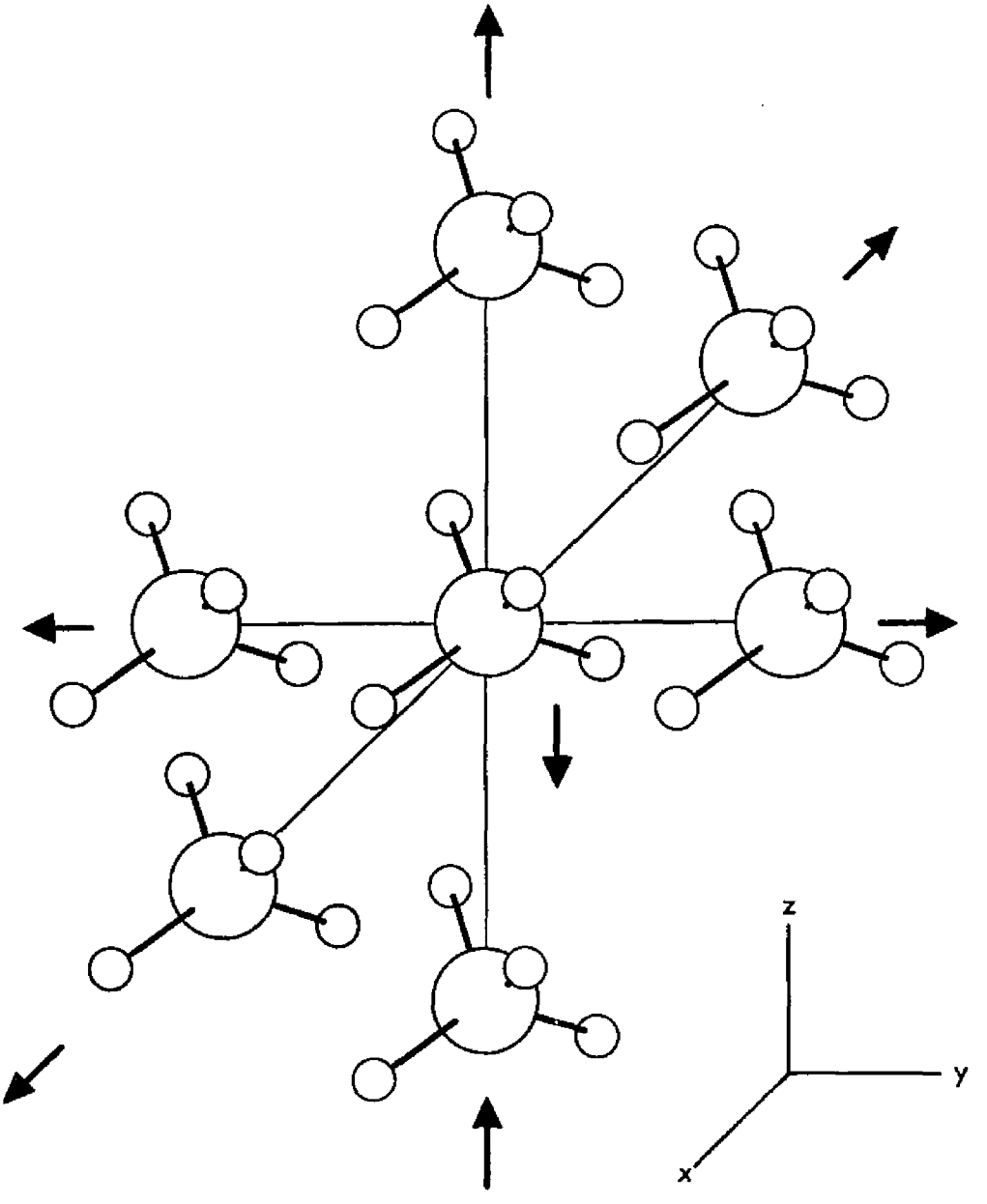

Figure 7. Asymmetric stretching of the 7-cluster in the z-direction coupled with symmetric stretching in the x- and y-directions.

molecular contributions and the final 36 elements are coefficients for the intermolecular contributions. From Table XI (p.87) and Figure 6 it can be seen that (s_{71},s_{83}), (s_{77},s_{89}) and (s_{95},s_{101}) are C_cC_s stretching coordinate pairs arranged in mutually orthogonal directions, so that each member of each pair is in a trans position to the other member of that pair. In q_{74},

$$\ell^{-1}_{74,71} \approx -\ell^{-1}_{74,83} \tag{258}$$

$$\ell^{-1}_{74,77} \approx -\ell^{-1}_{74,89} \tag{259}$$

$$\ell^{-1}_{74,95} \approx \ell^{-1}_{74,101} \approx 0 \tag{260}$$

The cluster is thus vibrating asymmetrically in two orthogonal directions and not at all in the third. In order to preserve the center of mass, the central molecule must be translating independently in the x- and y-directions. The frequency of q_{74} is therefore included in Equation (87). In normal mode q_{76},

$$\ell^{-1}_{76,71} \approx \ell^{-1}_{76,83} \tag{261}$$

$$\ell^{-1}_{76,77} \approx \ell^{-1}_{76,89} \tag{262}$$

$$\ell^{-1}_{76,95} \approx -\ell^{-1}_{76,101} \tag{263}$$

The cluster is thus stretching symmetrically in the x- and y-directions and asymmetrically in the z-direction. This implies a z-translation of the central molecule so that ν_{76} is also included in Equation (87).

A similar procedure is used to determine the rotational external modes of the central molecule of a medium cluster. Table XXIII shows two eigenvectors for a typical 3-cluster. The mode labeled q_{38} contains two torsional displacements, s_{32}-$\tau(H_2C_1C_6H_7)$ and s_{38}-$\tau(H_2C_1C_{11}H_{12})$, with non-zero amplitude coefficients. Since

$$\ell^{-1}_{38,32} \approx -\ell^{-1}_{38,38} \tag{264}$$

the two shell molecules may be visualized as rotating around the C-C-C axis in the same "sense" with respect to an external reference frame. This is shown in Figure 8. In order not to impart angular momentum to the entire cluster, the central molecule must rotate in an opposite sense around the y-axis. The frequency of this mode is therefore included in Equation (87). Eigenvector $\bar{\ell}^{-1}_{40,k}$ in Table XXIII shows a similar mode, but in this case

$$\ell^{-1}_{40,32} \approx \ell^{-1}_{40,38} \tag{265}$$

Table XXIII

Identification of Central External Eigenvectors - 3-Cluster Torsional Modes

Eigenvalue 38 = 40.990

0.00000	0.00001	0.00000	-0.00001	-0.00005	-0.00000	0.00005	-0.00005	0.00000	0.00005
0.00042	0.00045	0.00047	-0.00005	-0.00100	-0.00018	0.00072	-0.00051	0.00075	0.00023
-0.00022	-0.00004	-0.00004	0.00096	0.00105	0.00018	-0.00077	0.00055	-0.00075	-0.00027
0.00002	-0.21850	0.00001	0.01885	-0.00007	-0.01912	0.00002	0.21859	0.00001	0.01877
-0.00007	-0.02935								

Eigenvalue 40 = 40.835

-0.00007	0.00021	-0.00007	-0.00007	-0.00321	0.00076	0.00439	0.00039	-0.00312	0.00079
0.00001	-0.00009	0.00001	0.00007	0.00209	-0.00013	-0.00229	0.00029	0.00052	-0.00049
0.00001	-0.00010	0.00001	0.00008	0.00214	-0.00013	-0.00234	0.00035	0.00052	-0.00054
-0.00045	0.79088	0.00079	-0.15069	0.00008	-0.01317	-0.00045	0.79091	0.00076	0.03967
-0.00028	0.013210								

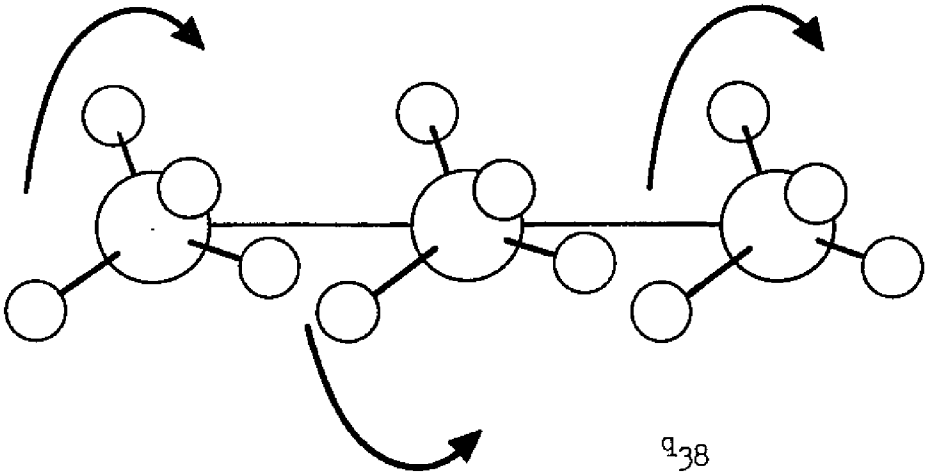

q_{38}

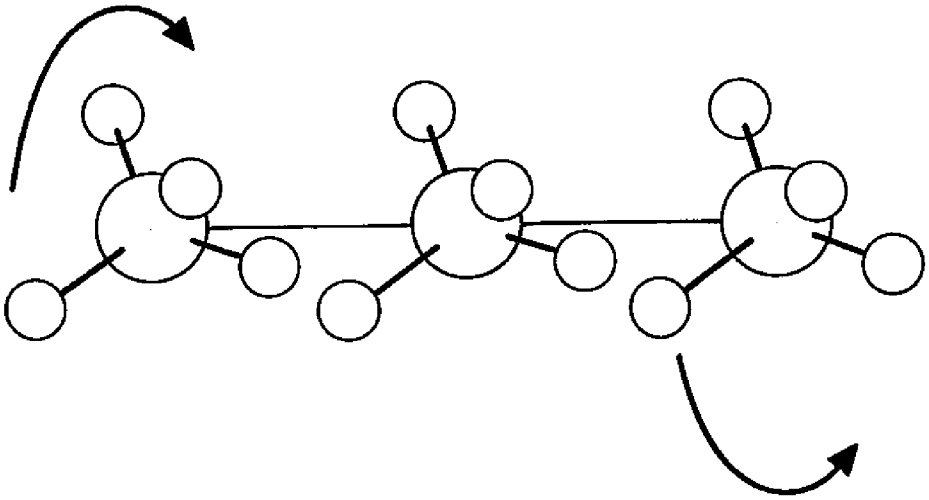

q_{40}

Figure 8. Torsional motion in the 3-cluster. No net rotation of the central molecule occurs in q_{40}.

The shell molecules are undergoing torsional motion in opposite senses so that no central molecular rotation around the y-axis is implied. Since torsional coordinate pairs in trans positions occur in all sized clusters, this type of analysis can always be performed.

Another set of examples illustrating the criteria used to assign external frequencies will now be given. The equilibrium configuration of a 3-cluster includes a C-C-C bond angle of 180°. The internal coordinates consisting of angles $H_2C_1C_6$ and $H_2C_1C_{11}$ are therefore supplementary. If, in 3-cluster mode q_i, one valence angle bend increases (positive $\ell^{-1}_{i,33}$) while its supplement decreases (negative $\ell^{-1}_{i,39}$), the mode represents a central molecular rotation around an axis normal to the $\{^{H}_{CCC}\}$ plane. Alternately, if one angle increases (or decreases) and its supplement increases (or decreases), the mode can be visualized as one in which the two shell molecules are wagging in the same direction in the $\{^{H}_{CCC}\}$ plane. In order to maintain the center of mass in this latter case, the central molecule must be translating in the opposite direction in the same plane. This is illustrated in Table XXIV and Figure 9. In q_{35},

$$\ell^{-1}_{35,33} \approx -\ell^{-1}_{35,39} \tag{266}$$

which implies a central molecular rotation; in q_{40}

$$\ell^{-1}_{40,33} \approx \ell^{-1}_{40,39} \tag{267}$$

Table XXIV

Identification of Central External Eigenvectors - 3-Cluster Central Nutational Modes

Eigenvalue 35 = 55.404

-0.00000	0.00000	0.00000	-0.00000	-0.00639	-0.04230	-0.00552	0.00503	0.04300	0.00618
0.00045	-0.00278	-0.00118	0.00007	0.00019	0.00045	0.00034	-0.00033	-0.00046	-0.00019
-0.00051	0.00094	0.00175	0.00034	-0.00216	0.00078	0.00652	-0.00602	-0.00138	0.00206
0.04519	-0.00057	-0.84278	-0.04511	0.00089	0.00022	0.06711	-0.00058	0.83904	0.04632
0.00048	-0.00487								

Eigenvalue 40 = 47.344

0.00067	-0.09726	-0.05826	0.00211	-0.00569	-0.00892	-0.00121	0.00121	0.00891	0.00570
0.00322	-0.08672	-0.04917	0.00187	0.00000	0.04726	-0.05238	-0.04721	0.05230	0.00003
0.00245	0.09721	-0.00743	-0.02127	-0.04598	-0.00892	0.03427	0.02178	0.00230	-0.00345
0.07421	-0.00067	0.72484	0.00620	0.00500	0.00210	0.06922	-0.00075	0.75789	0.00780
0.00021	-0.00555								

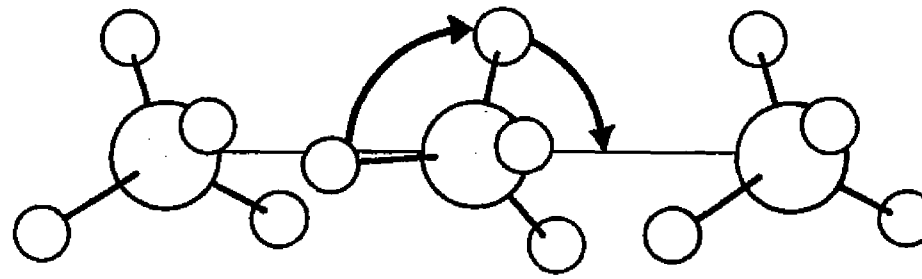

q_{35}

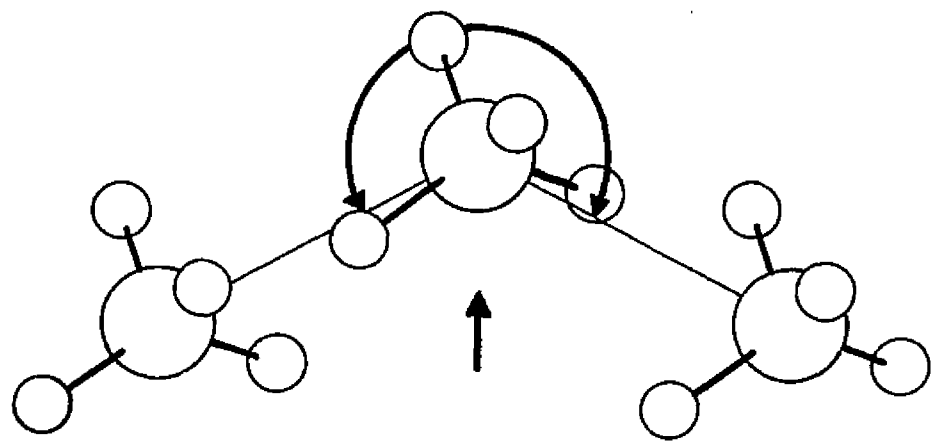

q_{40}

Figure 9. Central nutations in the 3-cluster. Both modes involve motion of the central molecule.

which implies a central molecular translation. Both ν_{35} and ν_{40} are therefore incorporated into the vpie A factor of Equation (85).

Table XXV and Figure 10 show two rotational modes for a 3-cluster which are predominantly manifestations of shell motion. These are not counted as external vibrations and do not enter into the calculation of the A factor in Equation (87).

The simple cell model of the liquid state allows six external modes for motion of the molecule under study — 3 translations and 3 rotations. In general, however, the process of eliminating non-central modes in the medium cluster model leaves more than the expected 6 external modes for the central molecule. This is a consequence of the anisotropic nature of the model and is most evident in the smaller clusters. The several central external modes must be reduced in number and combined in such a way as to be easily associated with molecular translation and rotation. Asymmetric C-C-C stretching in the 3-cluster, for example, can obviously be associated with translation along the y-axis, as was shown previously; but there are no carbon-carbon "bonds" in the x- or y-directions, so that translation in these directions must be viewed as being due to bending of the C-C-C angle. Such a C-C-C bend consists of simultaneous in-phase displacement of supplementary $H_cC_cC_s$ angles. One would not expect these three "translational" modes to be close in frequency since they are defined with respect to symmetrically different environments. Yet they should be degenerate because of the overall isotropy of the real liquid phase. For the purpose of elucidating the vapor pressure isotope effect, therefore, an average contribution from translational modes has been used to calculate the A factor. According

Table XXV

Identification of Central External Eigenvectors - 3-Cluster Shell Nutational Modes

Eigenvalue 41 = 38.078

-0.00000	-0.00034	-0.00034	0.00167	-0.00000	-0.00000	-0.00000	0.00000	0.00000	0.00000
0.00028	-0.00089	0.00100	0.00078	0.00109	-0.00000	-0.00055	-0.00055	0.00000	0.00000
-0.00000	0.00100	-0.00103	0.00004	-0.00000	0.00109	-0.00000	-0.00000	-0.00109	0.00000
-0.00616	0.00492	-0.00121	0.00677	-0.89981	0.07922	-0.00610	0.00503	0.00008	0.00033
-0.88015	0.08004								

Eigenvalue 42 = 36.000

0.00121	-0.00089	-0.00078	0.00121	0.00000	-0.00000	0.00000	0.00000	-0.00000	-0.00000
-0.00056	0.00078	0.00122	-0.00134	-0.00356	-0.00143	-0.00275	0.00355	0.00144	0.00275
0.07902	-0.01290	-0.03518	0.00045	0.01560	0.00089	0.00273	-0.01297	-0.00384	-0.00241
-0.03769	-0.00219	0.00079	0.00001	0.80479	0.60053	-0.03601	-0.00300	0.00029	0.00857
0.90019	0.62801								

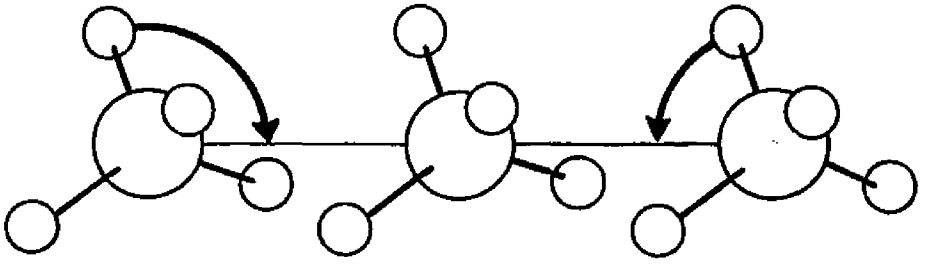

q_{41}

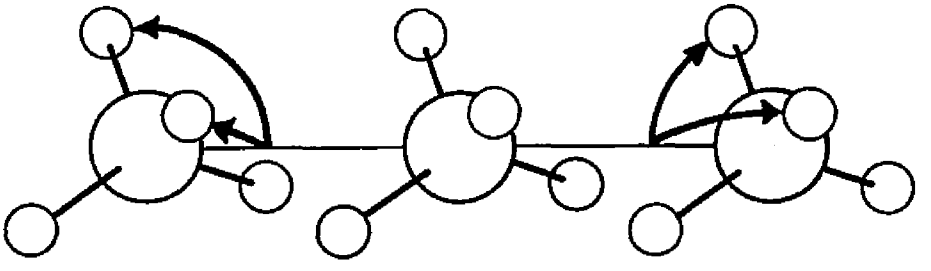

q_{42}

Figure 10. Two 3-cluster modes involving only shell nutational motion.

to Equations (42) and (43), to a first approximation, each mode contributes to the liquid-phase reduced partition function ratio as the square of its frequency (114),

$$\ell n \frac{s}{s}, f_c \propto \sum_i \Delta u_i^2 \approx \sum_i \Delta \lambda_i \tag{268}$$

so that a root mean square average of frequencies is the appropriate quantity to consider as the vpie-related translational frequency. An analogous situation exists for the central rotational modes, where simultaneous out-of-phase displacement of supplementary $H_c C_c C_s$ angles and $H_c C_c C_s H_s$ torsions are combined. In general, then, we have assumed

$$\sum_{\text{trans}}^{3} u_i^2 = \frac{3}{w} \sum_{\text{trans}}^{w} u^2_{\text{cluster}} \tag{269}$$

and

$$\sum_{\text{rot}}^{3} \Delta u_i^2 = \frac{3}{w} \sum_{\text{rot}}^{w} \Delta u^2_{\text{cluster}} \tag{270}$$

where the right sides of these equations span all w translational or rotational modes found in the analysis of MCM eigenvectors and the left sides are the two parts of the total external summation in Equation (87).

V. RESULTS AND DISCUSSION

With the medium cluster model, a methodology exists with which to examine the relationship between the vapor pressure isotope effect and molecular structure in the condensed phase. Specific interactions between a molecule in the liquid and the molecules that make up the surrounding medium can be evaluated. The model assumes

(a) the regularity of molecular position in any small neighborhood of the condensed phase,

(b) harmonic potentials for all modes of vibration in the liquid and gas phases as given by Equation (90), and

(c) that the central molecule of the cluster is a surrogate for the entire liquid phase as implied by Equations (77) and (78).

In this chapter, changes in the predicted vpie produced by variations of this hypothetical model of the condensed phase are presented. The A and B factors of Equation (85) have been examined as functions of MCM parameters such as cluster size, m, molecular orientation, $\underset{\sim}{\theta}_i^{(xyz)}$, and intermolecular separation, $|\vec{\rho}_i|$. General statistical mechanical treatments of conformational problems in liquids has been given elsewhere (115,116,117); consideration here is restricted to a treatment of analytical aspects relevent to the vapor pressure isotope

effect.

The MCM theory has been used to calculate the vpie of the spherical top methanes, $^{13}CH_4$, $^{14}CH_4$, and $^{12}CD_4$, all relative to $^{12}CH_4$ with "best-fit" $\underset{\sim}{F}$-matrices constructed for each different sized cluster via the techniques described in Section IV-3. The condensed phase force field was optimized for a cluster geometry based on the gear configuration (Section IV-1 and Figure 2) with the intermolecular distance, $|\vec{p}|$, equal to 3.817 Å. Non-zero elements of $\underset{\sim}{F}_m$ (m = 3,7,9,13) and $\underset{\sim}{F}_g$ are collected in Table XXVI. These matrices remain invariant as other medium cluster parameters are changed.

A major accomplishment of the present research has been the successful reproduction of the observed temperature dependence of equilibrium vapor pressure ratios for spherical top methane isotopes. In general, the results obtained via the MCM theory are closer to experiment than the results calculated by Bigeleisen, Cragg and Jeevanandam (40) through the use of the simple cell theory. Table XXVII compares vpie parameters A and B determined experimentally with values calculated from the simple cell model and the medium cluster model. It will be shown in Section V-3 that the MCM theory can also be used to calculate $\ell n(P'/P)$ for non-spherical top methanes.

V-1: The Vapor Pressure Isotope Effect and Molecular Orientation

An aggregate of m methane molecules can assume an infinite number of configurations depending on the relative orienta-

Table XXVI

Medium Cluster Model Force Field for Methane[b]

$\underset{\sim}{F}_m$[a]		f_r (mdyne/Å)	f_α (mdyne·Å)	f_{rr} (mdyne/Å)	$f'_{r\alpha}$ (mdyne)	$f'_{\alpha\alpha}$ (mdyne·Å)	$\underset{\sim}{F}_e$
$\underset{\sim}{F}_3$	f^c	5.4573	0.5654	0.1240	0.1901	0.0190	f_R = 0.0555 mdyne/Å
	f^s	5.4762	0.5657	0.1240	0.1776	0.0190	f_τ = 0.00375 mdyne·Å
$\underset{\sim}{F}_7$	f^c	5.4573	0.5612	0.1240	0.1993	0.0190	f_β = 0.00520 mdyne·Å
	f^s	5.4887	0.5668	0.1240	0.1707	0.0190	
$\underset{\sim}{F}_9$	f^c	5.4573	0.5590	0.1240	0.1989	0.0190	
	f^s	5.4903	0.5668	0.1240	0.1692	0.0190	
$\underset{\sim}{F}_{13}$	f^c	5.4573	0.5610	0.1240	0.1966	0.0190	
	f^s	5.4919	0.5673	0.1240	0.1676	0.0190	

(a) All other elements are zero
(b) Optimized for gear geometry; $|\vec{\rho}| = 3.817$ Å

Table XXVII

Comparison of Medium Cluster Model A and B Values
with Experimental Results for Spherical Top Methanes

	Molecule[a]	Experiment	MCM[b]				Simple cell model[c]
			3	7	9	13	
A ($^oK^2$)	$^{13}CH_4$	93.8 ± 6.1[d]	90.66	91.03	91.24	91.39	86.9
	$^{14}CH_4$	231.1 ±10.0[c]	171.01	171.71	172.13	172.44	163.9
	$^{12}CD_4$	894.77 ± 6.8[e]	917.92	924.93	928.09	932.44	943.2
	$^{12}CT_4$	-	1327.06	1304.12	-	-	-
B (^oK)	$^{13}CH_4$	0.535 ±0.06[d]	0.5519	0.5654	0.5425	0.5586	0.32
	$^{14}CH_4$	1.42 ±0.1 [c]	1.0169	1.0623	1.0195	1.0423	0.60
	$^{12}CD_4$	11.097 ±0.06[e]	10.9855	10.8884	11.0937	11.0349	11.92
	$^{12}CT_4$	-	14.9493	14.9260	-	-	-

(a) All species referred to $^{12}CH_4$

(b) Gear geometry; $|\vec{\rho}| = 3.817\text{Å}$

(c) Ref. (40)

(d) Ref. (34)

(e) Ref. (118)

tion, $\underset{\sim}{\theta}_i$, of each member. Medium cluster model calculations may be performed for any such configuration, and an evaluation of vapor pressure isotope effect parameters A and B as a function of orientation can be made. Since it would not be practicable — or particularly informative — to examine all possible orientations of methane in the liquid state, attention has been restricted to cluster configurations based on the parallel rocket, antiparallel staggered, and gear geometries mentioned in Section IV-1. The carbon-carbon distance was held constant at 3.817 Å.

We first considered a 3-cluster of $^{12}CH_4$ in a parallel rocket geometry with three corresponding CH bonds placed along the y-axis and the remaining CH bonds in an eclipsed conformation as shown in Figure 11. With the methods outlined in previous chapters, and using internal coordinates as defined in Section IV-2, the secular equation for this 15-atom aggregate was formulated and solved, and the eigenvectors representing central molecular vibration were identified. The corresponding eigenvalues expressed in wavenumbers were found to be

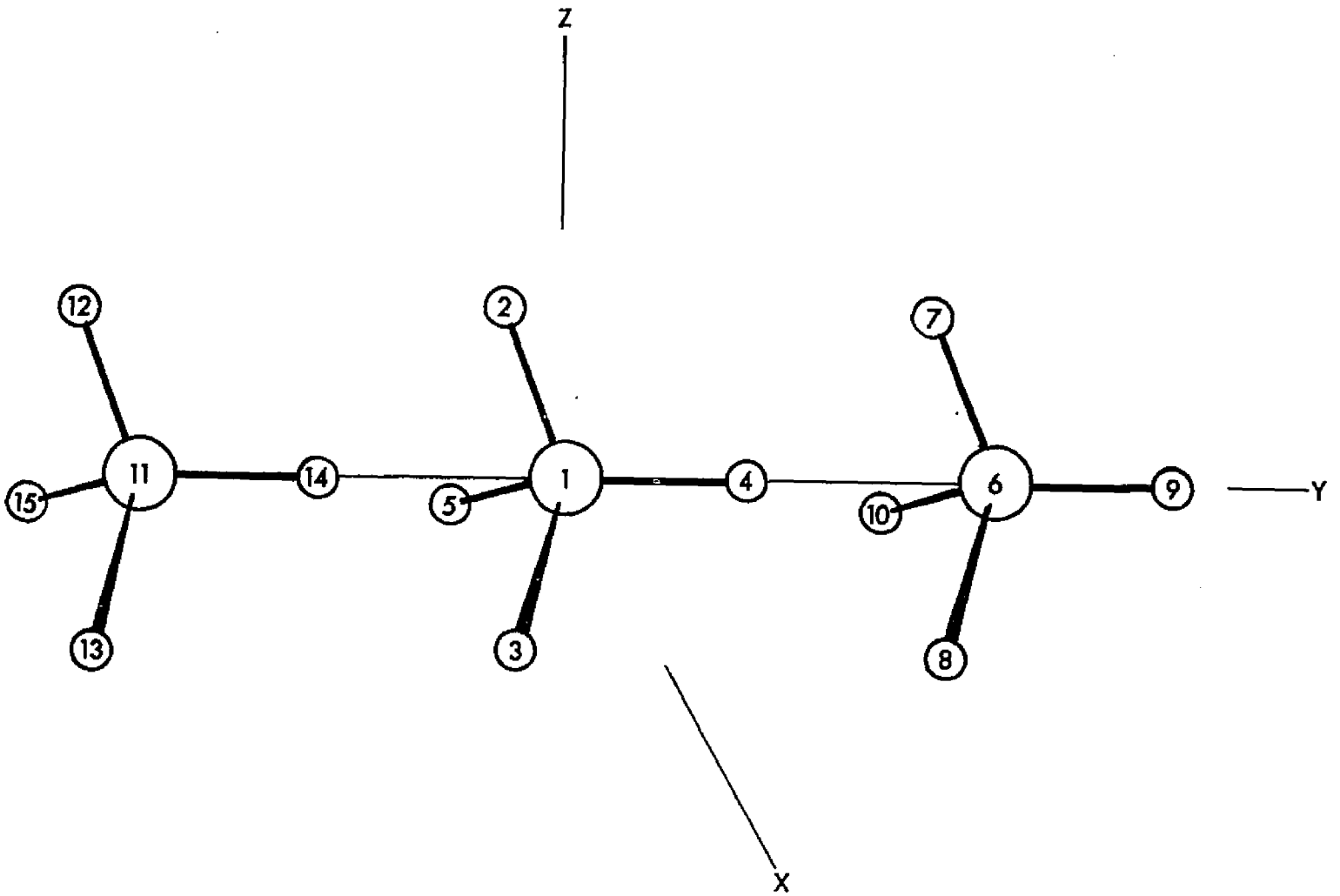

Figure 11. Methane 3-cluster in the rocket configuration. The shell molecule on the right is molecule 2; that on the left is molecule 3.

central optical modes	3133.624	ν_1 (A_1)	
	1573.200	ν_2 (E)	
	1571.633		
	3140.568	ν_3 (T_2)	
	3140.355		
	3140.347		
	1355.733	ν_4 (T_2)	
	1353.006		
	1351.511		
central acoustical modes	132.632	translation	
	10.426		
	10.310		
	75.570	rotation	
	74.157		
	54.065		

Comparison of the cluster optical frequencies for $^{12}CH_4$ with the simple liquid cell (BCJ) frequencies in Table VIII shows that the non-isotropic nature of the medium cluster model has broken the vibrational degeneracy observed for methane in the isotropic cell model. Nevertheless, the MCM frequencies can still be <u>loosely</u> associated with the gas-phase modes of methane given in Table III. The group-theoretical representation of CH_4 vibration, Γ_{vib}, is

$$\Gamma_{vib} = A_1 \oplus E \oplus 2T_2 \qquad (271)$$

These symmetry labels are indicated to the right of the associated MCM frequencies in the above list. The broken vibrational degeneracy of the central optical modes in the MCM theory reflects the observed phenomenon of broadening of spectral absorptions in the liquid phase (119).

The external frequencies of the $^{12}CH_4$ 3-cluster are also non-degenerate because of the anisotropy of the model. The simple cell theory gives identical eigenvalues for three translational motions dependent only on the total molecular mass [cf. Equations (149) and (150)], and three identical eigenvalues for rotational motion for spherical top molecules [Equation (151)]. However, in the linear 3-cluster model of the liquid state, translational vibration of the central CH_4 in the y-direction is more restricted (higher frequency) than x or z translation due to the presence of two shell molecules along the y-axis. Similarly, rotational vibration of the central CH_4 around the CCC axis is of low frequency because this motion involves only small tangential changes in the interatomic distances within the cluster, while rotational vibration of the central CH_4 around the x or z axis causes large radial changes in the interatomic distances, and the energy of vibration is therefore greater.

The vibrational frequencies of a 3-cluster of $^{13}CH_4$ in the same configuration were found in an analogous manner, and, with Equations (86) and (87), the A and B factors of $^{13}CH_4$ (with

$^{12}CH_4$ as the reference isotope) were evaluated. The conformation of the condensed phase clusters was then altered by rotating the central molecule around the y-axis, and again A and B were evaluated. By continuing this process — with each step requiring the solution of two 42 x 42 secular equations — a plot of the vpie parameters as a function of θ_1^y was obtained. The results for a full 360° rotation of the central molecule around the y-axis are shown in Figure 12. Evaluations were made at 20° intervals.

Simultaneous rotation of both shell molecules in the same sense, while keeping the central molecule fixed, naturally gives identical results to those of Figure 12:

$$B^{13}(-\theta_1^y) = B^{13}(\theta_2^y, \theta_3^y) \qquad (272)$$

$$A^{13}(-\theta_1^y) = A^{13}(\theta_2^y, \theta_3^y)$$

If only one shell molecule was rotated around the y-axis, however, the results obtained were somewhat different. Figures 13 and 14 show that rotation of the molecule on the right of the 3-cluster rocket configuration (molecule 2), which has a CH bond on the y-axis pointing away from the central molecule, has a larger effect on the $^{13}CH_4$ factors than does rotation of the methane on the left (molecule 3), which has a CH bond pointing toward the central molecule. Comparison of Figures

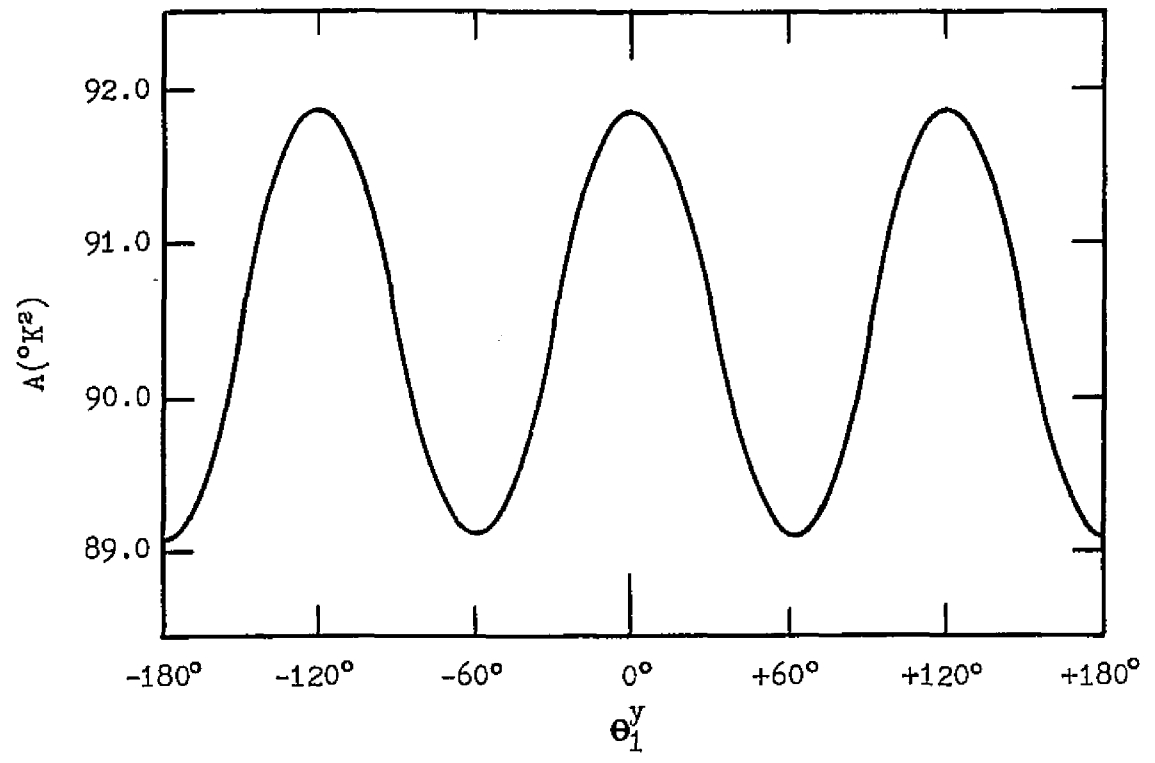

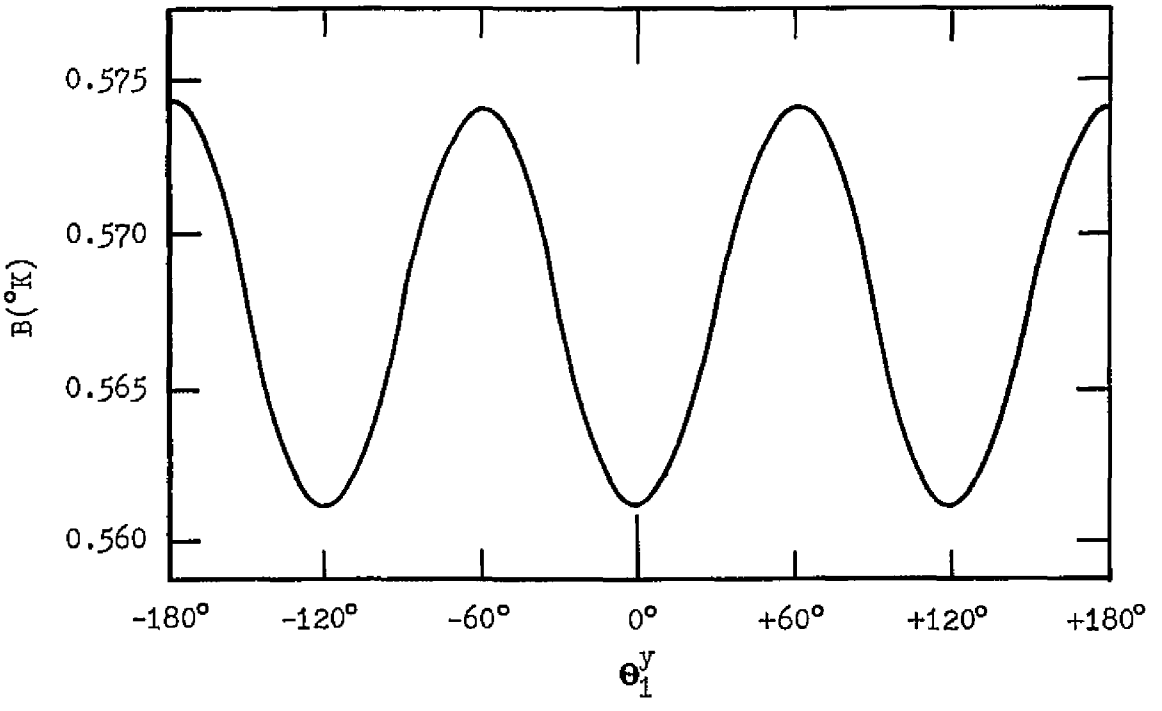

Figure 12. The vpie of $^{13}CH_4$ in the 3-cluster rocket configuration as a function of central molecular rotation around the y-axis.

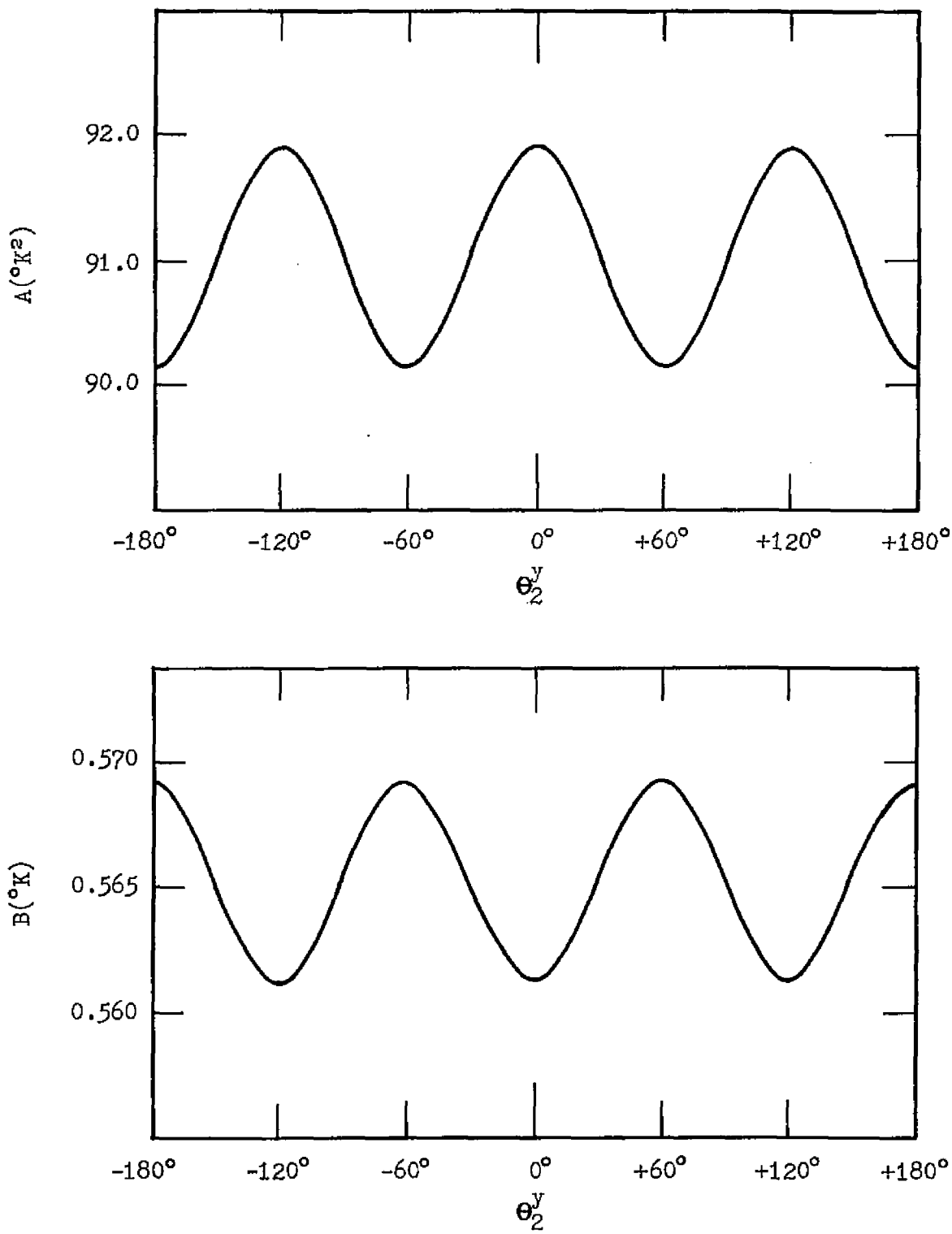

Figure 13. The vpie of $^{13}CH_4$ in the 3-cluster rocket configuration as a function of rotation of molecule 2 around the y-axis.

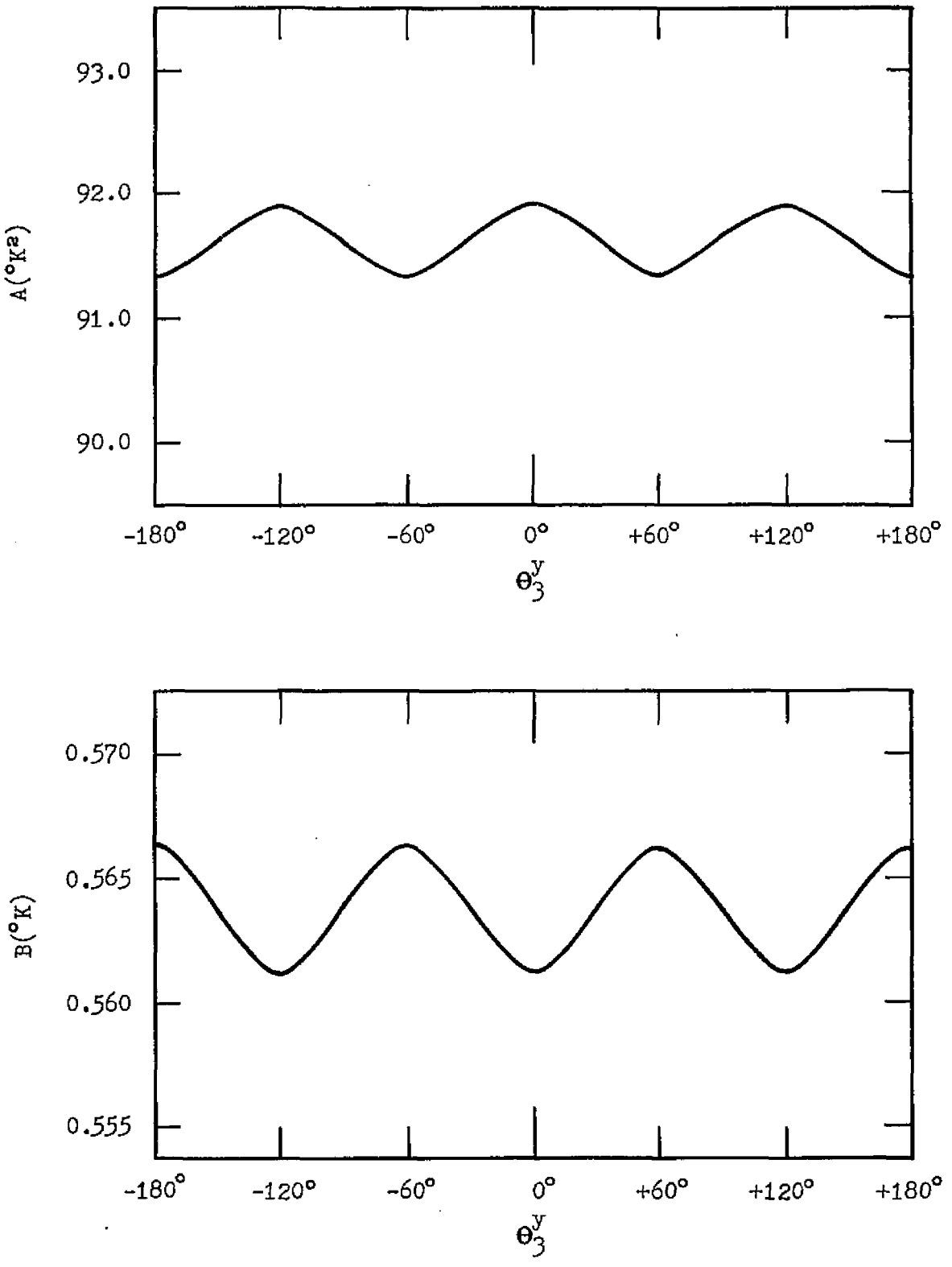

Figure 14. The vpie of $^{13}CH_4$ in the 3-cluster rocket configuration as a function of rotation of molecule 3 around the y-axis.

12 – 14 also shows that the rotational effect on the isotopic zero point energy shift difference is additive; that is, the change in B obtained by simultaneous rotation around the y-axis of the two shell molecules is equal to the sum of changes in B produced by rotation of the shell molecules separately,

$$B^{13}(\theta_3^y, \theta_2^y) = B^{13}(\theta_3^y) + B^{13}(\theta_2^y) \qquad (274)$$

The external frequency term is not exactly additive with respect to rotation around y:

$$A^{13}(\theta_3^y, \theta_2^y) \neq A^{13}(\theta_3^y) + A^{13}(\theta_2^y) \qquad (275)$$

Some limited conclusions can be drawn from these simple manipulations of the rocket 3-cluster. It is apparent that the sinusoidal behavior of A and B in Figures 12 - 14 is a result of variations in interaction energy between the hydrogen atoms not situated on the y-axis. Since an eclipsed conformation is generally associated with a higher potential energy, and the maximum A value is observed for the eclipsed rocket geometry, it follows that the A factor is a direct indicator of the potential behavior. This is in accordance with the Herzfeld-Teller relation given by Equation (7). Equation (275) shows that rotation of the shell molecules separately does not have the same effect on the accoustical spectrum as rotation together. This

is a result of the fact that the external coordinates defined with respect to each of the shell molecules have atoms in common with the central molecule, producing non-zero off diagonal terms in the $\underset{\sim}{G}_e$, $\underset{\sim}{G}_{ce}$, and $\underset{\sim}{G}_{se}$ regions of the $\underset{\sim}{G}$-matrix. Some of these elements of $\underset{\sim}{G}$ involve the reduced mass of the isotopically substituted carbon. Since a one-term approximation of the orthogonal polynomial expansion of $\ell n \frac{s}{s},f$, Equation (43), is given by (49,120)

$$\ell n \frac{s}{s},f \approx \frac{W_1}{24} \sum_i \Delta u_i^2 \tag{276}$$

or

$$\ell n \frac{s}{s},f \approx \frac{W_1}{24} \left(\frac{\hbar}{kT}\right)^2 \sum_i \sum_j f_{ij}(g'_{ij} - g_{ij}) \tag{277}$$

it can be seen that an effect on the reduced partition function ratio is produced by any elements of the 3-cluster $\underset{\sim}{G}_e$, $\underset{\sim}{G}_{ce}$ or $\underset{\sim}{G}_{se}$ for which

$$g'_{ij} - g_{ij} \neq 0 \tag{278}$$

Some of these same g_{ij} are orientation dependent as well. For example, the kinetic energy interaction term between central $\beta_2(H_3C_1C_6)$ nutation and shell $r_5(C_6H_8)$ stretching (in the $\underset{\sim}{G}_{se}$ region of $\underset{\sim}{G}$) is given by

$$g_{\beta_2 r_5} = \frac{\mu_C}{R} \sin \beta_3 \cos \tau_1 \qquad (279)$$

where R is the carbon-carbon distance, β_3 is the equilibrium H_8C_6C angle and τ_1 is the equilibrium $H_3C_1C_6H_8$ dihedral angle. This coordinate interaction is thus dependent on both mass (μ_C) and orientation (τ_1) with respect to rotation around the y-axis.

The zero point energy shift is additive since B is not strongly influenced by external coordinates and all elements in G_{ss} and G_{cs} are equal to zero [Equation (183)] and each shell molecule affects the central optical modes independently.

The magnitude and additivity of the y-axis rotational effect can be summarized by a list of the total amplitudes in Figures 12 - 14:

	$A^{13}_{max} - A^{13}_{min}$	$B^{13}_{max} - B^{13}_{min}$
(1) central rotation	2.77 °K²	0.0123 °K
(2) molecule 2 rotation	1.74 °K²	0.0073 °K
(3) molecule 3 rotation	0.54 °K²	0.0050 °K
total (2) + (3)	2.28 °K²	0.0123 °K

Figure 15 shows the effect of rotation of the central molecule around the z-axis for a 3-cluster of $^{13}CH_4$ in an eclipsed rocket geometry. A compound sinusoidal curve with period 2π is observed; the maximum A is found when the hydro-

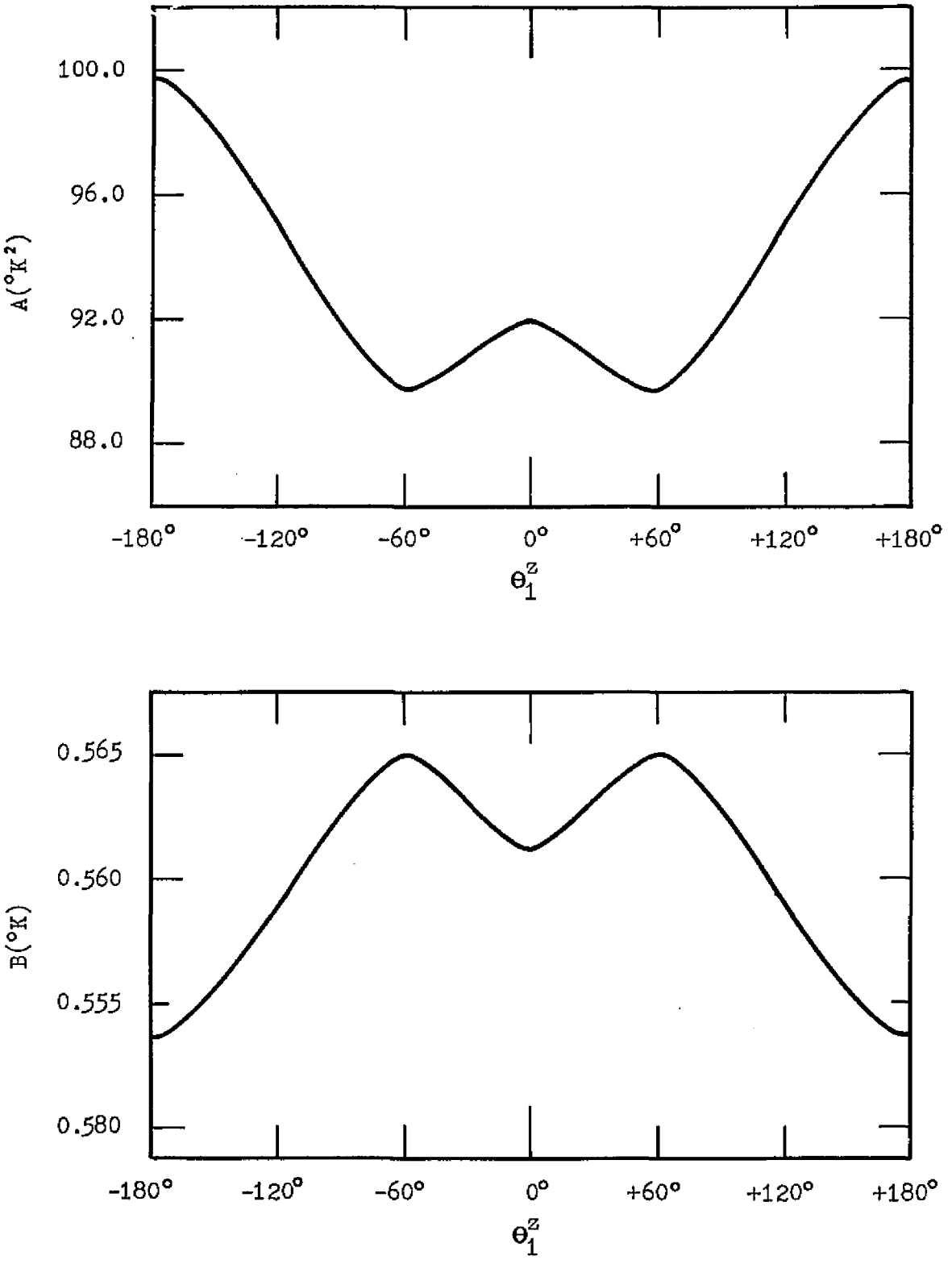

Figure 15. The vpie of $^{13}CH_4$ in the 3-cluster rocket configuration as a function of central molecular rotation around the z-axis.

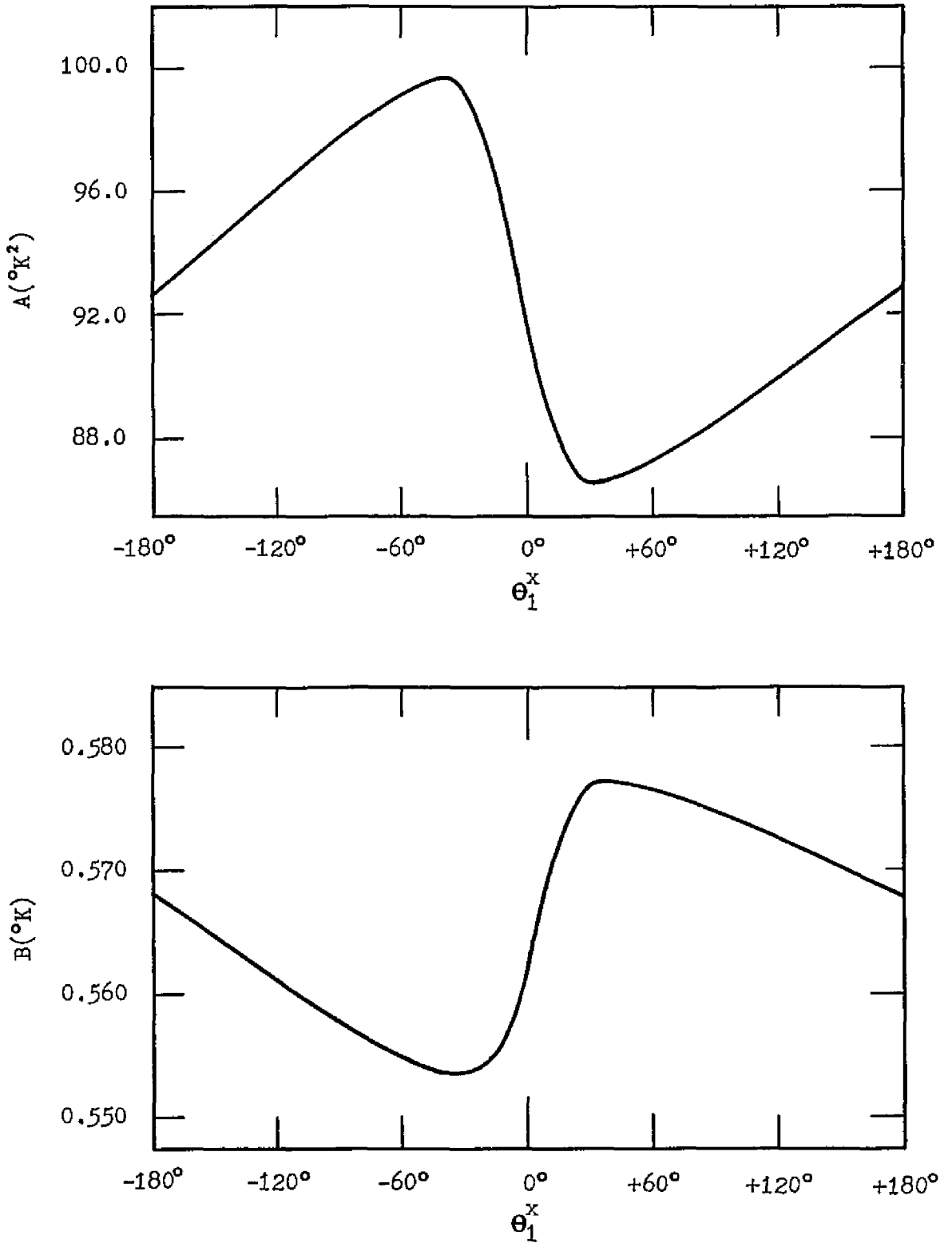

Figure 16. The vpie of $^{13}CH_4$ in the 3-cluster rocket configuration as a function of central molecular rotation around the x-axis.

gens on molecules 1 and 3 are pointed toward one another. Figure 16 shows the behavior of the vpie factors A and B as a function of rotational displacement of the central molecule around the x-axis. In this case, a rotation by 109° around x brings a second hydrogen (H_3) onto the y-axis (see Figure 11), so that the resulting geometry is equivalent to rotation of the central molecule around the y-axis by 180°. As expected, Figures 12 and 16 show that

$$B^{13}(\theta_1^x=109°) = B^{13}(\theta_1^y=180°)$$
$$A^{13}(\theta_1^x=109°) = A^{13}(\theta_1^y=180°) \qquad (280)$$

In Figures 17 - 19, the effects of central molecular orientation on A and B for a $^{12}CD_4$ 3-cluster in the rocket configuration is shown. In general, the variation of $\ell n \frac{s}{s},f(^{12}CD_4/^{12}CH_4)$ is seen to be larger with differing conformation than the corresponding variation of $\ell n \frac{s}{s},f(^{13}CH_4/^{12}CH_4)$. The variation in A and B over full 360° rotations of the central $^{12}CD_4$ around x, y, and z is about 10% (relative to the values at zero orientation change) while full rotations of $^{13}CH_4$ produce a 3% variation. This can be interpreted in terms of the orthogonal polynomial expansion of $\ell n \frac{s}{s},f$ as follows. As shown in Equation (277), a one-term approximation of the reduced partition function ratio is dependent on a linear

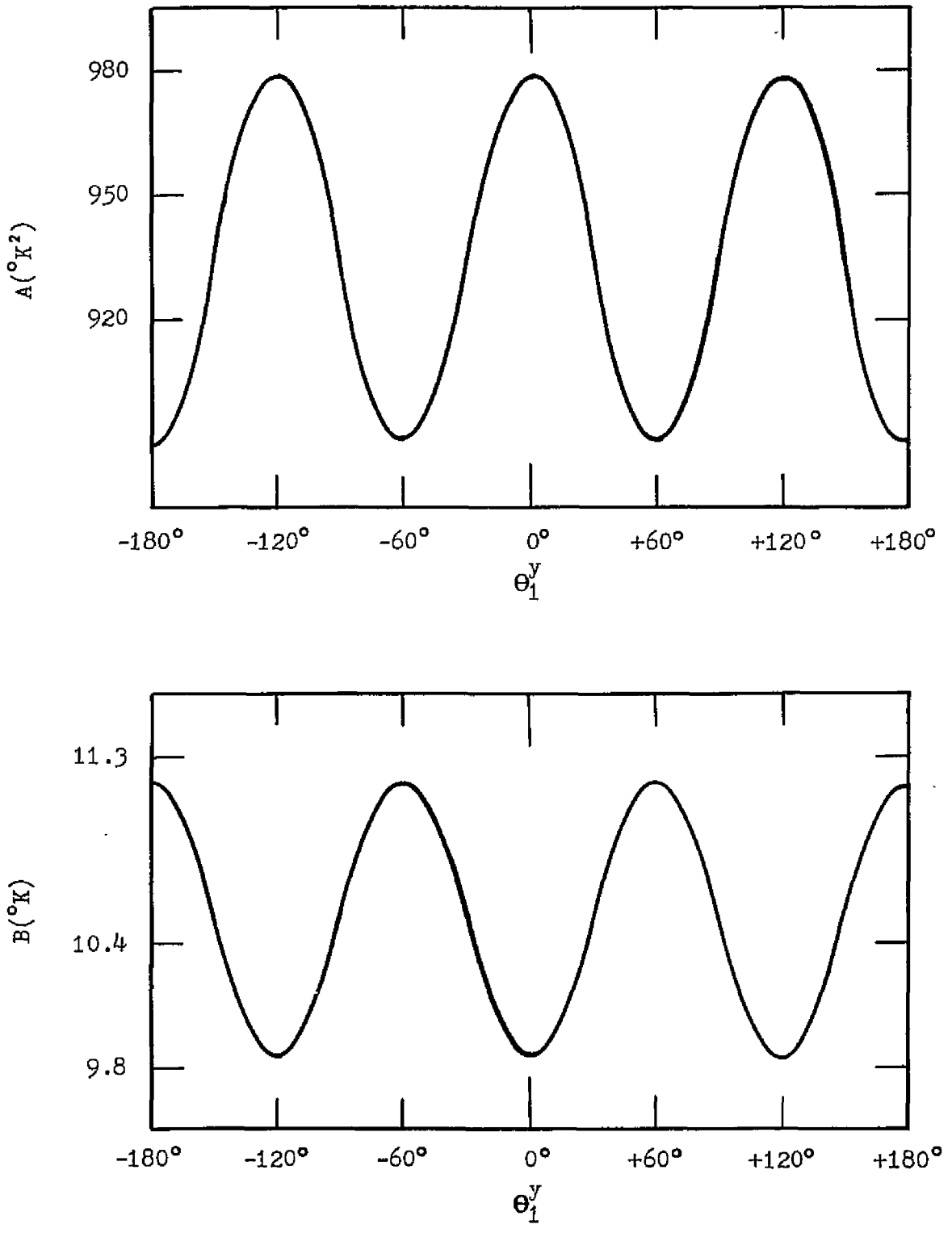

Figure 17. The vpie of $^{12}CD_4$ in the 3-cluster rocket configuration as a function of central molecular rotation around the y-axis.

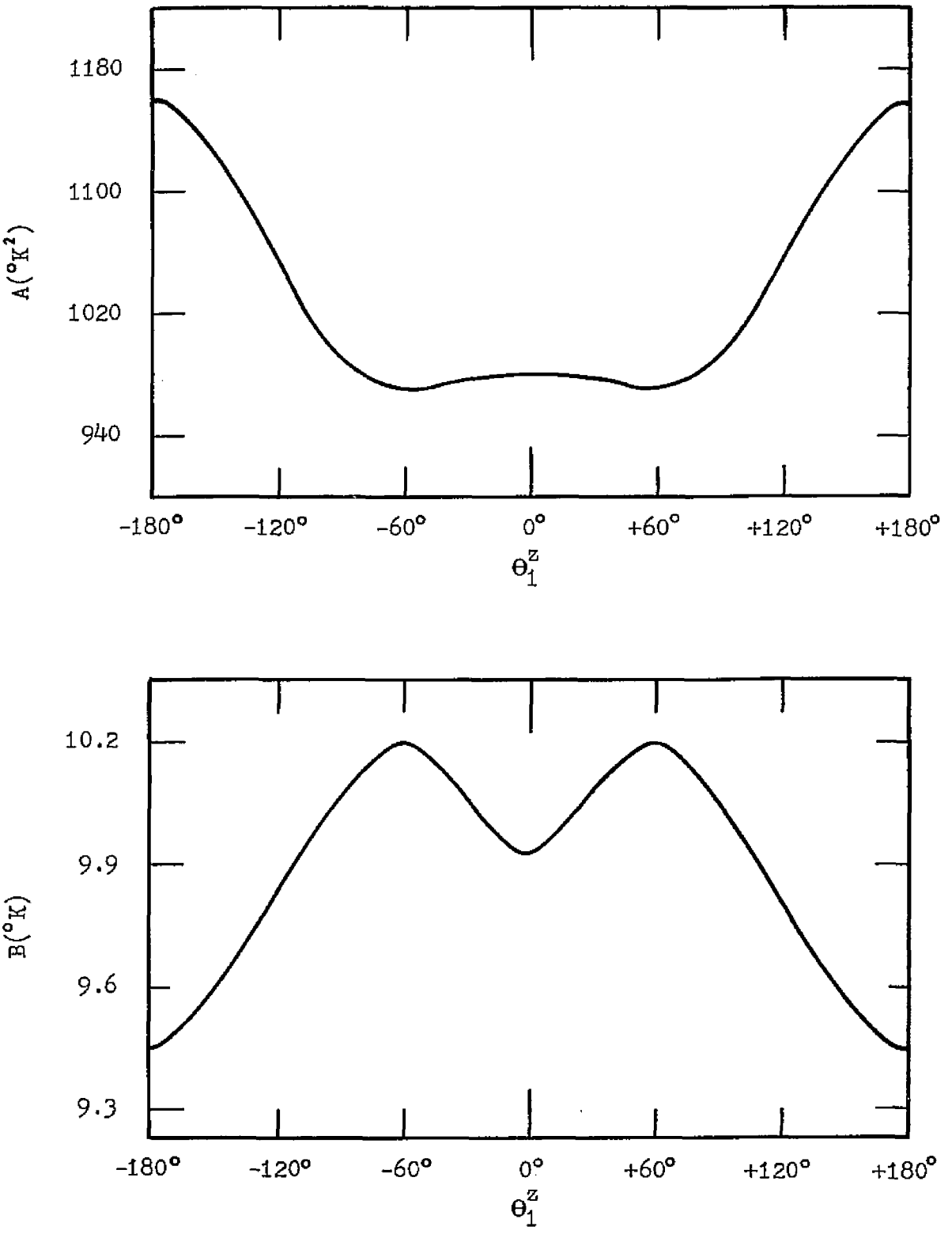

Figure 18. The vpie of $^{12}CD_4$ in the 3-cluster rocket configuration as a function of central molecular rotation around the z-axis.

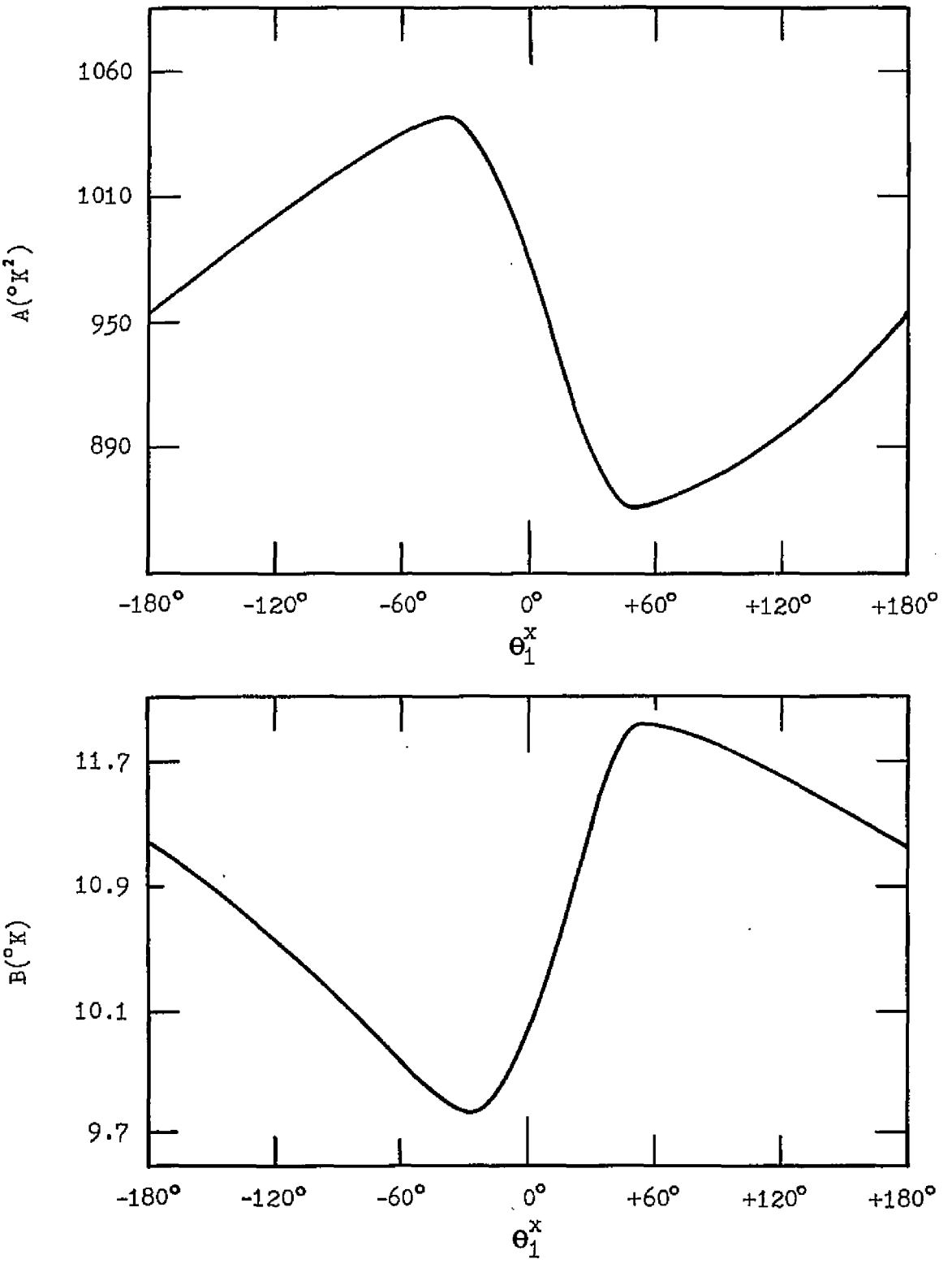

Figure 19. The vpie of $^{12}CD_4$ in the 3-cluster rocket configuration as a function of central molecular rotation around the x-axis.

difference of G-matrix elements, $g'_{ij}-g_{ij}$. In general, each of these elements g_{ij} is a sum of products of (a) a mass dependent part, expressible in terms of reduced masses, μ_i, and (b) a geometric part, expressible in terms of bond lengths and the equilibrium values of the bond angles also used to define nutational and torsional vibration, β_i and τ_i. Since orientation and geometry are the same for both the light and heavy condensed phase clusters, all non-vanishing $(g'_{ij}-g_{ij})$ terms are of the form

$$g'_{ij} - g_{ij} = (\mu'_i - \mu_i)\xi_{ij} \tag{281}$$

where ξ_{ij} is a function of orientation and geometry. The magnitude of the vapor pressure isotope effect of $^{12}CD_4$ is greater than that for $^{13}CH_4$ mainly because

$$(\mu'_i - \mu_i)_{^{12}CD_4} >> (\mu'_i - \mu_i)_{^{13}CH_4} \tag{282}$$

and the number of non-vanishing $\Delta\mu_i$ for $^{12}CD_4$ must be comparable to the number of non-vanishing $\Delta\mu_i$ for $^{13}CH_4$ since in $^{12}CD_4$ there are four atoms that are isotopically substituted, while in $^{13}CH_4$ every internal coordinate involves the central $^{13}C/^{12}C$ atom. However, because the terminal hydrogen atoms are involved in a greater number of internal coordinates for

which ξ_{ij} has a strong dependence on orientation, the vpie of $^{12}CD_4$ shows a greater relative variation with central molecular rotation than $^{13}CH_4$.

V-2: Total Orientational Effect -- The Larger Clusters

A more complete study of orientational effects on the vpie has also been performed using small perturbations of fixed intermolecular conformations for different sized clusters. The results presented in this section assume the invariance of the $\underset{\sim}{F}$-matrices given in Table XXVI and an intermolecular distance equal to 3.817 Å.

Figure 20 shows the A and B factors calculated for $^{13}CH_4$ (relative to $^{12}CH_4$) for 3-, 7-, and 9-clusters as a function of angular perturbation of the central molecule from a gear geometry. The midpoint of the abscissa of each graph in Figure 20 corresponds to a cluster geometry with each member molecule having the same orientation in space ("perfect" gear geometry). The central molecule of each cluster was rotated slightly around the x-, y-, or z-axis while holding the shell molecules in fixed orientations. The calculated A and B values change with respect to each of the three orthogonal rotations; this change is represented by three appropriately labeled curves for each sized cluster.

As shown in Figure 20, the variation of A and B caused by central molecular rotation is greatest for the 3-cluster, the most anisotropic of the different liquid phase models. As

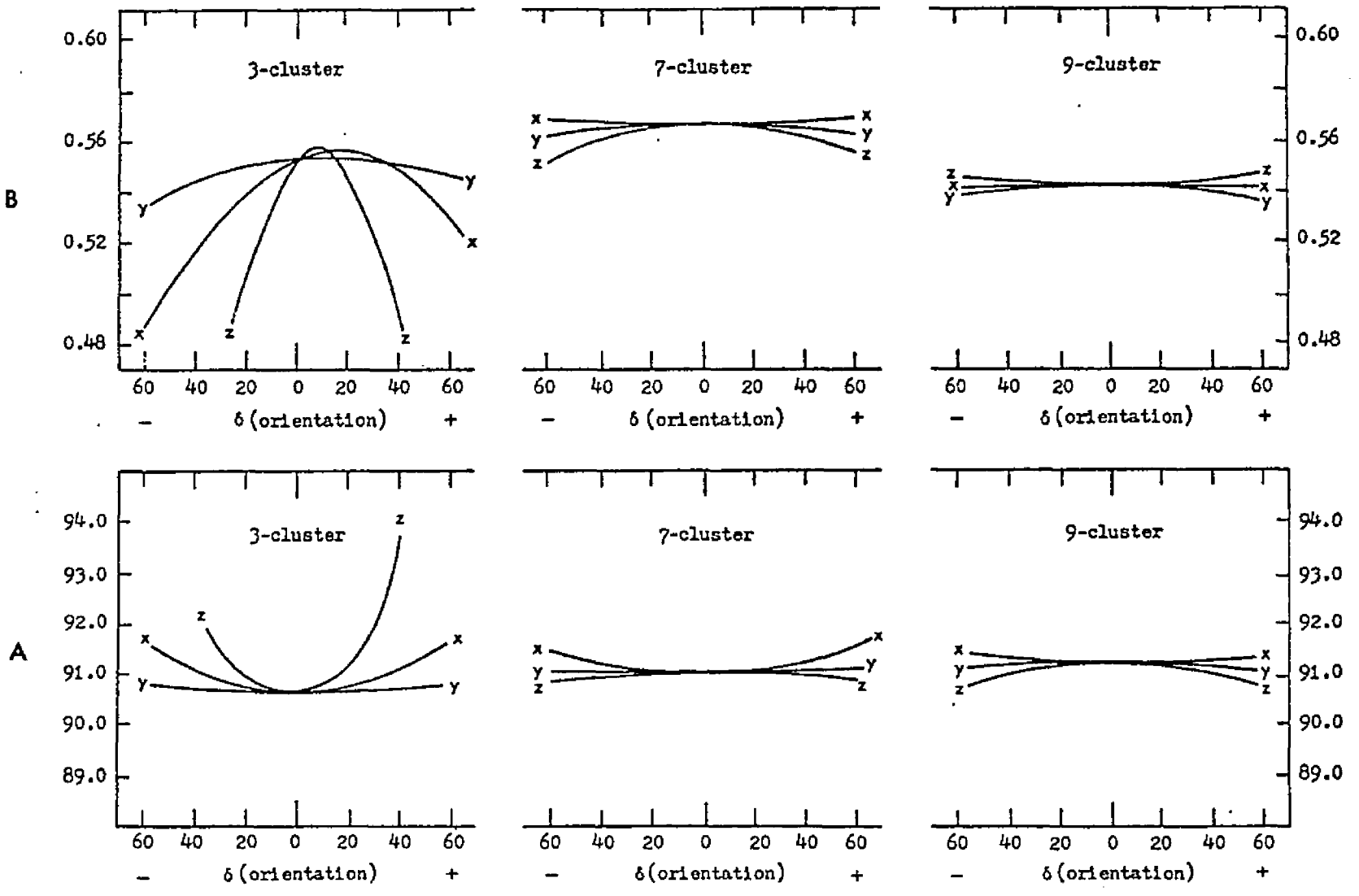

Figure 20. Total orientational effect of $^{13}CH_4$ in the gear geometry.

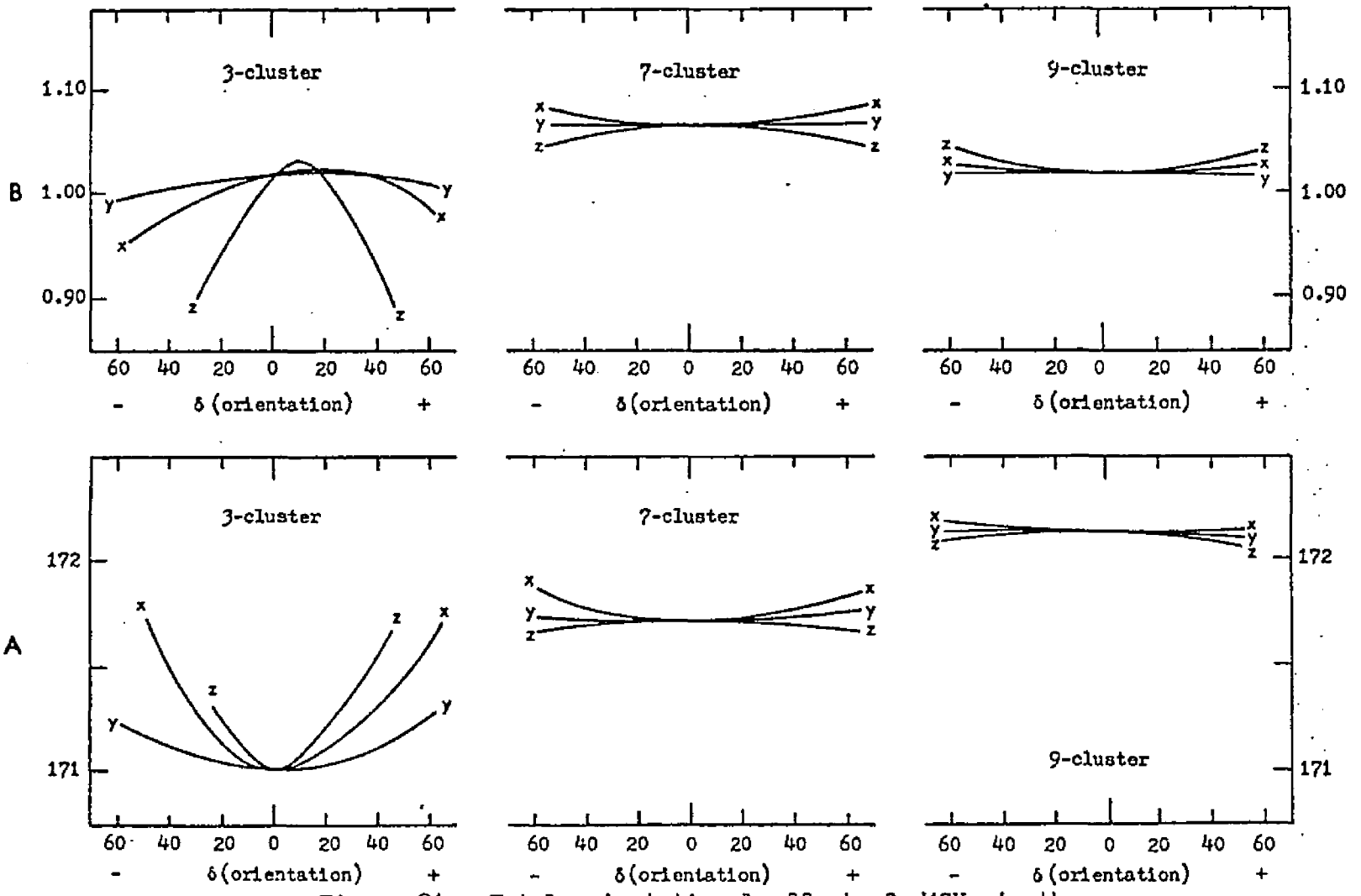

Figure 21. Total orientational effect of $^{14}CH_4$ in the gear geometry.

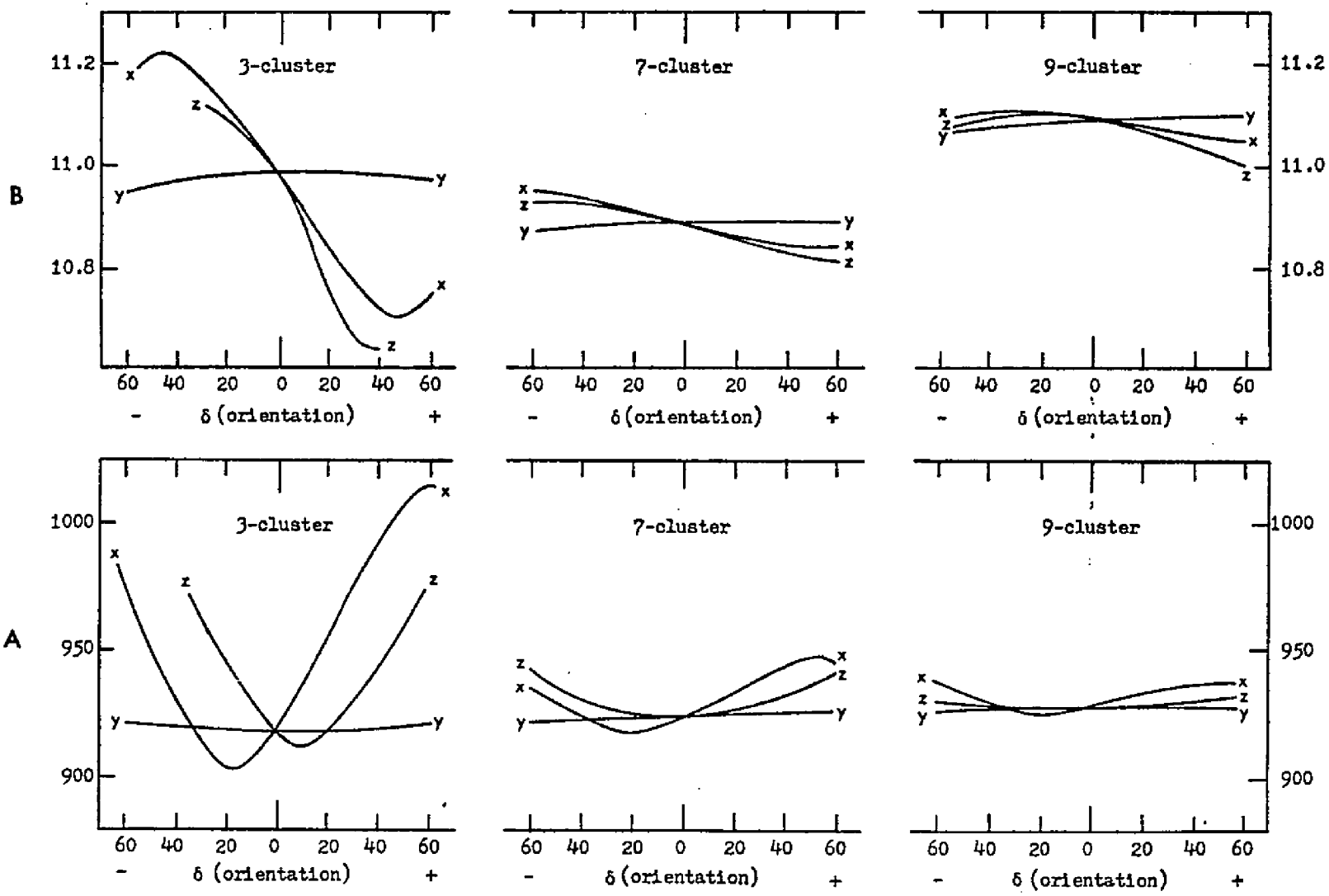

Figure 22. Total orientational effect of $^{12}CD_4$ in the gear geometry.

the cluster size increases, the liquid model becomes more isotropic as viewed from the central molecule, and the magnitude of A and B variation for equivalent angular distortion decreases markedly. While the absolute values for A and B for the perfect gear geometry are slightly different for the 3-, 7-, and 9-clusters (due to the different $\underset{\sim}{F}$-matrices used in each case), the relative effect of orientational distortion for $^{13}CH_4$ clusters obviously decreases with increasing m and increasing liquid-phase isotropy. The central molecule of a 13-cluster was similarly rotated by $\pm 20^\circ$ and $\pm 50^\circ$ around the x-, y-, and z-axes; the vpie parameters for this case (Table XXVIII) show virtually no change with gear geometry distortion, and x, y, and z rotation of the central $^{13}CH_4$ would produce a single, nearly horizontal line for A and B if plotted to the same scale as is used in Figure 20.

Figure 21 gives the results for an analogous study on the total orientational effect on the vpie of $^{14}CH_4$. The dependence of A and B on central molecular distortion from the gear geometry is similar to that for $^{13}CH_4$. Such similarity in the shapes of the A and B curves is reasonable since carbon is the isotopic substituent in each case.

The total orientational effect for $^{12}CD_4$ in the gear geometry is given in Figure 22. Because the hydrogens, rather than the carbons, are isotopically substituted, the shapes of the A and B curves as a function of central mole-

Table XXVIII

Total Orientational Effect for the 13-Cluster

Basic Geometry	δ(orientation)		$^{13}CH_4$ A(°K²)	$^{13}CH_4$ B(°K)	$^{14}CH_4$ A(°K²)	$^{14}CH_4$ B(°K)	$^{12}CD_4$ A(°K²)	$^{12}CD_4$ B(°K)
Gear	$\theta_x, \theta_y =$	+50	91.39	0.559	172.44	1.042	932.44	11.035
		+20	91.39	0.559	172.44	1.043	932.44	11.034
		-20	91.39	0.559	172.44	1.042	932.44	11.035
		-50	91.40	0.560	172.46	1.041	932.42	11.033
	$\theta_z =$	+50	91.41	0.561	172.49	1.043	932.44	11.031
		+20	91.40	0.562	172.47	1.042	932.44	11.033
		-20	91.40	0.562	172.47	1.042	932.45	11.035
		-50	91.41	0.560	172.48	1.043	932.44	11.034
Staggered Antipara.	$\theta_x =$	+50	91.40	0.559	172.45	1.044	932.44	11.035
		+20	91.40	0.559	172.45	1.044	932.44	11.034
		-20	91.39	0.559	172.45	1.044	932.43	11.035
		-50	91.39	0.560	172.45	1.044	932.43	11.036
	$\theta_y =$	+50	91.39	0.560	172.45	1.044	932.44	11.035
		+20	91.39	0.560	172.46	1.044	932.44	11.035
		-20	91.39	0.559	172.46	1.045	932.44	11.035
		-50	91.40	0.559	172.45	1.044	932.44	11.035
	$\theta_z =$	+50	91.40	0.560	172.45	1.045	932.45	11.034
		-50	91.40	0.560	172.45	1.044	932.44	11.035
Rocket	$\theta_x =$	+50	91.39	0.560	172.45	1.046	932.43	11.035
		+20	91.39	0.560	172.45	1.045	932.43	11.034
		-20	91.40	0.560	172.44	1.045	932.44	11.035
		-50	91.39	0.560	172.44	1.045	932.45	11.035
	$\theta_y =$	+50	91.41	0.561	172.46	1.045	932.46	11.036
		+20	91.40	0.559	172.46	1.045	932.45	11.036
		-20	91.40	0.559	172.46	1.045	932.45	11.036
		-50	91.39	0.559	172.45	1.045	932.44	11.035
	$\theta_z =$	+50	91.40	0.560	172.45	1.045	932.45	11.033
		-50	91.39	0.560	172.45	1.044	932.45	11.033

cular orientation are generally different from those of $^{13}CH_4$ and $^{14}CH_4$. The effect of increasing cluster size, however, is the same: as m increases, the variation of $\ell n \frac{s}{s}, f_c$ with differing intermolecular conformation becomes smaller. Variations in A and B for the $^{12}CD_4$ 13-cluster are again less than those observed for the 9-cluster (Table XXVIII).

Figures 23, 24, and 25 show the results of orientational studies obtained for $^{13}CH_4$, $^{14}CH_4$, and $^{12}CD_4$ with a starting geometry of each cluster (0° on the horizontal axes) based on the staggered antiparallel conformation. The symmetry of this configuration for the 3- and 7-clusters are such as to cause the variation of vpie parameters with central molecular rotation to be symmetric with respect to the $\theta_1^{(xyz)}=0°$ line. The results for the staggered antiparallel geometry distortion summarized in Figures 23 - 25 reinforce the conclusions reached in the gear geometry studies above.

The eclipsed rocket geometry, described in Section V-1, was used as the basis for the last group of total orientational studies. The effect on the vpie parameters A and B caused by deviation from a perfect rocket geometry of $^{13}CH_4$, $^{14}CH_4$, and $^{12}CD_4$ clusters is shown in Figures 26, 27, and 28, respectively. Results shown for $^{13}CH_4$ and $^{12}CD_4$ 3-clusters are the same as those given in the middle -60° to +60° segments of Figures 12 and 15 - 19. The variation in A and B with central rotation again shows a diminishing trend as the cluster

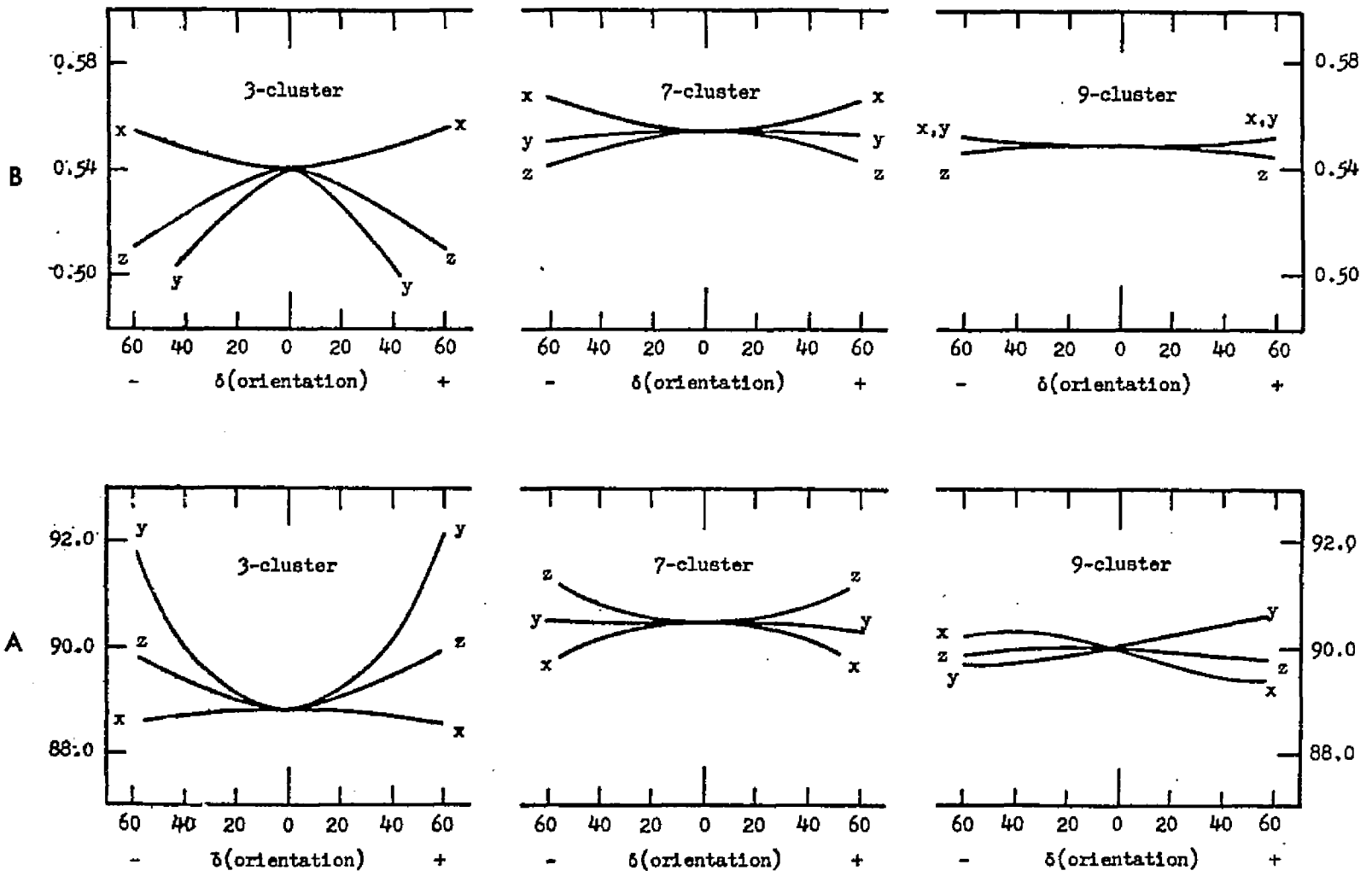

Figure 23. Total orientational effect of $^{13}CH_4$ in the staggered antiparallel geometry.

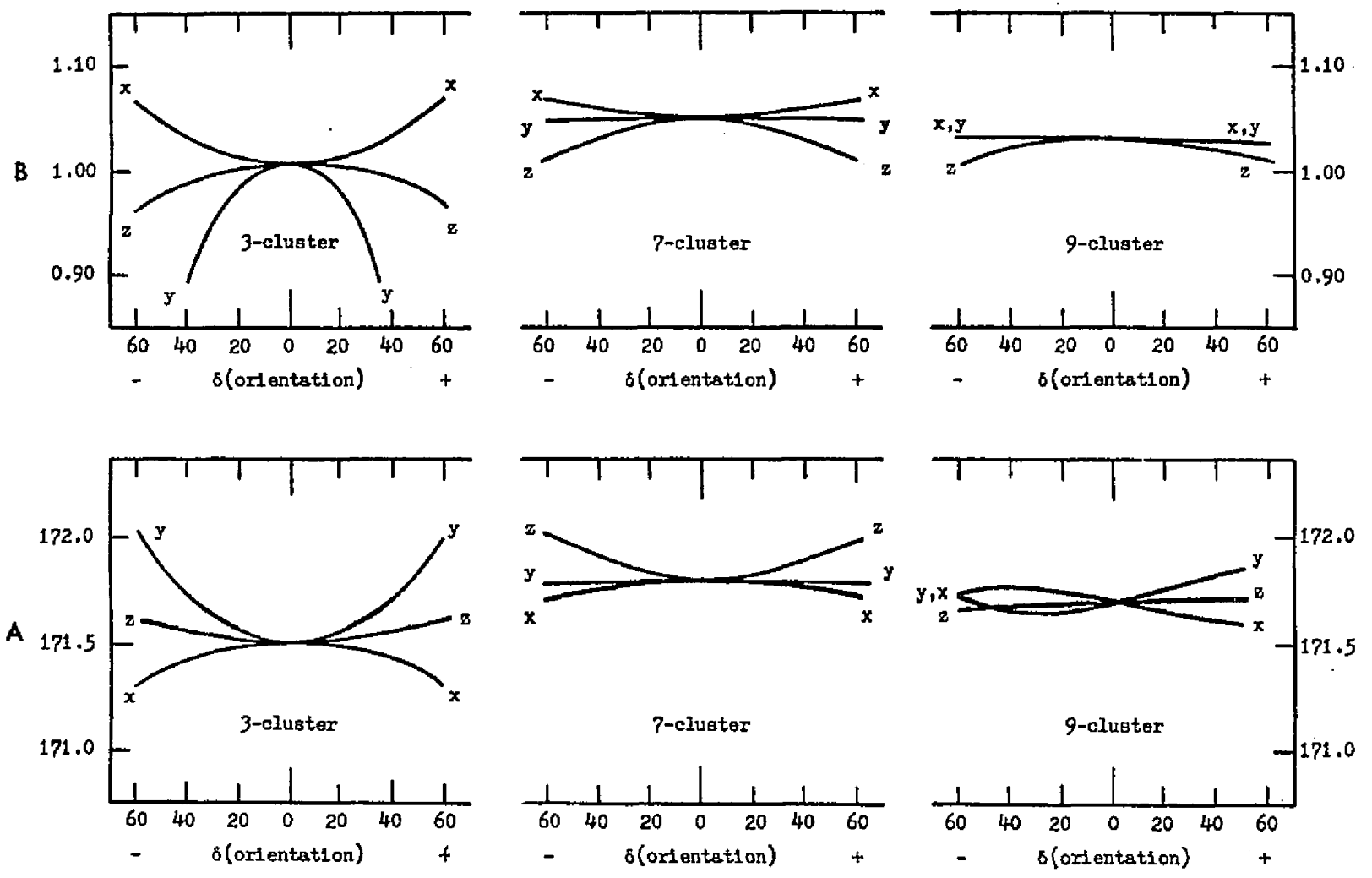

Figure 24. Total orientational effect of $^{14}CH_4$ in the staggered antiparallel geometry.

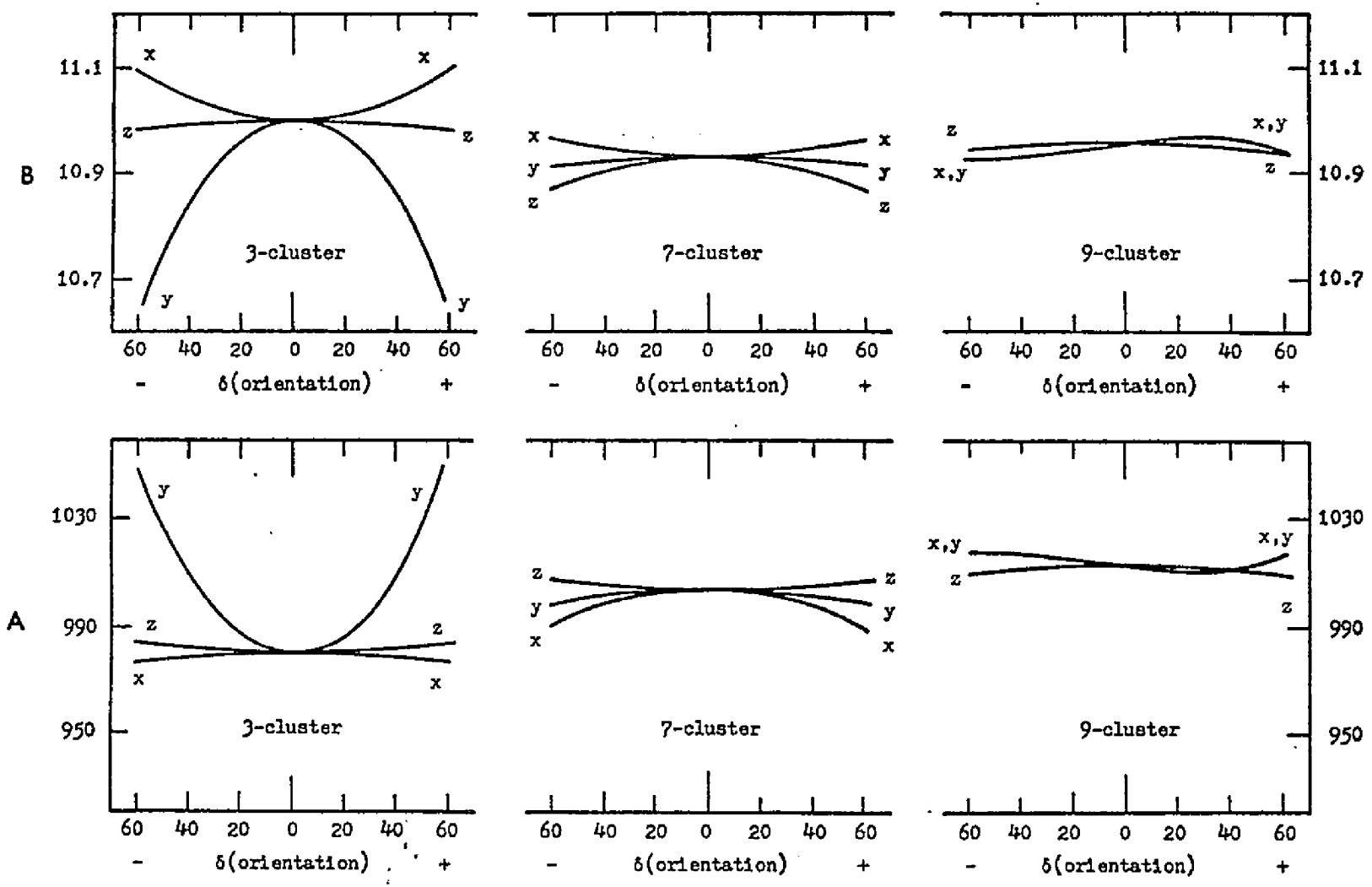

Figure 25. Total orientational effect of $^{12}CD_4$ in the staggered antiparallel geometry.

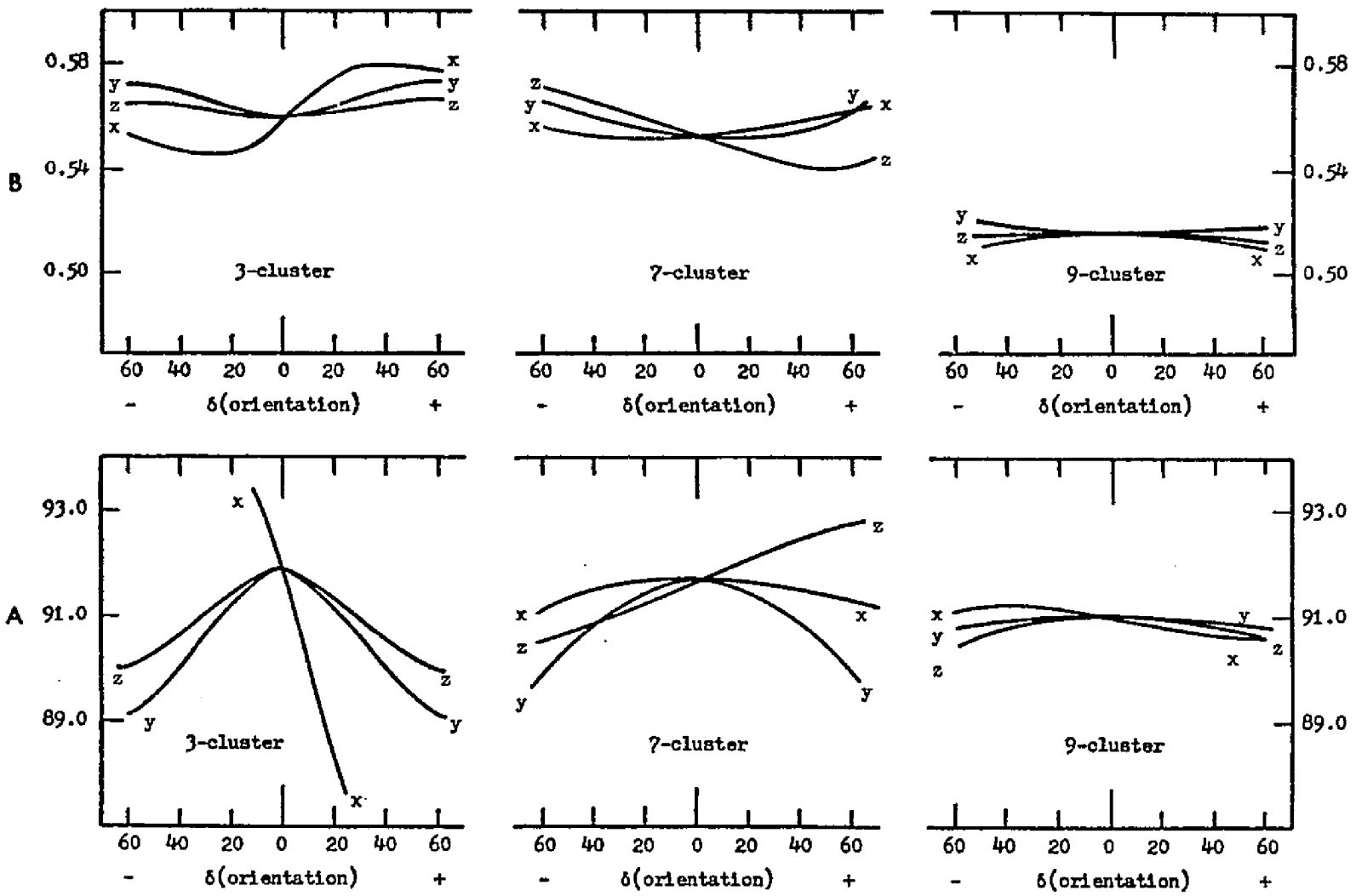

Figure 26. Total orientational effect of $^{13}CH_4$ in the rocket geometry.

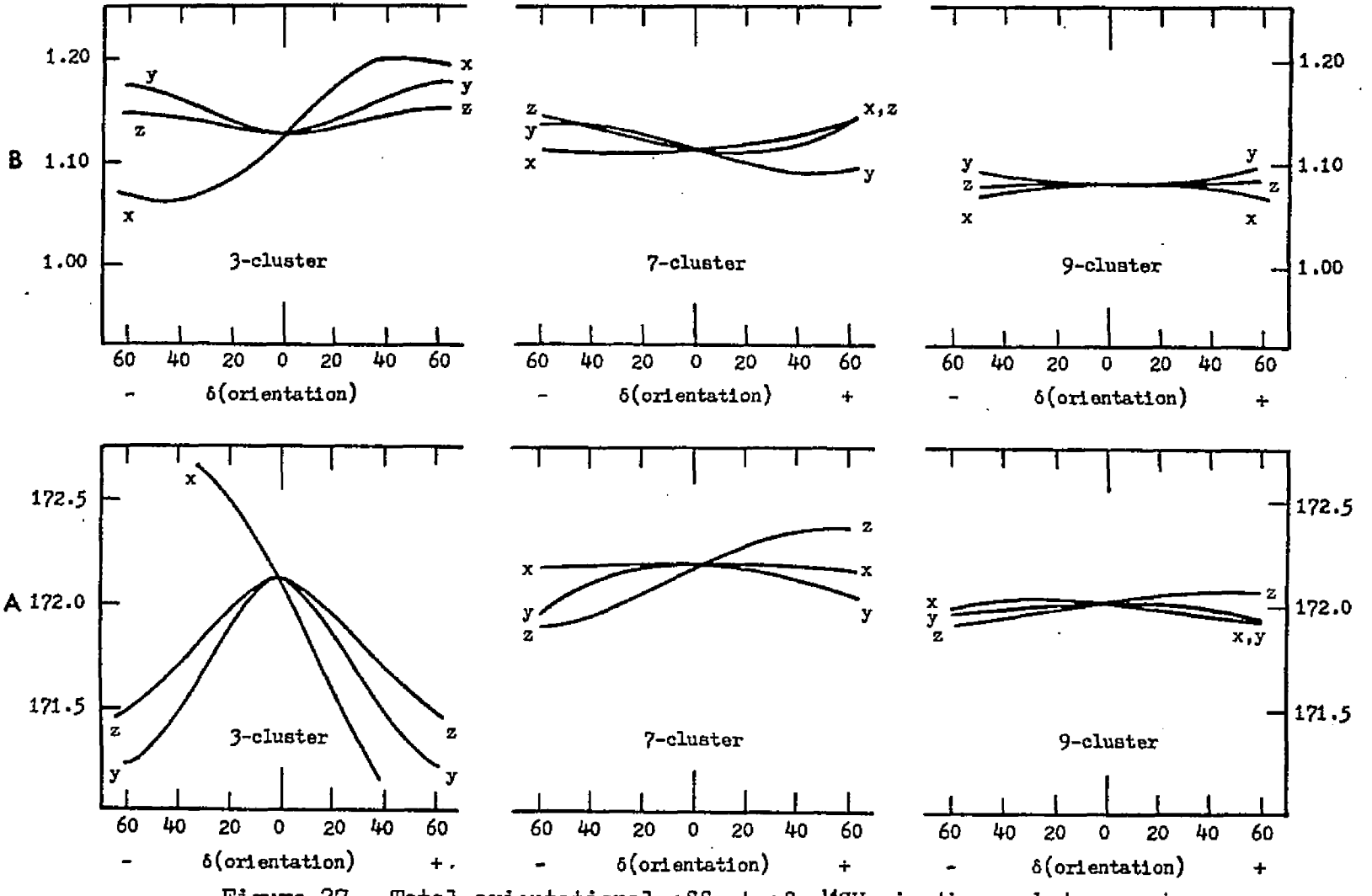

Figure 27. Total orientational effect of $^{14}CH_4$ in the rocket geometry.

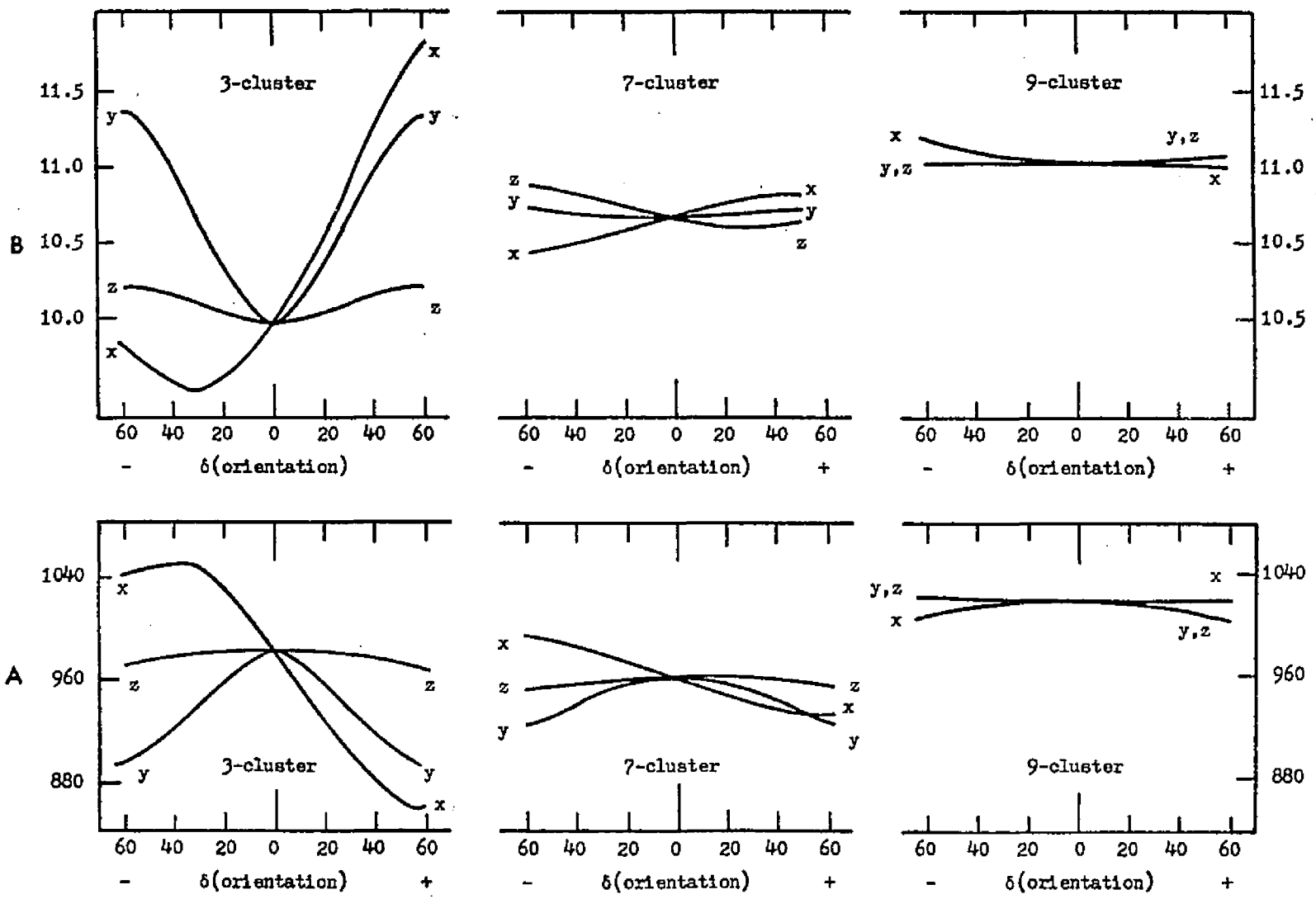

Figure 28. Total orientational effect of $^{12}CD_4$ in the rocket geometry.

size, m, is increased. The 13-cluster results are included in Table XXVIII.

Bigeleisen and Ishida (121) state that, in general, the vapor pressure isotope effect is a poor criterion of molecular geometry. The application of the medium cluster model presented in this section has shown that, in the absence of specific directional forces such as dipole-dipole interactions, the vpie is also a poor criterion of molecular orientation in the liquid phase. The general success of model calculations with harmonic external restoring forces in predicting the observed vpie of CH_4 isotopes is evidence for hindered molecular rotation in the methane condensed phase (40,122,123). However, the medium cluster model, with its consideration of specific intermolecular motion within a molecular — rather than external — reference frame, also shows that the vpie is not strongly dependent on the mutual orientations in which the molecules are constrained. For cluster sizes which simulate realistic coordination numbers (124,125) in the liquid phase (say, $m \approx 9$), the variation in vapor pressure isotope effect falls well below the level of experimental detectibility.

V-3: Non-spherical Top Methanes

The results presented in the previous section suggest that for large clusters ($m \geq 9$), the orientational influence on the condensed phase reduced partition function ratio is minimized. This fact can be used to extend the applicability of the

medium cluster model to non-spherical top methanes.

Within the Born-Oppenheimer approximation, molecules such as HD or CH_3D exhibit no permanent dipole (61) and, to a first approximation, will show no preferred orientation of deuterium atoms among condensed phase molecules. For this reason, a vapor pressure isotope effect calculation for $^{12}CH_3D$ using the medium cluster model would violate the Born-Oppenheimer principle unless results were averaged over all possible mutual orientations of the lone deuteriums. For a 3-cluster, each intermolecular conformation would require 4 x 4 x 4 separate cluster analyses, one for each combination of deuterium positions in the 15-atom aggregate. Some lone deuterium orientations are equivalent, and an appropriately weighted average of each orientational contribution to $\ell n \frac{s}{s}, f_c$ could be used. While this same violation occurs in larger clusters, the results of Section V-2 show that all orientational effects on the vpie become small as the model becomes more isotropic. The vpie results obtained for any arbitrary position of the lone deuterium in the central molecule of a 9- or 13-cluster of $^{12}CH_3D$ are representative of those for any other possible deuterium orientation.

The A and B factors calculated for some symmetric and asymmetric top methanes using a 9-cluster model in the gear geometry are shown in Table XXIX, together with results obtained for $^{13}CH_4$, $^{14}CH_4$, $^{12}CD_4$. The 9-cluster $\underset{\sim}{F}$-matrix in Table XXVI

Table XXIX

A and B Values for Methane Isotopes

Molecule	A (°K²)			B (°K)		
	Experiment[a]	Cell	MCM[b] 9-cluster	Experiment[a]	Cell	MCM[b] 9-cluster
$^{13}CH_4$	93.8± 6.1	86.9	91.2	0.535±0.06	0.32	0.543
$^{14}CH_4$	231.1±10.0	163.9	172.1	1.42 ±0.1	0.60	1.019
$^{12}CH_3D$	292.2± 3.7	282.8	290.7	2.995±0.03	2.86	2.931
$^{12}CH_3T$	502.8± 6.5	453.5	481.5	4.827±0.07	4.20	4.760
$^{12}CH_2D_2$	535.8± 5.3	529.4	529.0	5.854±0.05	5.78	5.798
$^{12}CHD_3$	748.5± 6.1	763.2	756.0	8.687±0.06	8.96	8.690
$^{12}CD_4$	894.7± 6.8	943.2	928.1	11.097±0.06	11.92	11.094

(a) Ref. (40)

(b) Gear geometry; $|\vec{\rho}| = 3.817$ Å

was used; the intermolecular separation was 3.817 Å. Since the $\underset{\sim}{F}$-matrix was calculated from a "best-fit" procedure with spherical top molecules only, the close agreement with the experimental vapor pressure isotope effects is especially interesting.

V-4: Variation of Intermolecular Separation

The final MCM parameter variation considered in this thesis research was alteration of the intermolecular distance, R ($= |\vec{\rho}|$). A gear conformation for all sized clusters was used and the $\underset{\sim}{F}$-matrices given in Table XXVI were assumed to be invariant with changing intermolecular separation.

Figures 29, 30, and 31 show the calculated A values as a function of $|\vec{\rho}|$ for m-clusters (m = 3,7,9,13) of $^{13}CH_4$, $^{14}CH_4$, and $^{12}CD_4$, respectively, relative to $^{12}CH_4$. Computations were done at 0.2 Å intervals over the range of $|\vec{\rho}| = 3$ Å to $|\vec{\rho}| = 10$ Å for m = 3, 7, and 9, and at 1.0 Å intervals for m = 13. For all isotopes, the A factor decreases monotonically as the intermolecular separation increases. This behavior is expected since the external modes for both the heavy and reference isotopic species become unrestricted at large separation and approach zero frequency. The curves in Figures 29 - 31 have a finite limit at infinite separation because of the assumption of pure harmonic motion: at larger intermolecular distances, the "true" potential begins to flatten, but the harmonic potential continues to increase indefinitely, becoming

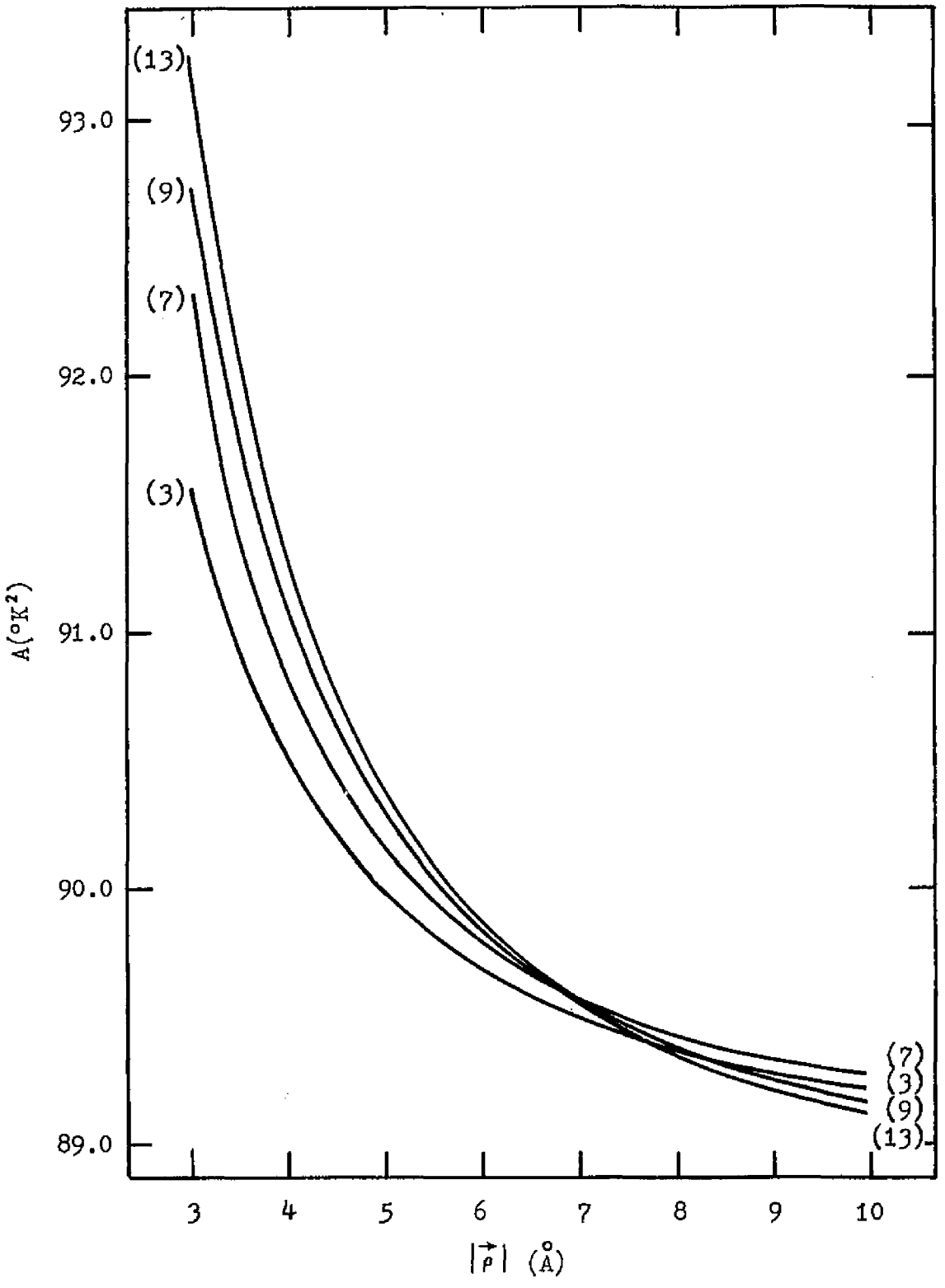

Figure 29. The vpie A factor for $^{13}CH_4$ as a function of intermolecular separation. The numbers in parentheses indicate cluster size.

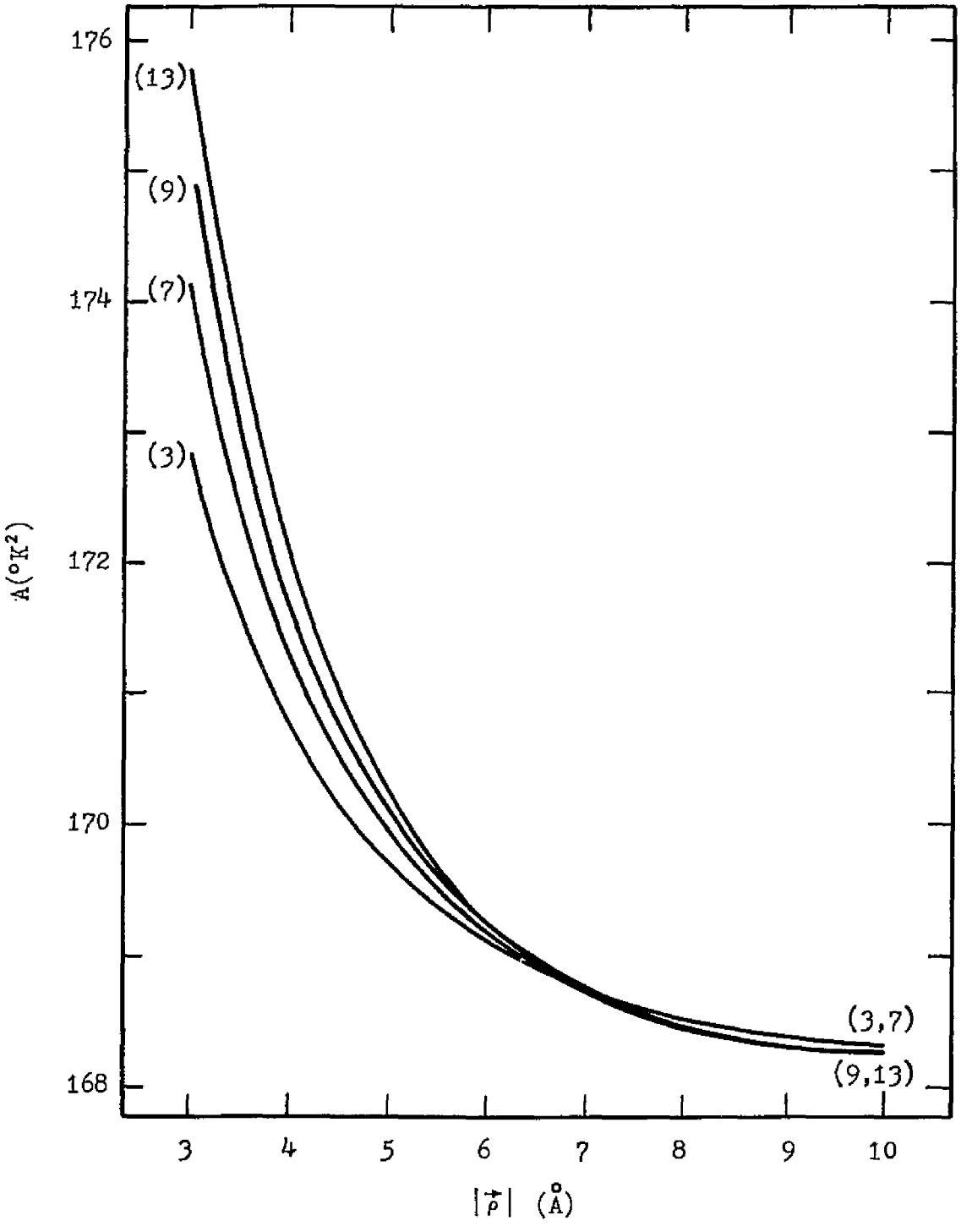

Figure 30. The vpie A factor for $^{14}CH_4$ as a function of intermolecular separation. The numbers in parentheses indicate cluster size.

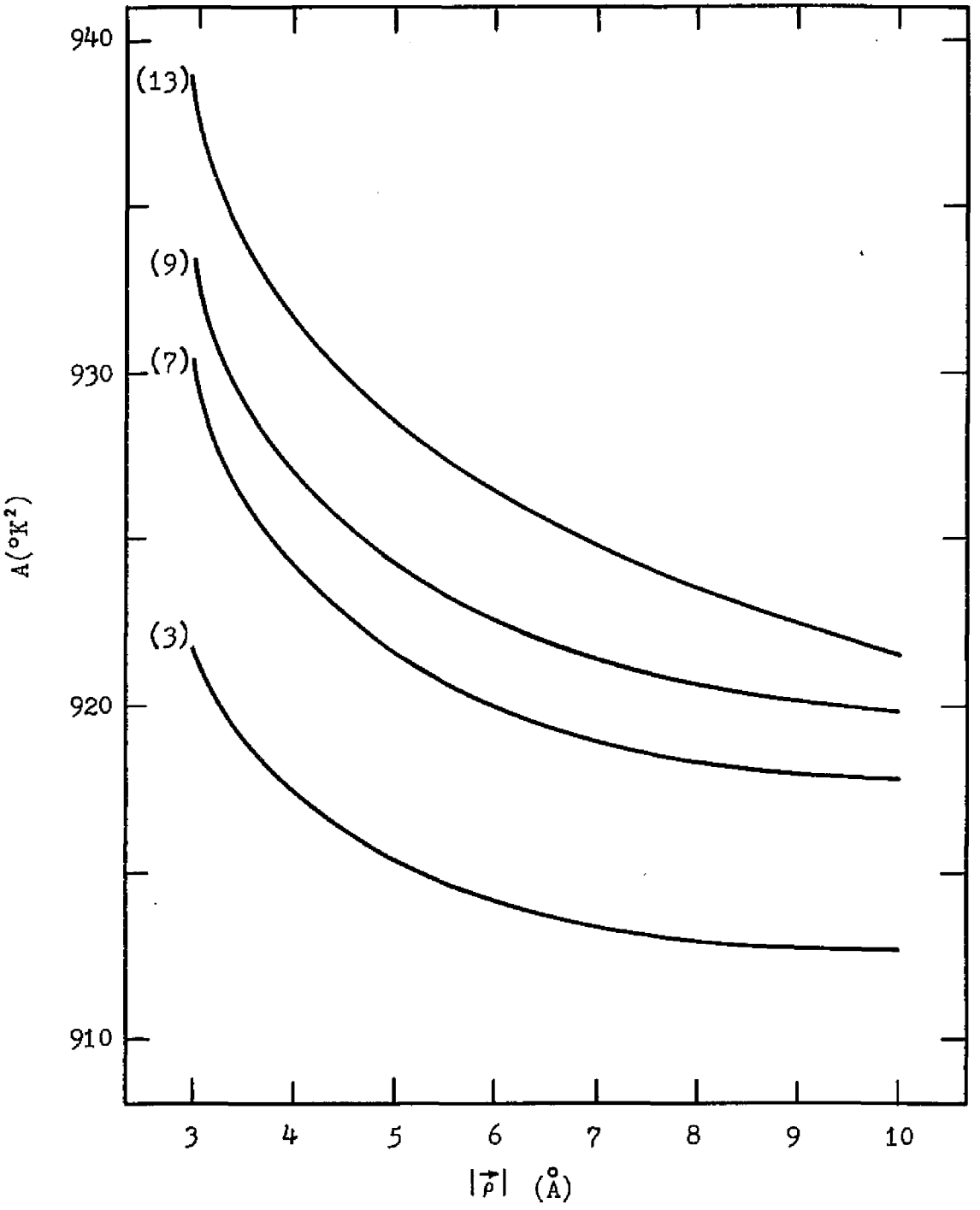

Figure 31. The vpie A factor for $^{12}CD_4$ as a function of intermolecular separation. The numbers in parentheses indicate cluster size.

a poorer and poorer approximation as the amplitude of external vibration gets larger (63). Since we are concerned with the general vapor pressure isotope effect behavior in the neighborhood of 4 Å separation, this artifact can be ignored. In general, all three spherical top methanes show a very weak dependence of A on intermolecular separation; the change in A for medium cluster models of 3, 7, 9, and 13 molecules is always less than $1\frac{1}{2}\%$ for $^{13}CH_4$ and $^{14}CH_4$ as $|\vec{\rho}|$ is varied by $\pm 50\%$ from 3 Å to 5 Å, and always less than $\frac{1}{2}\%$ for $^{12}CD_4$.

The effect of $|\vec{\rho}|$ variation on the B factors of $^{13}CH_4$, $^{14}CH_4$, and $^{12}CD_4$ is shown in Figures 32, 33, and 34, respectively. The variation in the isotopic zero point energy difference as $|\vec{\rho}|$ goes from 3 Å to 5 Å is about 1% for all isotopes. $^{12}CD_4$ shows, as expected, the monotonically decreasing B with increasing $|\vec{\rho}|$ for all m. The harmonic defect at large intermolecular separation, mentioned above in connection with the A factor, is also in evidence for B^D. The carbon-substituted methanes show the additional anomaly of monotonically increasing B values with increasing $|\vec{\rho}|$ for $m \geq 7$.

Because the internal coordinates of the central molecule do not involve changes in the carbon-carbon distance, the weak dependence of B on intermolecular separation must be due to a kinetic energy interaction between central internal coordinates and intermolecular external coordinates. These interactions are represented by elements in the $\underset{\sim}{G}^C_{ie}$ region of the $\underset{\sim}{G}$-matrix

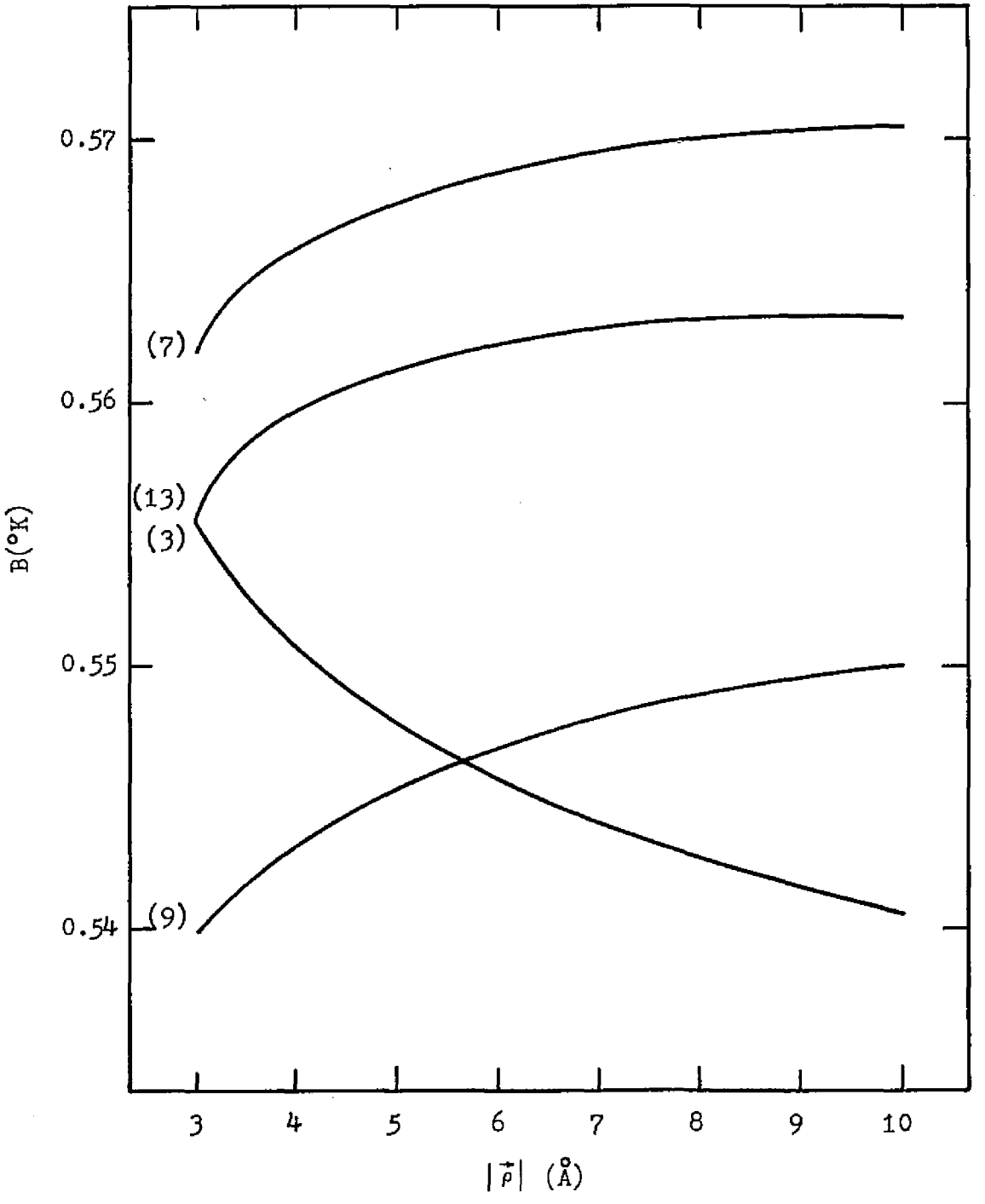

Figure 32. The vpie B factor for $^{13}CH_4$ as a function of intermolecular separation. The numbers in parentheses indicate cluster size.

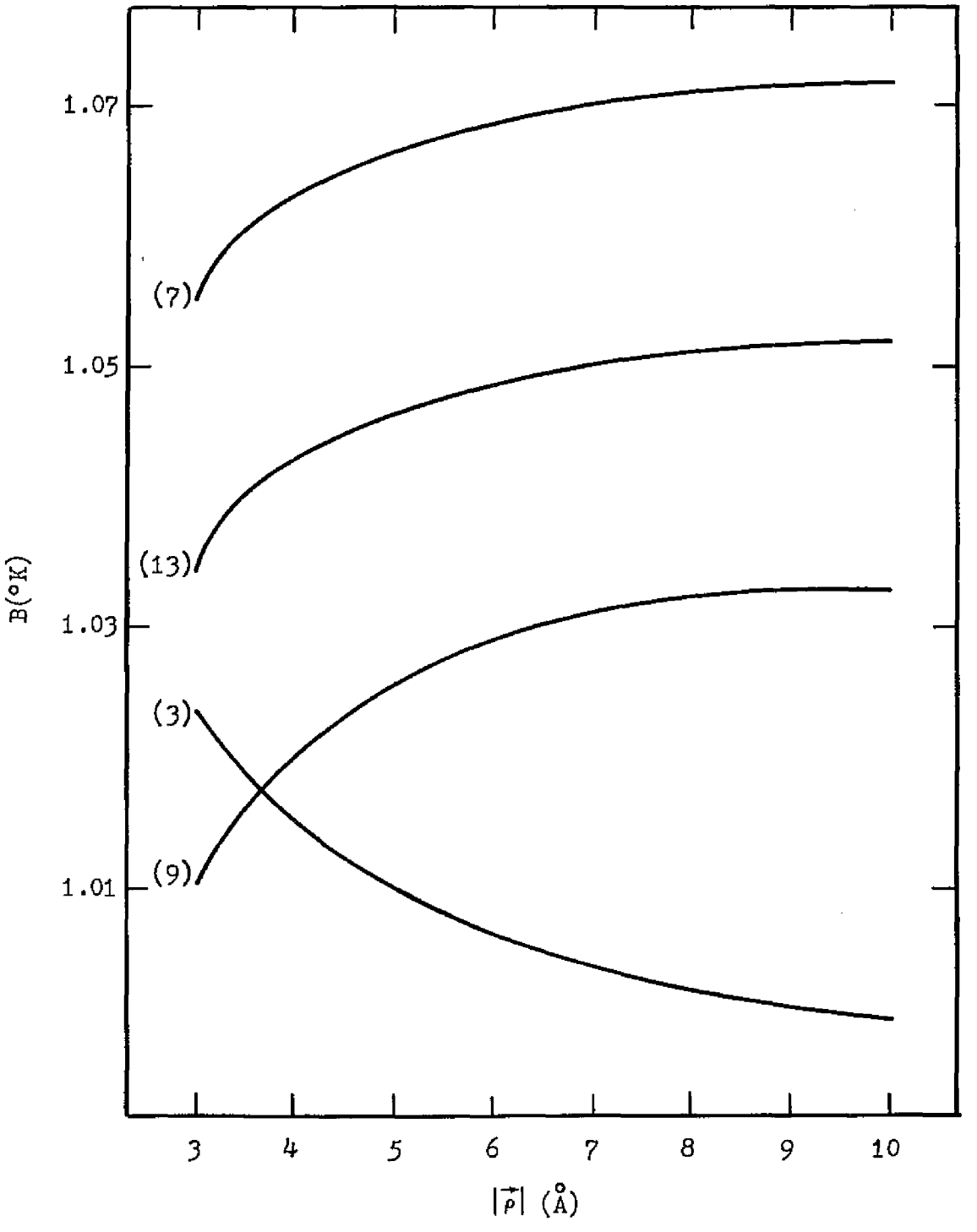

Figure 33. The vpie B factor for $^{14}CH_4$ as a function of intermolecular separation. The numbers in parentheses indicate cluster size.

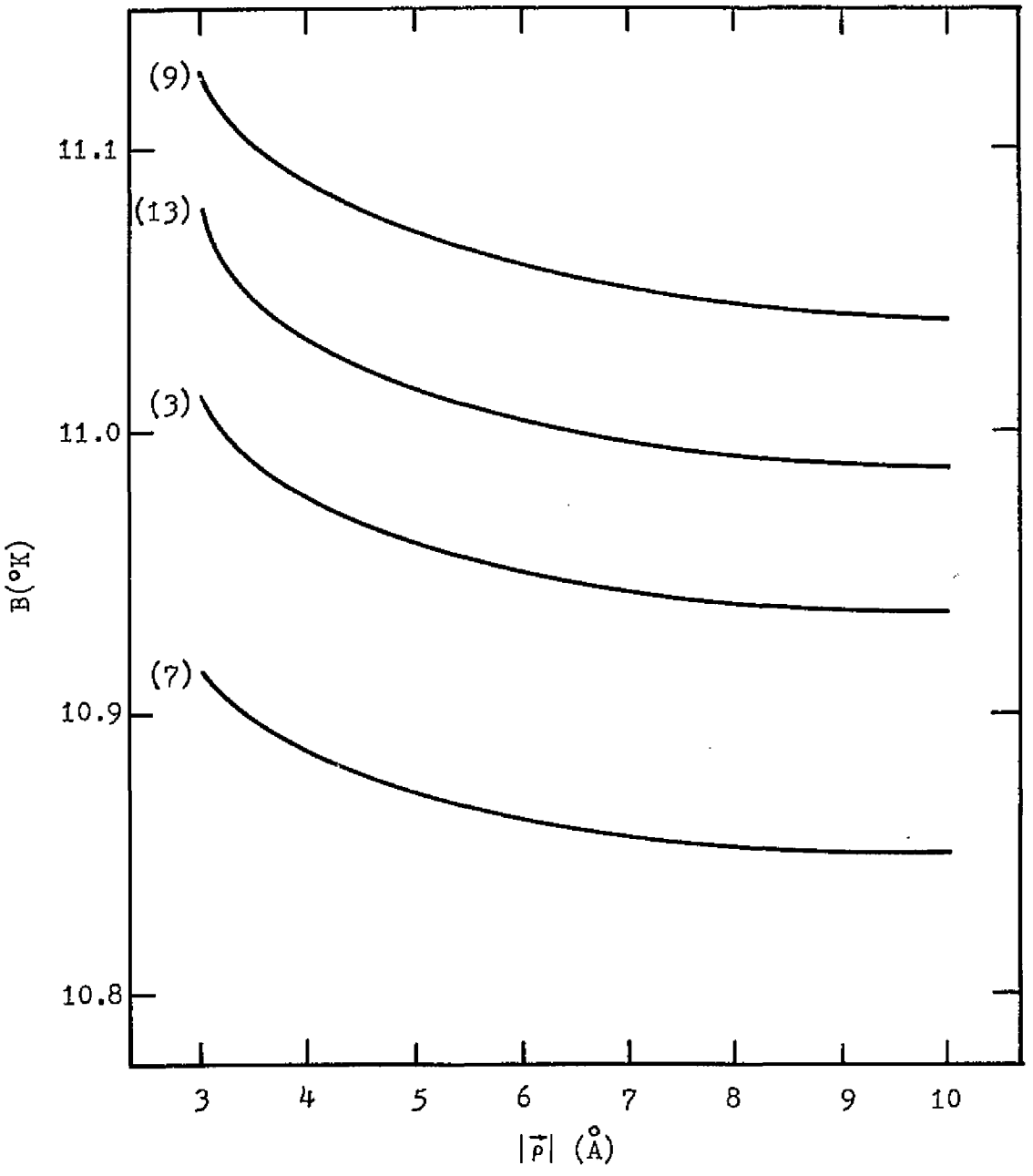

Figure 34. The vpie B factor for $^{12}CD_4$ as a function of intermolecular separation. The numbers in parentheses indicate cluster size.

shown in Equation (183). The interaction terms in this region are of six possible types: three represent the interaction of internal CH stretching with external CC stretching (g_{rR}), HCCH torsion ($g_{r\tau}$) or CCH nutation ($g_{r\beta}$), and three represent the interaction of internal HCH bending with external stretching ($g_{\alpha R}$), torsion ($g_{\alpha\tau}$), or nutation ($g_{\alpha\beta}$).

Table XXX lists the optical eigenvalues of the central molecule (in cm^{-1}) calculated for $^{12}CH_4$, $^{13}CH_4$ and $^{12}CD_4$ in both the 3- and 7-cluster for $|\vec{\rho}| = 3$ Å and $|\vec{\rho}| = 10$ Å. Gas-phase frequencies for each of the molecules are also listed for comparison. The difference in frequencies between the $|\vec{\rho}| = 10$ Å column and the gas-phase column is a result of the harmonic defect. No differences are observed between $|\vec{\rho}| = 3$ Å and $|\vec{\rho}| = 10$ Å for frequencies $\nu_1(A_1)$ or $\nu_2(E)$, and only very minor differences are seen for $\nu_3(T_2)$. The largest of the small frequency differences is exhibited by $\nu_4(T_2)$. Since ν_4 is an HCH bending mode only, to a first approximation, the intermolecular distance effect on B must be the result of $g_{\alpha R}$, $g_{\alpha\tau}$, and/or $g_{\alpha\beta}$ interactions.

To first order, $\ell n \frac{s}{s}, f$ is dependent on the sum of the products of corresponding $\underset{\sim}{F}$- and $\underset{\sim}{G}$-matrix elements as shown by Equation (277). In order to determine which kinetic energy interaction terms are primarily responsible for the intermolecular separation effect on the zero point energy (and the anomalous behavior of B^{13} and B^{14} vs. $|\vec{\rho}|$ for $m \geq 7$), the zero-

Table XXX

Central Internal Frequencies at Different Intermolecular Distances

		$^{12}CH_4$			$^{13}CH_4$			$^{12}CD_4$		
		$\|\vec{\rho}\|=10$ Å	$\|\vec{\rho}\|=3$ Å	gas	$\|\vec{\rho}\|=10$ Å	$\|\vec{\rho}\|=3$ Å	gas	$\|\vec{\rho}\|=10$ Å	$\|\vec{\rho}\|=3$ Å	gas
m = 3	ν_1	3133.624	3133.624	3143.741	3133.624	3133.624	3143.741	2216.648	2216.648	2223.804
	ν_2	1573.200	1573.200	1574.215	1573.200	1573.200	1574.215	1112.848	1112.848	1113.561
		1571.633	1571.633	1574.215	1571.633	1571.633	1574.215	1111.738	1111.738	1113.561
	ν_3	3140.568	3140.568	3154.097	3129.902	3129.902	3143.076	2320.618	2320.618	2333.201
		3140.356	3140.352	3154.097	3129.721	3129.717	3143.076	2320.075	2320.064	2333.201
		3140.348	3140.344	3154.097	3129.715	3129.711	3143.076	2320.034	2320.023	2333.201
	ν_4	1355.669	1355.735	1357.435	1347.016	1347.058	1348.914	1029.364	1029.354	1027.032
		1353.002	1352.999	1357.435	1344.377	1344.374	1348.914	1024.809	1024.806	1027.032
		1351.516	1351.502	1357.435	1342.675	1342.863	1348.914	1023.951	1023.926	1027.032
m = 7	ν_1	3133.624	3133.624	3143.741	3133.624	3133.624	3143.741	2216.648	2216.648	2223.804
	ν_2	1570.371	1570.371	1574.215	1570.364	1570.364	1574.215	1110.943	1110.942	1113.561
		1570.277	1570.277	1574.215	1570.276	1570.276	1574.215	1110.794	1110.793	1113.561
	ν_3	3139.725	3139.721	3154.097	3129.179	3129.175	3143.076	2318.982	2318.971	2333.201
		3139.722	3139.713	3154.097	3129.177	3129.169	3143.076	2318.951	2318.927	2333.201
		3139.710	3139.698	3154.097	3129.169	3129.159	3143.076	2318.879	2318.948	2333.201
	ν_4	1359.479	1359.462	1357.435	1350.757	1350.742	1348.914	1030.825	1030.791	1027.032
		1352.481	1352.644	1357.435	1343.760	1343.743	1348.914	1025.000	1024.984	1027.032
		1348.432	1348.383	1357.435	1339.670	1339.626	1348.914	1022.833	1022.752	1027.032

order $\underset{\sim}{F}$-matrices given in Table XXVI have been supplemented by the inclusion of non-zero $f_{\alpha R}$, $f_{\alpha\tau}$ and $f_{\alpha\beta}$ interaction terms. The results are shown in Table XXXI. The quantity Ω is defined as the difference between the zero point energy shifts for $|\vec{\rho}| = 3$ Å and $|\vec{\rho}| = 10$ Å,

$$\Omega = B(|\vec{\rho}| = 3\,\text{Å}) - B(|\vec{\rho}| = 10\,\text{Å}) \qquad (283)$$

A positive Ω represents a "normal", monotonically decreasing, B vs. $|\vec{\rho}|$ behavior.

As can be seen from Table XXXI, small changes in all equivalent $f_{\alpha R}$ and $f_{\alpha\beta}$ terms have the greatest influence on the behavior of B as the intermolecular distance is varied. Furthermore, there exists a range of values of $f_{\alpha R}$ for which Ω is positive for both carbon-substituted methane and hydrogen-substituted methane in 3- and 7-clusters.

While these results show that components of the molecular force field in the liquid phase far removed from the diagonal of $\underset{\sim}{F}$ can influence the general behavior of the reduced partition function ratio, the effect of varying the intermolecular separation is of very small magnitude.

V-5: Concluding Remarks

This research has developed a new model for condensed phase interactions derived within the framework of the Born-Oppenheimer and harmonic approximations. The general usefulness of the

Table XXXI

Separation Effects in the Zero Point Energy Shifts
with Augmented Liquid-phase Force Fields

$\underset{\sim}{F}_{ce}$		m = 3			m = 7		
		$\Omega(^{13}CH_4)$	$\Omega(^{14}CH_4)$	$\Omega(^{12}CD_4)$	$\Omega(^{13}CH_4)$	$\Omega(^{14}CH_4)$	$\Omega(^{12}CD_4)$
$f_{\alpha R}$ (mdyne)	-0.010	+0.0162	+0.0230	+0.0984	+0.0331	+0.0406	+0.0861
	-0.005	+0.0156	+0.0210	+0.0895	+0.0246	+0.0201	+0.0794
	0.000	+0.0151	+0.0191	+0.0622	-0.0091	-0.0167	+0.0641
	+0.005	+0.0150	+0.0186	+0.0556	-0.0228	-0.0307	+0.0246
	+0.010	+0.0148	+0.0184	+0.0501	-0.0290	-0.0376	+0.0125
$f_{\alpha\tau}$ (mdyne·Å)	-0.010	+0.0150	+0.0196	+0.0586	-0.0084	-0.0159	+0.0600
	-0.005	+0.0151	+0.0193	+0.0604	-0.0089	-0.0164	+0.0626
	0.000	+0.0151	+0.0191	+0.0622	-0.0091	-0.0167	+0.0641
	+0.010	+0.0150	+0.0196	+0.0677	-0.0096	-0.0170	+0.0685
$f_{\alpha\beta}$ (mdyne·Å)	-0.010	+0.0312	+0.0307	+0.1102	+0.0112	-0.0357	-0.0150
	-0.005	+0.0222	+0.0261	+0.0868	+0.0103	-0.0103	-0.0312
	0.000	+0.0151	+0.0191	+0.0622	-0.0091	-0.0167	+0.0641
	+0.005	-0.0030	+0.0104	+0.0344	-0.0292	-0.0311	-0.0097
	+0.010	-0.0086	+0.0006	-0.0018	-0.0302	-0.0360	-0.0152

medium cluster theory for predicting and interpreting the vapor pressure isotope effect has been demonstrated; in particular, the observed vpie for a series of isotopic methane derivatives has been successfully reproduced with better agreement with experiment than has been possible using the simple cell model. We have concluded, however, that insofar as the medium cluster model provides a reasonable picture of the liquid state, the vpie is not sufficiently sensitive to molecular orientation to permit an experimental determination of intermolecular orientation in the condensed phase through measurement of isotopic pressure ratios. The very fact that the MCM calculations have shown the virtual independence of the vpie on molecular orientation at large cluster sizes is a demonstration of the general acceptability of the cell model assumptions as far as the vpie is concerned.

Future applications of the MCM theory might include an examination of systems that exhibit strong association in the condensed phase. As mentioned in Section IV-3c, the external part of the MCM force field, $\underset{\sim}{F}_e$, consists of m-1 submatrices which were assumed to be identical in this study for the methane case [Equation (216)]. By assigning larger corresponding elements to one submatrix while keeping the others equal, a dimer-like interaction in the condensed phase is simulated, so that a correlation between molecular association and the vpie may be investigated. The methodology developed in this research will also be useful in other aspects of condensed phase theory such as the effects of "holes" and molecular dislocations.

APPENDIX

```
C
C     PROGRAM 9090
C
C     THE PURPOSE OF THIS PROGRAM IS TO CALCULATE AN X-MATRIX
C     FOR USE WITH THE 9071 PROGRAM.....
C     IF L = 1, AN ASSUMPTION OF PLATONIC CLUSTER SHAPE IS MADE
C     CLUSTER SIZE = M      MOLECULAR SIZE = N
C
C
      DOUBLE PRECISION PSI,THETA,PHI,A,B,RHO,X,TEMP
      DIMENSION A(13,13),B(13,13),RHO(13),X(13,3,6),PHI(13),
     1THETA(13),PSI(13),NCOL(3)
      REAL*8 MODEL(6) /'Z-Y-X','Z-X-Y','Y-Z-X','Y-X-Z',
     1'X-Z-Y','X-Y-Z'/
      INTEGER LABEL(3) /'Z','Y','X'/
      DATA A/14*0.,3*90.,45.,2*90.,0.,45.,3*0.,90.,2*0.,2*90.,45.,2*90
     1.,0.,45.,3*0.,90.,3*0.,90.,135.,2*90.,0.,45.,3*0.,90.,
     2,4*0.,135.,0.,90.,0.,45.,3*0.,90.,
     3 5*0.,180.,2*0.,135.,3*0.,90.,6*0.,180.,0.,135.,3*0.,90.,
     48*0.,135.,3*0.,30.,8*0.,135.,3*0.,30.,12*0.,30.,12*0.,150.,12*0.,
     5150.,12*0.,150./
      DATA B/28*0.,180.,120.,180.,120.,90.,0.,90.,3*0.,60.,
     13*0.,240.,90.,240.,180.,0.,180.,3*0.,120.,4*0.,270.,0.,270.,3*0
     2.,180.,12*0.,240.,8*0.,90.,3*0.,300.,8*0.,180.,3*0.,30.,8*0.,270.,
     33*0.,150.,12*0.,270.,12*0.,90.,12*0.,210.,12*0.,330./,PI/3.14159/
 2000 READ(5,1) IDENT,N,M,L
    1 FORMAT(4I6)
      IF(6+IDENT) 3000,20,3000
   20 DO 21 J=1,N
   21 READ (5,2) (X(1,K,J),K=1,3)
    2 FORMAT(3F14.6)
      IF(L.EQ.1) GO TO 22
      DO 13 I=2,M
   13 READ (5,3) RHO(I),A(M,I),B(M,I)
    3 FORMAT(F14.6,2F10.6)
      GO TO 17
   22 READ (5,4) RHO(2)
    4 FORMAT (F14.6)
      DO 23 I=3,M
   23 RHO(I)=RHO(2)
   17 CONTINUE
      WRITE(6,8) M
    8 FORMAT('1','THE X-MATRIX FOR THE ',I2,'-CLUSTER FOLLOWS')
      WRITE(6,483)
  483 FORMAT('+',38('_'))
      WRITE(6,484)
  484 FORMAT('0')
C
      DO 55 I=2,M
      X(I,1,1)=SNGL(X(1,1,1)+RHO(I)*DCOS(A(M,I)*1.7453292519944D-02))
      IF(DABS(X(I,1,1)).LE.(0.000001)) X(I,1,1)=0.0
      X(I,2,1)=SNGL(X(1,2,1)+RHO(I)*DSIN(A(M,I)*1.7453292519944D-02)
     1*DCOS(B(M,I)*1.7453292519944D-02))
      X(I,3,1)=SNGL(X(1,3,1)+RHO(I)*DSIN(A(M,I)*1.7453292519944D-02)
     1*DSIN(B(M,I)*1.7453292519944D-02))
      DO 55 J=2,N
      DO 56 K=1,3
   56 X(I,K,J)=X(1,K,J)
   55 CONTINUE
```

```
      DO 44 I=1,M
      READ (5,485) PSI(I),THETA(I),PHI(I),MODE
  485 FORMAT(3F14.6,I6)
      WRITE(6,7)
      WRITE(6,5) PSI(I),THETA(I),PHI(I),MODEL(MODE)
    5 FORMAT(' ',6X,'ROLL(Z)=',F12.6,' DEGREES',3X,
     1'YAW(Y)=',F12.6,' DEGREES',3X,'PITCH(X)=',F12.6,
     2' DEGREES',5X,'THE ROTATIONAL MODE IS ',A8)
      PSI(I)=PSI(I)*1.74532925199440-02
      THETA(I)=THETA(I)*1.74532925199440-02
      PHI(I)=PHI(I)*1.74532925199440-02
      GO TO (101,102,103,104,105,106),MODE
  101 CONTINUE
C     ROLL SUBSECTION
      DO 30 J=2,N
      TEMP=X(I,2,J)
      X(I,2,J)=-X(I,3,J)*DSIN(PSI(I))+X(I,2,J)*DCOS(PSI(I))
   30 X(I,3,J)=X(I,3,J)*DCOS(PSI(I))+TEMP*DSIN(PSI(I))
C     YAW SUBSECTION
      DO 31 J=2,N
      TEMP=X(I,3,J)
      X(I,3,J)=X(I,3,J)*DCOS(THETA(I))-X(I,1,J)*DSIN(THETA(I))
   31 X(I,1,J)=TEMP*DSIN(THETA(I))+X(I,1,J)*DCOS(THETA(I))
C     PITCH SUBSECTION
      DO 32 J=2,N
      TEMP=X(I,2,J)
      X(I,2,J)=X(I,2,J)*DCOS(PHI(I))+X(I,1,J)*DSIN(PHI(I))
   32 X(I,1,J)=-TEMP*DSIN(PHI(I))+X(I,1,J)*DCOS(PHI(I))
      GO TO 200
  102 CONTINUE
C     ROLL SUBSECTION
      DO 33 J=2,N
      TEMP=X(I,2,J)
      X(I,2,J)=-X(I,3,J)*DSIN(PSI(I))+X(I,2,J)*DCOS(PSI(I))
   33 X(I,3,J)=X(I,3,J)*DCOS(PSI(I))+TEMP*DSIN(PSI(I))
C     PITCH SUBSECTION
      DO 34 J=2,N
      TEMP=X(I,2,J)
      X(I,2,J)=X(I,2,J)*DCOS(PHI(I))+X(I,1,J)*DSIN(PHI(I))
   34 X(I,1,J)=-TEMP*DSIN(PHI(I))+X(I,1,J)*DCOS(PHI(I))
C     YAW SUBSECTION
      DO 35 J=2,N
      TEMP=X(I,3,J)
      X(I,3,J)=X(I,3,J)*DCOS(THETA(I))-X(I,1,J)*DSIN(THETA(I))
   35 X(I,1,J)=TEMP*DSIN(THETA(I))+X(I,1,J)*DCOS(THETA(I))
      GO TO 200
  103 CONTINUE
C     YAW SUBSECTION
      DO 36 J=2,N
      TEMP=X(I,3,J)
      X(I,3,J)=X(I,3,J)*DCOS(THETA(I))-X(I,1,J)*DSIN(THETA(I))
   36 X(I,1,J)=TEMP*DSIN(THETA(I))+X(I,1,J)*DCOS(THETA(I))
C     ROLL SUBSECTION
      DO 37 J=2,N
      TEMP=X(I,2,J)
      X(I,2,J)=-X(I,3,J)*DSIN(PSI(I))+X(I,2,J)*DCOS(PSI(I))
   37 X(I,3,J)=X(I,3,J)*DCOS(PSI(I))+TEMP*DSIN(PSI(I))
C     PITCH SUBSECTION
      DO 38 J=2,N
      TEMP=X(I,2,J)
      X(I,2,J)=X(I,2,J)*DCOS(PHI(I))+X(I,1,J)*DSIN(PHI(I))
   38 X(I,1,J)=-TEMP*DSIN(PHI(I))+X(I,1,J)*DCOS(PHI(I))
      GO TO 200
  104 CONTINUE
C     YAW SUBSECTION
      DO 39 J=2,N
```

```
      TEMP=X(I,3,J)
      X(I,3,J)=X(I,3,J)*DCOS(THETA(I))-X(I,1,J)*DSIN(THETA(I))
   39 X(I,1,J)=TEMP*DSIN(THETA(I))+X(I,1,J)*DCOS(THETA(I))
C     PITCH SUBSECTION
      DO 60 J=2,N
      TEMP=X(I,2,J)
      X(I,2,J)=X(I,2,J)*DCOS(PHI(I))+X(I,1,J)*DSIN(PHI(I))
   60 X(I,1,J)=-TEMP*DSIN(PHI(I))+X(I,1,J)*DCOS(PHI(I))
C     ROLL SUBSECTION
      DO 61 J=2,N
      TEMP=X(I,2,J)
      X(I,2,J)=-X(I,3,J)*DSIN(PSI(I))+X(I,2,J)*DCOS(PSI(I))
   61 X(I,3,J)=X(I,3,J)*DCOS(PSI(I))+TEMP*DSIN(PSI(I))
      GO TO 200
  105 CONTINUE
C     PITCH SUBSECTION
      DO 62 J=2,N
      TEMP=X(I,2,J)
      X(I,2,J)=X(I,2,J)*DCOS(PHI(I))+X(I,1,J)*DSIN(PHI(I))
   62 X(I,1,J)=-TEMP*DSIN(PHI(I))+X(I,1,J)*DCOS(PHI(I))
C     ROLL SUBSECTION
      DO 63 J=2,N
      TEMP=X(I,2,J)
      X(I,2,J)=-X(I,3,J)*DSIN(PSI(I))+X(I,2,J)*DCOS(PSI(I))
   63 X(I,3,J)=X(I,3,J)*DCOS(PSI(I))+TEMP*DSIN(PSI(I))
C     YAW SUBSECTION
      DO 64 J=2,N
      TEMP=X(I,3,J)
      X(I,3,J)=X(I,3,J)*DCOS(THETA(I))-X(I,1,J)*DSIN(THETA(I))
   64 X(I,1,J)=TEMP*DSIN(THETA(I))+X(I,1,J)*DCOS(THETA(I))
      GO TO 200
  106 CONTINUE
C     PITCH SUBSECTION
      DO 65 J=2,N
      TEMP=X(I,2,J)
      X(I,2,J)=X(I,2,J)*DCOS(PHI(I))+X(I,1,J)*DSIN(PHI(I))
   65 X(I,1,J)=-TEMP*DSIN(PHI(I))+X(I,1,J)*DCOS(PHI(I))
C     YAW SUBSECTION
      DO 66 J=2,N
      TEMP=X(I,3,J)
      X(I,3,J)=X(I,3,J)*DCOS(THETA(I))-X(I,1,J)*DSIN(THETA(I))
   66 X(I,1,J)=TEMP*DSIN(THETA(I))+X(I,1,J)*DCOS(THETA(I))
C     ROLL SUBSECTION
      DO 67 J=2,N
      TEMP=X(I,2,J)
      X(I,2,J)=-X(I,3,J)*DSIN(PSI(I))+X(I,2,J)*DCOS(PSI(I))
   67 X(I,3,J)=X(I,3,J)*DCOS(PSI(I))+TEMP*DSIN(PSI(I))
  200 DO 19 J=2,N
      DO 18 K=1,3
   18 X(I,K,J)=X(I,K,J)+X(I,K,1)
   19 CONTINUE
   43 CONTINUE
C
C
      WRITE (6,7)
    7 FORMAT('-')
      DO 46 K=1,3
   46 WRITE(6,9) LABEL(K),(X(I,K,J),J=1,N)
    9 FORMAT(' ',A4,6F14.6)
   45 CONTINUE
   44 CONTINUE
      NN=1
      DO 408 I=1,M
      DO 408 J=1,N
      WRITE(9,409) (K,NN,X(I,K,J),K=1,3)
  408 NN=NN+1
```

```
  409 FORMAT(3(2I3,F20.15))
      WRITE(9,777)
  777 FORMAT(1X,'-1')
 1000 CONTINUE
      GO TO 2000
 3000 CONTINUE
      END
```

```
C
C     THE FOLLOWING PROGRAM PRE-ASSEMBLES F
C
      IMPLICIT REAL*8 (A-H,O-Z)
      REAL*4 RECORD(18)
      DIMENSION NRO(339),NCO(339),NFO(339),Z(339)
      DIMENSION F(147,147),FI(20)
      NAMELIST/ERROR/K,NRO,NCO,NFO,Z
      READ(5,1) (RECORD(I),I=1,18)
    1 FORMAT(18A4)
      READ(5,2) NQ,NOZ,NF
    2 FORMAT(3I5)
      READ(5,3) (NRO(I),NCO(I),NFO(I),Z(I),I=1,NOZ)
    3 FORMAT(4(3I3,F9.6))
      READ(5,4) (FI(K),K=1,NF)
    4 FORMAT(6F12.6)
      DO 10 I=1,NQ
      DO 10 J=1,NQ
   10 F(I,J)=0.000
      DO 170 K=1,NOZ
      IF(NCO(K)-NQ.GT.0) GO TO 615
      IF(NRO(K)-NCO(K).GT.0) GO TO 615
      IF(NFO(K)-NF.GT.0) GO TO 615
      I=NRO(K)
      J=NCO(K)
      M=NFO(K)
      F(I,J)=F(I,J)+Z(K)*FI(M)
  170 F(J,I)=F(I,J)
      DO 179 I=1,NQ
  179 WRITE(12) (F(I,J),J=1,NQ)
      WRITE(6,1) (RECORD(I),I=1,18)
      DO 180 I=1,NQ
  180 WRITE(6,6) I,(F(I,J),J=1,NQ)
    6 FORMAT(5H0 ROWI4/(10F12.6))
      GO TO 90
  615 WRITE(6,ERROR)
   90 CONTINUE
      END
```

```
C     THIS IS A MODIFICATION OF 9071 AND COMPUTES COORDINATES USING
C     ISOTOPE-INDEPENDENT B-MATRIX FOR BOTH INTERNAL AND EXTERNAL
C     COORDINATES.  B IS COMPUTED FOR ISOTOPE 1 ONLY. PROGRAM 9071 IS
C     AN ISHIDA MODIFICATION OF SDW 9064I.  G MATRIX EVALUATION PROGRAM
C     FOR IBM 7090 MONITOR THIS PROGRAM EVALUATES G AND B MATRIX
C     ELEMENTS FOR UP TO 84 COORDINATES FOR MOLECULES CONTAINING UP TO
C     28 ATOMS.  THE G MATRIX MAY BE SYMMETRIZED G AND B ARE PUNCHED
C     ONTO CARDS IN A FORM SUITABLE FOR INPUT TO SD 9032.  THE MOMENT
C     OF INERTIA TENSOR AND THE TRANSFORMATION TO PRINCIPLE AXES ARE
C     EVALUATED.  THIS PROGRAM EVALUATES G AND B MATRIX ELEMENTS FOR 6
C     TYPES OF INTERNAL COORDINATES.(1)BOND STRETCHING,(2)VALENCE ANGLE
C     BENDING,(3)OUT OF PLANE WAGGING,(4)TORSION,(5)LINEAR VALENCE
C     ANGLE BENDING,AND(6)IN PLANE WAGGING FOR UP TO 28 ATOMS AND UP TO
C     84 INTERNAL COORDINATES.  THE INPUT DATA ARE THE MASSES AND THE
C     CARTESIAN COORDINATES OF THE ATOMS IN AN ARBITRARY REFERENCE
C     FRAME.
C
C
      IMPLICIT REAL*8(A-H,O-Z)
      DIMENSION X(3,66),WT(66),B(147,147),NI(147),NCOD(147),N1(147),
     1N2(147),N3(147),N4(147),N5(147),N6(147),G(147,147),
     2NROW(4),NCOL(4),DATIN(4),R(3),D(66,66)
      REAL*4 RECORD(36)
      INTEGER CONCAT
      COMMON X,WT,B,IND,NOPROB,NOAT,NQ,INT,NISO,NA,MJ,NOINT,NI,NCOD,N1,
     1N2,N3,N4,N5,N6,JOKER,NROB,NOP,NCA,NS,NCO,N7,N8
      EQUIVALENCE (G,D)
   90 READ (5,12) IND,NOP,NOAT,NQ,INT,NISO,CONCAT
   12 FORMAT(I3,I4,I2,4I3)
      IF(9+IND) 95,92,95
   95 CALL EXIT
   92 NOPROB=100*NOP
  100 READ(5,14) (RECORD(I),I=1,36)
   14 FORMAT(18A4)
  101 WRITE(6,50) NOPROB,NQ,NISO
   50 FORMAT(22H1 G MATRIX PROBLEM NO.I8,I6,12H COORDINATESI4,9H ISOTOPE
     1S)
C     READ X MATRIX. THE CARTESIAN COORDINATES OF THE ATOMS.
C        THE X MATRIX IS PUNCHED IN 18 COLUMN FIELDS,4 PER CARD. THE
C        FIRST THREE COLUMNS GIVE THE ROW NUMBER IDENTIFYING THE
C        CARTESIAN AXES. COLUMNS 4-6 GIVE THE COLUMN NUMBER OF THE X
C        MATRIX.THE ATOM NUMBER,AND COLUMNS 7-18 GIVE THE ELEMENT WITH
C        THE DECIMAL POINT BETWEEN COLUMNS 12-13 OR PUNCHED.THE
C        ROW NUMBER FOLLOWING THE LAST ELEMENT IS SET EQUAL TO -1.
  105 DO 107 I=1,3
      DO 107 J=1,NOAT
  107 X(I,J)=0.0D0
  108 IF(CONCAT.EQ.1) GO TO 2
      READ (5,16)           (NROW(L),NCOL(L),DATIN(L),L=1,3)
      GO TO 3
    2 READ(9,16) (NROW(L),NCOL(L),DATIN(L),L=1,3)
   16 FORMAT(3(2I3,F20.15))
    3 WRITE (6,21)           (NROW(L),NCOL(L),DATIN(L),L=1,3)
   21 FORMAT(1H 3(2I3,F20.15))
  109 DO 114 L=1,3
      IF(NROW(L))116,600,111
  111 IF(3-NROW(L))600,112,112
  112 IF(NOAT-NCOL(L))600,113,113
  113 I=NROW(L)
```

```
      J=NCOL(L)
  114 X(I,J)=OATIN(L)
      GO TO 108
  116 IF(NROW(L)+1)600,120,600
C       READ INTERNAL COORDINATE  VECTORS
C         A VECTOR OF 8 NUMBERS NI,NCOD,N1,N2,N3,N4,N5,N6 GIVING THE NO.
C        ASSINGED TO THE INTERNAL COORDINATE,NI, THE CODE IDENTFYING
C        THE TYPE OF COORDINATE,NCOD, AND THE NUMBERS OF THE ATOMS
C         DEFINING THE COORDINATE.
C       TYPE        CODE      N1    N2    N3    N4    N5    N6
C      STRETCHING    1        I     J
C      BENDING       2        I     J     K           IX    JX
C    OUT PLANE WAG   3        I     J     K     L     IX    JX
C      TORSION       4        I     J     K     L     IX    JX
C      LINEAR BEND   5        NO2   I     J     K     IX    JX
C   IN PLANE WAG     6        I     J     K     L     IX    JX
C CRAWFORD TORSION   7        I1    I2    I3    I4    I5    I6
C       IX AND JX GIVE THE BOND DISTANCE BY WHICH THE COORDINATE IS TO
C      WEIGHTED. IF IX=JX,NOT EQUAL TO ZERO, THE WEIGHTING FACTOR IS
C      SET EQUAL TO 1.0D0.
C      NOTE THAT FOR THE LINEAR BENDING TYPE N1=NO2 THE NO.OF THE
C      BENDING COORDINATE PERPENDICULAR TO NI.
C         THE INTERNAL COORDINATE VECTOR IS PUNCHED IN 24 COLUMN FIELDS,
C         3 COLUMNS FOR EACH OF THE 8 ELEMENTS IN THE ORDER NI,NCOD,N1
C         N2,N3,N4,N5,N6. THERE ARE THREE FIELDS PER CARD.
C      ATOM NUMBERS FOR WEIGHTING PURPOSE FOR CRAWFORD TORSION,N7(J) AND
C      N8(J), ARE PROVIDED IN CARDS DIRECTLY AFTER THE LAST INTERNAL
C      COORDINATE VECTOR CARD.
  120 READ (5,18)           (NI(J),NCOD(J),N1(J),N2(J),N3(J),N4(J),N5(J),
     1N6(J),J=1,INT)
   18 FORMAT(3(8I3))
      WRITE (6,15)             NOPROB
   15 FORMAT(51H0 THERE FOLLOWS COORDINATE VECTOR INPUT PROBLEM NO.I8)
      WRITE (6,19)             (NI(J),NCOD(J),N1(J),N2(J),N3(J),N4(J),N5(J
     1),N6(J),J=1,INT)
   19 FORMAT(3(8I3))
  122 DO 126 J=1,INT
      IF(NQ-NI(J))605,124,124
  124 IF(NCOD(J))605,605,125
  125 IF(7-NCOD(J))605,126,126
  126 CONTINUE
  130 NA=3*NOAT
      JOKER=0
  132 DO 134 I=1,NQ
      DO 134 J=1,NA
  134 B(I,J)=0.0D0
  135 MJ=0
  140 MJ=MJ+1
  142 IF(INT-MJ) 271,150,150
  150 NOINT=NI(MJ)
      MX=NCOD(MJ)
  152 GOTO (160,170,180,190,200,210,220),MX
C     STRETCHING SUBROUTINE
  160 CALL BOST
      IF(JOKER)140,140,610
C     BENDING SUBROUTINE
  170 CALL BEND
      IF(JOKER)140,140,610
C     OUT OF PLANE WAGGING SUBROUTINE
  180 CALL OPLA
      IF(JOKER)140,140,610
C     TORSIONAL SUBROUTINE
  190 CALL TORS
      IF(JOKER)140,140,610
C     LINEAR BENDING SUBROUTINE
  200 CALL LIBE
```

```
      IF(JOKER)140,140,610
C     IN PLANE WAGGING SUBROUTINE
  210 CALL PWAG
      IF(JOKER)140,140,610
C     CRAWFORD TORSION SUBROUTINE
  220 READ (5,900)          NOINT,N7,N8
  900 FORMAT (3I3)
      CALL TORC
      IF (JOKER) 140,140,610
  271 NS=1
C     READ ISOTOPE CONTROL CARD CONTAINING THE FOLLOWING INFORMATION
C        1.IN=-06  IDENTIFYING CARD. IN COLUMNS 1-3.
C        2.IFL=1, IF LIQUID PHASE.  ZERO OTHERWISE.  COLUMN 6.
C        3.IFLP=1, IF PRECEDING ISOTOPE IS LIQUID.  ZERO OTHERWISE.
  272 READ (5,2022) IN,IFL,IFLP,(RECORD(I),I=1,10)
      WRITE(8,58) NOPROB,NS,(RECORD(I),I=1,10)
 2022 FORMAT(3I3,10A4)
      IF(6+IN)620,276,620
C     READ MASSES
  276 READ (5,20)           (WT(I),I=1,NOAT)
   20 FORMAT(5F12.6)
   22 FORMAT(6F12.6)
      WRITE(8,22) (WT(I), I=1,NOAT)
      IF(NS-1)3005,3001,3005
 3001 MQ=NQ+6
      GO TO 3005
 3005 IF(IFL-1)2005,2010,2010
 2005 IF(IFLP-1)2740,2020,2020
 2010 IF(IFLP-1)2025,740,740
 2020 NQ=NQ-6
      GO TO 740
 2740 IF(NS-1)95,2025,740
 2025 NQ=NQ+6
  740 CALL MOMIN
      IF(NS-1)1005,1005,224
 1005 IF(IFL)95,1010,224
 1010 NQ=NQ-6
  224 DO 282 I=1,NQ
      DO 282 J=1,NQ
      G(I,J)=0.0D0
      DO 282 L=1,NOAT
      DO 282 M=1,3
      K=3*(L-1)+M
  282 G(I,J)=G(I,J)+B(I,K)*B(J,K)/WT(L)
      DO 300 I=1,NQ
      DO 300 J=1,NQ
      IF(0.00005-DABS(G(I,J)))300,294,294
  294 G(I,J)=0.00000
  300 CONTINUE
      WRITE (6,58)            NOPROB,NS,(RECORD(I),I=1,10)
   58 FORMAT(18H1 G MATRIX PROBLEMI8,8H ISOTOPEI3/12X,10A4)
      DO 284 I=1,NQ
      WRITE (6,54)            I,(G(I,J),J=1,NQ)
   54 FORMAT(4H0ROWI3/(10F12.6))
  284 WRITE(8,33) (G(I,J),J=I,NQ)
   33 FORMAT(4E18.9)
  390 NS=NS+1
  398 IF(NISO-NS)400,272,272
  400 DO 406 I=1,NOAT
      DO 406 J=1,NOAT
      DSQ=0.0D0
  403 DO 405 M=1,3
      R(M)=X(M,J)-X(M,I)
  405 DSQ=DSQ+R(M)*R(M)
  406 D(I,J)=DSQRT(DSQ)
  414 WRITE (6,68)            NOPROB
```

```
   68 FORMAT(28H1ATOM DISTANCE CHECK PROBLEMI8)
  416 DO 418 I=1,NOAT
  418 WRITE(6,70)I,(D(I,J),J=1,NOAT)
   70 FORMAT(5HOATOMI3/(12F10.6))
      IF(JOKER.GE.1) CALL EXIT
      GO TO 90
  600 WRITE (6,72)            NOPROB
   72 FORMAT(24HO X MATRIX ERROR PROBLEMI8)
      CALL EXIT
  605 WRITE (6,74)            NOPROB
   74 FORMAT(35HO INTERNAL COORDINATE ERROR PROBLEMI8)
      GO TO 400
  610 WRITE (6,76)            NOPROB,NOINT,MX,JOKER
   76 FORMAT(29HO ERROR IN SUBROUTINE PROBLEMI8,11H COORDINATEI3,5H CODE
     1I3,7H JOKER=I3)
      GO TO 400
  615 WRITE (6,78)            NOPROB,NS,L,NROW(L),NCOL(L),DATIN(L)
   78 FORMAT(23H U MATRIX ERROR PROBLEMI8,8H ISOTOPEI3,6H FIELDI3,6H REA
     1DS,I4,I4,F12.6)
      GO TO 400
  620 WRITE (6,80)            NOPROB
   80 FORMAT(22H ISOTOPE ERROR PROBLEMI8)
      GO TO 400
      END
      SUBROUTINE BOST
      IMPLICIT REAL*8(A-H,O-Z)
C     THIS SUBROUTINE COMPUTES THE B MATRIX ELEMENTS FOR A BOND STRETCH
C     AS DEFINED BY WILSON.
      DIMENSION X(3,66),WT(66),B(147,147),NI(147),NCOD(147),N1(147),
     1N2(147),N3(147),N4(147),N5(147),N6(147),RIJ(3)
      COMMON X,WT,B,IND,NOPROB,NOAT,NQ,INT,NISO,NA,MJ,NOINT,NI,NCOD,N1,
     1N2,N3,N4,N5,N6,JOKER
  100 IF(N6(MJ))130,101,130
  101 IF(N5(MJ))130,102,130
  102 IF(N4(MJ))130,103,130
  103 IF(N3(MJ))130,104,130
  104 IF(NOAT-N2(MJ))130,105,105
  105 IF(NOAT-N1(MJ))130,106,106
  106 I=N1(MJ)
      J=N2(MJ)
      DIJSQ=0.0D0
  109 DO 112 M=1,3
      RIJ(M)=X(M,J)-X(M,I)
  112 DIJSQ=DIJSQ+RIJ(M)*RIJ(M)
  114 DO 120 M=1,3
      NOCOL1=3*(I-1)+M
      NOCOL2=3*(J-1)+M
      B(NOINT,NOCOL1)=-RIJ(M)/DSQRT(DIJSQ)
  120 B(NOINT,NOCOL2)=-B(NOINT,NOCOL1)
      GO TO 132
  130 JOKER=1
  132 RETURN
      END
      SUBROUTINE BEND
      IMPLICIT REAL*8(A-H,O-Z)
C     THIS SUBROUTINE COMPUTES THE  B MATRIX ELEMENTS OF A VALENCE
C     ANGLE BENDING  COORDINATE AS DEFINED BY WILSON,
C      I AND K ARE THE NUMBERS  OF THE END ATOMS.
C      J= THE NUMBER OF THE CENTRAL ATOM
      DIMENSION X(3,66),WT(66),B(147,147),NI(147),NCOD(147),N1(147),
     1N2(147),N3(147),N4(147),N5(147),N6(147),RJI(3),RJK(3),RIXJX(3),
     2EJI(3),EJK(3)
      COMMON X,WT,B,IND,NOPROB,NOAT,NQ,INT,NISO,NA,MJ,NOINT,NI,NCOD,N1,
     1N2,N3,N4,N5,N6,JOKER
  100 IF(NOAT-N6(MJ))150,101,101
  101 IF(NOAT-N5(MJ))150,102,102
```

```
  102 IF(N4(MJ))150,103,150
  103 IF(NOAT-N3(MJ))150,104,104
  104 IF(NOAT-N2(MJ))150,105,105
  105 IF(NOAT-N1(MJ))150,106,106
  106 I=N1(MJ)
      J=N2(MJ)
      K=N3(MJ)
      IX=N5(MJ)
  110 JX=N6(MJ)
      DJISQ=0.0D0
      DJKSQ=0.0D0
      DXSQ=0.0D0
  115 DO 122 M=1,3
      RJI(M)=X(M,I)-X(M,J)
      RJK(M)=X(M,K)-X(M,J)
      RIXJX(M)=X(M,JX)-X(M,IX)
      DJISQ=DJISQ+RJI(M)*RJI(M)
      DJKSQ=DJKSQ+RJK(M)*RJK(M)
  122 DXSQ=DXSQ+RIXJX(M)*RIXJX(M)
  123 DJI=DSQRT(DJISQ)
      DJK=DSQRT(DJKSQ)
      DX=DSQRT(DXSQ)
      IF(DX)128,127,128
  127 DX=1.0D0
  128 DOTJ=0.0D0
  129 DO 132 M=1,3
      EJI(M)=RJI(M)/DJI
      EJK(M)=RJK(M)/DJK
  132 DOTJ=DOTJ+EJI(M)*EJK(M)
      IF(1.0D0-DABS(DOTJ))152,152,134
  134 SINJ=DSQRT(1.0D0-DOTJ*DOTJ)
  136 DO 144 M=1,3
      NOCOL1=3*(I-1)+M
      B(NOINT,NOCOL1)=(DX*(DOTJ*EJI(M)-EJK(M)))/(DJI*SINJ)
      NOCOL2=3*(K-1)+M
      B(NOINT,NOCOL2)=(DX*(DOTJ*EJK(M)-EJI(M)))/(DJK*SINJ)
      NOCOL3=3*(J-1)+M
  144 B(NOINT,NOCOL3)=-B(NOINT,NOCOL1)-B(NOINT,NOCOL2)
      GO TO 154
  150 JOKER=1
      GO TO 154
  152 JOKER=2
  154 RETURN
      END
      SUBROUTINE OPLA
      IMPLICIT REAL*8(A-H,O-Z)
C     THIS SUBROUTINE COMPUTES THE B MATRIX ELEMANTS FOR AN OUT OF
C     PLANE WAGGING COORDINATE AS DEFINED  BY WILSON, BUT MODIFIED SO
C     THAT WEIGHTING IS MADE NOT BY R0 BUT BY R0 X COS(ANGLE LJK/2).
C      I= THE END ATOM
C      J= THE APEX ATOM
C      K AND L = THE ANCHOR ATOMS.
      DIMENSION X(3,66),WT(66),B(147,147),NI(147),NCOD(147),N1(147),
     1N2(147),N3(147),N4(147),N5(147),N6(147),RJI(3),RJK(3),RJL(3),
     2RIXJX(3),EJI(3),EJK(3),EJL(3),C1(3),C2(3),C3(3)
      COMMON X,WT,B,IND,NOPROB,NOAT,NQ,INT,NISO,NA,MJ,NOINT,NI,NCOD,N1,
     1N2,N3,N4,N5,N6,JOKER
  100 IF(NOAT-N6(MJ))170,101,101
  101 IF(NOAT-N5(MJ))170,102,102
  102 IF(NOAT-N4(MJ))170,103,103
  103 IF(NOAT-N3(MJ))170,104,104
  104 IF(NOAT-N2(MJ))170,105,105
  105 IF(NOAT-N1(MJ))170,106,106
  106 I=N1(MJ)
      J=N2(MJ)
      K=N3(MJ)
```

```
      L=N4(MJ)
      IX=N5(MJ)
      JX=N6(MJ)
  112 DJISQ=0.0D0
      DJKSQ=0.0D0
      DJLSQ=0.0D0
  115 DXSQ=0.0D0
  116 DO 124 M=1,3
      RJI(M)=X(M,I)-X(M,J)
      DJISQ=DJISQ+RJI(M)*RJI(M)
      RJK(M)=X(M,K)-X(M,J)
      DJKSQ=DJKSQ+RJK(M)*RJK(M)
      RJL(M)=X(M,L)-X(M,J)
      DJLSQ=DJLSQ+RJL(M)*RJL(M)
      RIXJX(M)=X(M,JX)-X(M,IX)
  124 DXSQ=DXSQ+RIXJX(M)*RIXJX(M)
  126 DJI=DSQRT(DJISQ)
      DJK=DSQRT(DJKSQ)
      DJL=DSQRT(DJLSQ)
      DX=DSQRT(DXSQ)
  130 IF(DX) 132,131,132
  131 DX=1.0D0
  132 DO 136 M=1,3
      EJI(M)=RJI(M)/DJI
      EJK(M)=RJK(M)/DJK
  136 EJL(M)=RJL(M)/DJL
  137 C1(1)=EJK(2)*EJL(3)-EJK(3)*EJL(2)
      C1(2)=EJK(3)*EJL(1)-EJK(1)*EJL(3)
      C1(3)=EJK(1)*EJL(2)-EJK(2)*EJL(1)
      C2(1)=EJL(2)*EJI(3)-EJL(3)*EJI(2)
      C2(2)=EJL(3)*EJI(1)-EJL(1)*EJI(3)
      C2(3)=EJL(1)*EJI(2)-EJL(2)*EJI(1)
      C3(1)=EJI(2)*EJK(3)-EJI(3)*EJK(2)
      C3(2)=EJI(3)*EJK(1)-EJI(1)*EJK(3)
  139 C3(3)=EJI(1)*EJK(2)-EJI(2)*EJK(1)
  140 DET=EJI(1)*C1(1)+EJI(2)*C1(2)+EJI(3)*C1(3)
      DOTI=0.0D0
  142 DO 143 M=1,3
  143 DOTI=DOTI+EJK(M)*EJL(M)
  144 IF(1.0D0-DABS(DOTI))172,172,146
  146 SINI=DSQRT(1.0D0-DOTI*DOTI)
  147 SINT=DET/SINI
  148 IF(1.0D0-DABS(SINT))174,174,149
  149 COST=DSQRT(1.0D0-SINT*SINT)
  150 TANT=SINT/COST
  155 DO 168 M=1,3
      NOCOL1=3*(I-1)+M
  157 SMI    =((C1(M)/(COST*SINI))-(TANT*EJI(M)))/DJI
      B(NOINT,NOCOL1)=DX*SMI
      NOCOL2=3*(K-1)+M
  160 SMK=((C2(M)/(COST*SINI))-((TANT*(EJK(M)-DOTI*EJL(M)))/(SINI*SINI))
     1)/DJK
      B(NOINT,NOCOL2)=DX*SMK
      NOCOL3=3*(L-1)+M
  163 SML=((C3(M)/(COST*SINI))-((TANT*(EJL(M)-DOTI*EJK(M)))/(SINI*SINI))
     1)/DJL
      B(NOINT,NOCOL3)=DX*SML
      NOCOL4=3*(J-1)+M
  168 B(NOINT,NOCOL4)=-DX*(SMI+SMK+SML)
      GO TO 178
  170 JOKER=1
      GO TO 178
  172 JOKER=2
      GO TO 178
  174 JOKER=3
  178 RETURN
```

```
      END
      SUBROUTINE TORS
      IMPLICIT REAL*8(A-H,O-Z)
C     THIS SUBROUTINE COMPUTES  THE B MATRIX ELEMENTS FOR THE TORSION
C     AS DEFINED  BY WILSION.
C      I AND L = THE END ATOMS .  I NEARER OBSERVER.
C      J AND K = THE CENTRAL ATOMS. J NEARER OBSERVER.
      DIMENSION X(3,66),WT(66),B(147,147),NI(147),NCOD(147),N1(147),
     1N2(147),N3(147),N4(147),N5(147),N6(147),RIJ(3),RJK(3),RKL(3),
     2RIXJX(3),EIJ(3),EJK(3),EKL(3),CR1(3),CR2(3)
      COMMON X,WT,B,IND,NOPROB,NOAT,NQ,INT,NISO,NA,MJ,NOINT,NI,NCOD,N1,
     1N2,N3,N4,N5,N6,JOKER
  100 IF(NOAT-N6(MJ)) 180,101,101
  101 IF(NOAT-N5(MJ)) 180,102,102
  102 IF(NOAT-N4(MJ)) 180,103,103
  103 IF(NOAT-N3(MJ)) 180,104,104
  104 IF(NOAT-N2(MJ)) 180,105,105
  105 IF(NOAT-N1(MJ)) 180,106,106
  106 I=N1(MJ)
      J=N2(MJ)
      K=N3(MJ)
      L=N4(MJ)
      IX=N5(MJ)
  110 JX=N6(MJ)
  112 DIJSQ=0.0D0
      DJKSQ=0.0D0
      DKLSQ=0.0D0
  115 DXSQ=0.0D0
  116 DO 124 M=1,3
      RIJ(M)=X(M,J)-X(M,I)
      DIJSQ=DIJSQ+RIJ(M)*RIJ(M)
      RJK(M)=X(M,K)-X(M,J)
      DJKSQ=DJKSQ+RJK(M)*RJK(M)
      RKL(M)=X(M,L)-X(M,K)
      DKLSQ=DKLSQ+RKL(M)*RKL(M)
      RIXJX(M)=X(M,JX)-X(M,IX)
  124 DXSQ=DXSQ+RIXJX(M)*RIXJX(M)
  126 DIJ=DSQRT(DIJSQ)
      DJK=DSQRT(DJKSQ)
      DKL=DSQRT(DKLSQ)
      DX=DSQRT(DXSQ)
  130 IF(DX)132,131,132
  131 DX=1.0D0
  132 DO 136 M=1,3
      EIJ(M)=RIJ(M)/DIJ
      EJK(M)=RJK(M)/DJK
  136 EKL(M)=RKL(M)/DKL
  138 CR1(1)=EIJ(2)*EJK(3)-EIJ(3)*EJK(2)
      CR1(2)=EIJ(3)*EJK(1)-EIJ(1)*EJK(3)
      CR1(3)=EIJ(1)*EJK(2)-EIJ(2)*EJK(1)
      CR2(1)=EJK(2)*EKL(3)-EJK(3)*EKL(2)
      CR2(2)=EJK(3)*EKL(1)-EJK(1)*EKL(3)
  142 CR2(3)=EJK(1)*EKL(2)-EJK(2)*EKL(1)
  143 DOTPJ=0.0D0
      DOTPK=0.0D0
  145 DO 147 M=1,3
      DOTPJ=DOTPJ-EIJ(M)*EJK(M)
  147 DOTPK=DOTPK-EJK(M)*EKL(M)
  148 IF(1.0D0-DABS(DOTPJ))182,182,149
  149 IF(1.0D0-DABS(DOTPK))182,182,150
  150 SINPJ=DSQRT(1.0D0-DOTPJ*DOTPJ)
      SINPK=DSQRT(1.0D0-DOTPK*DOTPK)
  152 DO 164 M=1,3
      SMI=-CR1(M)/(DIJ*SINPJ*SINPJ)
  154 NOCOL1=3*(I-1)+M
      B(NOINT,NOCOL1)=B(NOINT,NOCOL1)+DX*SMI
```

```
  156 F1=(CR1(M)*(DJK-DIJ*DOTPJ))/(DJK*DIJ*SINPJ*SINPJ)
      F2=(DOTPK*CR2(M))/(DJK*SINPK*SINPK)
  157 SMJ=F1-F2
      NOCOL2=3*(J-1)+M
  158 B(NOINT,NOCOL2)=B(NOINT,NOCOL2)+DX*SMJ
      SML= CR2(M)/(DKL*SINPK*SINPK)
  160 NOCOL3=3*(L-1)+M
      B(NOINT,NOCOL3)=B(NOINT,NOCOL3)+DX*SML
  162 NOCOL4=3*(K-1)+M
  164 B(NOINT,NOCOL4)=B(NOINT,NOCOL4)-DX*(SMI+SMJ+SML)
      GO TO 186
  180 JOKER=1
      GO TO 186
  182 JOKER=2
  186 RETURN
      END
      SUBROUTINE LIBE
      IMPLICIT REAL*8(A-H,O-Z)
C     THIS SUBROUTINE COMPUTES THE B MATRIX ELEMENTS FOR A PAIR OF
C     PERPENDICULAR LINEAR BENDING COORDINATES.
C      N1=NO2 THE NUMBER OF THE SECOND COORDINATE,
C      I AND K = THE END ATOMS,
C      J= THE CNTRAL ATOM.
C     A GIVES THE CARTESIAN COORDINATES OF A POINT IN SPACE, SUCH
C      THAT THE VECTOR FROM ATOM J TO POINT A IS PERPENDICULAR TO
C      THE LINE I-J-K AND SERVES TO ORIENT THE COORDINATES IN SPACE.
      DIMENSION X(3,66),WT(66),B(147,147),NI(147),NCOD(147),N1(147),
     1N2(147),N3(147),N4(147),N5(147),N6(147),A(3),RJI(3),RJK(3),
     2RIXJX(3),UN(3),UNIT(3),UP(3),EJI(3),EJK(3)
      COMMON X,WT,B,IND,NOPROB,NOAT,NQ,INT,NISO,NA,MJ,NOINT,NI,NCOD,N1,
     1N2,N3,N4,N5,N6,JOKER
  100 IF(NOAT-N6(MJ))160,101,101
  101 IF(NOAT-N5(MJ))160,102,102
  102 IF(NOAT-N4(MJ))160,103,103
  103 IF(NOAT-N3(MJ))160,104,104
  104 IF(NOAT-N2(MJ))160,105,105
  105 IF(NQ-N1(MJ))160,106,106
  106 READ (5,24)              (A(I),I=1,3)
   24 FORMAT(3F12.6)
  108 I=N2(MJ)
      J=N3(MJ)
  110 K=N4(MJ)
      IX=N5(MJ)
      JX=N6(MJ)
  113 NO2=N1(MJ)
  114 DJISQ=0.0D0
      DJKSQ=0.0D0
      DXSQ=0.0D0
  116 DAJSQ=0.0D0
  117 DO 124 M=1,3
      RJI(M)=X(M,I)-X(M,J)
      DJISQ=DJISQ+RJI(M)*RJI(M)
      RJK(M)=X(M,K)-X(M,J)
      DJKSQ=DJKSQ+RJK(M)*RJK(M)
      RIXJX(M)=X(M,JX)-X(M,IX)
      DXSQ=DXSQ+RIXJX(M)*RIXJX(M)
      UN(M)=A(M)-X(M,J)
  124 DAJSQ=DAJSQ+UN(M)*UN(M)
  126 DJI=DSQRT(DJISQ)
      DJK=DSQRT(DJKSQ)
      DX=DSQRT(DXSQ)
      DAJ=DSQRT(DAJSQ)
  130 IF(DX)132,131,132
  131 DX=1.0D0
  132 DOTJ=0.0D0
      DOTP=0.0D0
```

```
  134 DO 140 M=1,3
      EJI(M)=RJI(M)/DJI
      EJK(M)=RJK(M)/DJK
      UNIT(M)=UN(M)/DAJ
      DOTJ=DOTJ+EJI(M)*EJK(M)
  140 DOTP=DOTP+EJI(M)*UNIT(M)
      TEST=(DABS(DOTJ)-1.000)
      IF(0.0001-DABS(TEST))162,142,142
  142 IF(0.00005-DABS(DOTP))162,143,143
  143 UP(1)=EJK(2)*UNIT(3)-EJK(3)*UNIT(2)
      UP(2)=EJK(3)*UNIT(1)-EJK(1)*UNIT(3)
      UP(3)=EJK(1)*UNIT(2)-EJK(2)*UNIT(1)
  146 DO 156 M=1,3
      NOCOL1=3*(I-1)+M
      B(NOINT,NOCOL1)=-DX*UNIT(M)/DJI
      B(NO2,NOCOL1)=-DX*UP(M)/DJI
      NOCOL2=3*(K-1)+M
      B(NOINT,NOCOL2)=-DX*UNIT(M)/DJK
      B(NO2,NOCOL2)=-DX*UP(M)/DJK
      NOCOL3=3*(J-1)+M
      B(NOINT,NOCOL3)=DX*(1.0D0/DJI+1.0D0/DJK)*UNIT(M)
  156 B(NO2,NOCOL3)=DX*(1.0D0/DJI+1.0D0/DJK)*UP(M)
      GO TO 164
  160 JOKER=1
      GO TO 164
  162 JOKER=2
  164 RETURN
      END
      SUBROUTINE PWAG
      IMPLICIT REAL*8(A-H,O-Z)
C     THIS SUBROUTINE COMPUTES THE B MATRIX ELEMENTS FOR AN IN PLANE
C     WAGGING COORDINATE  (SUCH AS BENZENE IN PLANE H WAG)
C      I= THE END ATOM.
C      J= THE APEX ATOM
C      K AND L= THE ANCHOR ATOMS.
      DIMENSION X(3,66),WT(66),B(147,147),NI(147),NCOD(147),N1(147),
     1N2(147),N3(147),N4(147),N5(147),N6(147),RJI(3),RJK(3),RJL(3),
     2EJI(3),EJK(3),EJL(3),RIXJX(3)
      COMMON X,WT,B,IND,NOPROB,NOAT,NQ,INT,NISO,NA,MJ,NOINT,NI,NCOD,N1,
     1N2,N3,N4,N5,N6,JOKER
  100 IF(NOAT-N6(MJ))180,101,101
  101 IF(NOAT-N5(MJ))180,102,102
  102 IF(NOAT-N4(MJ))180,103,103
  103 IF(NOAT-N3(MJ))180,104,104
  104 IF(NOAT-N2(MJ))180,105,105
  105 IF(NOAT-N1(MJ))180,106,106
  106 I=N1(MJ)
      J=N2(MJ)
      K=N3(MJ)
      L=N4(MJ)
      IX=N5(MJ)
      JX=N6(MJ)
  114 DJISQ=0.0D0
      DJKSQ=0.0D0
      DJLSQ=0.0D0
      DXSQ=0.0D0
  120 DO 130 M=1,3
      RJI(M)=X(M,I)-X(M,J)
      DJISQ=DJISQ+RJI(M)*RJI(M)
      RJK(M)=X(M,K)-X(M,J)
      DJKSQ=DJKSQ+RJK(M)*RJK(M)
      RJL(M)=X(M,L)-X(M,J)
      DJLSQ=DJLSQ+RJL(M)*RJL(M)
      RIXJX(M)=X(M,JX)-X(M,IX)
  130 DXSQ=DXSQ+RIXJX(M)*RIXJX(M)
      DI=DSQRT(DJISQ)
```

```
      DK=DSQRT(DJKSQ)
      DL=DSQRT(DJLSQ)
      DX=DSQRT(DXSQ)
  135 IF(DX)136,136,138
  136 DX=1.0D0
  138 COSIK=0.0D0
      COSIL=0.0D0
  140 DO 146 M=1,3
      EJI(M)=RJI(M)/ DI
      EJK(M)=RJK(M)/ DK
      EJL(M)=RJL(M)/ DL
      COSIK=COSIK+EJI(M)*EJK(M)
  146 COSIL=COSIL+EJI(M)*EJL(M)
  148 IF(1.0D0-DABS(COSIK))182,182,149
  149 IF(1.0D0-DABS(COSIL))182,182,150
  150 SINIK=DSQRT(1.0D0-COSIK*COSIK)
  151 SINIL=DSQRT(1.0D0-COSIL*COSIL)
  152 DO 170 M=1,3
      NOCOL1=3*(I-1)+M
      SMI=(COSIK*EJI(M)-EJK(M))/(2.0D00*SINIK*DI)-
     1(COSIL*EJI(M)-EJL(M))/(2.0D0*SINIL*DI)
      B(NOINT,NOCOL1)=DX*SMI
      NOCOL2=3*(K-1)+M
      SMK=(COSIK*EJK(M)-EJI(M))/(2.0D00*SINIK*DK)
      B(NOINT,NOCOL2)=DX*SMK
      NOCOL3=3*(L-1)+M
      SML=-(COSIL*EJL(M)-EJI(M))/(2.0D00*SINIL*DL)
      B(NOINT,NOCOL3)=DX*SML
      NOCOL4=3*(J-1)+M
  170 B(NOINT,NOCOL4)=-DX*(SMI+SMK+SML)
      GO TO 184
  180 JOKER=1
      GO TO 184
  182 JOKER=2
  184 RETURN
      END
      SUBROUTINE TORC
      IMPLICIT REAL*8(A-H,O-Z)
C     THIS SUBROUTINE COMPUTES THE B MATRIX ELEMENTS FOR THE TORSION AS
C     DEFINED BY CRAWFORD, AND WEIGHTING MADE BY ROX SIN(ANGLE 3-1-5/2),
C      I1 AND I2 = THE CENTRAL ATOMS.  I1 NEARER OBSERVER.
C      I3 AND I5 = THE END ATOMS ATTACHED TO I1.
C      I4 AND I6 = THE END ATOMS ATTACHED TO I2.
C     THIS SUBROUTINE REJECTS MOLECULES IN WHICH I3, I1 AND I5 OR I4, I2
C      AND I6 ARE COLINEAR AND THOSE IN WHICH THE BOND (I1-I2) IS NOT CO
C     PLANAR WITH PLANES (I1-I3-I5) AND (I2-I4-I6).
      DIMENSION X(3,66),WT(66),B(147,147),NI(147),NCOD(147),N1(147),
     1N2(147),N3(147),N4(147),N5(147),N6(147),R12(3),R13(3),R15(3),
     2R24(3),R26(3),E12(3),E13(3),E15(3),E24(3),E26(3),CR1(3),CR2(3),
     3R78(3)
      COMMON X,WT,B,IND,NOPROB,NOAT,NO,INT,NISO,NA,MJ,NOINT,NI,NCOD,N1,
     1N2,N3,N4,N5,N6,JOKER,NPROB,NOP,NCA,NS,NCD,N7,N8
  100 IF (NOAT-N6(MJ)) 180,101,101
  101 IF (NOAT-N5(MJ)) 180,102,102
  102 IF (NOAT-N4(MJ)) 180,103,103
  103 IF (NOAT-N3(MJ)) 180,104,104
  104 IF (NOAT-N2(MJ)) 180,105,105
  105 IF (NOAT-N1(MJ)) 180,106,106
  106 IF(NOAT-N7)180,107,107
  107 IF(NOAT-N8)180,108,108
  108 I1=N1(MJ)
      I2=N2(MJ)
      I3=N3(MJ)
      I4=N4(MJ)
      I5=N5(MJ)
  110 I6=N6(MJ)
```

```
112 D12SQ=0.0D0
    D13SQ=0.0D0
    D15SQ=0.0D0
    D24SQ=0.0D0
115 D26SQ=0.0D0
    D78SQ=0.0D0
116 DO 124 M=1,3
    R12(M)=X(M,I2)-X(M,I1)
    D12SQ=D12SQ+R12(M)*R12(M)
    R13(M)=X(M,I3)-X(M,I1)
    D13SQ=D13SQ+R13(M)*R13(M)
    R15(M)=X(M,I5)-X(M,I1)
    D15SQ=D15SQ+R15(M)*R15(M)
    R24(M)=X(M,I4)-X(M,I2)
    D24SQ=D24SQ+R24(M)*R24(M)
    R26(M)=X(M,I6)-X(M,I2)
    D26SQ=D26SQ+R26(M)*R26(M)
    R78(M)=X(M,N7)-X(M,N8)
124 D78SQ=D78SQ+R78(M)*R78(M)
126 D12=DSQRT(D12SQ)
    D13=DSQRT(D13SQ)
    D15=DSQRT(D15SQ)
    D24=DSQRT(D24SQ)
130 D26=DSQRT(D26SQ)
    D78=DSQRT(D78SQ)
132 DO 136 M=1,3
    E12(M)=R12(M)/D12
    E13(M)=R13(M)/D13
    E15(M)=R15(M)/D15
    E24(M)=R24(M)/D24
136 E26(M)=R26(M)/D26
138 CR1(1)=E13(2)*E15(3)-E13(3)*E15(2)
    CR1(2)=E13(3)*E15(1)-E13(1)*E15(3)
    CR1(3)=E13(1)*E15(2)-E13(2)*E15(1)
    CR2(1)=E26(2)*E24(3)-E26(3)*E24(2)
    CR2(2)=E26(3)*E24(1)-E26(1)*E24(3)
142 CR2(3)=E26(1)*E24(2)-E26(2)*E24(1)
143 DOT1=0.0D0
    DOT2=0.0D0
    DOT3=0.0D0
    DOT4=0.0D0
    DOT5=0.0D0
    DOT6=0.0D0
145 DO 147 M=1,3
    DOT1=DOT1+E13(M)*E15(M)
    DOT2=DOT2+E24(M)*E26(M)
    DOT3=DOT3+E12(M)*E13(M)
    DOT4=DOT4+E12(M)*E24(M)
    DOT5=DOT5+E12(M)*E15(M)
147 DOT6=DOT6+E12(M)*E26(M)
    IF(1.0D0-DABS(DOT1)) 182,182,200
200 IF(1.0D0-DABS(DOT2)) 182,182,202
202 IF(1.0D0-DABS(DOT3)) 182,203,204
203 IF(1.0D0-DOT3) 182,182,204
204 IF(1.0D0-DABS(DOT4)) 182,205,206
205 IF(1.0D0-DOT4) 182,182,206
206 IF(1.0D0-DABS(DOT5)) 182,207,208
207 IF(1.0D0-DOT5) 182,182,208
208 IF(1.0D0-DABS(DOT6)) 182,209,210
209 IF(1.0D0-DOT6) 182,182,210
210 DOTN1=0.0D0
    DOTN2=0.0D0
    DO 220 M=1,3
    DOTN1=DOTN1+E12(M)*CR1(M)
220 DOTN2=DOTN2+E12(M)*CR2(M)
    IF(0.000001-DABS(DOTN1)) 184,184,222
```

```
  222 IF(0.000001-DABS(DOTN2)) 184,184,224
  224 SIN1=DSQRT(1.0D0-DOT1*DOT1)
      SIN2=DSQRT(1.000-DOT2*DOT2)
      IF (D78)1111,1110,1111
 1110 D78=1.0D0
      GO TO 152
 1111 D78=D78*DSQRT((1.-DOT1)/2.0D0)
  152 DO 164 M=1,3
      NOCOL1=3*(I1-1)+M
      B(NOINT,NOCOL1)=CR1(M)*(D13*DOT3-D15*DOT5)*D78/(D13*D15*SIN1*SIN1)
      NOCOL2=3*(I2-1)+M
      B(NOINT,NOCOL2)=CR2(M)*(D24*DOT4-D26*DOT6)*D78/(D26*D24*SIN2*SIN2)
      NOCOL3=3*(I3-1)+M
      B(NOINT,NOCOL3)=CR1(M)*DOT5*D78/(D13*SIN1*SIN1)
      NOCOL4=3*(I4-1)+M
      B(NOINT,NOCOL4)=CR2(M)*DOT6*D78/(D24*SIN2*SIN2)
      NOCOL5=3*(I5-1)+M
      B(NOINT,NOCOL5)=-CR1(M)*DOT3*D78/(D15*SIN1*SIN1)
      NOCOL6=3*(I6-1)+M
  164 B(NOINT,NOCOL6)=-CR2(M)*DOT4*D78/(D26*SIN2*SIN2)
      GO TO 186
  180 JOKER=1
      GO TO 186
  182 JOKER=2
      GO TO 186
  184 JOKER=3
  186 RETURN
      END
      SUBROUTINE MOMIN
      IMPLICIT REAL*8(A-H,O-Z)
C        THIS SUBROUTINE COMPUTES THE MOMENT OF INERTIA TENSOR IN
C     CARTESIAN COORDINATES AND THE TRANSFORMATION TO THE PRINCIPAL
C     AXES.
      DIMENSION X(3,66),WT(66),B(147,147),NI(147),NCOD(147),N1(147),
     1N2(147),N3(147),N4(147),N5(147),N6(147),CM(3),C(3),R(29),
     2DNER(3,3),TR(3,3),A(3,66)
      COMMON X,WT,B,IND,NOPROB,NOAT,NO,INT,NISO,NA,MJ,NOINT,NI,NCOD,N1,
     1N2,N3,N4,N5,N6,JOKER,NROB,NOP,NCA,NS,NCD,N7,N8
  100 W=0.0D0
  102 DO 103 I=1,NOAT
  103 W=W+WT(I)
C     FIND THE CENTER OF MASS.
  105 DO 109 M=1,3
      CM(M)=0.0D0
      DO 108 I=1,NOAT
  108 CM(M)=CM(M)-WT(I)*X(M,I)
  109 C(M)=CM(M)/W
  110 DO 114 I=1,NOAT
      R(I)=0.0D0
      DO 114 M=1,3
  114 R(I)=R(I)+(X(M,I)+C(M))**2
C     TRANSLATE TO THE CENTER OF MASS.
C     COMPUTE THE MOMENT OF INERTIA TENSOR.
  116 DO 126 I=1,3
      DO 126 J=1,3
      DNER(I,J)=0.0D0
  119 DO 126 K=1,NOAT
      IF(I-J)123,121,123
  121 DNER(I,J)=DNER(I,J)+WT(K)*(R(K)-(X(I,K)+C(I))**2)
      GO TO 126
  123 DNER(I,J)=DNER(I,J)-WT(K)*(X(I,K)+C(I))*(X(J,K)+C(J))
  126 CONTINUE
  130 WRITE (6,80)            W,(C(M),M=1,3)
   80 FORMAT(7H1 MASS=F12.6,16H CENTER OF MASS 3F12.6)
  132 WRITE (6,82)
   82 FORMAT(27H0 MOMENT OF INERTIA TENSOR.)
```

```
  134 DO 135 I=1,3
  135 WRITE (6,84)              (DNER(I,J),J=1,3)
   84 FORMAT(1H03F12.6)
  136 NR=0
      N=3
      IEGEN=0
C     FIND THE PRINCIPAL MOMENTS AND THE TRANSFORMATION TO THE PRINCIPAL
C     AXES.
  140 CALL HDIAG(DNER,N,IEGEN,TR,NR)
  142 WRITE (6,86)              (DNER(I,I),I=1,3)
   86 FORMAT(20H0 PRINCIPAL MOMENTS 3F12.6,18H & TRANSFORMATION.)
      DO 141 I=1,NOAT,6
      K=I+5
      NCO=1
      L=NCO+K/6
  141 CONTINUE
   85 FORMAT(6F12.6,1HWI2,I2,I3)
  143 WRITE(8,87) (DNER(I,I), I=1,3),W
   87 FORMAT(4E18.9)
  144 DO 146 I=1,3
  146 WRITE (6,84)              (TR(I,J),J=1,3)
      IF (NS-1)148,150,148
  150 DO 160 I=1,3
      DO 160 K=1,NOAT
      A(I,K)=0.0D0
      DO 160 J=1,3
  160 A(I,K)=A(I,K)+TR(J,I)*(X(J,K)+C(J))
      DO 180 K=1,NOAT
      DO 180 J=1,3
      NOCOL=3*(K-1)+J
      B(NQ-5,NOCOL)=WT(K)*TR(J,1)/W
      B(NQ-4,NOCOL)=WT(K)*TR(J,2)/W
  180 B(NQ-3,NOCOL)=WT(K)*TR(J,3)/W
      DO 190 K=1,NOAT
      DO 190 L=1,3
      NOCOL=3*(K-1)+L
      IF(DNER(1,1))251,251,252
  251 B(NQ-2,NOCOL)=0.0D0
      GO TO 260
  252 B(NQ-2,NOCOL)=(WT(K)/DNER(1,1))*(A(2,K)*TR(L,3)-A(3,K)*TR(L,2))
  260 IF(DNER(2,2))261,261,262
  261 B(NQ-1,NOCOL)=0.000
      GO TO 270
  262 B(NQ-1,NOCOL)=(WT(K)/DNER(2,2))*(A(3,K)*TR(L,1)-A(1,K)*TR(L,3))
  270 IF(DNER(3,3))271,271,190
  271 B(NQ,NOCOL)=0.0D0
      GO TO 220
  190 B(NQ  ,NOCOL)=(WT(K)/DNER(3,3))*(A(1,K)*TR(L,2)-A(2,K)*TR(L,1))
C       WRITE B
  220 WRITE (6,52)              NOPROB
   52 FORMAT(18H0 B MATRIX PROBLEMI8)
      DO 222 I=1,NQ
  222 WRITE (6,54)              I,(B(I,J),J=1,NA)
   54 FORMAT(4HOROWI3/(10F12.6))
  148 RETURN
      END
      SUBROUTINE HDIAG(H,N,IEGEN,U,NR)
      IMPLICIT REAL*8(A-H,O-Z)
CHDIAGMIHDI3, FORTAN II DIAGONALIZATION OF A REAL SYMMETRIC MATRIX BY
C     THE JACOBI METHOD.
C     CALLING SEQUENCE FOR DIAGONALIZATION
C     CALL HDIAG( H, N, IEGEN, U, NR)
C     WHERE H IS THE ARRAY TO BE DIAGONALIZED.
C     N IS THE ORDER OF THE MATRIX, H.
C     IEGEN MUST BE SET UNEQUAL TO ZERO IF ONLY EIGENVALUES ARE TO BE
C     COMPUTED.
```

```
C     IEGEN MUST BE SET EQUAL TO ZERO IF EIGENVALUES AND EIGENVECTORS
C     ARE TO BE COMPUTED.
C     U IS THE UNITARY MATRIX USED FOR FORMATION OF THE EIGENVECTORS.
C     NR IS THE NUMBER OF ROTATIONS.
C     A DIMENSION STATEMENT MUST BE INSERTED IN THE SUBROUTINE.
C     DIMENSION H(N,N), U(N,N), X(N), IQ(N)
C     COMPUTER MUST OPERATE IN FLOATING TRAP MODE
C     THE SUBROUTINE OPERATES ONLY ON THE ELEMENTS OF H THAT ARE TO THE
C     RIGHT OF THE MAIN DIAGONAL. THUS, ONLY A TRIANGULAR
C     SECTION NEED BE STORED IN THE ARRAY H.
      DIMENSION H(3,3),U(3,3),X(3),IQ(3)
      DSIGNF(X1,X2)=DSIGN(X1,X2)
      IF (IEGEN) 15,10,15
   10 DO 14 I=1,N
      DO 14 J=1,N
      IF(I-J)12,11,12
   11 U(I,J)=1.0D0
      GO TO 14
   12 U(I,J)=0.
   14 CONTINUE
   15 NR = 0
      IF (N-1) 1000,1000,17
C     SCAN FOR LARGEST OFF DIAGONAL ELEMENT IN EACH ROW
C     X(I) CONTAINS LARGEST ELEMENT IN  ITH ROW
C     IQ(I) HOLDS SECOND SUBSCRIPT DEFINING POSITION OF ELEMENT
   17 NMI1=N-1
      DO 30 I=1,NMI1
      X(I) = 0.
      IPL1=I+1
      DO 30 J=IPL1,N
      IF(X(I)-DABS( H(I,J))) 20,20,30
   20 X(I)=DABS(H(I,J))
      IQ(I)=J
   30 CONTINUE
C     SET INDICATOR FOR SHUT-OFF,RAP=2**-27,NR=NO.OF ROTATIONS
      RAP=7.450580596E-9
      HDTEST=1.0038
C     FIND MAXIMUM OF X(I) S FOR PIVOT ELEMENT AND
C     TEST FOR END OF PROBLEM
   40 DO 70  I=1,NMI1
      IF (I-1) 60,60,45
   45 IF(XMAX-X(I)) 60,70,70
   60 XMAX=X(I)
      IPIV=I
      JPIV=IQ(I)
   70 CONTINUE
C     IS MAX. X(I) EQUAL TO ZERO, IF LESS THAN HDTEST,REVISE HDTEST
      IF (XMAX) 1000,1000,80
   80 IF( HDTEST) 90,90,85
   85 IF (XMAX - HDTEST) 90,90,148
   90 HDIMIN = DABS ( H (1,1) )
      DO 110  I=2,N
      IF (HDIMIN - DABS ( H (I,I))) 110,110,100
  100 HDIMIN=DABS (H(I,I))
  110 CONTINUE
      HDTEST = HDIMIN*RAP
C     RETURN IF MAX.H(I,J)LESS THAN(2**-27)DABS(H(K,K)-MIN)
      IF (HDTEST-XMAX) 148,1000,1000
  148 NR= NR+1
C     COMPUTE TANGENT, SINE AND COSINE,H(I,I),H(J,J)
  150 TANG=DSIGNF(2.0D00,(H(IPIV,IPIV)-H(JPIV,JPIV)))*H(IPIV,JPIV)/
     1(DABS(H(IPIV,IPIV)-H(JPIV,JPIV))+DSQRT((H(IPIV,IPIV)-
     2H(JPIV,JPIV))**2+4.0D0*H(IPIV,JPIV)**2))
      COSINE=1.0D0/DSQRT(1.0D0+TANG**2)
      SINE=TANG*COSINE
      HII=H(IPIV,IPIV)
```

```
      H(IPIV,IPIV)=COSINE**2*(HII+TANG*(2.0D0*H(IPIV,JPIV)+
     1TANG*H(JPIV,JPIV)))
      H(JPIV,JPIV)=COSINE**2*(H(JPIV,JPIV)-
     1TANG*(2.0D0*H(IPIV,JPIV)-TANG*HII))
      H(IPIV,JPIV)=0.
C     PSEUDO RANK THE EIGENVALUES
C     ADJUST SINE AND COS FOR COMPUTATION OF H(IK) AND U(IK)
      IF ( H(IPIV,IPIV) - H(JPIV,JPIV)) 152,153,153
  152 HTEMP = H(IPIV,IPIV)
      H(IPIV,IPIV) = H(JPIV,JPIV)
      H(JPIV,JPIV) =HTEMP
C     RECOMPUTE SINE AND COS
      HTEMP =DSIGNF(1.0D0, -SINE) * COSINE
      COSINE =DABS (SINE)
      SINE =HTEMP
  153 CONTINUE
C     INSPECT THE IQS BETWEEN I+1 AND N-1 TO DETERMINE
C     WHETHER A NEW MAXIUM VALUE SHOULD BE COMPUTE   SINCE
C     THE PRESENT MAXIMUM IS IN THE I OR J ROW.
      DO 350 I=1,NM11
      IF(I-IPIV)210,350,200
  200 IF (I-JPIV) 210,350,210
  210 IF(IQ(I)-IPIV) 230,240,230
  230 IF(IQ(I)-JPIV) 350,240,350
  240 K=IQ(I)
  250 HTEMP=H(I,K)
      H(I,K)=0.
      IPL1=I+1
      X(I) =0.
C     SEARCH IN DEPLETED ROW FOR NEW MAXIMUM
      DO 320 J=IPL1,N
      IF ( X(I) -DABS( H(I,J)) ) 300,300,320
  300 X(I) = DABS(H(I,J))
      IQ(I)=J
  320 CONTINUE
      H(I,K)=HTEMP
  350 CONTINUE
      X(IPIV) =0.
      X(JPIV) =0.
C     CHANGE THE ORDER ELEMENTS OF H
      DO 530 I=1,N
      IF (I-IPIV) 370,530,420
  370 HTEMP = H(I,IPIV)
      H(I,IPIV)= COSINE*HTEMP + SINE*H(I,JPIV)
      IF ( X(I) - DABS( H(I,IPIV)) )380,390,390
  380 X(I) = DABS(H(I,IPIV))
      IQ(I) = IPIV
  390 H(I,JPIV) = - SINE*HTEMP + COSINE*H(I,JPIV)
      IF ( X(I) - DABS ( H(I,JPIV)) ) 400,530,530
  400 X(I) = DABS(H(I,JPIV))
      IQ(I) = JPIV
      GO TO 530
  420 IF(I-JPIV) 430,530,480
  430 HTEMP = H(IPIV,I)
      H(IPIV,I) = COSINE*HTEMP + SINE*H(I,JPIV)
      IF ( X(IPIV) - DABS(H(IPIV,I)) ) 440,450,450
  440 X(IPIV) = DABS(H(IPIV,I))
      IQ(IPIV) = I
  450 H(I,JPIV) = - SINE*HTEMP + COSINE*H(I,JPIV)
      IF (X(I) - DABS( H(I,JPIV)) ) 400,530,530
  480 HTEMP = H(IPIV,I)
      H(IPIV,I) = COSINE*HTEMP + SINE*H(JPIV,I)
      IF ( X(IPIV) - DABS( H(IPIV,I)) ) 490,500,500
  490 X(IPIV) = DABS(H(IPIV,I))
      IQ(IPIV) = I
  500 H(JPIV,I) = - SINE*HTEMP + COSINE*H(JPIV,I)
```

```
      IF ( X(JPIV) - DABS( H(JPIV,I)) )510,530,530
  510 X(JPIV) = DABS(H(JPIV,I))
      IQ(JPIV) = I
  530 CONTINUE
C     TEST FOR COMPUTATION OF EIGENVECTORS
      IF(IEGEN) 40,540,40
  540 DO 550 I=1,N
      HTEMP=U(I,IPIV)
      U(I,IPIV)=COSINE*HTEMP+SINE*U(I,JPIV)
  550 U(I,JPIV)= -SINE*HTEMP+COSINE*U(I,JPIV)
      GO TO 40
 1000 RETURN
      END
```

```
C
C     G-MATRIX DIAGONALIZATION
C
      IMPLICIT REAL*8 (A-H,O-Z)
      REAL*4 STORY
      DIMENSION STORY(36),WT(66),TMOM(3),G(147,147),DG(147)
      DIMENSION A(147,147),W(147,147)
      EQUIVALENCE (G,W)
  100 READ(5,1) ISO,NOAT,NQ
    1 FORMAT(3I5)
      IF(ISO.EQ.0) CALL EXIT
      READ(8,6) (STORY(I),I=1,36)
      READ(8,10) (WT(I),I=1,NOAT)
      READ(8,7) (TMOM(I),I=1,3),TMASS
    7 FORMAT(4E18.9)
    6 FORMAT(18A4)
   10 FORMAT(6F12.6)
      DO 2020 I=1,NQ
      READ(8,7) (G(I,J),J=I,NQ)
      DO 2020 J=1,NQ
 2020 G(J,I)=G(I,J)
      NR1=0
      IEGEN=0
      DO 44 I=1,NQ
      DO 44 J=1,NQ
   44 A(I,J)=0.0D0
      CALL HDIAG(G,NQ,IEGEN,A,NR1)
      DO 147 J=1,NQ
      IF(0.0005D0-G(J,J)) 142,145,145
  145 DG(J)=0.0D0
      GO TO 147
  142 DG(J)=G(J,J)
  147 CONTINUE
      DO 150 J=1,NQ
      DO 150 I=1,NQ
  150 W(I,J)=A(I,J)*DSQRT(DG(J))
      WRITE(13) ((W(I,J),I=1,NQ),J=1,NQ)
      GO TO 100
      END
      SUBROUTINE HDIAG(H,N,IEGEN,U,NR)
      IMPLICIT REAL*8 (A-H,O-Z)
      REAL*4 RECORD,RECD,STORY
CHDIAGMIHDI3, FORTAN II DIAGONALIZATION OF A REAL SYMMETRIC MATRIX BY
C     THE JACOBI METHOD.
C     CALLING SEQUENCE FOR DIAGONALIZATION
C     CALL HDIAG( H, N, IEGEN, U, NR)
C     WHERE H IS THE ARRAY TO BE DIAGONALIZED.
C     N IS THE ORDER OF THE MATRIX, H.
C     IEGEN MUST BE SET UNEQUAL TO ZERO IF ONLY EIGENVALUES ARE TO BE
C     COMPUTED.
C     IEGEN MUST BE SET EQUAL TO ZERO IF EIGENVALUES AND EIGENVECTORS
C     ARE TO BE COMPUTED.
C     U IS THE UNITARY MATRIX USED FOR FORMATION OF THE EIGENVECTORS.
C     NR IS THE NUMBER OF ROTATIONS.
C     A DIMENSION STATEMENT MUST BE INSERTED IN THE SUBROUTINE.
C     DIMENSION H(N,N), U(N,N), X(N), IQ(N)
C     COMPUTER MUST OPERATE IN FLOATING TRAP MODE
C     THE SUBROUTINE OPERATES ONLY ON THE ELEMENTS OF H THAT ARE TO THE
C     RIGHT OF THE MAIN DIAGONAL. THUS, ONLY A TRIANGULAR
```

```
C       SECTION NEED BE STORED IN THE ARRAY H.
        DIMENSION H(147,147),U(147,147),X(147),IQ(147)
        DSIGNF(X,Y)=DSIGN(X,Y)
        CALL ERRSET (208,256,-1,1,0,0)
        CALL ERRSET (209,256,-1,1,0,0)
        IF (IEGEN) 15,10,15
   10   DO 14 I=1,N
        DO 14 J=1,N
        IF(I-J)12,11,12
   11   U(I,J)=1.0D0
        GO TO 14
   12   U(I,J)=0.0D0
   14   CONTINUE
   15   NR = 0
        IF (N-1) 1000,1000,17
C       SCAN FOR LARGEST OFF DIAGONAL ELEMENT IN EACH ROW
C       X(I) CONTAINS LARGEST ELEMENT IN  ITH ROW
C       IQ(I) HOLDS SECOND SUBSCRIPT DEFINING POSITION OF ELEMENT
   17   NMI1=N-1
        DO 30 I=1,NMI1
        X(I) = 0.0D0
        IPL1=I+1
        DO 30 J=IPL1,N
        IF(X(I)-DABS( H(I,J))) 20,20,30
   20   X(I)=DABS(H(I,J))
        IQ(I)=J
   30   CONTINUE
C       SET INDICATOR FOR SHUT-OFF,RAP=2**-27,NR=NO.OF ROTATIONS
        RAP=7.450580596D-9
        HDTEST=1.0D38
C       FIND MAXIMUM OF X(I) S FOR PIVOT ELEMENT AND
C       TEST FOR END OF PROBLEM
   40   DO 70  I=1,NMI1
        IF (I-1) 60,60,45
   45   IF(XMAX-X(I)) 60,70,70
   60   XMAX=X(I)
        IPIV=I
        JPIV=IQ(I)
   70   CONTINUE
C       IS MAX. X(I) EQUAL TO ZERO. IF LESS THAN HDTEST,REVISE HDTEST
        IF (XMAX) 1000,1000,80
   80   IF( HDTEST) 90,90,85
   85   IF (XMAX - HDTEST) 90,90,148
   90   HDIMIN = DABS ( H (1,1) )
        DO 110  I=2,N
        IF (HDIMIN - DABS ( H (I,I))) 110,110,100
  100   HDIMIN=DABS (H(I,I))
  110   CONTINUE
        HDTEST=HDIMIN*RAP
C       RETURN IF MAX.H(I,J)LESS THAN(2**-27)DABS(H(K,K)-MIN)
        IF (HDTEST-XMAX) 148,1000,1000
  148   NR= NR+1
C       COMPUTE TANGENT, SINE AND COSINE,H(I,I),H(J,J)
  150   TANG=DSIGN(2.D0,(H(IPIV,IPIV)-H(JPIV,JPIV)))*H(IPIV,JPIV)/(DABS(H
       1(IPIV,IPIV)-H(JPIV,JPIV))+DSQRT((H(IPIV,IPIV)-H(JPIV,JPIV))**2+
       24.000*H(IPIV,JPIV)**2))
        COSINE=1.0D0/DSQRT(1.0D0+TANG*TANG)
        SINE=TANG*COSINE
        HII=H(IPIV,IPIV)
        H(IPIV,IPIV)=COSINE**2*(HII+TANG*(2.0D0*H(IPIV,JPIV)+TANG*H(JPIV,
       1JPIV)))
        H(JPIV,JPIV)=COSINE**2*(H(JPIV,JPIV)-TANG*(2.0D0*H(IPIV,JPIV)-TANG
       1*HII))
        H(IPIV,JPIV)=0.0D0
C       PSEUDO RANK THE EIGENVALUES
C       ADJUST SINE AND COS FOR COMPUTATION OF H(IK) AND U(IK)
```

```
      IF ( H(IPIV,IPIV) - H(JPIV,JPIV)) 152,153,153
  152 HTEMP = H(IPIV,IPIV)
      H(IPIV,IPIV) = H(JPIV,JPIV)
      H(JPIV,JPIV) =HTEMP
C     RECOMPUTE SINE AND COS
      HTEMP = DSIGNF (1.0D0, -SINE) * COSINE
      COSINE =DABS (SINE)
      SINE =HTEMP
  153 CONTINUE
C     INSPECT THE IQS BETWEEN I+1 AND N-1 TO DETERMINE
C     WHETHER A NEW MAXIUM VALUE SHOULD BE COMPUTE   SINCE
C     THE PRESENT MAXIMUM IS IN THE I OR J ROW.
      DO 350 I=1,NMI1
      IF(I-IPIV)210,350,200
  200 IF (I-JPIV) 210,350,210
  210 IF(IQ(I)-IPIV) 230,240,230
  230 IF(IQ(I)-JPIV) 350,240,350
  240 K=IQ(I)
  250 HTEMP=H(I,K)
      H(I,K)=0.0D0
      IPL1=I+1
      X(I) =0.0D0
C     SEARCH IN DEPLETED ROW FOR NEW MAXIMUM
      DO 320 J=IPL1,N
      IF ( X(I) -DABS( H(I,J)) ) 300,300,320
  300 X(I) = DABS(H(I,J))
      IQ(I)=J
  320 CONTINUE
      H(I,K)=HTEMP
  350 CONTINUE
      X(IPIV) =0.0D0
      X(JPIV) =0.0D0
C     CHANGE THE ORDER ELEMENTS OF H
      DO 530 I=1,N
      IF (I-IPIV) 370,530,420
  370 HTEMP = H(I,IPIV)
      H(I,IPIV)= COSINE*HTEMP + SINE*H(I,JPIV)
     - IF ( X(I) - DABS( H(I,IPIV)) )380,390,390
  380 X(I) = DABS(H(I,IPIV))
      IQ(I) = IPIV
  390 H(I,JPIV) = - SINE*HTEMP + COSINE*H(I,JPIV)
      IF ( X(I) - DABS ( H(I,JPIV)) ) 400,530,530
  400 X(I) = DABS(H(I,JPIV))
      IQ(I) = JPIV
      GO TO 530
  420 IF(I-JPIV) 430,530,480
  430 HTEMP = H(IPIV,I)
      H(IPIV,I) = COSINE*HTEMP + SINE*H(I,JPIV)
      IF ( X(IPIV) - DABS(H(IPIV,I)) ) 440,450,450
  440 X(IPIV) = DABS(H(IPIV,I))
      IQ(IPIV) = I
  450 H(I,JPIV) = - SINE*HTEMP + COSINE*H(I,JPIV)
      IF (X(I) - DABS( H(I,JPIV)) ) 400,530,530
  480 HTEMP = H(IPIV,I)
      H(IPIV,I) = COSINE*HTEMP + SINE*H(JPIV,I)
      IF ( X(IPIV) - DABS( H(IPIV,I)) ) 490,500,500
  490 X(IPIV) = DABS(H(IPIV,I))
      IQ(IPIV) = I
  500 H(JPIV,I) = - SINE*HTEMP + COSINE*H(JPIV,I)
      IF ( X(JPIV) - DABS( H(JPIV,I)) )510,530,530
  510 X(JPIV) = DABS(H(JPIV,I))
      IQ(JPIV) = I
  530 CONTINUE
C     TEST FOR COMPUTATION OF EIGENVECTORS
      IF(IEGEN) 40,540,40
  540 DO 550 I=1,N
```

```
      HTEMP=U(I,IPIV)
      U(I,IPIV)=COSINE*HTEMP+SINE*U(I,JPIV)
  550 U(I,JPIV)= -SINE*HTEMP+COSINE*U(I,JPIV)
      GO TO 40
 1000 RETURN
      END
```

```
C
C     SOLUTION OF THE SECULAR EQUATION.  INPUT IS GAMMA
C     MATRIX (DIAGONALIZED G) AND F.
C
      IMPLICIT REAL*8 (A-H,O-Z)
      REAL*4 RECORD
      DIMENSION F(147,147),W(147,147),RECORD(36),DD(147)
      DIMENSION H(147,147),DV(147),EIG(147,147),C(147,147)
      EQUIVALENCE (H,EIG),(DD,DV)
  100 READ(5,1) IND,NOPROB,NQ,NOAT,ITHERM,IREP,NEXCO
    1 FORMAT(7I5)
      IF(9+IND)95,93,95
   95 CALL EXIT
   93 READ(5,2) (RECORD(I),I=1,36)
    2 FORMAT(18A4)
      WRITE(6,50) NOPROB,IND,(RECORD(I),I=1,36)
   50 FORMAT(13H1 PROBLEM NO,I8,I3/(12X,18A4))
      IF (NOPROB.NE.1) GO TO 99
      DO 98 I=1,NQ
   98 READ(12) (F(I,J),J=1,NQ)
   99 READ(13) ((W(I,J),I=1,NQ),J=1,NQ)
      DO 200 J=1,NQ
      DO 195 L=1,NQ
      DD(L)=0.0D0
      DO 195 K=1,NQ
  195 DD(L)=DD(L)+F(L,K)*W(K,J)
      DO 200 I=1,NQ
      H(I,J)=0.0D0
      DO 200 M=1,NQ
  200 H(I,J)=H(I,J)+W(M,I)*DD(M)
      NR=0
      IEGEN=0
      CALL HDIAG(H,NQ,IEGEN,C,NR)
      DO 208 I=1,NQ
  208 DV(I)=DSQRT(DABS(H(I,I)/5.88852D-7))
      DO 275 I=1,NQ
      DO 275 J=1,NQ
      EIG(I,J)=0.0D0
      DO 275 K=1,NQ
  275 EIG(I,J)=EIG(I,J)+W(I,K)*C(K,J)
      IF(IREP.EQ.1) GO TO 204
C  NQC=10 FOR METHANE AND PMM
      NQC=10
      MM=NQ-NEXCO
      DO 278 J=1,NQ
      IF(J.GT.MM) GO TO 280
      DO 272 JJ=1,NQC
      IF(DABS(EIG(JJ,J)).GE.(0.1)) GO TO 280
  272 CONTINUE
      GO TO 278
  280 WRITE(6,12) J,DV(J),(EIG(I,J),I=1,NQ)
   12 FORMAT(12H0 EIGENVALUEI3,2H= F12.6,
     120H EIGENVECTOR FOLLOWS/(10F12.6))
  278 CONTINUE
      GO TO 108
  204 DO 288 J=1,NQ
  288 WRITE(6,12) J,DV(J),(EIG(I,J),I=1,NQ)
  108 WRITE(6,61) NOPROB
   61 FORMAT(24H FREQUENCIES PROBLEM NO,I6)
```

```
      WRITE(6,63) (DV(I),I=1,NQ)
   63 FORMAT(6F12.6)
      GO TO 100
      END
      SUBROUTINE HDIAG(H,N,IEGEN,U,NR)
      IMPLICIT REAL*8 (A-H,O-Z)
      REAL*4 RECORD,RECD,STORY
CHDIAGMIHDI3, FORTAN II DIAGONALIZATION OF A REAL SYMMETRIC MATRIX BY
C     THE JACOBI METHOD.
C     CALLING SEQUENCE FOR DIAGONALIZATION
C     CALL HDIAG( H, N, IEGEN, U, NR)
C     WHERE H IS THE ARRAY TO BE DIAGONALIZED.
C     N IS THE ORDER OF THE MATRIX, H.
C     IEGEN MUST BE SET UNEQUAL TO ZERO IF ONLY EIGENVALUES ARE TO BE
C     COMPUTED.
C     IEGEN MUST BE SET EQUAL TO ZERO IF EIGENVALUES AND EIGENVECTORS
C     ARE TO BE COMPUTED.
C     U IS THE UNITARY MATRIX USED FOR FORMATION OF THE EIGENVECTORS,
C     NR IS THE NUMBER OF ROTATIONS.
C     A DIMENSION STATEMENT MUST BE INSERTED IN THE SUBROUTINE.
C     DIMENSION H(N,N), U(N,N), X(N), IQ(N)
C     COMPUTER MUST OPERATE IN FLOATING TRAP MODE
C     THE SUBROUTINE OPERATES ONLY ON THE ELEMENTS OF H THAT ARE TO THE
C     RIGHT OF THE MAIN DIAGONAL. THUS, ONLY A TRIANGULAR
C     SECTION NEED BE STORED IN THE ARRAY H.
      DIMENSION H(147,147),U(147,147),X(147),IQ(147)
      DSIGNF(X,Y)=DSIGN(X,Y)
      CALL ERRSET (208,256,-1,1,0,0)
      CALL ERRSET (209,256,-1,1,0,0)
      IF (IEGEN) 15,10,15
   10 DO 14 I=1,N
      DO 14 J=1,N
      IF(I-J)12,11,12
   11 U(I,J)=1.0D0
      GO TO 14
   12 U(I,J)=0.0D0
   14 CONTINUE
   15 NR = 0
      IF (N-1) 1000,1000,17
C     SCAN FOR LARGEST OFF DIAGONAL ELEMENT IN EACH ROW
C     X(I) CONTAINS LARGEST ELEMENT IN  ITH ROW
C     IQ(I) HOLDS SECOND SUBSCRIPT DEFINING POSITION OF ELEMENT
   17 NMI1=N-1
      DO 30 I=1,NMI1
      X(I) = 0.0D0
      IPL1=I+1
      DO 30 J=IPL1,N
      IF(X(I)-DABS( H(I,J))) 20,20,30
   20 X(I)=DABS(H(I,J))
      IQ(I)=J
   30 CONTINUE
C     SET INDICATOR FOR SHUT-OFF,RAP=2**-27,NR=NO.OF ROTATIONS
      RAP=7.450580596D-9
      HDTEST=1.0D38
C     FIND MAXIMUM OF X(I) S FOR PIVOT ELEMENT AND
C     TEST FOR END OF PROBLEM
   40 DO 70  I=1,NMI1
      IF (I-1) 60,60,45
   45 IF(XMAX-X(I)) 60,70,70
   60 XMAX=X(I)
      IPIV=I
      JPIV=IQ(I)
   70 CONTINUE
C     IS MAX. X(I) EQUAL TO ZERO, IF LESS THAN HDTEST,REVISE HDTEST
      IF (XMAX) 1000,1000,80
   80 IF( HDTEST) 90,90,85
```

```
   85 IF (XMAX - HDTEST) 90,90,148
   90 HDIMIN = DABS ( H (1,1) )
      DO 110  I=2,N
      IF (HDIMIN - DABS ( H (I,I))) 110,110,100
  100 HDIMIN=DABS (H(I,I))
  110 CONTINUE
      HDTEST=HDIMIN*RAP
C     RETURN IF MAX.H(I,J)LESS THAN(2**-27)DABS(H(K,K)-MIN)
      IF (HDTEST-XMAX) 148,1000,1000
  148 NR= NR+1
C     COMPUTE TANGENT, SINE AND COSINE,H(I,I),H(J,J)
  150 TANG=DSIGN(2.D0,(H(IPIV,IPIV)-H(JPIV,JPIV)))*H(IPIV,JPIV)/(DABS(H
     1(IPIV,IPIV)-H(JPIV,JPIV))+DSQRT((H(IPIV,IPIV)-H(JPIV,JPIV))**2+
     24.000*H(IPIV,JPIV)**2))
      COSINE=1.0D0/DSQRT(1.0D0+TANG*TANG)
      SINE=TANG*COSINE
      HII=H(IPIV,IPIV)
      H(IPIV,IPIV)=COSINE**2*(HII+TANG*(2.0D0*H(IPIV,JPIV)+TANG*H(JPIV,
     1JPIV)))
      H(JPIV,JPIV)=COSINE**2*(H(JPIV,JPIV)-TANG*(2.0D0*H(IPIV,JPIV)-TANG
     1*HII))
      H(IPIV,JPIV)=0.0D0
C     PSEUDO RANK THE EIGENVALUES
C     ADJUST SINE AND COS FOR COMPUTATION OF H(IK) AND U(IK)
      IF ( H(IPIV,IPIV) - H(JPIV,JPIV)) 152,153,153
  152 HTEMP = H(IPIV,IPIV)
      H(IPIV,IPIV) = H(JPIV,JPIV)
      H(JPIV,JPIV) =HTEMP
C     RECOMPUTE SINE AND COS
      HTEMP = DSIGNF (1.0D0, -SINE) * COSINE
      COSINE =DABS (SINE)
      SINE =HTEMP
  153 CONTINUE
C     INSPECT THE IQS BETWEEN I+1 AND N-1 TO DETERMINE
C     WHETHER A NEW MAXIUM VALUE SHOULD BE COMPUTE   SINCE
C     THE PRESENT MAXIMUM IS IN THE I OR J ROW.
      DO 350 I=1,NMI1
      IF(I-IPIV)210,350,200
  200 IF (I-JPIV) 210,350,210
  210 IF(IQ(I)-IPIV) 230,240,230
  230 IF(IQ(I)-JPIV) 350,240,350
  240 K=IQ(I)
  250 HTEMP=H(I,K)
      H(I,K)=0.0D0
      IPL1=I+1
      X(I) =0.0D0
C     SEARCH IN DEPLETED ROW FOR NEW MAXIMUM
      DO 320 J=IPL1,N
      IF ( X(I) -DABS( H(I,J)) ) 300,300,320
  300 X(I) = DABS(H(I,J))
      IQ(I)=J
  320 CONTINUE
      H(I,K)=HTEMP
  350 CONTINUE
      X(IPIV) =0.0D0
      X(JPIV) =0.0D0
C     CHANGE THE ORDER ELEMENTS OF H
      DO 530 I=1,N
      IF (I-IPIV) 370,530,420
  370 HTEMP = H(I,IPIV)
      H(I,IPIV)= COSINE*HTEMP + SINE*H(I,JPIV)
      IF ( X(I) - DABS( H(I,IPIV)) )380,390,390
  380 X(I) = DABS(H(I,IPIV))
      IQ(I) = IPIV
  390 H(I,JPIV) = - SINE*HTEMP + COSINE*H(I,JPIV)
      IF ( X(I) - DABS ( H(I,JPIV)) ) 400,530,530
```

```
  400 X(I) = DABS(H(I,JPIV))
      IQ(I) = JPIV
      GO TO 530
  420 IF(I-JPIV) 430,530,480
  430 HTEMP = H(IPIV,I)
      H(IPIV,I) = COSINE*HTEMP + SINE*H(I,JPIV)
      IF ( X(IPIV) - DABS(H(IPIV,I)) ) 440,450,450
  440 X(IPIV) = DABS(H(IPIV,I))
      IQ(IPIV) = I
  450 H(I,JPIV) = - SINE*HTEMP + COSINE*H(I,JPIV)
      IF (X(I) - DABS( H(I,JPIV)) ) 400,530,530
  480 HTEMP = H(IPIV,I)
      H(IPIV,I) = COSINE*HTEMP + SINE*H(JPIV,I)
      IF ( X(IPIV) - DABS( H(IPIV,I)) ) 490,500,500
  490 X(IPIV) = DABS(H(IPIV,I))
      IQ(IPIV) = I
  500 H(JPIV,I) = - SINE*HTEMP + COSINE*H(JPIV,I)
      IF ( X(JPIV) - DABS( H(JPIV,I)) )510,530,530
  510 X(JPIV) = DABS(H(JPIV,I))
      IQ(JPIV) = I
  530 CONTINUE
C     TEST FOR COMPUTATION OF EIGENVECTORS
      IF(IEGEN) 40,540,40
  540 DO 550 I=1,N
      HTEMP=U(I,IPIV)
      U(I,IPIV)=COSINE*HTEMP+SINE*U(I,JPIV)
  550 U(I,JPIV)= -SINE*HTEMP+COSINE*U(I,JPIV)
      GO TO 40
 1000 RETURN
      END
```

REFERENCES

1. W.H. Keesom and J. Haantjes, Physica 2, 986 (1935).
2. H.G. East and H. Kuhn, J. Sci Instrum. 23, 185 (1956).
3. E.W. Becker and O. Stehl, Z. Angew. Phys. 4, 20 (1952).
4. M.W. Lee, D.M. Eshelman and J. Bigeleisen, J. Chem. Phys. 56, 5053 (1972).
5. J. Bigeleisen and E. Roth, J. Chem. Phys. 35, 68 (1961).
6. J. Bigeleisen, F.P. Brooks, T. Ishida and S.V. Ribnikar, Rev. Sci. Instrum. 39, 352 (1968).
7. G. Boato, G. Scoles and M.E. Vallauri, Nuovo Cimento 14, 735 (1959).
8. J. Bigeleisen and S.V. Ribnikar, J. Chem. Phys. 35, 1297 (1961).
9. I. Dostrovsky, D.R. Leewellyn and B.H. Vroman, J. Chem. Soc., 3509 (1952).
10. J. Bigeleisen, M.J. Stern and W.A. Van Hook, J. Chem. Phys. 38, 497 (1963).
11. G. Thomaes and R. Steenwinkel, Mol. Phys. 5, 307 (1962).
12. M. Benedict and T.H. Pigford, "Nuclear Chemical Engineering," McGraw-Hill, New York, 1957.
13. K. Cohen, "The Theory of Isotope Separation," McGraw-Hill, New York, 1957.
14. T. Ishida and H. Wieck in "Proceedings of the International Meeting on the Isotope Effects of Physical and Chemical Processes," Inst. for Stable Isotopes, Cluj, Rumania, 1973, in press.
15. F.A. Lindeman, Phil. Mag. 38, 173 (1919).
16. O. Stern (1914) unpublished; see ref (17).
17. W.H. Keesom and H. van Dijk, Proc. Acad. Sci. Amsterdam 34, 42 (1931).
18. R.B. Scott, F.C. Brickwedde, H.C. Urey and M.H. Wahl, J. Chem. Phys. 2, 454 (1934).
19. K.F. Herzfeld and E. Teller, Phys. Rev. 54, 912 (1938).

20. E. Wigner, Phys. Rev. 40, 749 (1932).

21. L.D. Landau and E.M. Lifshitz, "Statistical Physics," Addison-Wesley, Reading, Mass., 1969.

22. H. Friedmann, Adv. Chem. Phys. 4, 225 (1962).

23. J. Bigeleisen, J. Chem. Phys. 23, 2264 (1955).

24. I. Oppenheim and A.S. Friedman, J. Chem. Phys. 35, 35 (1961).

25. G. Casanova, A. Levi and N. Terzi, Physica 30, 937 (1964).

26. J. Bigeleisen, M.W. Lee and F. Mandel, Acc. Chem. Res. 8, 179 (1975).

27. F. Mandel, J. Chem. Phys. 57, 3929 (1972).

28. L. Verlet, Phys. Rev. 159, 98 (1967).

29. J.S. Rowlinson, Mol. Phys. 9, 197 (1965).

30. R.D. Present and C.T. Chen, J. Che,. Phys. 55, 2391 (1971); J. Chem. Phys. 54, 58 (1971).

31. See for example, M.J. Stern, W. Spindel and E.U. Monse, J. Chem. Phys. 48, 2908 (1968); J. Chem. Phys. 52, 2022 (1970); T. Ishida, Z.C. Kornblum and J.S. Pollin in "Proceedings of the International Conference on Isotopes in Nature," Gera, E. Germany, 1975, in press.

32. J. Bigeleisen, J. Chim. Phys. 60, 35 (1963).

33. M. Wolfsberg, J. Chim. Phys. 60, 15 (1963).

34. T. John in "Proceedings of the International Symposium on Isotope Separation," J. Kistemaker, J. Bigeleisen and A.O.C. Nier, Eds., North-Holland Publishing Co., Amsterdam, 1958.

35. G.G. Devyatkh, Zh. Fiz. Khim. 31, 1445 (1957); Tr. Khim. Tekhnol. 2, 229 (1958).

36. I.B. Rabinovych, "Influence of Isotopy on the Physicochemical Properties of Liquids," Consultants Bureau, New York, 1970.

37. J. Bigeleisen, J. Chem. Phys. 34, 1485 (1961).

38. M.J. Stern, W.A. Van Hook and M. Wolfsberg, J. Chem. Phys. 39, 3179 (1963).

39. T. Ishida and J. Bigeleisen, J. Chem. Phys. 49, 5498 (1968).

40. J. Bigeleisen, C.B. Cragg and M. Jeevanandam, J. Chem. Phys. 47, 4335 (1967).

41. W.A. Van Hook, J. Chem. Phys. 46, 1907 (1966).

42. J. Bigeleisen, J. Chem. Phys. 39, 769 (1963); J. Chem. Phys. 39, 1356 (1963).

43. I.N. Levine, "Quantum Chemistry," Wiley, New York, 1975.

44. J. Bigeleisen and M.G. Mayer, J. Chem. Phys. 15, 261 (1947).

45. J. Bigeleisen, Science 147, 463 (1965).

46. J. Bigeleisen, J. Chem. Phys. 21, 1333 (1953).

47. J. Bigeleisen in ref. (34).

48. G. Vojta, Z. Physik. Chem. 217, 337 (1961).

49. J. Bigeleisen and T. Ishida, J. Chem. Phys. 48, 1311 (1968).

50. T. Ishida, W. Spindel and J. Bigeleisen in "Isotope Effects in Chemical Processes," W. Spindel, Ed., Adv. in Chem. Ser. No. 89, American Chemical Society, Washington, D.C., 1969; Proc. Nat Acad. Sci. 67, 113 (1970).

51. W.A. Van Hook and A.Y. Fang, J. Chem. Phys. 60, 3513 (1974).

52. F.H. Varekamp and J. Beenakker, Physika 25, 889 (1959).

53. W. Göpel and T. Dorfmüller, Z. Phys. Chem. 82, 54 (1972).

54. P.W. Bridgman, J. Chem. Phys. 3, 597 (1935).

55. J. Walkley and J.H. Hildebrand, J. Am. Chem. Soc. 81, 4439 (1959).

56. J.O. Hirschfelder, C.F. Curtiss and R.B. Bird, "Molecular Theory of Gases and Liquids," Wiley, New York, 1954.

57. D.J. McGinty, J. Chem. Phys. 58, 4733 (1973); see also ref. (56).

58. G. Jansco and W.A. Van Hook, Chem. Rev. 74, 689 (1974).

59. J. Bigeleisen, M.W. Lee and F. Mandel, Ann. Rev. Phys. Chem. 24, 407 (1973).

60. M. Wolfsberg and L.I. Kleinman in "Isotopes and Chemical Principles," P.A. Rock, Ed. ACS Symposium Series No. 11, American Chemical Society, Washington, D.C., 1975.

61. W. Kolos and L. Wolniewicz, J. Chem. Phys. 43, 2429 (1965).

62. E.B. Wilson, Jr., J.C. Decius and P.C. Cross, "Molecular Vibrations," McGraw-Hill, New York, 1955.

63. G. Herzberg, "Infrared and Ramen Spectra of Polyatomic Molecules," Van Nostrand-Reinhold, New York, 1945.

64. J.C. Decius, J. Chem. Phys. 17, 1315 (1949).

65. E.B. Wilson, Jr., J. Chem. Phys. 7, 1047 (1939).

66. R. Courant and D. Hilbert, "Methods of Mathematical Physics," Interscience, New York, 1953.

67. E.P. Wigner, "Group Theory," Academic Press, New York, 1959.

68. L.M. Sverdlov, M.A. Kovner and E.P. Krainov, "Vibrational Spectra of Polyatomic Molecules," Wiley, New York, 1974.

69. Y. Morino and K. Kuchitsu, J. Chem. Phys. 20, 1809 (1952).

70. J.H. Schachtschneider and R.G. Snyder, Spectrochim. Acta. 19, 117 (1963).

71. J.C. Decius, J. Chem. Phys. 38, 241 (1963).

72. G. Thyagarajan, C.R. Sarma and M.K. Snbhedar, J. Mol. Spectrosc. 33, 100 (1969).

73. L.H. Jones and R.R. Ryan, J. Chem. Phys. 52, 2003 (1970).

74. L.H. Jones, Coord. Chem. Rev. 1, 351 (1966).

75. R.L. Redington and A.L.K. Aljibury, J. Mol. Spectrosc. 37, 494 (1971).

76. D.C. McKean and J.L. Duncan, Spectrochim. Acta. 27A, 1879 (1971).

77. P. Pulay, Mol. Phys. 17, 197 (1969).

78. J. Gerritt and I.M. Mills, J. Chem. Phys. 49, 1719 (1968).

79. J. Gerritt and I.M. Mills, J. Chem. Phys. 49, 1730 (1968).

80. P. Sivanstrøm, K. Thomsen and P. Yde, Mol. Phys. 20, 1135 (1971).

81. W. Meyer and P. Rosmus, J. Chem. Phys. 63, 2356 (1975).

82. W.J. Stevens, G. Das, A.C. Wahl, M. Krauss and D. Newman, J. Chem. Phys. 61, 3687 (1974).

83. L.H. Jones, "Inorganic Vibrational Spectroscopy," Marcel Dekker, New York, 1971.

84. L.H. Jones and R.S. McDowell, J. Mol. Spectrosc. 3, 633 (1959); L.H. Jones and M. Goldblatt, J. Mol. Spectrosc. 2, 103 (1958).

85. S.R. Hartshorn and V.J. Shiner, Jr., J. Am. Chem. Soc. 94, 9002 (1972).

86. A. Babloyantz, Mol. Phys. 2, 39 (1959).

87. P.A. Egelstaff, E. Page and J.G. Powels, Mol. Phys. 20, 881 (1971).

88. L.J. Lowden and D. Chandler, J. Chem. Phys. 61, 5228 (1974).

89. W. Press, J. Chem. Phys. 56, 2597 (1972).

90. W. Press, B. Dorner and G. Will, Phys. Letters 31A, 253 (1970).

91. R.T. Birge, Revs. Mod. Phys. 13, 233 (1941).

92. "Handbook of Chemistry and Physics," 53rd Ed., Chemical Rubber Co., 1973.

93. A. Bondi, "Physical Properties of Molecular Crystals, Liquids and Glasses," Wiley, New York, 1968.

94. D.A. Gyorog and E.F. Obert, A.I.Ch.E. Journal 10, 621 (1964).

95. A.G. DeRocco and J.O. Halford, J. Chem. Phys. 28, 1152 (1958).

96. W.F. Vogel and R.C. Ahlert, J. Phys. Chem. 73, 2304 (1969).

97. R.C. Ahlert and W.F. Vogel, A.I.Ch.E. Journal 12, 1025 (1969).

98. K.E. Gubbins and J.P. O'Connell, J. Chem. Phys. 60, 3449 (1974).

99. S.W. Brelvi and J.P. O'Connell, A.I.Ch.E. Journal 18, 1239 (1972).

100. F.A. Cotton and C.S. Kraihänzel, J. Am. Chem. Soc. 84, 4432 (1962).

101. M.F. Crawford, H.L. Welch and J.H. Harrold, Can. J. Chem. 30, 81 (1952).

102. A. Ben-Naim, J. Chem. Phys. 56, 2864 (1972); J. Chem. Phys. 59 6535 (1973).

103. R.F.W. Bader, P.M. Beddal and J. Peslak, J. Chem. Phys. 58, 557 (1973).

104. R.F.W. Bader and P.M. Beddall, J. Chem. Phys. 56, 3320 (1972).

105. R.F.W. Bader, W.H. Henneker and P.E. Cade, J. Chem. Phys. 46, 3341 (1973).

106. S. Srebrenik, H. Weinstein and R. Pauncz, J. Chem. Phys. 61, 5050 (1974).

107. P. Hohenberg and W. Kohn, Phys. Rev. B 136, 864 (1964).

108. H. Eves, "Matrix Theory," Allyn and Bacon, Boston, 1966.

109. L.A. Pipes and S. Hovenessian, "Matrix-Computer Methods in Engineering," Wiley, New York, 1969.

110. F. Scheid, "Numerical Analysis," McGraw-Hill, New York, 1968.

111. R.P. Tewarson, "Sparse Matrices," Academic Press, New York, 1973.

112. R.P. Tewarson, Int. J. Comp. Math. 2, 247 (1970).

113. G.E. Ewing, J. Chem. Phys. 40, 179 (1964).

114. J. Bigeleisen in ref. (60).

115. A. J. Hopfinger, "Conformational Properties of Macromolecules," Academic Press, New York, 1973.

116. L.J. Lowden and D. Chandler, J. Chem. Phys. 59, 6587 (1973).

117. S.A. Rice and P. Gray, "Statistical Mechanics of Simple Liquids," Wiley, New York 1965.

118. G.T. Armstrong, F.G. Brickwedde and R.B. Scott, J. Res. Natl. Bur. Std. 55, 39 (1955).

119. R.B. Wright, M. Shwartz and C.H. Wang, J. Chem. Phys. 58, 5125 (1973).

120. J. Bigeleisen, T. Ishida and W. Spindel, J. Chem. Phys. 55, 5021 (1971).

121. J. Bigeleisen and T. Ishida, J. Chem. Phys. 62, 80 (1975).

122. D.E. O'Reilly, J. Chem. Phys. 56, 2924 (1972).

123. G.B. Savitsky and D.F. Horing, J. Chem. Phys. 36, 2635 (1962).

124. P.A. Egelstaff, "Introduction to the Liquid State," Academic Press, New York, 1967.

125. J.H. Hildebrand and R.B. Scott, "Regular Solutions," Prentice-Hall, Englewood Cliffs, New Jersey, 1962; see also ref. (89).